

UNIVERSITY OF SOUTHAMPTON

FACULTY OF ENGINEERING AND THE ENVIRONMENT

National Centre for Advanced Tribology at Southampton

**Improved Testing Methodologies for Evaluating the Corrosion
Resistance of Paint Systems and Materials for Aging Military
Aircraft**

by

Rachael Hayley Collins

Supervised by Dr Julian Wharton & Professor Keith Stokes

A thesis submitted in partial fulfilment of the requirements for the degree of Doctorate of
Philosophy

January 2018

Abstract

The prediction of in-service performance of military aircraft materials in corrosive environments has long relied on atmospheric exposure test sites. There are established accelerated test methods for assessing the performance of aerospace coatings however, these are often far removed from the environments experienced by aircraft during typical operations and do not provide predictive information regarding expected service life. Often tests incorporate salt spray and ultraviolet radiation whilst exposing the metal to continuous or cyclic conditions dissimilar to those of the corrosive environment. Consequently, coatings which pass these standard tests sometimes prematurely fail in-service, leading to corrosion and failure of structural components. The divergence between laboratory and real world performance is exacerbated when comparing chromate containing to chromate free technologies. In general, salt spray and other accelerated environmental tests provide a ranking of materials in terms of their resistance to a particular environment. For example, the salt spray test provides a comparison between chromate levels present in chromated systems but is not necessarily valid to non-chromated systems. The validity of accelerated tests when evaluating materials and coatings for use in conditions which are not directly related is, therefore, of doubtful benefit in the prediction of service life. It is however, necessary to implement screening tests to enable down-selection and ranking of the best performing systems.

The quantitative link between real world exposure and laboratory based accelerated testing was explored through the implementation of a large scale time-optimised four factorial experimental design. The design encompassed two base materials, aircraft aluminium alloy (AA) 2024-T3 and AA7075-T6. The base materials were used in conjunction with 6 coating systems, each including; a pre-treatment, a primer and a topcoat, this resulted in twelve distinct coupon types, each consisting of three sections; primer, primer-topcoat and topcoat. The twelve coupon types were subjected to nine experiments, four 18 month external exposure tests and five accelerated laboratory tests. The four external tests were defined as either tropical or temperate in climate and coastal or inland in location. The first of the accelerated laboratory tests was the standard neutral BS 9227 - Corrosion tests in artificial atmospheres, salt spray test [1]. The remaining four accelerated tests utilise a cyclic design that aims to replicate the weather patterns associated with the tropical and temperate locations used for exposure testing. Accelerated test protocols 1 and 2 utilised controlled temperature and humidity cycles in a chamber, whilst accelerated tests 3 and 4 were a variant on a Scab test [2]. Time remained a key factor linking all experiments with all tests split by seven equal time points, allowing for interrogation throughout the process of exposure and enabling the pursuit of similarities between failure mechanisms of different coupon types.

List of Contents

Abstract.....	i
List of Contents.....	iii
List of Figures.....	vii
List of Tables.....	xv
List of Equations.....	xvii
Acknowledgements.....	xxi
Definitions and Abbreviations.....	xxiii
Nomenclature.....	xxv
1. Introduction.....	1
1.1. Project aim.....	2
1.2. Project overview.....	2
1.3. Environmental test chamber - background & context.....	2
1.4. Thesis structure.....	4
2. Protecting aircraft.....	7
2.1. Introduction.....	7
2.2. Aircraft coating technology.....	8
2.3. Conversion coatings.....	10
2.4. Polymeric coatings.....	11
2.4.1. Chromate inhibition mechanism.....	12
2.4.2. Future alternatives to chromates.....	12
2.4.3. Magnesium additives.....	15
2.4.4. Sol-gel coatings.....	16
2.4.5. The Al-alloy substrate.....	21
2.4.6. AA2024-T3 microstructure.....	22
2.4.7. AA7075-T6 microstructure.....	24
2.5. Experimental.....	27
2.5.1. Coating application.....	29
2.6. Zero time point analysis.....	31
2.6.1. Film thickness measurements.....	31
2.6.2. Success of coating application.....	33
2.6.3. Gloss measurements.....	39
2.6.1. Hardness measurements.....	41

2.7.	Summary.....	42
3.	Understanding the Exposure Environment.....	45
3.1.	Introduction.....	45
3.2.	Objective.....	55
3.3.	Experimental.....	55
3.3.1.	Materials.....	55
3.3.2.	Field exposures.....	56
3.3.3.	Gloss measurements.....	63
3.3.4.	Film thickness measurements.....	64
3.3.5.	Colorimetry measurements.....	64
3.3.6.	Hardness measurements.....	65
3.3.7.	Pulsed thermography measurements.....	65
3.4.	Results and discussion.....	67
3.4.1.	Coating component gloss changes with exposure.....	67
3.4.2.	Film thickness change with exposure.....	69
3.4.3.	Colour change with exposure.....	71
3.4.4.	Hardness increase with exposure.....	72
3.4.5.	The quantified corroded surface.....	73
3.5.	Summary.....	77
4.	Incompatibility of the Standard BS EN ISO 9227 Performance with Natural Exposures.....	79
4.1.	Introduction.....	79
4.1.1.	Accelerated corrosion tests.....	80
4.1.2.	Corrosion.....	85
4.1.3.	Atmospheric and bulk solution corrosion.....	87
4.1.4.	Corrosion of aluminium and aluminium alloys.....	87
4.2.	Experimental Objective.....	96
4.3.	Experimental.....	96
4.3.1.	Materials.....	96
4.3.2.	Field exposures.....	97
4.3.3.	Understanding the accelerated exposure environment.....	97
4.3.4.	BS EN ISO 9227.....	101
4.3.5.	Post exposure analytics.....	101
4.4.	Results and discussion.....	102
4.5.	Summary.....	112
5.	Exploring Replication of a Tropical Coastal Environment.....	115
5.1.	Introduction.....	115

5.2.	Objective	117
5.3.	Experimental	117
5.3.1.	Materials	117
5.3.2.	The field exposure.....	118
5.3.3.	The accelerated exposure experiment	118
5.3.4.	Post exposure analytics	119
5.4.	Results and discussion	119
5.4.1.	Gloss change	120
5.4.2.	Colour change	124
5.5.	Summary	127
6.	Alternative Approaches to Salt Spray	129
6.1.	Introduction.....	129
6.2.	Objectives	130
6.3.	The importance of rain.....	130
6.3.1.	Materials	132
6.3.2.	Experimental procedure	132
6.4.	Trials with oxidants.....	134
6.4.1.	Materials	135
6.4.2.	Experimental procedure	136
6.5.	Results and discussion	137
6.5.1.	Studying the effect of rain.....	137
6.5.2.	Studying the effect of oxidants	143
6.6.	Summary	159
7.	The Factorial Design.....	163
7.1.	Introduction.....	163
7.2.	Objectives	163
7.3.	The factorial design.....	163
7.4.	Data collection	165
7.5.	Analysis.....	165
7.5.1.	Factorial design response to Q1	166
7.5.2.	Factorial design response to Q2	166
7.5.3.	Factorial design response to Q3	166
7.5.4.	Additional analysis.....	167
7.6.	Summary	167
8.	Conclusions.....	169

8.1.	Response to Thesis Questions	169
8.2.	Wider learnings.....	171
9.	Future Work.....	173
9.1.	The factorial design	173
9.2.	The current data set.....	173
9.2.1.	With permission for chemical analysis	173
9.3.	Future experiments	174
10.	Bibliography	177
11.	Appendix	185
11.1.	Coating systems supplied by AkzoNobel	185
11.2.	Coating Systems supplied by PPG	187
11.3.	Natural exposure rack design.....	190
11.4.	Additional data from testing of Ascott chamber.....	193
11.5.	Full factorial design as analysed.....	196

List of Figures

FIGURE 1: MILITARY AEROSPACE COATING SCHEMATIC.....	9
FIGURE 2: BIS-SILANE BONDING SCHEMATIC WITH AN ALUMINIUM SUBSTRATE.....	17
FIGURE 3: CHEMICAL STRUCTURE AND FORMULA OF BIS-[3-(TRIETHOXSILYL)- PROPYL]TETRASULFIDE $[(H_3C_2O)_3SI(CH_2)_3S_4(CH_2)_3SI(OC_2H_5)_3]$	18
FIGURE 4: AA2024-T3 MICROSTRUCTURES, KELLER'S REAGENT, 500X MAGNIFICATION, (A) SOLUTION HEAT TREATED (495°C) AND COOLED IN STILL AIR, (B) SOLUTION HEAT TREATED (495°C) AND COOLED IN AIR BLAST, (C) SOLUTION HEAT TREATED (495°C) AND QUENCHED IN BOILING WATER [56].	23
FIGURE 5: MICROSTRUCTURE OF AA7075-T6, SCALE BAR IS A LENGTH OF 100 MM [5]......	25
FIGURE 6: SECTIONED VIEW OF COATED COUPON SYSTEM.....	27
FIGURE 7: EXAMPLE OF AS-COATED AKZONOBEL COATING SYSTEM 1 - PANEL NUMBER 49 (AA2024-T3 SUBSTRATE).	29
FIGURE 8: COATING APPLICATION IN BOOTH AT 1710 NAVAL AIR SQUADRON.	30
FIGURE 9: BACKING COATING AFTER 7 DAY'S TESTING AT 60°C WITH CONSTANT 5 WT.% SALT FOG.	31
FIGURE 10: FILM THICKNESS MEASUREMENTS OF AKZONOBEL COATING SYSTEM 1. THE MEASUREMENTS ILLUSTRATE TRENDS IN FILM THICKNESS ASSOCIATED WITH SPRAYING LOCATION ON BOARD 1.	34
FIGURE 11: FILM THICKNESS MEASUREMENTS OF AKZONOBEL COATING SYSTEM 2. THE MEASUREMENTS ILLUSTRATE TRENDS IN FILM THICKNESS ASSOCIATED WITH SPRAYING LOCATION ON BOARD 2.	35
FIGURE 12: FILM THICKNESS MEASUREMENTS OF AKZONOBEL COATING SYSTEM 3. THE MEASUREMENTS ILLUSTRATE TRENDS IN FILM THICKNESS ASSOCIATED WITH SPRAYING LOCATION ON BOARD 3.	35
FIGURE 13: FILM THICKNESS MEASUREMENTS OF AKZONOBEL COATING SYSTEM 4. THE MEASUREMENTS ILLUSTRATE TRENDS IN FILM THICKNESS ASSOCIATED WITH SPRAYING LOCATION ON BOARD 4.	36
FIGURE 14: FILM THICKNESS MEASUREMENTS OF AKZONOBEL COATING SYSTEM 5. THE MEASUREMENTS ILLUSTRATE TRENDS IN FILM THICKNESS ASSOCIATED WITH SPRAYING LOCATION ON BOARD 5.	36
FIGURE 15: FILM THICKNESS MEASUREMENTS OF AKZONOBEL COATING SYSTEM 6. THE MEASUREMENTS ILLUSTRATE TRENDS IN FILM THICKNESS ASSOCIATED WITH SPRAYING LOCATION ON BOARD 6.	37
FIGURE 16: MAP OF RAF AND RNAS BASES IN THE UNITED KINGDOM WHEREBY MILITARY AIRCRAFT ARE STATIONED, DATA COLLECTED FROM [74].	46
FIGURE 17: WORLD MAP OF PERMANENT RAF AND RNAS BASES WHERE UK MILITARY AIRCRAFT ARE STATIONED [74].	47
FIGURE 18: CURRENT MOD OPERATIONS ENVIRONMENTS AS IDENTIFIED PUBLICALLY BY THE MOD [75-77].	48

FIGURE 19: EXAMPLE OF CALIBRATION IMAGES FOUND IN BS EN ISO 4628, BLISTER SIZE 4, QUANTITY RANGE (LEFT TO RIGHT) 2 3, 4, 5. IMAGES ADAPTED FROM [90]	54
FIGURE 20: SOUTHAMPTON OUTDOOR EXPOSURE RIG.....	58
FIGURE 21: PORTSMOUTH OUTDOOR EXPOSURE RIG.....	58
FIGURE 22: LOCATIONS OF POSSIBLE PANAMA EXPOSURE SITES.	59
FIGURE 23: TROPICAL COASTAL EXPOSURE SITE AT 336 DAYS EXPOSURE.	60
FIGURE 24: TROPICAL INLAND EXPOSURE SITE AT 336 DAYS EXPOSURE.	61
FIGURE 25: FILM THICKNESS MEASUREMENT PATTERN.....	64
FIGURE 26: PULSED THERMOGRAPHY EXPERIMENTAL SETUP.....	66
FIGURE 27: COATING SYSTEM 3 PRIMER 60 DEGREE GLOSS VS. EXPOSURE TIME.	67
FIGURE 28: COATING SYSTEM 4 TOPCOAT 60 DEGREE GLOSS VS. EXPOSURE TIME.....	67
FIGURE 29: COATING SYSTEM 5 TOPCOAT 85 DEGREE GLOSS VS. EXPOSURE TIME.....	68
FIGURE 30: COATING SYSTEM 6 TOPCOAT 60 DEGREE GLOSS VS. EXPOSURE TIME.....	69
FIGURE 31: COATING SYSTEM 1 PRIMER MEASURED CHANGE IN FILM THICKNESS POST EXPOSURE VS. EXPOSURE TIME.....	70
FIGURE 32: COATING SYSTEM 6 TOPCOAT MEASURED CHANGE IN FILM THICKNESS POST EXPOSURE VS. EXPOSURE TIME.....	70
FIGURE 33: COATING 1 PRIMER CALCULATED ΔE 2000 COLOUR DIFFERENCE VS. EXPOSURE TIME.	71
FIGURE 34: COATING 6 PRIMER CALCULATED ΔE 2000 COLOUR DIFFERENCE VS. EXPOSURE TIME.	71
FIGURE 35: COATING SYSTEM 1 PRIMER KONIG HARDNESS VS. EXPOSURE TIME.....	72
FIGURE 36: TROPICAL INLAND FIELD EXPOSURE SITE.....	73
FIGURE 37: PULSED INFRARED THERMOGRAPHY FRAMES OF COATING SYSTEM 6 ON AA2024-T3 EXPOSED FOR 252 DAYS TO EITHER A TEMPERATE INLAND ENVIRONMENT (LEFT) OR TROPICAL COASTAL ENVIRONMENT (RIGHT).....	74
FIGURE 38: COATING SYSTEM 1 TOPCOAT PERCENTAGE SURFACE AREA CORROSION COVERAGE VS. EXPOSURE TIME.....	75
FIGURE 39: COATING SYSTEM 2 TOPCOAT PERCENTAGE SURFACE AREA CORROSION COVERAGE VS. EXPOSURE TIME.....	75
FIGURE 40: COATING SYSTEM 4 TOPCOAT PERCENTAGE SURFACE AREA CORROSION COVERAGE VS. EXPOSURE TIME.....	76
FIGURE 41: COATING SYSTEM 5 TOPCOAT PERCENTAGE SURFACE AREA CORROSION COVER VS. EXPOSURE TIME.	77
FIGURE 42: SCHEMATIC DIAGRAM OF AQUEOUS CORROSION AT METAL SOLUTION INTERFACE.	86
FIGURE 43: POURBAIX (E-PH) DIAGRAM FOR THE ALUMINIUM-WATER SYSTEM AT 25°C ($E /$ V VS. SHE) [9].	88
FIGURE 44: MODE OF CORROSION BASED ON EXPERIMENTAL DATA FOR AA5086 IN THE PRESENCE OF 0.5 M SODIUM CHLORIDE [116].	89
FIGURE 45: SIMPLIFIED ELECTROCHEMICAL MECHANISM OF PIT GROWTH ON ALUMINIUM SHOWING ITS AUTOCATALYTIC SELF-STIMULATING NATURE.	91

FIGURE 46: PITTING SCHEMATIC: (1) TYPICAL EXCHANGE CURRENT DENSITIES, (2) DEALLOYING OF S PHASE AND DEPOSITION OF CU AND (3) TRENCHING OF ANODIC DISPERSOID FREE ZONE AROUND THE INTERMETALLIC PARTICLE.	92
FIGURE 47: SCHEMATIC DETAILING CHEMICAL REACTIONS ASSOCIATED WITH FILIFORM CORROSION [121].	93
FIGURE 48: FILIFORM CORROSION: (A) TRANSVERSE SECTION AND (B) PLANE VIEW.	93
FIGURE 49: THE EVOLUTION OF EXFOLIATION CORROSION: (A) UNCORRODED MICROSTRUCTURE, (B) INTERGRANULAR CORROSION, (C) ONSET OF DELAMINATION CAUSED BY WEDGING EFFECT OF CORROSION PRODUCTS AND (D) LEAFING AND LOSS OF STRUCTURAL INTEGRITY.	94
FIGURE 50: EXFOLIATION CORROSION IN A 7000 SERIES ALUMINIUM ALLOY [122].	95
FIGURE 51: UNIVERSITY OF SOUTHAMPTON CYCLIC CORROSION CHAMBER.	98
FIGURE 52: EXPOSURE SEQUENCE USED IN THERMOCOUPLE STUDY.	98
FIGURE 53: SAMPLE LOCATION SEQUENCE USED IN THERMOCOUPLE STUDY OF ASCOTT CCT CHAMBER.	99
FIGURE 54: THERMOCOUPLE EXPERIMENT ASCOTT CYCLIC CORROSION CHAMBER CYCLE 1 (SEE FIGURE 53).	100
FIGURE 55: AVERAGED TRIPLICATE 60° GLOSS MEASUREMENTS POST EXPOSURE FOR PRIMER SECTION OF COATING SYSTEM 6.	103
FIGURE 56: AVERAGED TRIPLICATE 60° GLOSS MEASUREMENTS POST EXPOSURE FOR PRIMER SECTION OF COATING SYSTEM 2.	103
FIGURE 57: AVERAGED TRIPLICATE 60° GLOSS MEASUREMENTS POST EXPOSURE FOR PRIMER SECTION OF COATING SYSTEM 4.	104
FIGURE 58: AVERAGED TRIPLICATE 60° GLOSS MEASUREMENTS POST EXPOSURE FOR PRIMER SECTION OF COATING SYSTEM 5.	104
FIGURE 59: AVERAGED TRIPLICATE 60° GLOSS MEASUREMENTS POST EXPOSURE FOR PRIMER SECTION OF COATING SYSTEM 3.	105
FIGURE 60: AVERAGED TRIPLICATE 60° GLOSS MEASUREMENTS POST EXPOSURE FOR PRIMER SECTION OF COATING SYSTEM 1.	105
FIGURE 61: COATING SYSTEM 1 ON AA7075-T6 EXPOSED TO TROPICAL COASTAL NATURAL EXPOSURE FOR 420 DAYS.	106
FIGURE 62: AVERAGE ACCELERATION FACTOR BOUND BY STANDARD DEVIATION COMPARING COATING PERFORMANCE WHEN EXPOSED TO BS EN ISO 9227 SALT FOG VS. TROPICAL INLAND NATURAL EXPOSURE ON AA2024-T3, PERFORMANCE MEASURED WITH % AREA CORROSION BENEATH TOPCOAT IDENTIFIED USING PULSED THERMOGRAPHY.	107
FIGURE 63: AVERAGE CALCULATED ACCELERATION FACTOR BOUND BY STANDARD DEVIATION COMPARING COATING PERFORMANCE WHEN EXPOSED TO BS EN ISO 9227 SALT FOG VS. TROPICAL INLAND NATURAL EXPOSURE ON AA7075-T6, PERFORMANCE MEASURED WITH % AREA CORROSION BENEATH TOPCOAT IDENTIFIED USING PULSED THERMOGRAPHY.	108

FIGURE 64: AVERAGE CALCULATED ACCELERATION FACTOR BOUND BY STANDARD DEVIATION COMPARING COATING PERFORMANCE WHEN EXPOSED TO BS EN ISO 9227 SALT FOG VS. TROPICAL COASTAL NATURAL EXPOSURE ON AA7075-T6, PERFORMANCE MEASURED WITH % AREA CORROSION BENEATH TOPCOAT IDENTIFIED USING PULSED THERMOGRAPHY.108

FIGURE 65: AVERAGE CALCULATED ACCELERATION FACTOR BOUND BY STANDARD DEVIATION COMPARING COATING PERFORMANCE WHEN EXPOSED TO BS EN ISO 9227 SALT FOG VS. TEMPERATE COASTAL NATURAL EXPOSURE ON AA7075-T6, PERFORMANCE MEASURED WITH % AREA CORROSION BENEATH TOPCOAT IDENTIFIED WITH PULSED THERMOGRAPHY109

FIGURE 66: AVERAGE CALCULATED ACCELERATION FACTOR BOUND BY STANDARD DEVIATION FOR COATING SYSTEM 5, COMPARING PERFORMANCE OF EXPOSURE TO BS EN ISO 9227 SALT FOG AND NATURAL EXPOSURES ON BOTH AA2024-T3 AND AA7075-T6. PERFORMANCE WAS MEASURED WITH % AREA OF CORROSION BENEATH THE TOPCOAT USING PULSED THERMOGRAPHY.110

FIGURE 67: AVERAGE CALCULATED ACCELERATION FACTOR BOUND BY STANDARD DEVIATION FOR COATING SYSTEM 3, COMPARING PERFORMANCE OF EXPOSURE TO BS EN ISO 9227 SALT FOG AND NATURAL EXPOSURES ON BOTH AA2024-T3 AND AA7075-T6. PERFORMANCE WAS MEASURED WITH % AREA OF CORROSION BENEATH THE TOPCOAT USING PULSED THERMOGRAPHY.111

FIGURE 68: ASCOTT ANALYTICAL GRAPH SHOWING STANDARD RANGE OF TEMPERATURE/HUMIDITY CONTROL FOR A CCT CHAMBER AND HOW THIS MAY BE EXTENDED BY THE ADDITION OF OPTIONAL ACCESSORIES [126].116

FIGURE 69: CYCLE FOR ACCELERATED TESTING PROTOCOL 1 – CYCLE A FROM 0 MINUTES TO 240 MINUTES, CYCLE B FROM 240 MINUTES TO 480 MINUTES.....118

FIGURE 70: AVERAGED TRIPLICATE 85° GLOSS MEASUREMENTS POST EXPOSURE FOR TOPCOAT SECTION OF COATING SYSTEM 1.120

FIGURE 71: COATING SYSTEM 1 IN AA2024-T3 EXPOSED TO THE TROPICAL COASTAL SITE FOR 504 DAYS (COUPON #58).....121

FIGURE 72: AVERAGED TRIPLICATE 85° GLOSS MEASUREMENTS POST EXPOSURE FOR TOPCOAT SECTION OF COATING SYSTEM 2.122

FIGURE 73: LEFT - COATING SYSTEM 1 IN AA7075-T6 EXPOSED TO THE BS EN ISO 9227 FOR 84 DAYS (COUPON NO. 391). RIGHT- COATING SYSTEM 1 IN AA2024-T3 EXPOSED TO THE ACCELERATED EXPOSURE PROTOCOL FOR 84 DAYS (COUPON NO. 27).....122

FIGURE 74: AVERAGED TRIPLICATE 85° GLOSS MEASUREMENTS POST EXPOSURE FOR TOPCOAT SECTION OF COATING SYSTEM 4.123

FIGURE 75: AVERAGED TRIPLICATE 85° GLOSS MEASUREMENTS POST EXPOSURE FOR TOPCOAT SECTION OF COATING SYSTEM 5.123

FIGURE 76: COATING 4 PRIMER CALCULATED ΔE 2000 COLOUR DIFFERENCE.....125

FIGURE 77: COATING 5 PRIMER CALCULATED ΔE 2000 COLOUR DIFFERENCE.....125

FIGURE 78: COATING 6 PRIMER CALCULATED ΔE 2000 COLOUR DIFFERENCE.....126

FIGURE 79: TEMPERATURE AND HUMIDITY CYCLE FOR SEASONAL ACCELERATED PROTOCOL.....	133
FIGURE 80: POST EXPOSURE IMAGE OF COATING SYSTEM 1 (COUPON #20) APPLIED TO AA7075-T6 EXPOSED FOR 84 DAYS TO THE LABORATORY BASED ACCELERATED TEST PROTOCOL 2; TEMPERATURE RANGE OF 30 °C TO 0 °C, RELATIVE HUMIDITY RANGE OF 95 % TO 45 %, [NACL] RANGE OF 0.444 G L ⁻¹ TO 1.333 G L ⁻¹ AND WASH OFF VOLUME OF 25 ML PER COUPON.	137
FIGURE 81: POST EXPOSURE IMAGE OF COATING SYSTEM 1 (COUPON #62) APPLIED TO AA7075-T6 EXPOSED FOR 504 DAYS TO THE TEMPERATE INLAND FIELD EXPOSURE....	138
FIGURE 82: POST EXPOSURE IMAGE OF COATING SYSTEM 1 (COUPON #379) APPLIED TO AA7075-T6 EXPOSED FOR 84 DAYS TO THE TEMPERATE INLAND FIELD EXPOSURE.....	139
FIGURE 83: POST EXPOSURE IMAGE OF COATING SYSTEM 1 (COUPON #381) APPLIED TO AA7075-T6 EXPOSED FOR 252 DAYS TO THE TEMPERATE INLAND FIELD EXPOSURE....	139
FIGURE 84: POST EXPOSURE IMAGE OF COATING SYSTEM 1 (COUPON #60) APPLIED TO AA7075-T6 EXPOSED FOR 336 DAYS TO THE TEMPERATE INLAND FIELD EXPOSURE....	140
FIGURE 85: POST EXPOSURE IMAGE OF COATING SYSTEM 6 (COUPON #321) APPLIED TO AA2024-T3 EXPOSED FOR 84 DAYS TO THE LABORATORY BASED ACCELERATED TEST PROTOCOL 2; TEMPERATURE RANGE OF 30 °C TO 0 °C, RELATIVE HUMIDITY RANGE OF 95 % TO 45 %, [NACL] RANGE OF 0.444 G L ⁻¹ TO 1.333 G L ⁻¹ AND WASH OFF VOLUME OF 25 ML PER COUPON.	141
FIGURE 86: POST EXPOSURE IMAGE OF COATING SYSTEM 6 (COUPON #377) APPLIED TO AA2024-T3 EXPOSED FOR 504 DAYS TO THE TEMPERATE INLAND FIELD EXPOSURE....	141
FIGURE 87: POST EXPOSURE IMAGE OF COATING SYSTEM 6 (COUPON #316) APPLIED TO AA7075-T6 EXPOSED FOR 168 DAYS TO THE TEMPERATE INLAND FIELD EXPOSURE....	142
FIGURE 88: POST EXPOSURE IMAGE OF COATING SYSTEM 6 (COUPON #328) APPLIED TO AA7075-T6 EXPOSED FOR 84 DAYS TO THE BS EN ISO 9227 SALT SPRAY TEST, EXPOSURE TEMPERATURE 35 °C WITH A CONTINUOUS 5 WT.% NA CL SOLUTION DEPOSITED AT A RATE OF 1.5 ML H ⁻¹ 80 CM ⁻²	143
FIGURE 89: COATING SYSTEM 1 COUPON NUMBER 230 (LEFT) AND 379 (RIGHT) POST 84 DAYS EXPOSURE TO TEMPERATE INLAND SITE, COUPON 230 EXPOSURE AUGMENTED WITH THE ADDITION OF 1 ML OF 3 WT. % H ₂ O ₂ SOLUTION TWICE PER WEEK.....	144
FIGURE 90: COATING SYSTEM 2 COUPON NUMBER 104 (LEFT) AND 82 (RIGHT) AFTER 84 DAYS EXPOSURE TO TEMPERATE INLAND SITE, COUPON 104 EXPOSURE AUGMENTED WITH THE ADDITION OF 1 ML 3 WT. % H ₂ O ₂ SOLUTION TWICE PER WEEK.	145
FIGURE 91: COATING SYSTEM 3 COUPON NUMBER 167 (LEFT) AND 127 (RIGHT) AFTER 84 DAYS EXPOSURE TO TEMPERATE INLAND SITE, COUPON 167 EXPOSURE AUGMENTED WITH THE ADDITION OF 1 ML OF 3 WT. % H ₂ O ₂ SOLUTION TWICE PER WEEK.....	146
FIGURE 92: COATING SYSTEM 4 COUPON NUMBER 251 (LEFT) AND 190 (RIGHT) AFTER 84 DAYS EXPOSURE TO TEMPERATE INLAND SITE, COUPON 251 EXPOSURE AUGMENTED WITH THE ADDITION OF 1 ML 3 WT. % H ₂ O ₂ SOLUTION TWICE PER WEEK.	147

FIGURE 93: COATING SYSTEM 5 COUPON NUMBER 293 (LEFT) AND 253 (RIGHT) AFTER 84 DAYS EXPOSURE TO TEMPERATE INLAND SITE, COUPON 293 EXPOSURE AUGMENTED WITH THE ADDITION OF H ₂ O ₂	148
FIGURE 94: COATING SYSTEM 6 COUPON NUMBER 356 (LEFT) AND 316 (RIGHT) AFTER 84 DAYS EXPOSURE TO TEMPERATE INLAND SITE, COUPON 356 EXPOSURE AUGMENTED WITH THE ADDITION OF 1 ML 3 WT. % H ₂ O ₂ SOLUTION TWICE PER WEEK.	148
FIGURE 95: COATING SYSTEM 1, COUPON 160 (LEFT) EXPOSED TO TEMPERATE INLAND SITE AFTER 84 DAYS WITH ADDITION OF 1 ML 0.03 WT. % H ₂ O ₂ SOLUTION TWICE PER WEEK, COUPON 41 (RIGHT) EXPOSED TO TEMPERATE INLAND SITE FOR 84 DAYS WITH ADDITION OF 1 ML 3 WT. % H ₂ O ₂ SOLUTION TWICE PER WEEK.	150
FIGURE 96: COATING SYSTEM 2, COUPON 97 (LEFT) EXPOSED TO TEMPERATE INLAND SITE AFTER 84 DAYS WITH ADDITION OF 1 ML 0.03 WT. % H ₂ O ₂ SOLUTION TWICE PER WEEK, COUPON 104 (RIGHT) EXPOSED TO TEMPERATE INLAND SITE FOR 84 DAYS WITH ADDITION OF 1 ML 3 WT. % H ₂ O ₂ SOLUTION TWICE PER WEEK.	150
FIGURE 97: COATING SYSTEM 3, COUPON 181 (LEFT) EXPOSED TO TEMPERATE INLAND SITE AFTER 84 DAYS WITH ADDITION OF 1 ML 0.03 WT. % H ₂ O ₂ SOLUTION TWICE PER WEEK, COUPON 167 (RIGHT) EXPOSED TO TEMPERATE INLAND SITE FOR 84 DAYS WITH OF 1 ML 3 WT. % H ₂ O ₂ SOLUTION TWICE PER WEEK.	151
FIGURE 98: COATING SYSTEM 4, COUPON 250 (LEFT) EXPOSED TO TEMPERATE INLAND SITE AFTER 42 DAYS WITH ADDITION OF 1 ML 0.03 WT. % H ₂ O ₂ SOLUTION TWICE PER WEEK, COUPON 346 (RIGHT) EXPOSED TO TEMPERATE INLAND SITE FOR 42 DAYS WITH OF 1 ML 3 WT. % H ₂ O ₂ SOLUTION TWICE PER WEEK.	151
FIGURE 99: COATING SYSTEM 5, COUPON 286 (LEFT) EXPOSED TO TEMPERATE INLAND SITE AFTER 84 DAYS WITH ADDITION OF 1 ML 0.03 WT. % H ₂ O ₂ SOLUTION TWICE PER WEEK, COUPON 293 (RIGHT) EXPOSED TO TEMPERATE INLAND SITE FOR 84 DAYS WITH ADDITION OF 1 ML 3 WT. % H ₂ O ₂ SOLUTION TWICE PER WEEK.	152
FIGURE 100: COATING SYSTEM 6, COUPON 361 (LEFT) EXPOSED TO TEMPERATE INLAND SITE AFTER 84 DAYS WITH ADDITION OF 1 ML 0.03 WT. % H ₂ O ₂ SOLUTION TWICE PER WEEK, COUPON 356 (RIGHT) EXPOSED TO TEMPERATE INLAND SITE FOR 84 DAYS WITH ADDITION OF 1 ML 3 WT. % H ₂ O ₂ SOLUTION TWICE PER WEEK.	152
FIGURE 101: PULSED THERMOGRAPHY FRAME OF COUPON 172, COATING SYSTEM 3, AA7075-T6 EXPOSED FOR 336 DAYS AT THE TROPICAL COASTAL SITE. IMAGE EXTRACTED 100 FRAMES AFTER CAMERA FLASH.	154
FIGURE 102: PULSED THERMOGRAPHY FRAME OF COUPON 356, COATING SYSTEM 6, AA2024-T3 EXPOSED FOR 84 DAYS AT THE TEMPERATE INLAND SITE WITH ADDITION OF 1 ML 3 WT. % H ₂ O ₂ SOLUTION APPLIED TWICE PER WEEK. IMAGE EXTRACTED 100 FRAMES AFTER CAMERA FLASH.	154
FIGURE 103: PULSED THERMOGRAPHY FRAME OF COUPON 41, COATING SYSTEM 1, AA2024-T3 EXPOSED FOR 84 DAYS TO THE TEMPERATE INLAND SITE WITH ADDITION OF 1 ML 3 WT. % H ₂ O ₂ SOLUTION APPLIED TWICE PER WEEK. IMAGE EXTRACTED 100 FRAMES AFTER CAMERA FLASH.	155

FIGURE 104: COATING SYSTEM 2, COUPON 96 (LEFT) EXPOSED TO TEMPERATE INLAND SITE FOR 70 DAYS WITH ADDITION OF 1 ML 0.03 WT. % H ₂ O ₂ SOLUTION APPLIED TWICE PER WEEK, COUPON 84 (RIGHT) EXPOSED FOR 70 DAYS TO THE NOVEL ACCELERATED PROTOCOL 2 (SECTION 6.3).....	156
FIGURE 105: COATING SYSTEM 3, COUPON 159 (LEFT) EXPOSED TO TEMPERATE INLAND SITE FOR 70 DAYS WITH ADDITION OF 1 ML 0.03 WT. % H ₂ O ₂ SOLUTION APPLIED TWICE PER WEEK, COUPON 145 (RIGHT) EXPOSED FOR 70 DAYS TO THE NOVEL ACCELERATED PROTOCOL 2 (SECTION 6.3).....	156
FIGURE 106: COATING SYSTEM 4, COUPON 223 (LEFT) EXPOSED TO TEMPERATE INLAND SITE FOR 84 DAYS WITH ADDITION OF 1 ML 0.03 WT. % H ₂ O ₂ SOLUTION APPLIED TWICE PER WEEK, COUPON 335 (RIGHT) EXPOSED FOR 84 DAYS TO THE NOVEL ACCELERATED PROTOCOL 2 (SECTION 6.3).....	157
FIGURE 107: COATING SYSTEM 5, COUPON 285 (LEFT) EXPOSED TO TEMPERATE INLAND SITE FOR 70 DAYS WITH ADDITION OF 1 ML 0.03 WT. % H ₂ O ₂ SOLUTION APPLIED TWICE PER WEEK, COUPON 271 (RIGHT) EXPOSED FOR 70 DAYS TO THE NOVEL ACCELERATED PROTOCOL 2 (SECTION 6.3).....	158
FIGURE 108: COATING SYSTEM 6, COUPON 361 (LEFT) EXPOSED TO TEMPERATE INLAND SITE FOR 84 DAYS WITH ADDITION OF 1 ML 0.03 WT. % H ₂ O ₂ SOLUTION APPLIED TWICE PER WEEK, COUPON 321 (RIGHT) EXPOSED FOR 84 DAYS TO THE NOVEL ACCELERATED PROTOCOL 2 (SECTION 6.3).....	158
FIGURE 109: POST PULSED PHASE THERMOGRAPHY ANALYSIS OF EXPOSED COUPON.	175
FIGURE 110: EXAMPLE OF AN AS-COATED AKZONOBEL COATING SYSTEM 2 – COUPON # 122 (AA2024-T3 SUBSTRATE).	185
FIGURE 111: EXAMPLE OF AN AS-COATED AKZONOBEL COATING SYSTEM 3 – COUPON # 177(AA2024-T3 SUBSTRATE).	186
FIGURE 112: EXAMPLE OF AN AS-COATED PPG COATING SYSTEM 4 – COUPON # 199 (AA7075-T6 SUBSTRATE).	187
FIGURE 113: EXAMPLE OF AN AS-COATED PPG COATING SYSTEM 5 – COUPON # 273 (AA2024-T3 SUBSTRATE).	188
FIGURE 114: EXAMPLE OF AN AS-COATED PPG COATING SYSTEM 6 – COUPON # 197 (AA2024-T3 SUBSTRATE).	189
FIGURE 115: EXPOSURE RIG DRAWINGS PAGE 1.	190
FIGURE 116: EXPOSURE RIG DRAWINGS PAGE 2.	191
FIGURE 117: EXPOSURE RIG DRAWINGS PAGE 3.	192
FIGURE 118: UNDERSTANDING THE ACCELERATED ENVIRONMENT THERMOCOUPLE SAMPLE ARRANGEMENT 2.....	193
FIGURE 119: UNDERSTANDING THE ACCELERATED ENVIRONMENT THERMOCOUPLE SAMPLE ARRANGEMENT 3.....	194
FIGURE 120: UNDERSTANDING THE ACCELERATED ENVIRONMENT THERMOCOUPLE SAMPLE ARRANGEMENT 4.....	194

FIGURE 121: UNDERSTANDING THE ACCELERATED ENVIRONMENT THERMOCOUPLE

SAMPLE ARRANGEMENT 5.....195

List of Tables

TABLE 1: SUMMARY OF ASCOTT CYCLIC CORROSION TEST CHAMBER PERFORMANCE:.....	4
TABLE 2: THESIS QUESTIONS	5
TABLE 3: TYPICAL TWO-PART AIRCRAFT EPOXY PRIMER FORMULATION [20]	11
TABLE 4: THE INTERNATIONAL ALLOY DESIGNATION SYSTEM SERIES DESCRIPTIONS [56].	21
TABLE 5: TEMPER CLASSES FOR ALUMINIUM ALLOYS [56].....	22
TABLE 6: SUBDIVISION OF THE T - TEMPER [56].....	22
TABLE 7: ALLOYING CONSTITUENTS OF AA2024.....	23
TABLE 8: COMPOSITION OF AA2024-T3 AS DETERMINED BY BOAG ET AL. [59].....	24
TABLE 9: ALLOYING CONSTITUENTS OF ALUMINIUM ALLOY 7075.....	24
TABLE 10: EXPERIMENTAL COATING SYSTEM DESCRIPTIONS.....	28
TABLE 11: ZERO TIME POINT FILM THICKNESS DATA.....	32
TABLE 12: ZERO TIME POINT GLOSS MEASUREMENTS.....	40
TABLE 13: ZERO TIME POINT HARDNESS MEASUREMENTS.....	41
TABLE 14: DEFINITION OF KOPPEN MODEL 1 ST AND 2 ND LETTERS	49
TABLE 15: DEFINITION OF KOPPEN MODEL 3RD LETTER	49
TABLE 16: BS EN ISO 9223 CATEGORISATION OF ATMOSPHERIC CORROSIVITY FOR ALUMINIUM [78].....	51
TABLE 17: TYPICAL ATMOSPHERIC ENVIRONMENTS DESCRIBED IN BS ISO EN 9223 [78]	52
TABLE 18: BS EN ISO 4628 - RATING SCHEME FOR DESIGNATING THE SIZE OF DEFECT, ADAPTED FROM [89].	53
TABLE 19: BS EN SI 4628 - RATING SCHEME FOR DESIGNATING THE INTENSITY OF CHANGES, ADAPTED FROM [90].	54
TABLE 20: ACT ELEMENTAL COMPOSITION OF AA2024-T3 COUPONS.....	56
TABLE 21: ACT ELEMENTAL COMPOSITION OF AA7075-T6 COUPONS.....	56
TABLE 22: FIELD EXPOSURE SITE DEFINITIONS [78, 79]	57
TABLE 23: GRID REFERENCES FOR THE PANAMA EXPOSURE SITES	60
TABLE 24: COUPON ALLOCATIONS FOR TROPICAL FIELD EXPOSURES.....	62
TABLE 25: COUPON ALLOCATIONS FOR TEMPERATE FIELD EXPOSURES.....	63
TABLE 26: DEFINITION OF COLLECTED DATA USING PULSED THERMOGRAPHY.....	65
TABLE 27: CURRENT ACCELERATED TEST PROTOCOLS.....	81
TABLE 28: BS EN ISO 9227 EXPERIMENTAL COUPONS	97
TABLE 29: COUPON ALLOCATIONS FOR ACCELERATED TEST 1.....	117
TABLE 30: COUPON ALLOCATIONS FOR ACCELERATED TESTING PROTOCOL 2.....	132
TABLE 31: SEASONAL WASH OFF AND CORRODENT LOADING EVENTS	134
TABLE 32: COUPON ALLOCATIONS FOR ACCELERATED TESTING PROTOCOL 3 COUPON DEFINITIONS	136
TABLE 33: COUPON ALLOCATIONS FOR ACCELERATED TESTING PROTOCOL 4.....	136
TABLE 34: OVERVIEW OF FACTORIAL DESIGN FACTORS AND LEVELS	164
TABLE 35: POST EXPOSURE DATA COLLECTION.....	165

TABLE 36: FACTORIAL DESIGN DATA SET	165
TABLE 37: FACTORIAL DESIGN RESEARCH QUESTIONS	166

List of Equations

EQUATION 1: FORMATION OF CONVERSION COATING.....	10
EQUATION 2: FORMATION OF METALLO-SILOXANE INTERFACIAL BONDS.....	17
EQUATION 3: FORMATION OF SILOXANE FILM.....	17
EQUATION 4: RATE OF CORROSION.....	50
EQUATION 5: CALCULATED DIFFERENCE IN FILM THICKNESS PRE AND POST EXPOSURE....	64
EQUATION 6: REDOX CORROSION REACTION.....	86
EQUATION 7: OXIDATIVE HALF-CELL REACTION.....	86
EQUATION 8: REDUCTIVE HALF-CELL REACTION.....	86
EQUATION 9: ANODIC HALF REACTION - METAL DISSOLUTION.....	86
EQUATION 10: CATHODIC HALF REACTION - OXYGEN REDUCTION REACTION.....	86
EQUATION 11: CATHODIC HALF REACTION - HYDROGEN EVOLUTION REACTION.....	86
EQUATION 12: CALCULATION OF ACCELERATION FACTOR.....	101

Academic Thesis: Declaration of Authorship

I, Rachael Hayley Collins

declare that this thesis entitled

Improved Testing Methodologies for Evaluating the Corrosion Resistance of Paint Systems and Materials for Aging Military Aircraft

and the work presented in it are my own and has been generated by me as the result of my own original research

I confirm that:

1. This work was done wholly or mainly while in candidature for a research degree at this University;
2. Where any part of this thesis has previously been submitted for a degree or any other qualification at this University or any other institution, this has been clearly stated;
3. Where I have consulted the published work of others, this is always clearly attributed;
4. Where I have quoted from the work of others, the source is always given. With the exception of such quotations, this thesis is entirely my own work;
5. I have acknowledged all main sources of help;
6. Where the thesis is based on work done by myself jointly with others, I have made clear exactly what was done by others and what I have contributed myself;
7. None of this work has been published before submission,

Signed:

Date...25/01/2018.....

Acknowledgements

I must express my continuing gratitude to my supervisors Dr Julian Wharton and Keith Stokes for their seemingly ceaseless patience, vital conversation and trust, without which I am sure I would not be where I find myself today.

I must also thank Dr Kaliope Mylona, Dr Matt Mishon, Luisa de Wong and those at 1710 Naval Air Squadron for their invaluable contributions to my research

Finally, thank you to DSTL for the opportunity to explore this challenge

Separately, I wish to acknowledge my ever longsuffering husband and family for their endless support and belief.

Definitions and Abbreviations

AA	Aluminium alloy
Al	Aluminium
ASM	American Society for Metals
ASTM	American Society for Testing and Materials
Bis amino silane	Bis-[trimethyloxysilylpropyl]amine
BS	British Standard
CCT	Cyclic corrosion test
CPVC	Critical pigment volume concentration
Cr^{III}	Trivalent chromium
Cr^{VI}	Hexavalent chromium
d	Day
DEF STAN	Defence Standard
DFT	Dry film thickness
DoD	Department of Defence
DSTL	Defence Science and Technology Laboratory
e⁻	Electron
FFC	Filiform corrosion
GU	Gloss Unit
h	Hour
ha	Hectare
IM	Intermetallic
IR	Infrared
ISO	International Organisation for Standardization
MOD	Ministry of Defence
Ox	Oxidation species
PTFE	Polytetrafluoroethylene
PVC	Pigment volume concentration
RAF	Royal Air Force
REACH	Registration, Evaluation, Authorization and restriction of Chemicals
Red	Reduction species
RH	Relative humidity
RNAS	Royal Naval Air Service
SCE	Saturated calomel electrode
SEM	Scanning electron microscopy
SVHC	Substances of very high concern

TCP	Trivalent chrome process
ToW	Time-of-wetness
U.K.	United Kingdom
UV	Ultra-violet radiation
XPS	X-ray Photoelectron spectroscopy

Nomenclature

E_{corr}	Corrosion potential	V
r_{corr}	Corrosion rate	$\text{g m}^{-2} \text{y}^{-1}$
wt. %	Weight percent	%
A	Acceleration factor	
r_{SF}	% thermography result BS EN ISO 9227 Salt Fog	%
t_{SF}	Exposure length for BS EN ISO 9227 Salt Fog	d
r_{NE}	% thermography result Natural Exposure	%
t_{NE}	Exposure length for Natural Exposure	d

1. Introduction

In the current economic climate military aircraft are remaining in-service for far longer than originally intended [3]. This is a direct result of the increasing costs of replacement equipment and reduced military funding. Due to extended operational lifetimes, the significance of an aging aircraft's ability to resist corrosive stimuli is of increasing importance. Protective coatings are utilised to extend operational lifetimes of these aircraft by shielding them from their immediate operating environment.

Traditionally aircraft were protected with a multi-layer coating system comprising of a chromate conversion coating, a polymeric hexavalent chromium primer and a topcoat to provide barrier protection and the preferred surface finish. This system although able to protect the aircraft effectively, as a technology coatings containing hexavalent chromium are subject to a 'sunset date' after which they will not be available without specific permission. The 'sunset date' is a result of hexavalent chromium compounds being included on the list of substances of very high concern (SVHC) compiled as a part of REACH (Registration, Evaluation, Authorization and restriction of Chemicals) legislation [4]. As a result of this, novel non chromate technologies are being researched to identify a viable replacement.

Coating testing is completed using either individually or a combination of static field exposures or accelerated laboratory based protocols. Field exposure experiments give results most representative of service life. However they are time consuming, with modern coatings requiring exposures of many years to yield useful results [5]. Laboratory accelerated tests provide a rapid way of assessing a set of coatings performance against one another, and they allow for comparison between laboratories. Such tests are accepted within industry and academia as not being representative of service life.

1.1. Project aim

The project aimed to define methodologies capable of more accurately determining the in-service performance of both chromated and non-chromated paint systems. These methods were then applied to the development of new testing regimes enabling the selection of a coating for service to be made from a more informed position.

1.2. Project overview

A quantified comparison was completed between real world exposures and laboratory based accelerated testing through the implementation of a large scale time-optimised four factorial experimental design. The design encompassed nine experiments, four 18 month field exposure tests and five accelerated laboratory tests. The four field tests were defined as either tropical or temperate in climate and coastal or inland in location. The four sites were selected to scope the boundaries of in-service conditions for military aircraft, and the effect the local microclimate had on the protective lifetime of a given coating. Completed alongside the field exposure tests were the five accelerated tests. The first of the accelerated laboratory tests was the British standard (BS) neutral BS 9227 - Corrosion tests in artificial atmospheres, salt spray tests [1]. Two of the remaining four accelerated tests utilise a cyclic design that aims to replicate in an accelerated manner the weather patterns associated with the tropical and temperate locations used for exposure testing. The remaining two experiments were variants of a Scab test, where the application of aqueous oxidant was used in place of the NaCl solution specified in the standard. Time was the key factor linking all of the experiments, each protocol was split into seven equal time points, allowing for interrogation of the progression of degradation throughout exposure. The samples tested included two base materials, aircraft aluminium alloy (AA) 2024-T3 and AA7075-T6. The base materials were used in conjunction with six coating systems, creating a total of 12 coupon variants.

1.3. Environmental test chamber - background & context

To protect valuable assets coatings are often used as a final line of defence between the substrate and the potentially corrosive atmosphere. The decision of what coating should be employed is not one that should be made arbitrarily. Often the decision is informed through a combination of field exposures and accelerated laboratory tests. Field tests often provide the most realistic evaluation of a coatings performance, they however have a number of negative effects that should be considered. Firstly, it is not possible for all potential environments for service to have an accompanying field site for testing, meaning any judgements of performance prior to service would have to be

extrapolated from a site deemed as similar. Secondly, 'real world' sites are uncontrolled, meaning the experience of testing coupons could vary from month to month and year to year. Thirdly, field exposure tests of complete coating systems can often last far longer than is practicably possible.

In response to these issues a number of laboratory based environmental chambers have been designed for use alongside predefined repeatable testing protocols. The earliest and simplest is the salt spray test, which was standardised first in ASTM B117 [6]. The salt spray test is still widely used in industry and academia to audit the performance of coatings within a repeatable environment. The environment in question is a $35^{\circ}\text{C} \pm 2^{\circ}\text{C}$ with a constantly atomised 5 wt. % NaCl salt fog for a period of up to 2000 h. The fog is produced through aerosolization of the 5 wt. % NaCl solution, has a deposition rate over 80 cm^2 of 1.5 mL h^{-1} . The popularity of salt spray test is based in its simplicity and the historical bank of data that has been collected over the many years it has been used. This is especially true for Cr(VI) coatings where the response to salt fog tests were able to predict in-service lifespan of a coating as a result of this bank of knowledge.

The inability of the salt spray test to predict 'real world' performance was first identified by the automotive industry during the 1980's. In response to the weaknesses of the salt spray test, Cyclic Corrosion Testing (CCT) was created. The key difference between the two methodologies was the inclusion of sequential changes of temperature and humidity with the programming of cyclic corrosion test protocols to more closely resemble real world environments. Since the 1980s many protocols have been developed by both standardising authorities such as ASTM as well as by individual end users such as Renault and Volvo [7]. Although many protocols exist there has yet to be an internationally accepted industry standard protocol for CCT. There are however known similarities between most defined protocols, typically all of the protocols include a combination of a number of known phases in varying orders. The phases in question include:

1. Pollution application i.e. NaCl or acetic acid,
2. An air drying phase either at ambient or elevated temperatures,
3. A condensation humidity phase,
4. A controlled humidity phase.

Due to the inclusion of dynamic phases in testing CCT testing is more representative of service conditions. However, CCT protocols typically have a narrow range defined conditions, meaning the effect of different potential changes to the service environment, be that seasonal or geographical do not feature. Therefore, CCT as it stands is still only able to provide a comparative study between coatings for the specific testing environment defined. The opportunity for standardised dynamic environments within CCT testing means that its potential is still not fully explored for the prediction of service life of aircraft coatings. Exploring this potential was one of the aims of the research of this thesis.

The similarity between CCT and salt spray testing and the continued popularity of both methods, CCT chambers are often design to also meet the requirement of salt spray standards such as BS EN ISO 9227 [1]. The University of Southampton has a CCT chamber which was used for some of the laboratory exposures completed during the course of this research. The specification of the chamber are detailed in Table 1.

Table 1: Summary of Ascott cyclic corrosion test chamber performance:

Mode	Variables	Range
Wetting mode	Temperature	Adjustable from ambient to +60 °C
	Humidity	Fixed at 95% - 100% RH
Salt spray mode	Temperature	Adjustable from ambient to +50 °C
	Salt spray fall-out rates	Adjustable from 0.5 to 2.5 mL per 80 cm ² per hour
Drying mode	Temperature	Adjustable from ambient to +50 °C
	Humidity	Uncontrolled

1.4. Thesis structure

The tasking defined by DSTL in simplistic terms was to create a quantitative accelerated corrosion testing protocol capable of predicting in-service lifetime of any aircraft coating technology. As a result of the expansive nature of the question, the research took on a broad set of topics that did not easily lend themselves to what could be considered a traditional thesis structure. Rather each chapter aims to gather information on specific topics lead by a set of questions, which once put together build a cohesive discussion of the overarching question.

To enable a systematic approach to the fulfilment of the research aims, this document is structured to answer a number of questions. Each of the questions works together to build a single narrative which hopes to identify if it is possible to create an accelerated corrosion protocol which can provide quantitative evidence regarding the service life of CrVI alternative coating systems. The questions are divided into specific chapters. The questions can be found in Table 2 alongside the section where by the specific question is addressed.

Table 2: Thesis questions

Question	Section
Why does a new accelerated corrosion test need to be identified?	1
What are the materials that need to be explored	2.2
Do different environments result in varied performance for coatings?	3
What is the current state of the art for accelerated corrosion testing used in academia and industry?	4.1.1
Does the most widely used testing protocol provide any results representative of a field exposure?	4
Is it possible to implement a procedure into a standard corrosion test chamber that is able to replicate coating performance in a tropical coastal field exposure?	5
Is it possible to implement a procedure into a cyclic corrosion chamber that is able to replicate a coatings performance in a temperate field exposure	6.3
Does the inclusion of a wash-off step create a more representative accelerated testing protocol?	6.3
Should UV be considered in isolation?	6.4
Rather than replicating environments inside a test chamber, is it better to accelerate the degradation experienced in a field exposure?	6.4
Could the application of an aqueous oxidant accelerate coating degradation?	6.4
Can further information be extracted through the use of a factorial design?	7

2. Protecting aircraft

2.1. Introduction

High strength AA2024-T3 and AA7075-T6 are both age hardened aluminium alloys which are often used in aircraft manufacture. AA2024-T3 is used for its high strength to weight ratio and its ability to withstand fatigue cracking. Typically within aging aircraft AA2024-T3 is used for lower wing skins and fuselage components [8]. Its strength to weight ratio of approximately $173 \text{ MPa g}^{-1} \text{ cm}^{-3}$ is because of the alloy's composition and temper [9]. In addition to the alloying elements being of benefits to age hardened aluminium alloys, they are also the basis of their accompanying weaknesses. A result of the main alloying constituents in AA2024-T3 being copper and magnesium, the alloy is particularly susceptible to localised corrosion, specifically pitting and exfoliation corrosion. AA7075-T6 is used in either forged or plate form typically for stringers, bulkheads and fuselage skins [10]. The main alloying elements of AA7075-T6 are zinc, magnesium and copper; it is known to have extremely high tensile strengths and a strength to weight ratio of approximately $203.55 \text{ MPa g}^{-1} \text{ cm}^{-3}$. These properties mean AA7074-T3 lends itself well to aircraft manufacture, however, it is prone to stress corrosion cracking [11].

Military aircraft see an extremely wide variety of operating environments varying from desert to Antarctic conditions. This variability in operational scenarios can accelerate degradation of protective polymeric coatings (thin films/paints) and can severely decrease the operating lifespan and continued availability of these aircraft. Current testing used in industry and academia for assessing the performance of coating systems implement standard tests which are often far removed from the actual environments that are experienced during operations. Consequently, although coatings may pass these standard tests they can prematurely fail in-service, leading to corrosion and wear of components and their subsequent failure [12]. This has been observed, for

example, on chromate-free systems, where performance under accelerated test conditions such as salt spray (ASTM B117) have shown equivalent resistance to corrosion as that exhibited by the well proven chromate systems [6]. However, when deployed the performance of these non-chromated systems has proven to be disappointing when directly compared to the standard chromate-containing paints [13]. The poor performance may be as a result of environments often encountered by the coatings in-service bearing little resemblance to the original screening technique used to select the service options. Laboratory tests also fall short when considering operational damage, and coating application error, both of which are known points of weakness when considering the lifetime of coating systems in-service.

In general, salt spray and other accelerated environmental tests are known to provide a ranking of materials in terms of their resistance to a particular environment. For example, the salt spray test provides a comparison between chromate levels present and barrier properties of chromated systems but is not necessarily valid to compare different non-chromated systems. The validity of accelerated tests when evaluating materials and coatings for use in conditions which are not directly related is, therefore, of doubtful benefit. Industrially it is, however, necessary to implement screening tests to enable down-selection and ranking of the best performing systems. Meaning an accelerated test that is able to provide information regarding expectations of in-service performance would be beneficial to DSTL and to other industry partners.

2.2. Aircraft coating technology

To successfully explore test method development for aerospace coatings it was important to understand the currently accepted technology, i.e. hexavalent chromate coatings as well as the state of the art replacement options being developed in academia and industry. Once the breath of coating opportunities was understood it was then possible to direct the discussion with the contacted suppliers to ensure the range of coatings tested covered as many of the possibilities as possible. With a greater breadth of coatings tested it was hoped that the analysis and exposure procedures would be biased towards a particular coating technology.

Current military aircraft coating technologies employ a three layer coating system to protect the aluminium substrate. Figure 1 shows a schematic of the current coating system. The first layer is formed using a chromate conversion coating; it is the final layer of corrosion defence and performs as an adhesion enhancer for the second layer. The second layer is typically an epoxy primer. The primer coating is the main defence against corrosion. The active pigment included in the coating is characteristically strontium chromate (SrCrO_4). The coating also contains non-active pigments which are used to alter final finish and performance of the dry film. The protection afforded by the chromate primer is only effective if it is above the 'minimum inhibition concentration', chromate containing primers currently used by the military have a leaching rate above this minimum to

ensure optimal performance. The final layer is a polyurethane topcoat, which normally contains no active pigment, rather it is used to seal the underlying layers from the environment [14]. The conversion coating is a thin layer between 10-60 nm, the preferred primer coating thickness is 25 μm but in reality this can range from 5 to 200 μm due to variations that occur during coating application. The polyurethane topcoat is typically applied to a thickness of 125 - 175 μm [15-17].

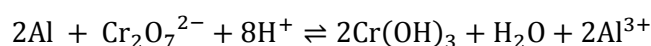


Figure 1: Military aerospace coating schematic.

2.3. Conversion coatings

The current conversion coating technology applied to military aircraft performs two roles; it acts to increase adhesion between the metal substrate and further polymeric coatings and increases corrosion resistance of the substrate. Conversion coatings are applied by immersing the substrate in an acid chromate and fluoride solution [18]. The protective film is believed to be formed through disruption of the aluminium passive film by the fluoride ions prior to the reduction of chromate ions by the exposed aluminium, Equation 1 shows a possible reaction, however, the speciation and hydration states of the products are variable [19].

Equation 1: Formation of conversion coating



The 10-60 nm film is normally comprised of $\text{Cr}(\text{OH})_2$ and $\text{Al}(\text{OH})_2$ [20]. Other species have been identified using Raman spectroscopy such as CrO_4^{2-} , $\text{Cr}_2\text{O}_7^{2-}$ and possibly a polymeric oxide, there was a lack of distinctive bands for Cr(III) species, however, this could be a result of weaker Raman scattering than the Cr(VI) species [19]. The mechanism proposed for the corrosion protection afforded by the chromate conversion coating is attributed to dynamic repair, where upon Cr(VI) ions are released into solution from within the conversion coating. They then migrate to the reactive (damaged) site and are reduced to Cr(III) oxide, the resulting film is a cathodic passivator [19].

When heterogeneous aluminium alloys are treated with conversion coatings the film formed is equally heterogeneous. Different classes of intermetallic particles act to retard or enhance the chromate reduction. It has been found that cathodic intermetallic particles act as nucleation points for the conversion coating, until such a time that they are covered with an oxide film, whereby the reduction will spread across the remaining surface. It should be noted that copper-rich zones have been identified as being able to retard the growth of the oxide film resulting in heterogeneities across the oxide film [21].

2.4. Polymeric coatings

Once an aircraft's aluminium component has been protected with the application of a conversion coating, further protection is achieved through the application of polymeric coatings. The first, a chromate containing epoxy primer provides the bulk of the corrosion protection. The chromate ion is typically introduced to the paint system in the form of an active pigment either strontium chromate or zinc chromate ($\text{SrCrO}_4 / \text{H}_2\text{CrO}_4\text{Zn}$) [20]. Table 3 shows a typical formulation of an aircraft chromate containing two-part epoxy primer.

Table 3: Typical two-part aircraft epoxy primer formulation [20]

Part A	wt. %	Part B	wt. %
Strontium chromate and other pigments	37.5	Polyamide resin	31.6
Epoxy resin	22.9	Glycol ether	15.0
Additives	0.2	Toluene / Xylene	54.4
Methyl isobutyl ketone	21.0		
Xylene	7.6		
Toluene	10.8		

The mechanism by which the epoxy primer is able to protect the underlying substrate from corrosive attack relies on the solubility of hexavalent chromium and its uniform distribution throughout the polymer film. The uniform distribution is afforded by the inclusion of the active material as a pigment and the dispersion of pigment during coating manufacture and preparation. The solubility is an inherent property of the chromate ions. The mechanism begins with the solubilisation of the chromate ion, it then diffuses to the area of damage, whereby it undergoes a reduction reaction from Cr(VI) to Cr(III) on the bare aluminium alloy surface affording a passive film through deposition of reduction products [20].

The final coating layer applied to protect aircraft from corrosion is a polyurethane topcoat. This is used to provide a barrier between the underlying substrate and the environment. Its purpose is to restrict the transport of water, oxygen and electrolyte to the active surface [22]. The topcoat also provides the final coating finish for the aircraft for military aircraft this is often a matt finish, the matt finish (low gloss) can be produced one of two ways; the first is an increase in pigment volume concentration (PVC) resulting a high pigment to binder ratio, the second is through the addition of large pigmented polymer beads, which allows for a reduction in gloss without increasing the PVC [23]. This is beneficial as when a coating is designed with a high PVC void formation results. The voids reduced the ability of the coating to control corrosion of the substrate, due to its increased porosity and a greater influx of electrolyte [22].

2.4.1. Chromate inhibition mechanism

Hexavalent chromium is a passivation inhibitor; it protects the underlying material by undergoing reactions on active sites such as inter-metallic particles, and grain boundaries. The protection can be attributed to the Cr(VI) inhibitor ion being reduced to form its oxide, the resulting oxide film acts as a barrier to the electrolyte (chloride ions) [20]. McCreery et al. used UV-Vis spectroscopy to assist in the development of a model describing the release mechanism of Cr(VI) within chromate conversion coatings and epoxy primers. The concentration was scrutinized by exploiting a linear relationship between absorption at 340 nm and concentration of Cr(VI) irrespective of solution pH. The mechanism for release of Cr(VI) is different depending on whether a conversion coating is considered or an epoxy primer. In the case of the primer Cr(VI) release is not controlled by Langmuir type relationship with the solution, instead Cr(VI) is released until the interpenetrating solution phase within the coating reaches saturation. The solution can be If used Cr(VI) ions are replaced from the remaining SrCrO_4 to maintain saturation until all of the SrCrO_4 is consumed. In the case of the conversion coating release of Cr(VI) from the 3D porous matrix is driven by a Langmuir type equilibrium between the film and the bulk solution interface [24].

In 1995 Kendig et al. described the combination of properties which ensure the success of hexavalent chromium as a corrosion inhibitor. Chromates are noted to be good oxidisers, they have the correct level of solubility in water, any reduction products are passive in nature, they are low cost and are easy to apply [25]. It is the combination of all of these properties which makes chromate corrosion inhibition such a difficult system to replace, there are however, many other systems being developed which will attempt to supersede this technology. The range of approaches currently being explored provides a challenge for any new selection test, as not all methods aim to provide aim like for like replacement of Cr(VI), instead completely new approaches are being explored. Differing mechanisms of protection will produce weakness to a range environmental stimuli, all of which cannot be overlooked in a replacement test.

2.4.2. Future alternatives to chromates

The following discussion gives a brief overview of some of the potential non-chromate containing alternatives currently in development for aerospace applications. It is important to note that currently it appears that it is unlikely that a non-toxic inorganic pigment could be identified that replicates the performance of hexavalent chromium in its protection of aluminium alloys from corrosion [13]. The combination of solubility of the Cr(VI) species and insolubility of the Cr(III) species alongside the innocuous pH of the saturated solution with respect to coating degradation, means the task of a like for like replacement appears to be insurmountable [13]. . The discussion remains broad as the specific technologies utilised in the work are unknown due to the legalities of the collaborations with the coating manufacturers. However, a broad range of coatings was still required as a part of the collaboration. The lead to testing of polyurethane, epoxy and sol gel based

coatings as well as other technologies such as adhesion promoters. Unlike the magnesium and chromate technologies that were specifically requested for testing the pigment and active pigments of other coatings tested were undefined by the manufacturer. Potentially any of those coating could have contained any of the technologies defined below either in combination or isolation.

Instead of replacing chromium completely one technique which has seen some success in laboratory testing is to avoid using the carcinogenic hexavalent form of chromium and instead focus on only using the less toxic trivalent form. The trivalent chromium process (TCP) has been developed as a commercial alternative to hexavalent chromium conversion coatings. The technique employs immersion of the substrate in a bath of hexafluorozirconate (K_2ZrF_6), trivalent chrome oxides (Cr_2O_3 or $Cr(OH)_3$), chromium sulfate ($Cr_2(SO_4)_3$) and a fluoborate salt (BF_4^-). The resultant coating is biphasic in nature with a hydrated zirconia ($ZrO_2 \cdot 2H_2O$) exterior with an interior of potassium fluoroaluminate (K_xAlF_{3+x}). The hydrated zirconia layer is typically 50 – 100 nm in thickness and is co-precipitated with Cr(III) oxide [26]. TCP has reduced adhesion when compared to hexavalent chromium conversion coatings and any corrosion protection offered to the underlying substrate is a result of increased breakdown potential and suppression of the oxygen reduction reaction [27]. TCP has been identified as more environmentally friendly as it does not contain and cannot be oxidised to form the carcinogenic hexavalent species. However, Swain et al. has previously identified the transient oxidation of trivalent chromium to hexavalent chromium within a TCP coating using Raman spectroscopy. The mechanism of formation is postulated to be a reduction of O_2 to H_2O_2 at cathodic copper sites, followed by oxidation of the trivalent chromium to hexavalent chromium by the H_2O_2 . However, although the study was able to identify hexavalent chromium as well as a relationship between oxygen concentration and its formation, it was unable to directly prove the existence of H_2O_2 as the oxidising species. The newly formed hexavalent chromium was identified to be transient in nature, meaning it was able to diffuse away from its site of production, resulting in the possibility of active healing similar to chromate conversion coatings [26]. As an environmentally friendly alternative to chromate conversion coatings, the identification of transient oxidised hexavalent chromium in TCP coatings places some doubt on such claims. Nevertheless, the concentrations of hexavalent chromium identified were not discussed within the bounds of the study; therefore the potential risks cannot be properly assessed.

Potentially any of the following alternatives to Cr(VI) may have been used by manufacturers for use in the experimental campaign. Sinko reviewed a range of inorganic salts which possessed the possibility to act as replacement for strontium chromate salts in anti-corrosive coatings for aircraft, the review stated that inorganic chemistry could not provide a nontoxic, cost effective, equally effective inhibitor pigment for the replacement of strontium chromate [13]. Although forewarned by Sinko many researchers have been attempting to identify a direct replacement for chromates. Molybdates,

vandates and permangates are all oxoanions in the form of $\text{MeO}_4^{(n-8)}$, all are analogous to the currently successful chromates and all are being explored as replacement pigments [28-31].

As a cathodic inhibitor with a complex mechanism dependent on concentration, it was identified that permanganates potential is greater as a pre-treatment than as a direct replacement for hexavalent chromium [29]. A more promising inhibitor tested was sodium molybdate. Sodium molybdates inhibitive performance was tested in solution by Lopez-Garity and Frankel. The work concluded that molybdate is an oxygen dependant inhibitor; when added to a non-aerated solution corrosion resistance decreased. The effective inhibition concentration is a minimum of 50 mM and a relatively high concentration ratio of molybdate to NaCl is required for successful corrosion inhibition [28]. Although productively probing the mechanism associated with inhibition and the performance possibilities with AA2024-T3, Frankel and Lopez-Garity have made no comparison between corrosion inhibitive performances of sodium molybdate with strontium chromate and so it is difficult to make any successful conclusions regarding sodium molybdate as a possible replacement for strontium chromate.

One mechanistic approach applied to the replacement of strontium chromate inhibitors is to identify alternative oxygen reduction reaction inhibitors, able to work in a similar fashion to hexavalent chromium [32]. Vandate ions are not only an oxoanion they are also an oxygen reduction inhibitor. Tetrahedral vandates have been identified as inhibiting the cathodic oxygen reduction reaction, by constraining the dissolution of magnesium from copper containing intermetallic particles of AA2024. This prevents the strengthening of cathodic nature of these particles as would typically be the case in the corrosion mechanism of AA2024-T3. It should be noted that vandates in their octahedral form have been found to increase corrosion of AA2024-T3, these possible changes in coordination of vandates are a function of concentration and pH [30, 31]. Again, work is still on-going and comparisons to Cr(VI) have yet to be completed by the investigators.

Another inhibitor of which much testing has been devoted but which is not an oxianion is cerium nitrate. Cerium is of interest for two reasons, the first is its ability to retard the oxygen reduction reactions, whilst the second is its change in solubility associated with its transition from Ce(III) to Ce(IV). The effectiveness of aqueous cerium nitrate in comparison to hexavalent chromium was explored by Thompson and Curioni et al. at the University of Manchester [33, 34]. In solution the team at Manchester identified using electrochemical noise analysis that cerium nitrate performs equally to hexavalent chromium with regard to corrosion protection [34]. This is in direct opposition to the highly cited work by Aramaki, which stated that not only was cerium nitrate less effective than hexavalent chromium but it was also unable to produce a self-healing oxide film such as hexavalent chromium [35]. The resultant ambiguity surrounding the performance of

cerium nitrate in solution has not prevented researchers from testing this inhibitor as a part of a coating.

Mansfeld et al. have explored the use of cerium salts as sealing agents for non-chromium containing anodizing processes. Cerium acetate, cerium sulphate and cerium nitrate were all tested on AA2024-T6 and AA7075-T6. Cerium nitrate performed differently on the two substrates, when used to seal the anodized surface of AA7075-T6 two time constants were identified using EIS, meaning the pores were successfully blocked with cerium hydroxide. When tested on AA2024-T3 a single time constant was seen with a very low pore resistance being identified, this illustrates that the pores were not sealed. The performance of these sealed anodized substrates when exposed to a salt spray test reflected this, with AA7075-T6 passing whilst AA2024-T3 failed [36].

In 2005 Van Ooij et al. discussed the possibility of using cerium nitrate as a replacement for the chromate containing conversion coatings. This was achieved by adding cerium nitrate as an inhibiting pigment to a silane based sol gel. The resulting film was able to restrict oxygen reduction, as was the free cerium nitrate in solution. It was also able to impart a certain amount of self-healing as the cerium was leached out of the sol-gel when the surrounding environment became alkaline in nature [37]. The performance was not compared a hexavalent chromium containing pre-treatment, and so the future success of cerium nitrate as a hexavalent chromium replacement cannot be further examined.

2.4.3. Magnesium additives

An alternate methodology used to overcome the difficulties of replacing hexavalent chromium was developed at Dakota State University and utilizes magnesium to cathodically protect aluminium in the same way zinc is used to protect steel [38-46]. Two distinct coatings have since been developed by Beirwagen and co-workers. The first is a two pack epoxy-polyamide utilising 30 – 40 μm magnesium particles at a 46% PVC, and the second utilizes a silane modified interpenetrating polymer network matrix and 50% PVC of magnesium particles [46]. Utilising electrochemical testing, it was identified that these coatings offer a two stage protection mechanism. Initially the magnesium particles cathodically polarise the underlying aluminium substrate, whilst precipitated products then act to impart secondary protection by partially blocking pores in the polymer matrix reducing ingress of electrolyte [44]. Interestingly it was also identified that the coatings are able to repassivate previously active pits in the substrate, as well as prevent growth of new pits [39]. With respect to exposure testing, when undergoing prohesion testing the epoxy-polyamide coating was able to withstand up to 1000 h with no signs of damages, whilst the modified silane has better barrier properties and so is able to withstand up to 3000 h without any visible signs of corrosion [46]. So great has been the success of this research that the technology

has been licenced by AkzoNobel and after further development is now being tested on in service aircraft [38].

2.4.4. Sol-gel coatings

In response to the difficulties associated with active corrosion inhibitor replacement in polymeric coatings, alternative coating technologies are concurrently being established to fulfil the needs of the aerospace market. Sol-gel coatings are one type of technology prolifically being explored, the Air Force Research Laboratory of the United States have been developing this technology for many years [47-50]. Sol-gels result in the formation of an oxide network directly on the substrate surface. Hydrolysis and condensation reactions occurring between metal or metalloid alkoxide precursors in a low molecular weight organic solvent result in the growth of polymeric oxide particles. The film is formed by the agglomeration of these particles which is driven by the evaporation of the solvent and condensation products [42]. Typical application methods include dip or spin coating; however, spraying and electrodeposition are both being explored as alternate application methods [42].

Sol-gels can be organic, inorganic or organic-inorganic hybrids, with hybrid systems being favoured for corrosion resistant coatings. Purely inorganic coatings are unfavourable as they are brittle, require high processing temperatures (400 °C to 800 °C) and are unable to form thick films; film of thicknesses greater than 1 µm are prone to cracking. For the favoured hybrid systems, there are numerous combinations to be exploited from three distinct categories. The first is category is comprised of mixtures of organic and inorganic constituents, with no chemical bonding between the two phases. The second category uses hydrolysed inorganic precursors to react with existing functional groups found on the selected polymeric species. The third category is made up of alkoxy silanes ($\text{Si}(\text{OR})_{4-n}$) the R group being a secondary polymerizable functional group [42].

Alkoxy silanes can be mono-silanes or bis-silanes, bis-silanes have been found to produce the most effect corrosion resistant coatings. Figure 2 illustrates the bonding motif for bis-silanes with an aluminium substrate. The bis-silane is able to form a high density interfacial layer as well as concurrently form a fully cross-linked silane matrix. This simultaneous bonding is not possible with mono silanes.

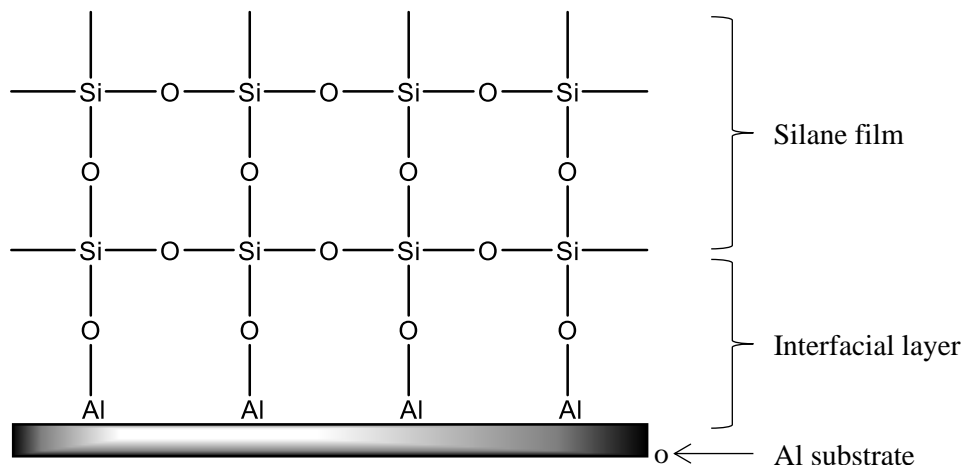
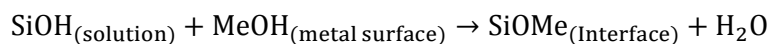


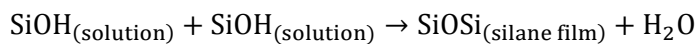
Figure 2: Bis-silane bonding schematic with an aluminium substrate.

Both the siloxane and the co-valent metallo-siloxane bonds are formed by condensation reactions between hydroxides. Equation 2 shows the reaction to form the interfacial bonds, whilst Equation 3 shows the self-condensation reaction required to form a siloxane film.

Equation 2: Formation of metallo-siloxane interfacial bonds



Equation 3: Formation of siloxane film



One hybrid system that has been extensively studied is bis-[3-(triethoxysilyl)propyl]tetrasulfide, which can be seen Figure 3 and shall referred to as bis-sulfur-silane. Van Ooij et al. have completed many studies exploring the potential bis-sulphur-silane as a protective coating for multiple substrates [37, 51-54].

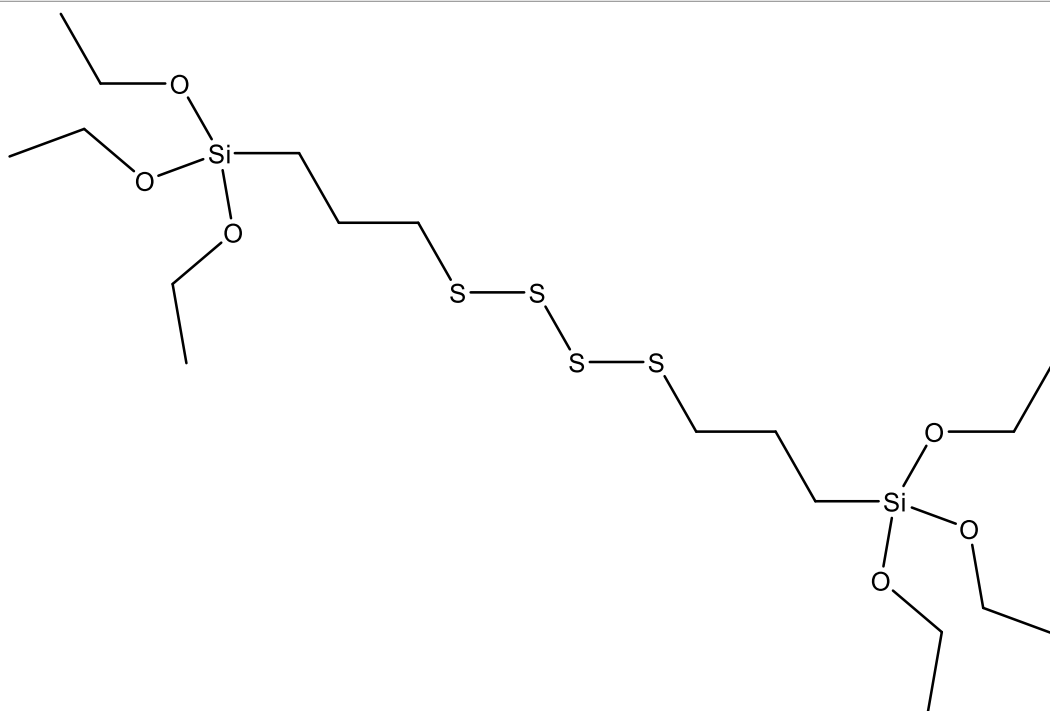


Figure 3: Chemical structure and formula of bis-[3-(triethoxysilyl)propyl]tetrasulfide



Van Ooij et al. investigated the corrosion protection mechanism afforded to AA2024-T3 by bis-sulfur-silane using polarisation experiments and EIS. EIS identified three electrochemically distinct layers each characterised by a specific feature apparent in the spectra. The spectrum includes two time constants, and a diffusion tail. The high frequency time constant was attributed to the outer most silane layer, the mid-frequency time constant is the interfacial layer whilst the tail is the Al surface. The polarisation experiments identified a decrease in cathodic current for AA2024-T3 when coated with bis-sulfur-silane. This is evidence that the coating provides only a physical barrier to corrosion. The cathodic current decreases because the newly formed covalent metallo-siloxane bonds block the cathodic sites preventing reaction [52].

Although viable for use on AA2024-T3, bis-sulfur silane has underperformed when tested on hot dipped galvanised steel [53]. The poor performance is attributed to the hydrophobicity of the coating, with a surface energy of 30-40 mJ m⁻², bis-sulfur silane is proposed to be unable to wet the zinc oxide top layer found on hot dip galvanised steel [53, 55]. The poor performance on hot dipped galvanised steel brings into question the possible performance of bis-sulfur silane on AA7075-T6, with a zinc alloy percentage of 5-6 %. This researcher is unable to identify any reference to the testing of bis-sulfur silane on AA7075-T6, a material historically used alongside AA2024-T3 in aircraft manufacture [10]. However, the proficiency of bis-sulfur silane as a barrier inhibitor if applied to AA7075-T6 is now called into question, a result of the discreet inclusions of zinc within the alloy microstructure.

In order to improve the performance of bis-sulfur silane, Van Ooij et al. blended it in a 3:1 ratio with a more hydrophilic silane, bis-[trimethoxysilylpropyl]amine (bis-amino silane) [53, 55]. When used alone bis-amino silane has poor corrosion performance on both AA2024-T3 and hot dipped galvanised steel. Bis-amino silanes increased hydrophilicity causes the attraction of chloride ions and water, which result in hydrolysis of the co-valent metallo-siloxane bonds and delamination of the coating. However, when blended with bis-sulfur silane the mixtures resulting corrosion performance exceeds that of bis-sulfur silane [53]. It was postulated that the increased performance of the mixed system is a result of the a more condensed film forming due to bis-amino silane having a catalytic effect on the condensation of bis-sulfur silane leading to the formation of more silanols [55]. A point of contention between the 2004 and 2006 investigations of the blended coatings by Van Ooij at al. regards the barrier properties of the mixed material. In 2004 it is stated that the inclusion of hydrophilic bis-amino silane has no tangible effect on the uptake of chloride ions and water [53]. Whilst in 2006 the same coating was tested using neutron reflectivity and it was identified as having an increase in hydrophilicity equivalent to the volume of bis-sulfur silane replaced by bis-amino silane [55]. Being aware of this inconsistency it is difficult to conclude if the addition of bis-amino silane has any direct effect on the performance of bis-sulfur silane in operational conditions. Van Ooij et al. have been unable to conclusively identify the additions effect, and any conclusions which have been postulated have been made using full immersion testing only, meaning they cannot be directly correlated to in service performance. To be more conclusive, testing must be performed which more closely replicated service conditions and uses addition substrates used in aircraft such as AA7075-T6.

The corrosion resistive performance of silane films can be further altered by the inclusion inhibiting additives. Van Ooij et al. have investigated the corrosion inhibition properties of a number of inorganic and organic additives. Inhibitors including cerium nitrate, benzotriazole, tolyltriazole and nano-silicate particles have all been tested. When silicate particles (\approx approx. 1 μm) are added to a bis-sulfur silane they are thought to suppress the cathodic reaction by passivating the aluminium substrate. The beneficial properties are only available when the volume of silicate particles is kept below the critical pigment volume concentration (CPVC) of the coating. If too much silicate is added the film becomes porous and the possible benefits are lost [54].

Low volatile organic compound, water based silanes are attractive as they are more environmentally friendly than sol-gels formed in low molecular weight organic solvents. However, the resulting water-based films are unable to match the performance of the organic solvent formed films. The performance deficit is attributed to less crosslinking within the films and a more hydrophilic surface. The greater hydrophilicity causes two distinct problems. The first is ingress of electrolyte is increased, whilst the second is increased hydrolysis of covalent metallo-siloxane bonds, resulting in reduction of adhesion [37]. Cerium nitrate, benzotriazole and tolyltriazole

were all tested to identify the possibility of improving the performance of water-based silane coating [37]. Both the organic inhibitors tolytriazole and benzotriazole were able to improve corrosion resistance through blocking of cathodic sites, leading to a reduction in cathodic current. Inorganic cerium nitrate was able to reduce cathodic current by forming a semi-permeable hydroxide blocking pores, it was also able to be leached out of the coating and provide some self-healing similarly to what is expected from chromium-based systems [37].

2.4.5. The Al-alloy substrate

Two substrates are being tested throughout this study as a result of aging military aircraft structures being typically built from AA2024-T3 or AA7075-T6, both of which are considered materials of interest. The two materials are often used when testing aerospace coatings. This is because the different alloy compositions potentially may interact with the coatings of interest differently. If this is the case it is important that this is known prior to service as a disparity could result in unidentified weaknesses causing concern for the safety of aircraft users. The following discussion provides context to the substrate names relative to the international alloy designation system alongside a discussion of expected microstructures of the two materials.

The names are derived using the international alloy designations system, which the most widely accepted naming scheme for wrought alloys [56]. Each alloy is given a four-digit number, where the first digit indicates the major alloying elements. Table 4 details each of the eight series' within the system and their main alloying elements alongside some specific properties. When describing an aluminium alloy, after the series number and a hyphen the temper of the material is described. The first digit describes the class of treatment, and the second a specific combination of treatments from within the class. Table 5 outlines the temper classes and Table 6 the subdivision of the 'T' class. Only the specific tempers of the 'T' class are listed as both of the materials of interest are members of the T-classification.

Table 4: The International Alloy Designation System series descriptions [56]

Series	Description
1000 series	Minimum 99% aluminium content, can be work hardened
2000 series	Main alloy element is copper, can be precipitation hardened with final strengths comparable to steel. Historically this series was the most common aerospace aluminium. It has been superseded by the 7000 series because of its tendency to undergo stress corrosion cracking.
3000 series	Main alloy element is manganese, can be work hardened
4000 series	Main alloy element is silicon
5000 series	Main alloy element is magnesium
6000 series	Main alloy elements are magnesium and silicon. Are known to be easy to machine and can be precipitation hardened but not the extent of the 2000 or 7000 series.
7000 series	Main alloy element is zinc. The 7000 series can be precipitation hardened to the highest strengths of any aluminium alloy
8000 series	Main alloy element is lithium.

Table 5: Temper classes for aluminium alloys [56]

Temper Designation	Description
F	Fabricated, no control of thermal conditions, no additional working to achieve explicit properties
O	Annealed, heat treated to reduced strength of final temper
H	Strain hardened, to increase strength
W	Solution treated, materials spontaneously age after solution heat treatment
T	Thermal treated, must produce other stable tempers than F, O or H

Table 6: Subdivision of the T - temper [56]

Temper	Sequential description
T1	Cooled after shaping process and naturally aged
T2	Cooled after shaping process, cold worked and naturally aged
T3	Solution heat treated, cold worked and naturally aged
T4	Solution heat treated and naturally aged
T5	Cooled after shaping process and artificially aged
T6	Solution heat treated and artificially aged
T7	Solution heat treated and over-aged
T8	Solution heat treated, cold worked and artificially aged
T9	Solution heat treated, artificially aged and cold worked
T10	Cooled after shaping process, cold worked and artificially aged

One material of interest, AA2024-T3 is a member of the 2000 series which means its main alloying element is copper. As the temper is defined by T3 it is also now known that AA2024-T3 has been solution heat treated, cold worked and then naturally aged. The resultant microstructure is important as the distribution of heterogeneities that drive the corrosion forms observed; this information shall be used when discussing different corrosion mechanisms identified post exposure [57].

2.4.6. AA2024-T3 microstructure

The 2000 series alloys are age hardening. The main alloying constituent of this series is copper and the resultant inhomogeneous microstructure of AA2024-T3 is particularly prone to localised attack. This attack is a result of galvanic coupling between copper-rich zones and copper depleted zones [57]. The average elemental composition of AA2024-T3 can be seen in Table 7 [58]. Figure 4 is composed of three images of the microstructure of AA2024-T3, after application of Keller's reagent. The apparent change in microstructure between the three images is purely a result of the quenching method after solution heat treatment. These changes aid in the illustration of the

variations possible for the microstructure of AA2024-T3 only through processing differences, the discrepancy increases once again if differences in composition are considered.

Table 7: Alloying constituents of AA2024

Alloying Element	Al	Cu	Mg	Mn	Fe	Si	Zn	Ti	Cr
wt.%	90.7-94.7	3.80-4.90	1.20-1.80	0.30-0.90	max 0.50	max 0.50	max 0.25	max 0.15	max 0.10

The views regarding the microstructure of AA2024-T3 vary between researchers. However, there is agreement regarding the fundamental structural masses of a granular α -matrix and a secondary phase of intermetallic particles. It is the composition and frequency of the intermetallic particles of which there is some uncertainty between the various reported studies. The α -phase is a solid solution of mainly aluminium which has been identified as having up to 2 atomic percent (at.%) copper in solid solution and 1 (at.%) magnesium [58].

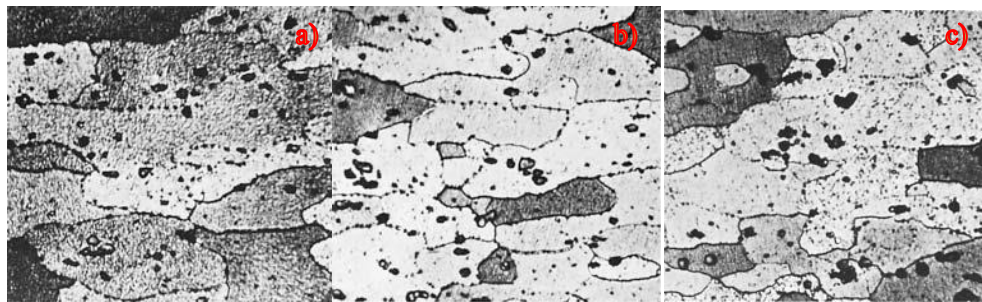


Figure 4: AA2024-T3 microstructures, Keller's reagent, 500X magnification, (a) Solution heat treated (495°C) and cooled in still air, (b) Solution heat treated (495°C) and cooled in air blast, (c) Solution heat treated (495°C) and quenched in boiling water [56].

The simplest description of the secondary phases of AA2024-T3 was proposed by Buchheit [57]. Buchheit et al. used SEM and EDS to identify the composition and frequency of the secondary phase particles of a diameter greater than 0.2 μm [57]. Only 2.7% of the total surface area was identified as being that of intermetallic particles, of this 2.7% 60% were identified as being S-phase (Al_2CuMg) [57]. The remaining 40% were attributed to $\text{Al}_6(\text{Cu,Fe,Mn})$ (12.3%), $\text{Al}_7\text{Cu}_2\text{Fe}$ (5.2%), $(\text{Al,Cu})_6\text{Mn}$ (4.3%) and the final 16.9% were defined as indeterminate [57]. The average particle size identified was 4 μm with a single standard deviation range of 1-7 μm [57]. A weakness of this study is a result of the experimental limitation of interaction volume which is associated with the X-ray emission volume, resulting in a level of uncertainty associated with the data collected describing the composition of particles with a diameter smaller than 0.7 μm [57]. The result of mass effect is an overestimation of the levels of aluminium present in particles, as some of the surrounding metal matrix is included in the EDS measurement of the particle.

One of the greatest areas for contention associated with the Buchheit paper is the lack of evidence for θ -phase (Al_2Cu). Boag et al. identified nine distinct phases which can be seen in Table 8, and which identifies 0.298 % of the total surface as θ -phase [59].

Table 8: Composition of AA2024-T3 as determined by Boag et al. [59]

Phase label	Measured stoichiometry	Area(% of total)
Matrix	$\text{Al}_{96}\text{Cu}_2\text{Mg}_5$	Residual
(Al, Cu)₂(Mn, Fe)₄Si	$\text{Al}_{77}\text{Cu}_5\text{Mn}_5\text{Fe}_{10}\text{Si}_4$	0.742
Al₂CuMg	$\text{Al}_{61}\text{Cu}_{20}\text{Mg}_{15}$	0.381
Al₇Cu₃Fe	$\text{Al}_{70}\text{Cu}_{18}\text{MnFe}_6$	0.089
(Al, Cu)₉₃(Fe, Mn)₅(Mg, Si)₂	$\text{Al}_{90}\text{Cu}_3\text{MgMn}_2\text{Fe}_3\text{Si}$	0.252
Al₁₀(Cu, Mg)	$\text{Al}_{90}\text{Cu}_7\text{Mg}_2$	0.983
Al₃(Cu, Fe, Mn)	$\text{Al}_{73}\text{Cu}_{11}\text{Mn}_4\text{Fe}_{10}\text{Si}$	0.062
Periphery	$\text{Al}_{81}\text{Cu}_{12}\text{Mg}_4\text{MnFe}$	0.018
Al₂Cu	$\text{Al}_{70}\text{Cu}_{27}$	0.298

Within standard texts such as Aluminium: properties and physical metallurgy by Hatch, the final microstructure for wrought AA2024-T3 is said to consist of four types of intermetallic particle; $\text{Al}_{12}\text{CuMg}$, $(\text{Mg, Fe})_3\text{Si}$, Al_{12} , $\text{Al}_7\text{Cu}_2\text{Fe}$, $\text{Al}_{20}\text{Mn}_3\text{Cu}_2$ [60]. The much debated θ - and S-particles are not discussed, Hatch states that both should dissolve back into the bulk during heat treatment [60]. However, based on more recent evidence such as the work by Boag and Buchheit the validity of these assumptions is still open to debate [57, 59].

2.4.7. AA7075-T6 microstructure

The second material used structurally in aging military aircraft is the 7000 series alloy AA7075-T6. The 7000 series alloys are age hardening, and have zinc as their key alloying element. The 7000 series are typically tertiary systems with Al-Zn and Mg.

Table 9: Alloying constituents of aluminium alloy 7075

Alloying Element	Al	Zn	Mg	Cu	Cr	Fe	Si	Mn	Ti
wt.%	87.10-	5.10-	2.10-	1.20-	0.18-	max	max	max	max
	91.40	6.10	2.90	2.00	0.28	0.50	0.40	0.30	0.20

Such tertiary systems are prone to stress corrosion cracking which is alleviated through the addition of copper, typically between 1.2 and 2.0 wt.%. The inclusion of copper also increases the materials response to age hardening resulting in an increased tensile strength [61]. AA7075-T6 is one of the 7000 series which include copper as one of its main alloying elements. The average composition of AA7075-T6 can be seen in Table 9.



Figure 5: Microstructure of AA7075-T6, scale bar is a length of 100 μm [5].

The additional alloying elements are used for various reasons including strengthening, weldability and in the cases of manganese controlling grain size [62]. AA7075-T6 has a microstructure containing α -phase matrix and three distinct types of secondary intermetallic particle [63]. The metal matrix has an approximate composition of Al, Zn (3 - 4 wt.%), Mg (2 - 3 wt.%) and Cu (0.5 - 1.0 wt.%), the exact composition varies depending on the specific formulation and temper [64]. The three distinct type of intermetallic identified are constituent particles (2 - 5 μm), dispersoids (0.5 - 2 μm) and hardening particles (extremely fine) [65]. The secondary phase particles are found along the grain boundaries, which are bound on either side by a precipitate free zone for between 30 nm and 70 nm [66]. Figure 5 shows a three-dimensional rendering of the microstructure of AA7075-T3, the darker points are the intermetallic particles aligning along the grain boundaries in the rolled direction. Dispersoids have been identified as having a typical compositions of $\text{Al}_{20}\text{Cu}_2\text{Mn}_3$ and $\text{Al}_{18}\text{Mg}_3\text{Cr}_2$, whilst hardening precipitates are generally of the

composition related to η -phase (Zn_2Mg) [67]. The composition of the constituent particles is slightly more complex, with differing opinions observable between researchers. Gao et al. report that there are two compositions associated with constituent particles, $Al_{23}Fe_4Cu$ and SiO_2 [68]. This is, however, dismissed by other researchers who consider that constituent particles of AA7075-T6 can be any of the following; Al_7Cu_2Fe , Al_2Zn , Al_3Zr or Mg_2Si [64, 69]. Further work has simplified the groupings of intermetallic particles with Ryl et al. having concluded that there are only two types in constituent intermetallic particle affecting localised corrosion of AA7075. The first is Mg_2Si and the second is $AlFe(Cu,Mn,Cr)$ which are anodic and cathodic respectively when compared to the matrix [70].

To develop an accelerated weathering test it must be possible to benchmark changes in coating performance due to exposure. Often test method development trials are completed using simplified coating systems, unrelated to those used in-service. It is possible that by simplifying the coating system, a mechanism of failure found in-service is made unavailable resulting in an environmental variable of importance to that mechanism may be overlooked in the design of the test. A test method developed using a single coating system, simplified or otherwise may also limit the effectiveness of the test designed when applied to wider coating options.

The difficulty lies in the complexity of the question, specifically for aerospace applications; is it possible to predict the failure of a polymeric heterogeneous multilayer systems applied to protect a metallurgical diverse substrate from a multitude of complex and constantly varying environments?

Any new test designed must be able to provide performance information for all possible coatings, not one specific technology. It is important that the methodological approach is from the environmental variables towards the coating response. With the goal to accelerate the in-service exposure environment, any coating can be tested without bias to a specific mechanism. The coatings being tested must be as close to the in-service systems as possible, using all components of the service systems including any preparative steps and the application processes.

2.5. Experimental

With the understanding of typically utilised aerospace substrates and the potential range of coating technologies a number of coatings were procured from two well know coating manufacturers; AkzoNobel and PPG. Coatings were then applied by the qualified engineers at 1710 Naval Air Squadron. The intension was that by testing commercially developed coatings as they would have been applied in service it would provide the best starting point for replicating the service life of coatings.

Three coating systems were been supplied by AkzoNobel, with the remaining three being supplied by PPG. The term ‘coating system’ was used as each of the six supplied factors included up to three distinct layers; a pre-treatment, a primer and a topcoat (Figure 6). The AkzoNobel coating systems all used the same topcoat, a white low gloss polyurethane topcoat. Similarly, the PPG systems also utilised a common top coat, a black low gloss military grade high solid polyurethane coating. The primers provided were unique to each of the coating systems tested, there was some variability within the individual manufacturers coating systems regarding application of pre-treatments. Table 10 illustrates the individual coating systems utilised. A two-thirds – two-thirds overlapped spraying design of primer and topcoat was selected for three reasons. The first was to allow a deeper interrogation of the performance of the individual coating layers, the second was to ensure meaningful data was collected in the relatively short 18 month field exposures, and the third reason was to look at different in-service scenarios such as miss sprays, which are not dealt with within the typical test panel design.

The AkzoNobel pre-treatment was an adhesion promoter, the method of adhesion promotion was however unknown. The pre-treatments supplied by PPG included a polyurethane pre-treatment traded as Desoprime 7530 pre-treatment and a sol-gel sold under the trade name of Desogel.

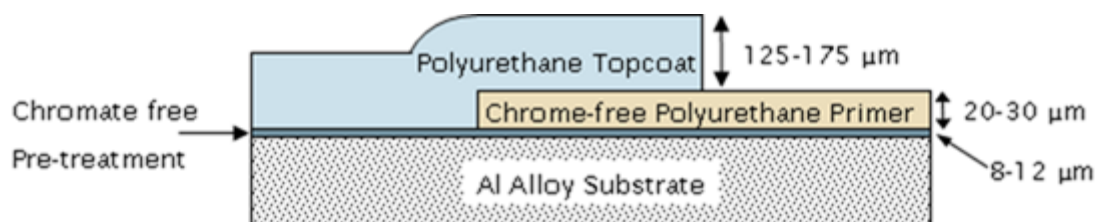


Figure 6: Sectioned view of coated coupon system.

Table 10: Experimental coating system descriptions

	AkzoNobel 1	AkzoNobel 2	AkzoNobel 3	PPG 4	PPG 5	PPG 6
Pre-treatment	Metaflex SP 1050	No pre-treatment	Metaflex SP 1050	Desoprime 7530 pre-treatment	Desogel	no pre-treatment
Primer	Aerodur 2100 Mg rich primer	Aerodur HS 2118 Primer	XP 304	Desoprime (PU)	CA7502	PR205
Top Coat	Aerodur 5000	Aerodur 5000	Aerodur 5000	Desothane top coat	Desothane top coat	Desothane top coat

Figure 7 shows a typical coupon panel prepared using AkzoNobel coating system 1, coating system 1 included a magnesium component such as those described in Section 2.4.3 to sacrificially protect the underlying aluminium. Specifically, the imaged panel, panel 49 was used as a zero exposure panel for the tropical coastal experiment, its substrate was AA2024-T3. Examples of AkzoNobel system 2, which utilised the Aerodur HS 2118 Primer (a high solid epoxy primer) and AkzoNobel system 3 can be seen in the Appendix section 11.1. Examples of the PPG systems 4, 5 and 6 can be found in in the Appendix section 11.2.

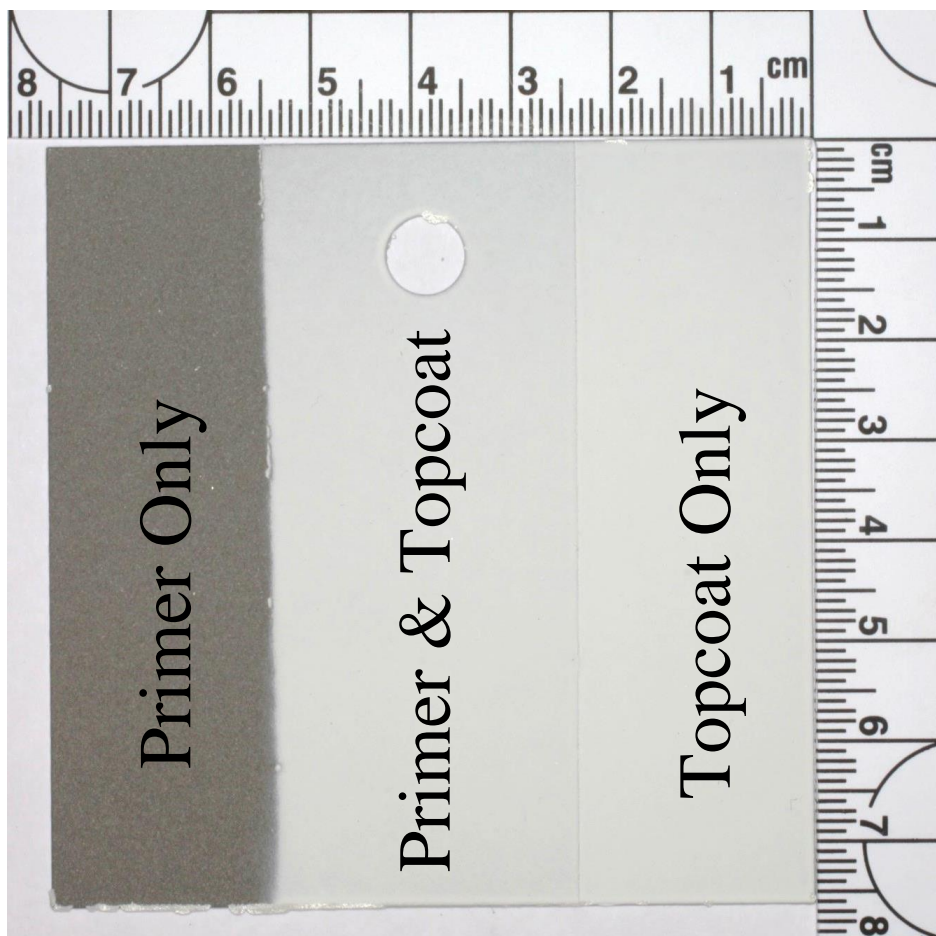


Figure 7: Example of as-coated AkzoNobel coating system 1 - Panel number 49 (AA2024-T3 substrate).

2.5.1. Coating application

In total of 396 coated coupons were prepared in the week commencing 2nd February 2015 by naval engineers from 1710 Naval Air Squadron. Coupons were initially abraded using scotch bright pads before being wiped with butan-2-one, coatings were applied following the guidance from the manufactures. Coupons were sprayed in batches defined by the coating system, to achieve this coupons were attached to 1 m × 1 m square medium density fibre board using double sided tape, which allowed for easy removal.



Figure 8: Coating application in booth at 1710 Naval Air Squadron.

Coupons were identified using a unique coupon number ensuring the entire process was traceable. After 72 h curing the coating thickness was measured using a Positector 6000 film thickness gauge; further analysis of these measurements can be found in Section 2.6.1. The coupons were left to cure undisturbed for seven days, once cured the front of the coupons were covered with plain paper and masking tape before being fastened face down onto the painting boards. The backs of the coupons were cleaned with acetone before being painted with one coat of PPG sigma cover 2; a two pack epoxy coating. The backing coating was applied to afford electronic neutrality from the steel weathering rigs and to prevent corrosion beginning on the reverse of coupons resulting in artificial damage to the front. Ideally the backs of the coupons would have been painted with the same coatings applied to the front; however, time constraints with the sprayers at 1710 prevented this from being possible. The suitability of this coating was tested by subjecting 2 coupons to a 60°C 5% NaCl salt fog for 7 days. As can be seen in Figure 9 no visible damage could be identified after 7 days exposure to this extreme environment. Once dry vinyl identification barcodes were applied to the reverse of the coupons and each coupon was photographed and organised into its relevant experiment and time point. Photographs were taken with a Canon EDS 550D camera using a 50 mm Canon compact macro lens and a Canon MR-14EX macro ring lite.

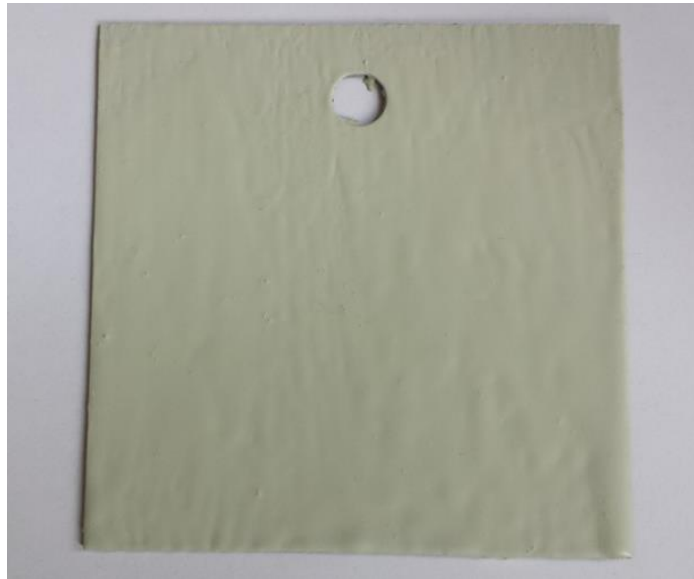


Figure 9: Backing coating after 7 day's testing at 60°C with constant 5 wt.% salt fog.

2.6. Zero time point analysis

After the application a number of analysis methods were used to provide information about the coatings and variations in the application process. Film thickness, gloss and coating hardness measurements provide information about the coatings prior to exposure. The hardness and gloss measurements provide information regarding the formulation of the coatings, whilst film thickness is also a feature of the formulation, it can provide additional information regarding the success of application. The data collected at the 0 time point will be used as points of comparison along with other methods of analysis to evaluate the exposure tests.

2.6.1. Film thickness measurements

When considering the overall quality of an individual coating application, two measures of success were considered. Firstly, success was considered by comparing the dry film thicknesses (DFT) achieved by a qualified technician to the ideal film thicknesses defined by the coating manufacturer. Secondly, the success of the spraying was defined by consistency achieved by the technician when comparing coupons of the same coating type. Since, for the current study all specimens of each coating system were sprayed as one larger coupon board, it was also possible to identify trends in the technician's spraying behaviour and/or performance.

Dry film thickness measurements were made in triplicate on all coupons and for each of the defined coupon regions. The measurements were made using a Positector 6000 film thickness gauge, and were recorded utilising both the coupon identification but also board location. Table 11 shows the mean dry film thicknesses for each of the primers and top coats sprayed. It must be noted that the film thickness is slightly over estimated in some cases through the application of a pretreatment to

the surface. Due to the pace of the spraying operation at 1710 Naval Air Squadron it was not possible to measure the film thickness of any of the pretreatments applied. Both systems 1 and 3 had metaflex adhesion promoter wiped across the surface and washed off with clean water prior to application of their respective primers. The remaining AkzoNobel system 2 underwent no pretreatment regime. System 4 from PPG had a pretreatment sprayed on the surface and was allowed to dry, unfortunately the film thickness remains unknown. Coupons from system 5 were pretreated with the application of a sol-gel. The coupons were sprayed with the solution and the excess was removed with compressed air, leaving behind a transparent blue film. System 6 does not utilise a pretreatment of any kind.

Table 11: Zero time point film thickness data

Coating Type	Literature DFT / μm	Mean DFT / μm	Standard deviation of measured film thickness
Coating 1 Primer	25 -35	64	9.7
Coating 2 Primer	15- 30	39	7.1
Coating 3 Primer	Unknown – experimental	38	5.5
Coating 4 Primer	20-30	48	12.5
Coating 5 Primer	20-30	48	11.3
Coating 6 Primer	15-25	32	6.1
Coating 1 Topcoat	45-75	34	5.7
Coating 2 Topcoat	45-75	41	7.8
Coating 3 Topcoat	45-75	56	9.6
Coating 4 Topcoat	35-45	45	6.7
Coating 5 Topcoat	35-45	40	12.8
Coating 6 Topcoat	35-45	29	4.4

From Table 11 it is apparent that the DFT quoted by the manufacturers for the primers supplied is difficult to achieve. All measured values are thicker than the preferred film thicknesses quoted by the manufacturer. This was unexpected as all application instructions from the manufacturer were followed throughout spraying. It is interesting to note that the film thicknesses measured for the top coats vary dramatically within the individual coating. AkzoNobel systems 1, 2 and 3 are all the same top coat sprayed from the same batch at the same time. However, the values for the film thickness vary by a factor of 1.6. A large range was also measured for the PPG systems 4, 5 and 6.

2.6.2. Success of coating application

As previously stated, the success of application was not only judged on the average achieved DFT, but also on the homogeneity of the application. To understand the effect of human on the final DFT the collected data was viewed pictorially. Figure 10 illustrates the DFT data collected for coating system 1. It should be noted that each coupon had nine measurements made, three for each of the applied films sections. Individual coupons are highlighted by the white overlaid grid system present on each of the pictorial figures. The repetitive vertical patterning visible is a result of the two thirds - two thirds coating application design selected for this work. Although quantitatively useful, it is this qualitative representation that yields the most information about the application itself. Figure 10 shows that the technician applied more primer specifically to the top three rows of panels. This could be a result of increased speed as the spraying continued or adding an additional layer on the top section due to a perceived need for additional coverage. It may be thought that this inconsistency means that the spraying for coating system 1 was not as successful as hoped. Whereas in reality the opposite is true, the variation caused by the operator during spraying could be of importance with regard to the degradation of the coating. Whilst the often used draw down bar method would have produced a perfect film of known thickness, it is clear from this panel alone that that would not have been representative of the coatings when actually used in-service.

Coating system 2 as seen in Figure 11 has high DFT towards the left and right edges of the boards. This could be a result of slower movements by the sprayer or due to a change in angle of the spray gun relative to the board face. The spray booth also had localised overhead lighting, which could have resulted in a shadow being cast on the lower edge of the board. When this is combined with the beige colour of the primer it could have resulted in a perceived coverage difference, which was then over compensated for. Again, these differences are not a sign of unsuccessful work, but instead result in coupons more representative of the real world than those which have the coating applied using a draw down bar.

The top section of the coating system 3 board (Figure 12) has a significantly thicker primer coat than the bottom section of the board. With the linear nature of the difference it would appear that the thicker film is a result of an additional pass made over the top three rows of coupons. Once again the primer is beige in colour, making the coverage difficult to judge, which in combination with the localised lighting could have played a role in this choice to add another layer of coating to the primer layer.

There are some localised thicker primer film sections that can be identified on coating board 4 (Figure 13). This could have been a result of the minute changes made by the sprayer during application, either slowing down or changing angle could account for this pattern. Due to the stochastic nature of the changes it is less likely to be a result of the application of additional coats

of paint, however, localised spots can have additional coating applied, if the sprayer perceives a discrepancy in coverage.

The top half of board for coating system 5 (Figure 14) shows that the panels have slightly thicker primer films than the lower half of the board. This implies either the sprayer moved slightly slower over the top few passes, or an additional light coat was added to the top half of the board.

The left side and central band of the board for coating system 6 (Figure 15) have thicker films than the rest of the board. This could be due to the angle of the spray gun changing as the sprayer approached the left side of the board. As well as a slower coat of primer in the central section. The central band is not linear enough in shape to be a result of a secondary application of the paint. Instead it is more likely to be a result of changes made by the sprayer.

To summarise, there are numerous differences that can be seen in the resulting film thicknesses created by spraying coatings that would not be achieved by application with a draw down bar. The importance of these variations will be explored further to see if they produce any identifiable trends in the outputs of the later exposure studies

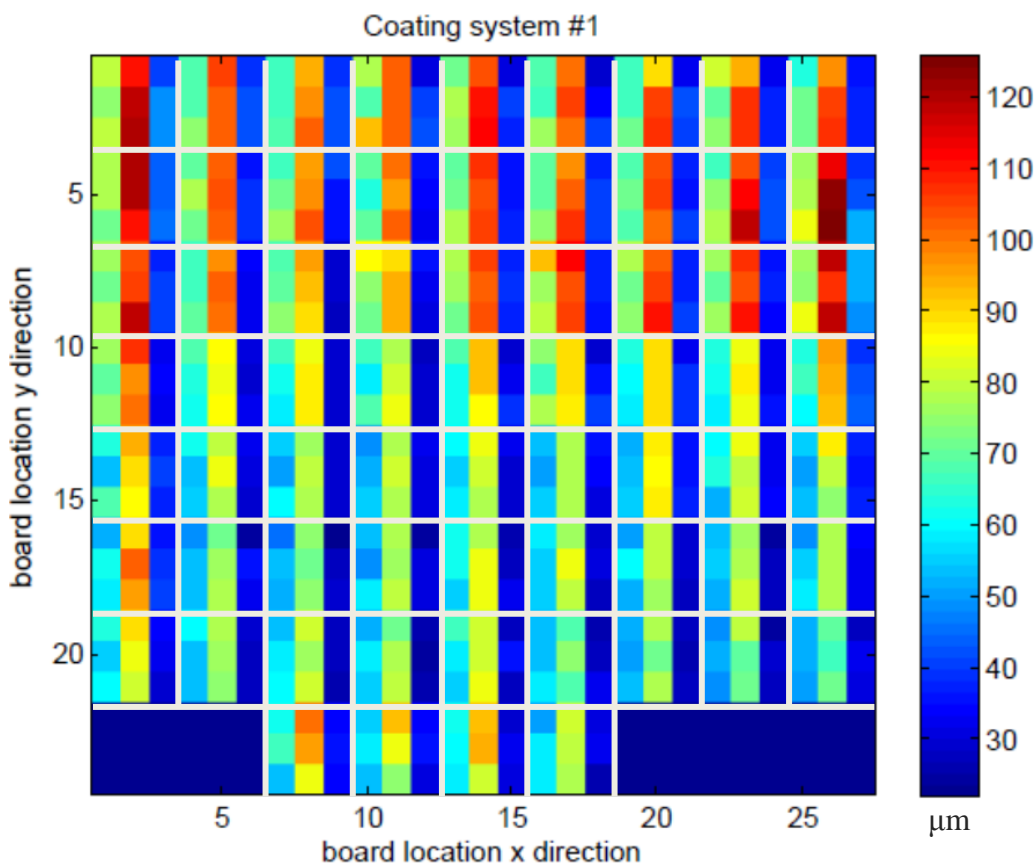


Figure 10: Film thickness measurements of AkzoNobel coating system 1. The measurements illustrate trends in film thickness associated with spraying location on Board 1.

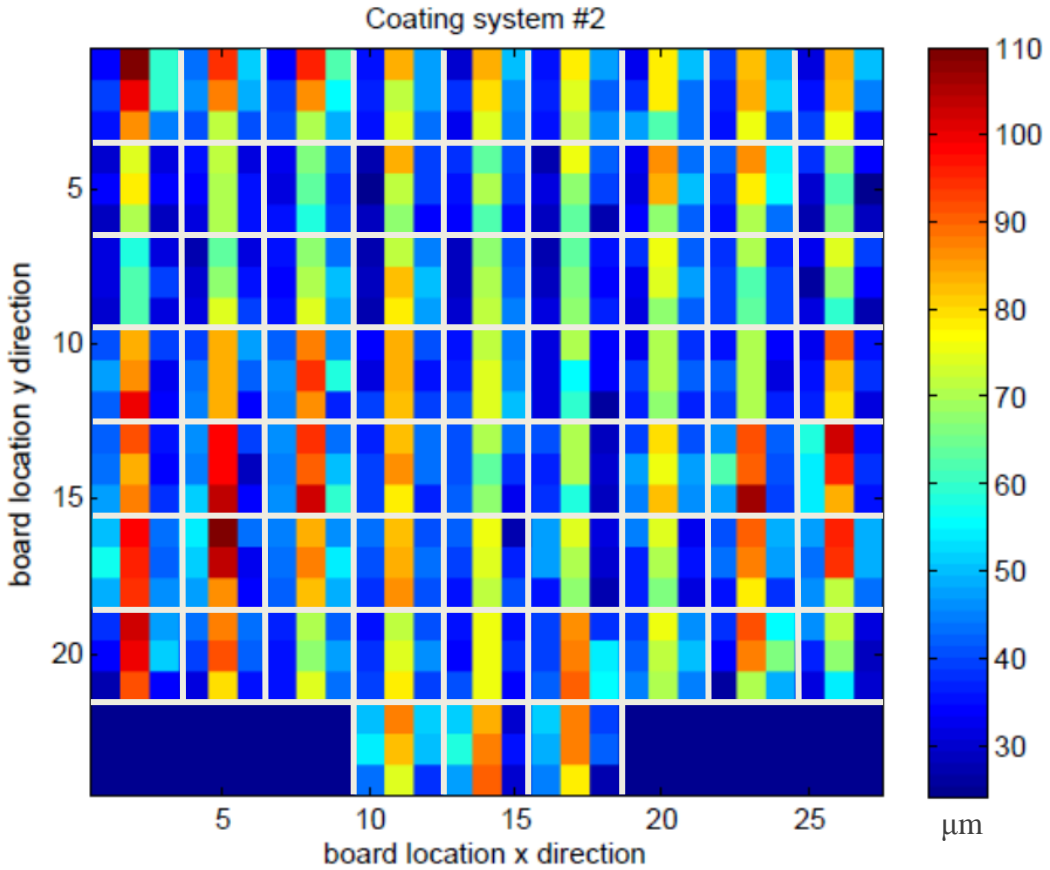


Figure 11: Film thickness measurements of AkzoNobel coating system 2. The measurements illustrate trends in film thickness associated with spraying location on Board 2.

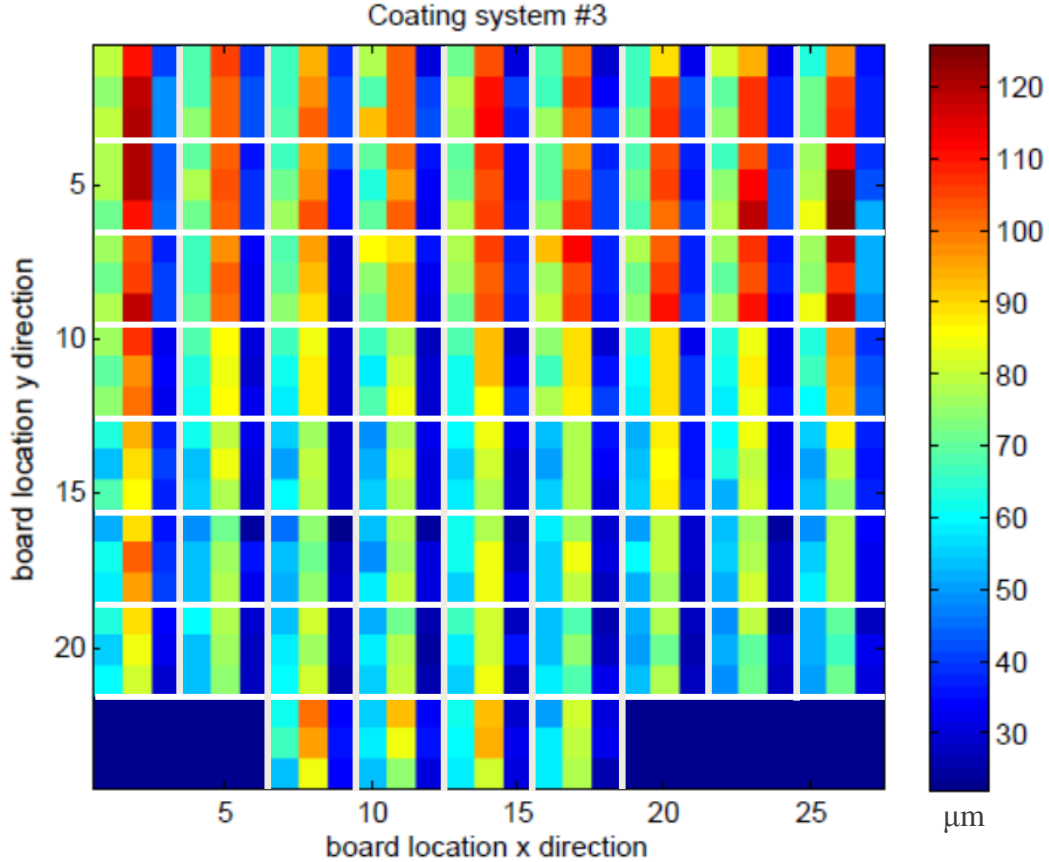


Figure 12: Film thickness measurements of AkzoNobel coating system 3. The measurements illustrate trends in film thickness associated with spraying location on Board 3.

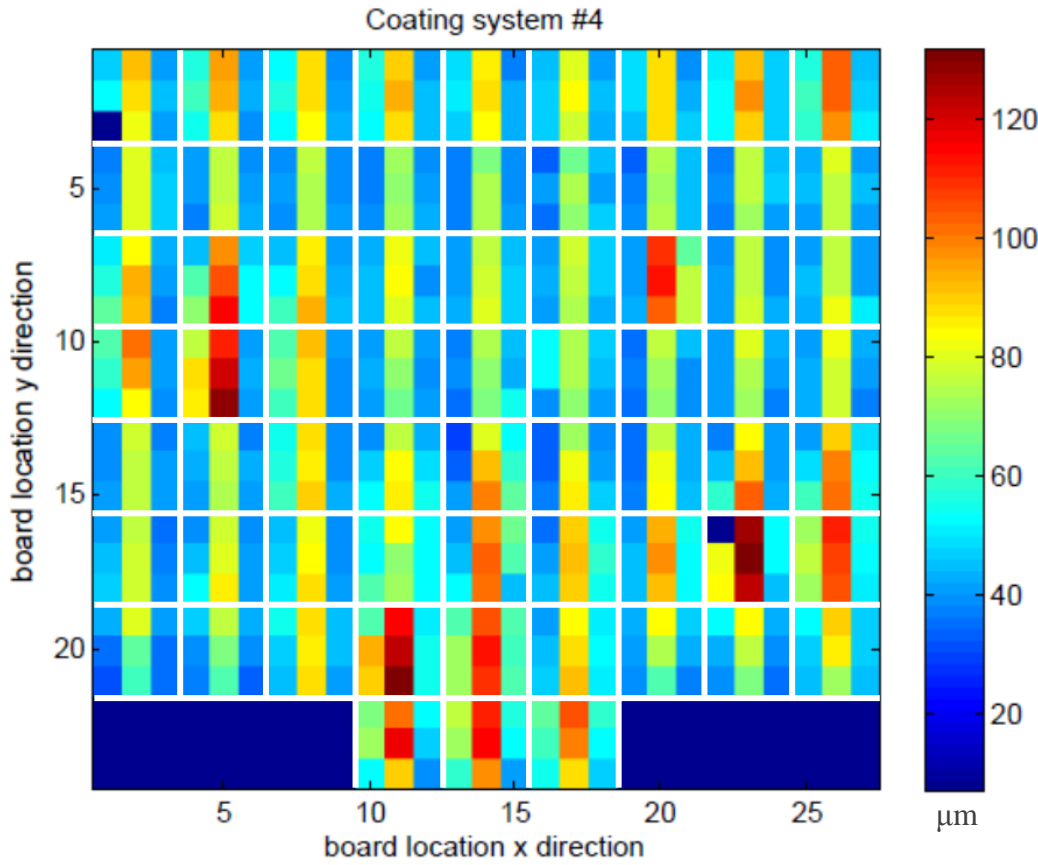


Figure 13: Film thickness measurements of AkzoNobel coating system4. The measurements illustrate trends in film thickness associated with spraying location on Board 4.

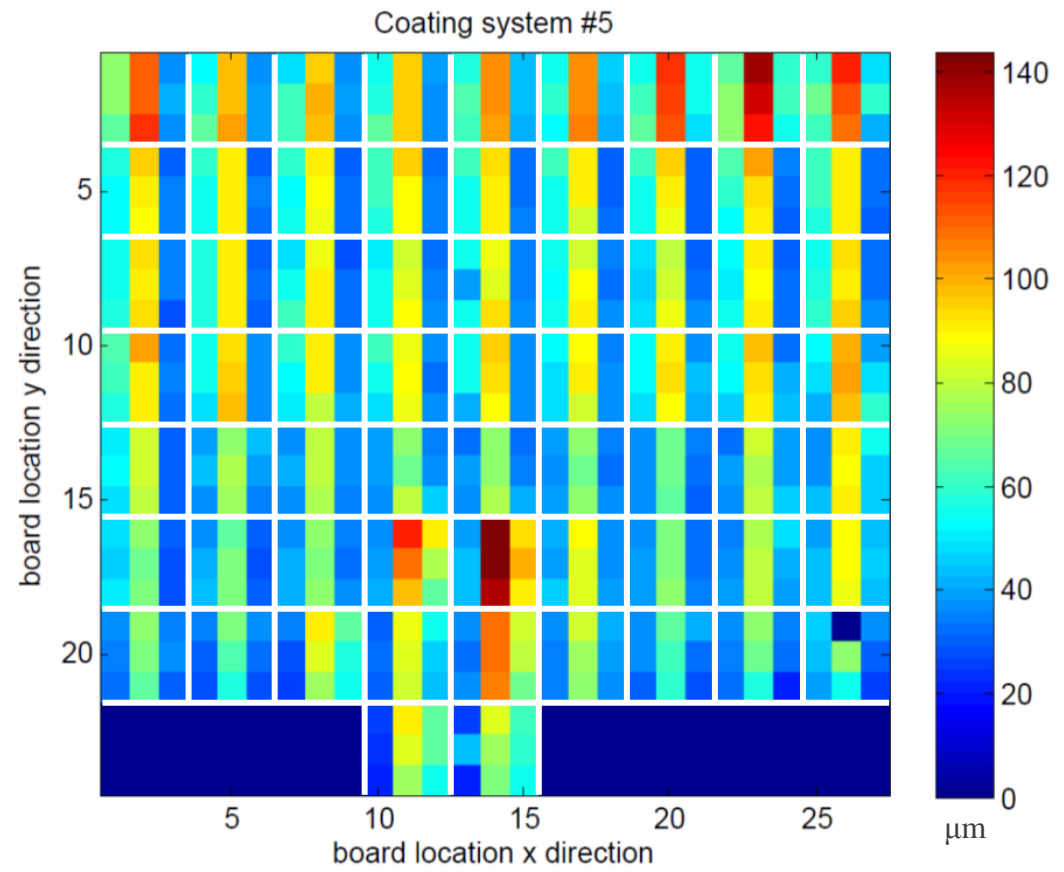


Figure 14: Film thickness measurements of AkzoNobel coating system 5. The measurements illustrate trends in film thickness associated with spraying location on Board 5.

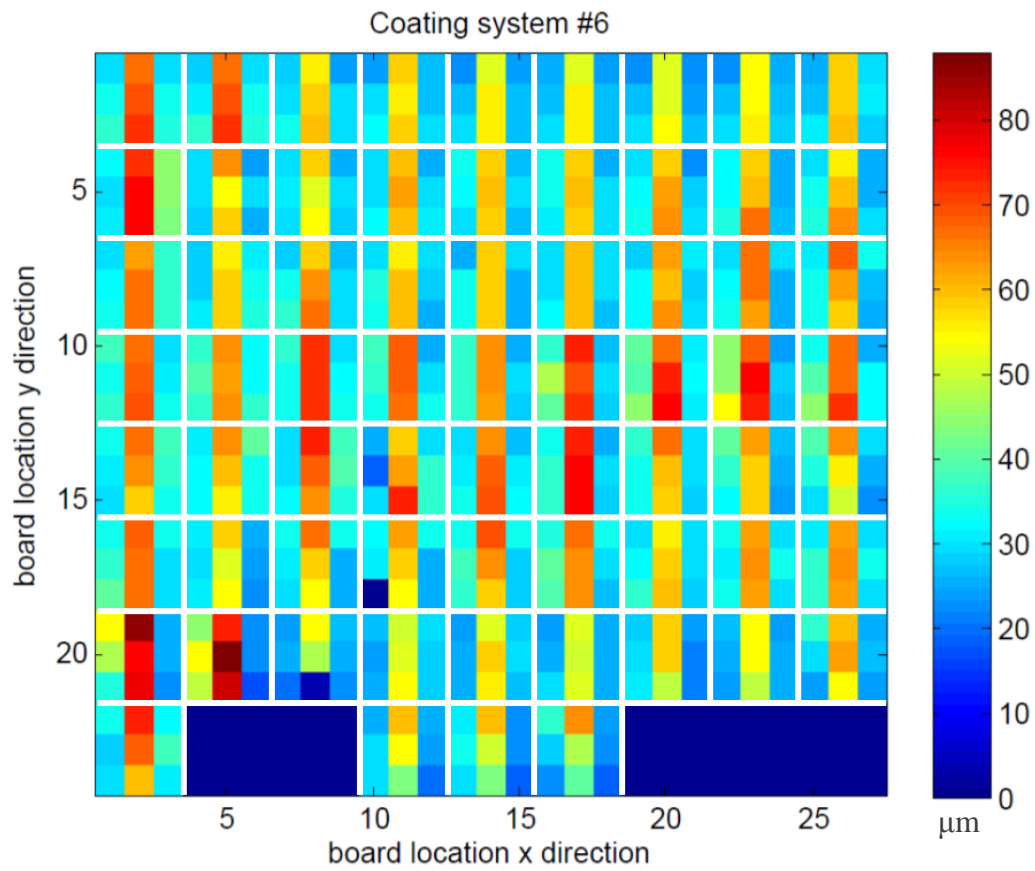


Figure 15: Film thickness measurements of AkzoNobel coating system 6. The measurements illustrate trends in film thickness associated with spraying location on Board 6

2.6.3. Gloss measurements

The gloss measurements on unexposed coupons provided information regarding variability of gloss between the coatings of interest as supplied by the manufactures. However, the main function was to provide a baseline for identification of changes in gloss resulting from variations in exposure. Variations in gloss can be attributed to a number of surface changes possible during exposure of a polymeric coating.

Gloss is a variable associated with surface finish that was used to compare coatings and their performance during aging or after exposure. Gloss is a measure of specular reflected light, the more matt a surface the more diffusely scattered incident light will be. To measure gloss, reflectometric equipment is employed to obtain the ratio of the gloss of a specified coating against a standard reference material. The reference material used is a polished black glass with a refractive index of 1.567 at a specified wavelength of 587.6 nm. The resulting value is expressed in gloss units (GU's), which are scaled values from 100 to 0, with 100 being the polished black glass standard and 0 being a perfectly matt substrate.

Gloss measurements must be made from a known direction and at specified incident angles. Industrially and hence within accepted reference standards, such as BS EN ISO 2813:2014, the incident angles commonly used are 20°, 60° and 85°. Gloss measurements were made using a Sheen Tri-glossmaster at 20°, 60° and 85°, each section of each coupon was measured three times and an average quoted. The measurements were made sequentially from left to right due to limitations of coupon size and the required surface area for the 20° measurement.

The resultant gloss measurements were averaged for each coating section on each coupon, and can be seen below. The gloss values are quoted to 0 decimal places as is defined within the BS EN ISO 2813 standard.

Table 12: Zero time point gloss measurements

Substrate	Coating System	GU – Primer			GU - Primer Topcoat			GU – Topcoat		
		20°	60°	85°	20°	60°	85°	20°	60°	85°
2024	1	0	2	1	1	2	3	1	3	3
7075	1	0	1	1	1	2	3	1	3	3
2024	2	9	40	38	1	3	4	1	3	4
7075	2	8	32	15	1	3	4	1	3	4
2024	3	48	80	91	1	3	4	1	3	4
7075	3	44	73	77	2	3	4	1	3	4
2024	4	3	21	56	1	7	21	1	7	21
7075	4	2	20	58	0	6	21	1	6	22
2024	5	14	55	77	0	5	20	1	6	23
7075	5	10	48	76	0	4	16	1	5	19
2024	6	2	18	41	1	6	18	0	5	18
7075	6	2	19	42	0	5	17	0	5	18

Primer gloss measurements for each of the coating systems identifies that for commercially available primers a range of surface finishes are possible, coating system 1 providing the lowest gloss measurement. Within the literature magnesium based primers tend to have PVC values close to the CPVC that allow for contact between all of the Mg particles and the aluminium substrate [44]. The pigment to pigment and pigment to substrate contact is important to enable the coating to cathodically polarise the substrate, resulting in the desired sacrificial protection mechanism. The high PVC results in a low gloss measurement, and the reactivity of the surface means that the gloss measurement is subject to change as the surface is exposed. The primer from system 3 has the highest gloss value, although the coatings protection mechanism is unknown the polymer is unusually a polyurethane. However, it is difficult to attribute the gloss to a feature of the formulation. However, it will be interesting to see how this value changes during environmental exposure. The remaining primers gloss values can be found between these upper and lower limits and degradation due to exposure could result in large shift in gloss from the as applied measurements.

In the ‘as applied’ condition the primer-topcoat and topcoat sections of the coupons can be discussed as single area, this is a result of the topcoat dictating the surface finish. This can be illustrated by the comparison of the primer-topcoat sections of coating system 1 and coating system 3. The primer of coating system 3 provides the highest gloss primer surface, whilst system 1 provides the lowest gloss base. The difference between the two surfaces is as much as 90 GU, the large gloss difference between the primers it is not reflected in the overlaid topcoat, with both gloss

profiles being nominally the same. Once exposed this relationship potentially could change depending on the activity of the primer.

2.6.1. Hardness measurements

Hardness of the coating was tested using a Persoz and König Pendulum Hardness Tester from Elcometer. Due to equipment restriction the Persoz pendulum was used, with the number of oscillation required for deflection from 6° to 3° measured as defined within the König Standard. The greater the number of oscillations the harder the coating. Typically the Persoz pendulum and König pendulum tests are separate standardised tests and so the data collected within the study although valid is not comparable to measurement's made externally using either of the standards. The Person pendulum affords 430 oscillations \pm 15 oscillations on the standard float glass standard specimen.

The zero time point averages for each of the coatings and substrate combinations can be seen in Table 13. The values are quoted to zero decimal places as the measurements are of completed oscillations of a pendulum.

Table 13: Zero time point hardness measurements

Substrate	Coating	Oscillations - Primer	Oscillations - Primer-topcoat	Oscillations - Topcoat
2024	1	114	32	21
7075	1	116	34	29
2024	2	93	30	24
7075	2	64	29	23
2024	3	176	26	19
7075	3	150	29	27
2024	4	140	112	125
7075	4	135	96	102
2024	5	233	126	112
7075	5	225	133	123
2024	6	152	119	113
7075	6	171	124	116

The trend of most consequence identified by the zero time point hardness measurement is the difference in performance between the topcoat supplied by AkzoNobel and the topcoat supplied by PPG. The PPG topcoat has a far higher number of oscillations, meaning the coating provided less damping to the pendulum than the AkzoNobel variant. The reduction in damping is a feature of a harder surface. The hardness measurements of 'as coated' coupons prior to environmental exposure will provide contextual information to the coupons that have been exposed. This will allow for identification of either hardening or softening of the polymer due to contact with different exposure environments. Hardening could be a result of further cross linking upon exposure.

Softening would be expected due to breakdown of inter and intra molecular bonds through mechanisms such as chain scission [71] .

2.7. Summary

The purpose of the chapter was to define what materials needed to be explored. This included substrate and coating options. This was achieved through examination of the following:

1. The current coating standard utilised by the UK military for protection of aircraft;
2. Potential replacements for Cr(VI) coatings developed within academia;
3. Typical structural aircraft aluminium alloys;
4. Coatings selected by manufacturers for testing and their application by 1710 Naval Air Squadron;
5. Pre-exposure testing, including evaluation of sprayer performance utilising film thickness measurements.

There is an incentive within industry to develop an alternative to Cr(VI) protective mechanism, as a result of the sunset date defined by REACH legislation. Many technologies have been developed to fill the gap that will occur once Cr(VI) is no longer an option. The UK military has yet to adopt a replacement technology, and finds itself in somewhat of unique position, enabling continued use of Cr(VI) until an option providing equal or better performance is identified. The difficulty of this task is compounded by the decision made by the UK military to align their testing procedures to the BS EN ISO 9227 protocol. In spite an awareness that BS EN ISO 9227 does not provide an accurate prediction of in-service performance, hence the decision made by DSTL to task Southampton University with this research.

The alignment with the BS EN ISO 9227 protocol is a positive decision when attempting to a compare coatings quickly within a standardised atmosphere. However, the BS EN ISO 9227 was developed alongside the uptake of Cr(VI) coatings, meaning known correlation between BS EN ISO 9227 results and in service lifetimes are biased towards coatings utilising Cr(VI) technology. The abstracted nature of the BS EN ISO 9227 from service conditions results in an inability to predict lifetimes in-service of coatings which deviate in chemistry from the Cr(VI) class of coatings.

Multiple coatings were used for all test method development describe in this thesis in response to the specificity of the BS EN ISO 9227 and the historic use of its results for the prediction of service life. The use of multiple coating systems was an attempt to create test protocols that were able to encompass all current and future coatings systems, ensuring any novel accelerated protocol could be applied to any coating system without a biased towards a particular technology. Six coating systems were tested, the first of the coatings systems was the Cr(VI) system currently in service, and the remaining five were all commercially identified replacements for Cr(VI). The decision to

test six coating systems was made to balance two competing concerns: (i) fewer than six coating systems may not have provided enough band width across the technology space, (ii) but more than six would have made the testing space too broad to be managed by a single researcher. The balance of six coatings does result in a limitation to be aware of, as only five alternative systems were tested not all possibilities defined within the literature could be tested. However, the five Cr(VI) replacement coatings selected were defined by multinational coating manufacturers as being promising commercial replacements for Cr(VI). The success of the range of the limited data set can only be confirmed when the testing protocols and field exposure are repeated with additional coating technologies and then compared with service exposed coatings, which would have to be completed as a part of future activities.

The six coating systems selected for testing were defined, alongside the creation of test coupons with 1710 Naval Air Squadron. Some pre-exposure analysis of film thickness, gloss and hardness was completed. The link between application and measured variation of film thickness was identified. The grid like application of film thickness measurements not only provides greater information regarding the application of coatings to coupons used for this work, but has the potential to be applied to other geometries as a training aid for sprayers to assist with meeting application tolerances in the field.

The other pre-exposure measurements defined the variation in coatings formulations, the differences in measured values of gloss for primer appear to be related to method of protection afforded by the primer. Coating system 1 which utilises a sacrificial protection mechanism has a very high PVC and so has a low gloss value to reflect this. The differences in gloss between coatings is beneficial and can provide some information regarding protection mechanism, especially, when as is the case for this present study, chemical analysis is forbidden.

The chapter aimed to identify what the materials of interest are. The substrates of interest were AA2024-T3 and AA7075-T6, both of which are well-established as structural materials used in aircraft manufacture. The replacement of Cr(VI) coating systems has led to the creation of a number of alternatives and this need for this development to be applicable to any coating system resulted in the selection of six coating systems. The effect of the variability of the in-service environment on the set of coating systems introduced shall be explored in the subsequent chapters.

3. Understanding the Exposure Environment

3.1. Introduction

The purpose of this chapter is to identify if different environments result in varied performance of materials selected for study. Whilst exploring the effect potential service condition via field exposure have on the performance of each of the coatings throughout exposure for up to 504 days to one of the field sites using a number of quantitative analytical tests.

When considering the weakness of a structure to atmospheric corrosion both the materials employed and the microclimate the structure is exposed to must be considered. For an aircraft the microclimates considered must encompass all those experienced during the lifetime of service. In broad terms the lifecycle can be split into flight hours, service readiness and periodic maintenance. The impact of hours in flight will not be considered for this study, due to the limited time military aircraft spend in flight. The total flying hours for RAF Typhoon aircraft for the year of 2014 was 16445 hours [72]. The RAF in 2014 had a fleet of 123 Typhoons, therefore assuming the possibility of planes in the fleet not being in service an estimate average of flight hours for a typhoon aircraft in 2014 is 134 h [73]. This equates to only 1.5 % of the year in flight, for the remaining 98.5 % of the year, the aircraft would be held ready for service or undergoing periodic maintenance at one of a number of sites. Service ready sites include both locations of permanent military bases and the transient sites of ongoing military operations, such as an aircraft carrier.

Permanent service ready sites for the purpose of this study are identified as working U.K. military bases, Figure 16 illustrates locations of Royal Air force (RAF) and Royal Naval Air Squadron (RNAS) bases in the U.K. that store aircraft and Figure 17 shows permanent U.K. military bases in other countries. The transient service ready sites are challenging to identify, but all current MOD

operational locations are illustrated in Figure 18, it assumed that the range of transient sites hosting aircraft would be captured within the locations identified. The figures highlight the range of locations across the globe that military aircraft are located, and hence the variability of microclimate aircraft can be exposed to.



Figure 16: Map of RAF and RNAS bases in the United Kingdom whereby military aircraft are stationed, data collected from [74].



Figure 17: World map of permanent RAF and RNAs bases where UK military aircraft are stationed [74].



Figure 18: Current MOD operations environments as identified publicly by the MOD [75-77].

The task of creating a predictive accelerated test procedure is simplified if when a coating is exposed to differing environments the deterioration of the coating is unaffected. However in the event the response is different the ability to create a single predictive test becomes less likely. The variation in possible climates military aircraft can be exposed to provide a challenge when approaching the development of an accurate and precise novel testing regime. To ensure any new test was realistic a base line for performance had to be defined. Instead, an exploration of a number of concepts for multiple environments would have to be undertaken.

Climate classification methods are used across many fields of research from climate change to corrosion science [78]. Köppen devised one such climate classification model, the model uses monthly temperature averages and precipitation to subdivide land masses based upon measureable climate differences [79]. The Köppen model allows for 33 distinct climates, each defined using three letters, the first is one of 5 broad climate groups, the second identifies the seasonal precipitation and the third is the temperature [79].

Table 14: Definition of Köppen model 1st and 2nd Letters

1 st Letter	2 nd Letter				
	W	F	M	S	T
A (Tropical)	Savannah with dry winter	Rain forest	Monsoon	Savannah with dry summer	
B (Dry)	Desert			Stepp (semi arid)	
C (Temperate)	Dry winter	Fully humid		Dry summer	
D (Continental)	Snow with dry winter			Snow with dry summer	
E (Polar)		Frost			Tundra

Table 15: Definition of Köppen model 3rd letter

3 rd Letter	H	K	A	B	C	D
Description	HOT ARID	COLD ARID	HOT SUMMER	WARM SUMMER	COOL SUMMER	COLD SUMMER

Although well used in climate science the Köppen model is not used when defining corrosivity of climates, rather the United Kingdom utilises an assemblage of BSI standard publications. Currently, four documents are used to define the effect of an atmosphere on an uncoated metallic substrate; the BS EN ISO 9223, BS EN ISO 9224: 2012, BS EN ISO 9225:2012 and the BS EN ISO 9226: 2012 [78, 80-82]. The four standards when combined define the corrosivity of an environment from the measured performance over the course of twelve months. It should be noted that if unusual climatic events occur over the course of the measured twelve months i.e. a volcanic eruption, it is possible that the typical environmental response may be misrepresented.

BS EN ISO 9223 – ‘Corrosivity of atmospheres classification, definition and estimation’ was defined to classify the corrosivity of an atmosphere relative for a small selection of homogeneous metallic substrates [78]. Classification is preferably made using the measured first year uniform corrosion data or this set of standard materials; carbon steel, zinc, copper and aluminium. The material specifications and processes required for the collection of this data are described in BS EN ISO 9226 – Determination of corrosion rate of standard specimens for the evaluation of corrosivity [82]. Specifically of interest to this work was the use of BS EN ISO 9223 and the development of the description of individual environments corrosivity with respect to aluminium substrates and the ineffectual state of the standard when applying this standard to characterise aircraft materials.

The BS EN ISO 9223 standard includes two methods of devising the corrosivity of an environment; the first is the direct method calculated from weight loss measurements made using the previously introduced BS EN ISO 9226 standard; the second involves calculation of the approximate corrosion rate using averaged environmental data [78, 82].

When employing the direct method; a 100 mm × 150 mm × 1 mm sample of aluminium with a minimum aluminium content of 99.5 wt.% is weighed using a four decimal place balance [82]. The sample exposed for one year in accordance with ISO standard 8565 beginning in spring or autumn [83]. Post exposure the corrosion products are removed following ISO standard 8407 [84]. The sample is then reweighed using the same four decimal place balance. The rate of corrosion is the calculated using the Equation 4 [82].

Equation 4: Rate of Corrosion

$$r_{\text{corr}} = \frac{\Delta_{\text{mass}}}{\text{Area} \cdot \text{time}}$$

The calculated corrosion rate does assume uniform corrosion of the substrate, an unrealistic assumption for aluminium. Aluminium is more prone to localised attack at mechanical defects resulting in the formation of deep pits at flaws or grain boundaries than uniform attack across the surface [85], the mechanism of aluminium corrosion shall be expanded upon in Section 4.1.4

Nevertheless, as the accepted methodology, the calculated uniform corrosion rate is the used to assess the severity of the environments using BS EN ISO 9223. Table 16 illustrates the standard strata applied to categorisation of environmental corrosivity against aluminium [78].

Table 16: BS EN ISO 9223 categorisation of atmospheric corrosivity for aluminium [78]

Corrosivity category	Corrosivity	Corrosion rate / $\text{g m}^{-2} \text{y}^{-1}$
C1	Very low	Negligible
C2	Low	$r_{\text{corr}} \leq 0.6$
C3	Medium	$0.6 < r_{\text{corr}} \leq 2$
C4	High	$2 < r_{\text{corr}} \leq 5$
C5	Very High	$5 < r_{\text{corr}} \leq 10$
CX	Extreme	$r_{\text{corr}} > 10$

The standard also describes typical environments that can be attributed to the defined corrosion categories, these descriptions can be seen in Table 17 [78]. The descriptions include discussions regarding three key factors, pollution by SO_2 , airborne salinity and the temperature humidity complex which is evaluated as time-of-wetness. The environmental descriptions used in BS EN ISO 9223 illustrate the intrinsic link between climate and atmospheric contaminants. The second technique described by BS EN ISO 9223 for defining the corrosivity of an environment takes advantage of this connection. BS EN ISO 9223 provides an equation derived from field work that is able to calculate predicted corrosion rate of aluminium in a specific environment using a set of environmental parameters [78]. The parameters include; temperature, relative humidity, average daily chloride deposition, and average daily sulfur dioxide deposition [78].

The calculation use of four parameters appears to try to simplify a very complex phenomena, however, with the quoted level of uncertainty for aluminium being - 50 % to + 100 %, the success of this simplification is called into doubt [78]. Regardless of the level of uncertainty the source and effect of these parameters must be considered to enable understanding of their effect in service and their importance in accelerated testing procedures.

The first concept to be explored was to identify if exposure conditions, i.e., climate, was responsible for differing performance of coatings, and if so, what are the bounds of this performance. Early discussions resulted in eight potential environments of interest initially being for further investigation. The eight identified environments were tropical coastal, tropical inland, temperate coastal, temperate inland, glacial coastal, polar inland and arid. The eight environments were selected in response to the detail of the Koppen model compared with the over simplicity of the British standard.

Table 17: Typical atmospheric environments described in BS ISO EN 9223 [78]

Corrosivity category	Corrosivity	Typical Outdoor Environment
C1	Very low	‘Dry or cold zone, atmospheric environment with very low pollution and time-of-wetness, e.g., certain deserts, Central Arctic/ Antarctica’
C2	Low	‘Temperate zone, atmospheric environment with low pollution (SO ₂ , 5 µg m ⁻³), e.g., rural areas, small towns. Dry or cold zone, atmospheric environment with short time of wetness, e.g., deserts, subarctic areas’
C3	Medium	‘Temperate zone, atmospheric environment with medium pollution (SO ₂ : 5 µg m ⁻³ to 30 µg m ⁻³) or some effect of chlorides, e.g., urban area, coastal areas with low deposition of chlorides. Subtropical and tropical, atmosphere with low pollution’
C4	High	‘Temperate zone, atmospheric environment with high pollution (SO ₂ : 30 µg m ⁻³ to 90 µg m ⁻³) or substantial effects of chlorides, e.g., polluted urban areas, industrial areas, coastal areas without spray of salt water or exposure to strong effects of de-icing salts. Subtropical and tropical zone, atmosphere with medium pollution’
C5	Very High	‘Temperate and subtropical zone, atmospheric environment with very high pollution (SO ₂ : 90 µg m ⁻³ to 250 µg m ⁻³) and/or significant effect of chlorides, e.g., industrial areas, coastal areas, sheltered positions on coastline’
CX	Extreme	‘Subtropical and tropical zone (very high time-of-wetness), atmospheric environment with very high SO ₂ pollution (higher than 250 µg m ⁻³) including accompanying and production factions and/or strong effect of chlorides, e.g., extreme industrial areas, coastal and offshore areas, occasional contact with salt spray

The environmental factors that are historically known to affect corrosion are not the only factors that must be considered when testing coatings. Other important environmental factors include:

- UV dosage [86];
- Atmospheric oxidants [87];
- Hygrothermal effects [5];
- Surface water [86] ;
- Interaction with substrate [88].

A coatings physical response to exposure can be qualified using BS EN ISO 4628. BS EN ISO 4628 is used to evaluate degradation of coatings through description of the quantity and size of defects and the intensity of uniform changes in appearance. BS EN ISO 4628 contains nine sections which define a process for the assessment of seven variables each which may be result of a weathering of a coating. The variables that can be assessed using BS EN ISO 4628 include; blistering, rusting, cracking, flaking, chalking by tape, chalking by velvet, delamination and corrosion around a scribe or other artificial defect and degree of filiform corrosion [89].

The most pertinent variable for this research was blistering, which is defined in part 2 of BS EN ISO 4628 and assesses blistering by size of blisters and density [90]. The density of blisters is defined using a numerical scale of 0 to 5, see Table 18.

Table 18: BS EN ISO 4628 - Rating scheme for designating the size of defect, adapted from [89].

Density score	Definition
0	None
1	Very Few , barely significant
2	Few but significant
3	Moderate number of defects
4	Considerable number of defects
5	Dense Pattern of defects

Table 19: BS EN SI 4628 - Rating scheme for designating the intensity of changes, adapted from [90].

Size score	Definition
0	Not visible under 10 x magnification
1	Only visible under 10 x magnification
2	Just visible with normal corrected vision (up to 0.2 mm)
3	Clearly visible with normal corrected vision (larger than 0.2 mm to 0.5 mm)
4	Larger than 0.5 mm up to 5 mm
5	Larger than 5 mm

To assist with the qualification of blistering part 2 of BS EN ISO 4628 provides a suit of images to compare against, which can be used to calibrate optical imaging systems. The qualification scale leads to subjective responses by operators if analysis is completed using the image guided method. The standard also provides no numerical guidance on ranges for optical imaging systems.

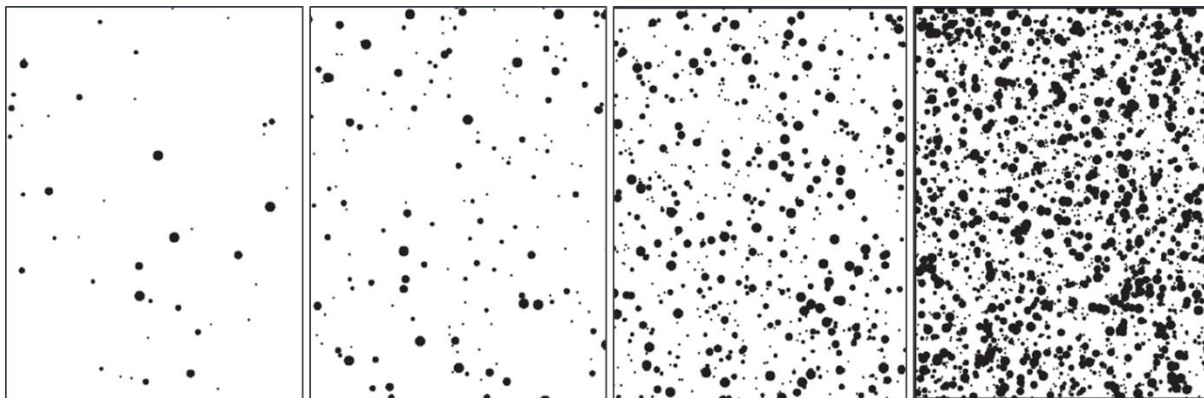


Figure 19: Example of calibration images found in BS EN ISO 4628, blister size 4, quantity range (left to right) 2 3, 4, 5. Images adapted from [90].

3.2. Objective

The objective of this study was to evaluate the resistance to weathering of six different coating systems throughout four field exposures and to identify if the coatings weathering performance differs between each of the field exposure sites. The resistance to weathering was quantified through measurements of gloss, dry film thickness, colour difference, changes to hardness and the percent corroded surface area.

3.3. Experimental

Although all eight selected environments or even 33 Koppen model environments described could be used in the storage of aircraft, the exploration of the concepts of realistic exposure tests and the benchmarking of real world performance did not require for proof of concept the uptake of all possible environments. Instead four environments were selected based upon availability of access to sites and ease of conversion of the environmental parameters to conventional accelerated corrosion chambers. The importance of the ability to convert natural exposure conditions into a traditional accelerated corrosion shall be explored in Chapter 5. The four environments selected were the tropical coastal, tropical inland, temperate coastal and temperate inland. The four experiments were individually considered of interest as they are able to provide comparison across different climate features. The change from tropical coastal to tropical inland was identifying if a change in salinity in an environment of high temperature and humidity averages creates a difference in performance of coatings. The change from tropical coastal to temperate coastal is looking to identify the effects attributed to changes in the temperature and humidity complex at high salinity levels. The tropical inland and temperate inland sites are looking at the changes in the temperature and humidity complex when the salinity levels are relatively low, identifying if the effects of temperature and humidity are exacerbated by high salinity levels. The four experiments aimed to see if these changes in environment had any quantifiable effect on coating performance over

3.3.1. Materials

The experiments were completed using coupons of the six coating systems defined in Chapter 1. The coupons used included both AA2024-T3 and AA7075-T6 which are commonly used structural materials in military aircraft. The coupons were sourced from ACT Test Panels LLC. The elemental composition of each of the materials as defined by the manufacturer is as follows:

Table 20: ACT elemental composition of AA2024-T3 coupons

Element	ACT Specification
Mn	0.63
Si	0.05
Cu	4.5
Ti	0.03
Fe	0.15
Zn	0.08
Mg	1.5
Al	Balance

Table 21: ACT elemental composition of AA7075-T6 coupons

Element	ACT Specification
Mn	0.03
Si	0.07
Cr	0.2
Cu	1.5
Ti	0.03
Fe	0.19
Zn	5.6
Mg	2.5
V	0.01
Zr	0.01
Al	Balance

3.3.2. Field exposures

The field exposures were completed by exposing coated coupons to one of four possible field exposure sites for up to 504 days. Coupons were also removed for analysis at 84 day intervals, once removed the samples were imaged, cleaned in distilled water to remove surface contaminants, dried with compressed air, imaged a second time and stored away from sunlight under normal laboratory conditions. Once this initial processing was complete the coupons were analysed to identify changes resultant from the field exposures. The four field exposures included a tropical coastal site, a tropical inland site, a temperate coastal site and a temperate inland site.

The four environments selected can be described using both the Köppen model and the corrosivity definition created for the British standard, each of site definitions can be found in Table 22.

Table 22: Field exposure site definitions [78, 79]

Environment	Köppen Model Definition	British Standard Definition
Tropical Coastal	Am	CX
Tropical Inland	Aw	C3/4
Temperate Coastal	Cfb	C4
Temperate Inland	Cfb	C3

The temperate inland exposure site was created at the University of Southampton, on the roof of the Lanchester Building, Highfield Campus (Latitude 50.934189, Longitude -1.3956848); it was selected as it gave unfettered access to the samples enabling additional measurements to be made. The Southampton site is defined as the temperate and non-coastal in spite of Southampton being a port, due to the non-central location of the university the bulk of the marine atmosphere was unable to penetrate so far inland, with salinity levels known to drop dramatically a few hundred metres from the shore [91]. The site was equipped to make climatic measurements this included continual monitoring of environmental factors such as temperature, humidity, wind speed, solar exposure, UV exposure, precipitation volume, precipitation frequency and air pressure with a Davis Vantage Pro 2 Weather Station. The sample material temperature was also being continually monitored using a Pico TC-08 (USB) thermocouple data logger and Omega surface adhesive k-type thermocouples mounted on the reverse of four samples.

Prior to exposure of samples at the Southampton site, the design and installation of a new exposure rack was completed. The racking is for full exposure and adheres to the guidelines set forth in British Standard 5466 [92]. By conforming to BS 5466 the samples will be exposed using a rack with a southerly exposure, a minimum height of 0.5 m, and an inclination of 45°. Detailed plans of the rack can be found in the Appendix Section 11.3. The completed site can be seen in Figure 20.



Figure 20: Southampton outdoor exposure rig.

The second natural exposure experiment utilised a newly installed site at Portsmouth Naval docks, on the roof of Unicorn Building (Latitude 50.8031, Longitude -1.0951); access to the site was granted by 1710 Naval Air Squadron. The Portsmouth site was defined as ‘temperate and coastal’ in nature, its coastal location resulted in higher salinity levels than the Southampton site, but its climate is relatively similar. A new exposure rack was installed following the design implemented at Southampton University, see Figure 21. However, due to radio transmission limitations it was not possible to measure local climatic data at this exposure location.



Figure 21: Portsmouth outdoor exposure rig.

The two remaining exposure sites were made available through DSTL; both were tropical exposure sites in Panama managed by the United States Department of Defense (DoD). The two sites selected included a breakwater site and an inland site at Cerro Tigre; fulfilling coastal and non-coastal exposures respectively. The locations are illustrated in Figure 22. The Horoko site was also considered, however, it was dismissed based upon its proximity to Panama Bay.

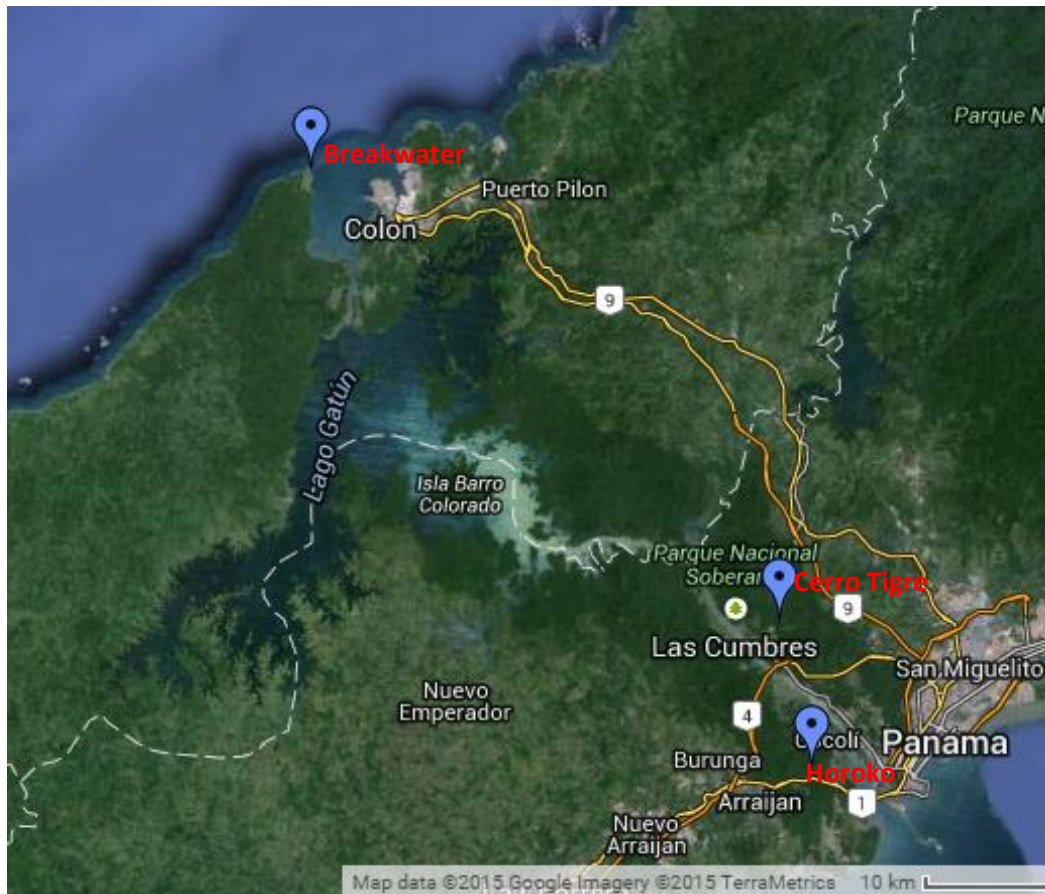


Figure 22: Locations of possible Panama exposure sites.

The breakwater exposure site is located on the Atlantic side of the Panama Isthmus, it has average temperatures ranging between 21 °C and 34 °C, and relative humidity can range between 51 % and 98%. Rain fall at the breakwater was expected on average for 216 days of the year with an expected rain fall of 267 cm. The Cerro Tigre site is located on the Pacific side of the Isthmus, test area is open canopy, with low salinity and UV levels. The site has average temperatures ranging between 18 °C and 37 °C, relative humidity can range between 64 % and 99%. Rain fall can be expected on average for 269 days of the year with a total expected rain fall of 185 cm. The grid references for the sites are defined in Table 23.

Table 23: Grid references for the Panama exposure sites

Exposure Site	Latitude	Longitude
Breakwater site	9°22'24.84"N	79°56'50.42"W
Cerro Tigre	9°3'55.01"N	79°37'43.70"W

The specific experimental combinations of substrate, coating, exposure site and exposure length that were used are defined in Table 24 and Table 25. The specific details of the exposures sites and arrangements can be seen in Figure 23 and Figure 24, respectively. The Figure 23 image was taken after the removal of coupons at 336 days at the tropical coastal site, as was the image in Figure 24 at the tropical inland site.



Figure 23: Tropical coastal exposure site at 336 days exposure.



Figure 24: Tropical inland exposure site at 336 days exposure.

Table 24: Coupon allocations for tropical field exposures

<i>Exposure Site</i>	Substrate	Coating	Exposure length						
			0	84	168	252	336	420	504
<i>Tropical Coastal</i>	2024	1	49			52	46		58
<i>Tropical Coastal</i>	2024	2			156	73	109	110	
<i>Tropical Coastal</i>	2024	3	189	161	177				174
<i>Tropical Coastal</i>	2024	4		239	240	148			166
<i>Tropical Coastal</i>	2024	5	301				298	299	300
<i>Tropical Coastal</i>	2024	6		204	366	367		362	
<i>Tropical Coastal</i>	7075	1		50	51			47	
<i>Tropical Coastal</i>	7075	2	112	365	114				111
<i>Tropical Coastal</i>	7075	3				180	172	115	
<i>Tropical Coastal</i>	7075	4	237			209	235	236	
<i>Tropical Coastal</i>	7075	5		302	304	311			48
<i>Tropical Coastal</i>	7075	6	364				32		363
<i>Tropical Inland</i>	2024	1		57	121	59		54	
<i>Tropical Inland</i>	2024	2				122	347		125
<i>Tropical Inland</i>	2024	3	56					5	188
<i>Tropical Inland</i>	2024	4		247			242	201	244
<i>Tropical Inland</i>	2024	5	308	309	307				
<i>Tropical Inland</i>	2024	6	371		373	374	179		
<i>Tropical Inland</i>	7075	1	385	243			53		55
<i>Tropical Inland</i>	7075	2	119	120	139			117	
<i>Tropical Inland</i>	7075	3		246	184	185	144		
<i>Tropical Inland</i>	7075	4	245		380	248			
<i>Tropical Inland</i>	7075	5				345	305	306	118
<i>Tropical Inland</i>	7075	6		372			193	369	370

Table 25: Coupon allocations for temperate field exposures

<i>Exposure Site</i>	Substrate	Coating	Exposure length						
			0	84	168	252	336	420	504
<i>Temperate Coastal</i>	2024	1	320		387	388			384
<i>Temperate Coastal</i>	2024	2		71				68	69
<i>Temperate Coastal</i>	2024	3	133	134		136			279
<i>Temperate Coastal</i>	2024	4	196		198		67	194	
<i>Temperate Coastal</i>	2024	5			324		256	257	
<i>Temperate Coastal</i>	2024	6		197		325	319		
<i>Temperate Coastal</i>	7075	1		386		128	382	383	
<i>Temperate Coastal</i>	7075	2	70		72	90	323		
<i>Temperate Coastal</i>	7075	3		7	135		130	131	
<i>Temperate Coastal</i>	7075	4	217	238		199			195
<i>Temperate Coastal</i>	7075	5	392	260		262			258
<i>Temperate Coastal</i>	7075	6	322		318			165	132
<i>Temperate Inland</i>	2024	1	63		31			61	
<i>Temperate Inland</i>	2024	2			65		123	394	64
<i>Temperate Inland</i>	2024	3		127	254	3	312		
<i>Temperate Inland</i>	2024	4	252	190			249	173	
<i>Temperate Inland</i>	2024	5		253		255			314
<i>Temperate Inland</i>	2024	6	329			1		376	377
<i>Temperate Inland</i>	7075	1		379		381	60		62
<i>Temperate Inland</i>	7075	2	129	82		66		261	
<i>Temperate Inland</i>	7075	3	186					187	36
<i>Temperate Inland</i>	7075	4			191	192			378
<i>Temperate Inland</i>	7075	5	315		16		116	313	
<i>Temperate Inland</i>	7075	6		316	317		375		

3.3.3. Gloss measurements

Gloss measurements were made using a Sheen Tri-glossmaster at incident angles of 60° and 85°, each of the three sections of each coupon were measured three times. The gloss meter has a measurement range of 0 – 1000 GU (Gloss Units) at 60° and 0 – 160 GU at 85°, mirror like samples can be measured using the 20° option which has a range of 0 – 2000 GU. The average of the three values was then calculated and used to compare the effect of the field exposure sites.

3.3.4. Film thickness measurements

The post exposure thickness measurements were completed using an Elcometer 456 dual FNF integral coating thickness gauge. The gauge has a sensitivity of $\pm 2.5 \mu\text{m}$ and a range of 0 – 13 mm. The measurements were made from top to bottom of each of the coupon sections as illustrated by Figure 25. The difference in film thickness between pre and post exposure was then calculated for each of the measurements using the following Equation 5.

Equation 5: Calculated difference in film thickness pre and post exposure

$$\Delta f = f - f_0$$

Where Δf is the change in film thickness (μm), f is the film thickness post exposure and f_0 is the pre-exposure film thickness. The three Δf values for each section were then averaged to represent the section in its entirety.



1	4	7
2	5	8
3	6	9

Figure 25: Film thickness measurement pattern.

3.3.5. Colorimetry measurements

The colorimetry measurements were made using an Elcometer 6085S Portable Sphere Spectrophotometer. The spectrophotometer used had a spectral range of 400 nm to 700 nm, and data was collected as L a* b* values. Data was collected both pre and post exposure following the same pattern described in Figure 25. The average L a* and b* value for each of the sections at each time point was then calculated. The average L a* and b* values were then used to calculate the change in colour as a result of exposure. This change was quantified using the CIE Δ_E 2000 formula as defined in ASTM D2244. The calculations were completed using an excel calculator created by Sharma et al. [93].

3.3.6. Hardness measurements

Post exposure coating hardness was measured following the procedure defined in Section 2.6.1.

3.3.7. Pulsed thermography measurements

The inherent differences in emissivity of aluminium alloys, their corrosion products and polymeric coatings was exploited through the application of pulsed thermography to quantify the under coating corrosion product. A diagram of the experimental set up used for pulsed thermography measurements of coupons can be found in Figure 26. Pulsed thermography measurements were made using an FLIR SC5000 with a 320×256 pixel format Indium Antimonide focal plane array. The frame rate for capture was 380 Hz and the measurements were made with 30 cm between the coupon and lens, this resulted the highest possible resolution for measurement. The coupons were image for 10 second capturing the cannon camera flash used to thermally excite the samples. The remaining frames captured the sample cooling. Once imaged the data was analysed relative to a single frame extracted 100 frames after the camera flash. The frame was then exported as a .jpg image for quantitative analysis using Image J software. The images created were easily segmented and analysed using a repeatable processes. The images were imported into ImageJ and the scale was set using the coupon width. The area of interest was cropped from the image and was segmented using the Weka trainable segmentation plugin. The segmented image was then thresholded and the area of imaged corrosion calculated. The data collected for each segment of each coupon are detailed in Table 26.

Table 26: Definition of collected data using pulsed thermography

Number of incidents of corrosion
Total area of corrosion
Average size of corrosion incidents
% area of corrosion
Average circularity of corrosion incidents
Average perimeter of incidents

Although multiple data sets were collected for this work only the percentage (%) area of corrosion was used for further analysis.

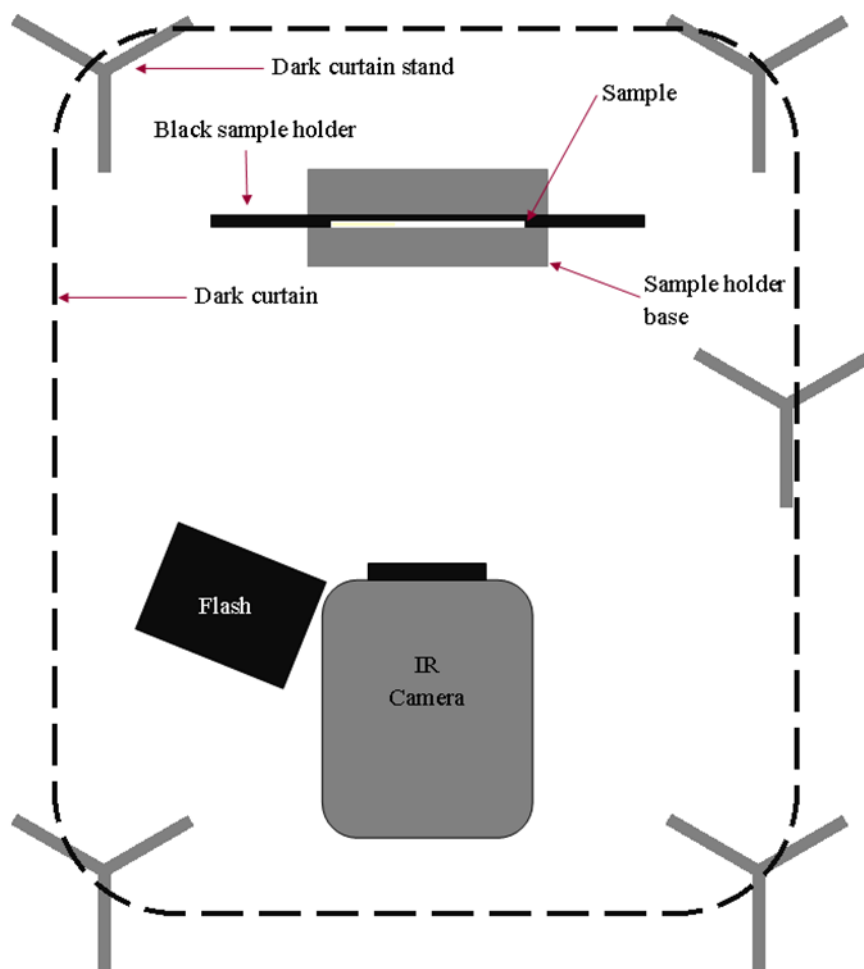


Figure 26: Pulsed thermography experimental setup.

3.4. Results and discussion

A selection of the collected data is presented. Data collected but which provided no additional information to the discussion was not included. The data sets provided are coating system and coating section specific, all analysis was completed for each of the sections. Hence analysis is completed for each of the sections; primer, primer topcoat and topcoat in isolation.

3.4.1. Coating component gloss changes with exposure

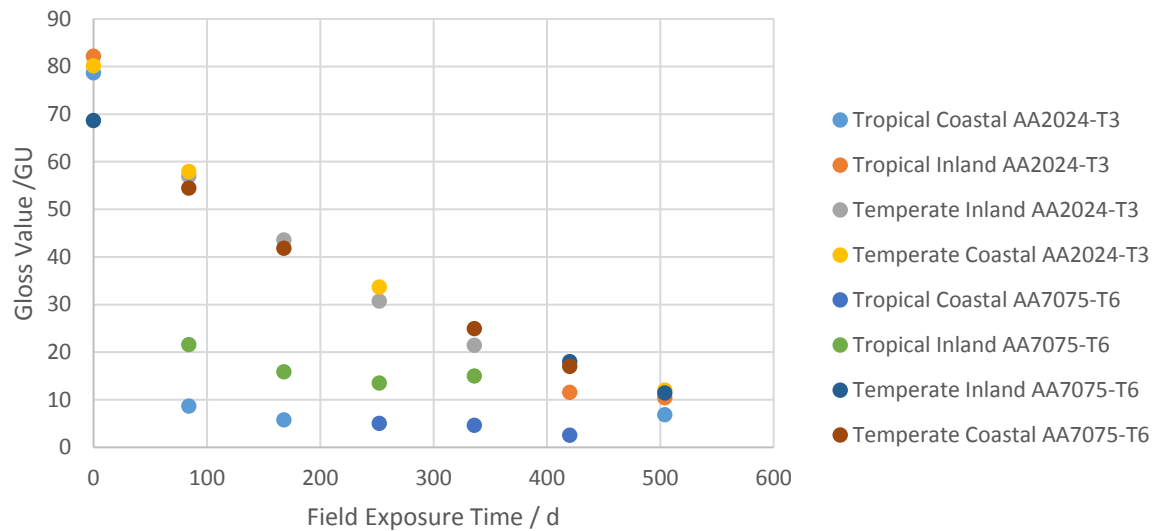


Figure 27: Coating System 3 Primer 60 degree gloss vs. exposure time.

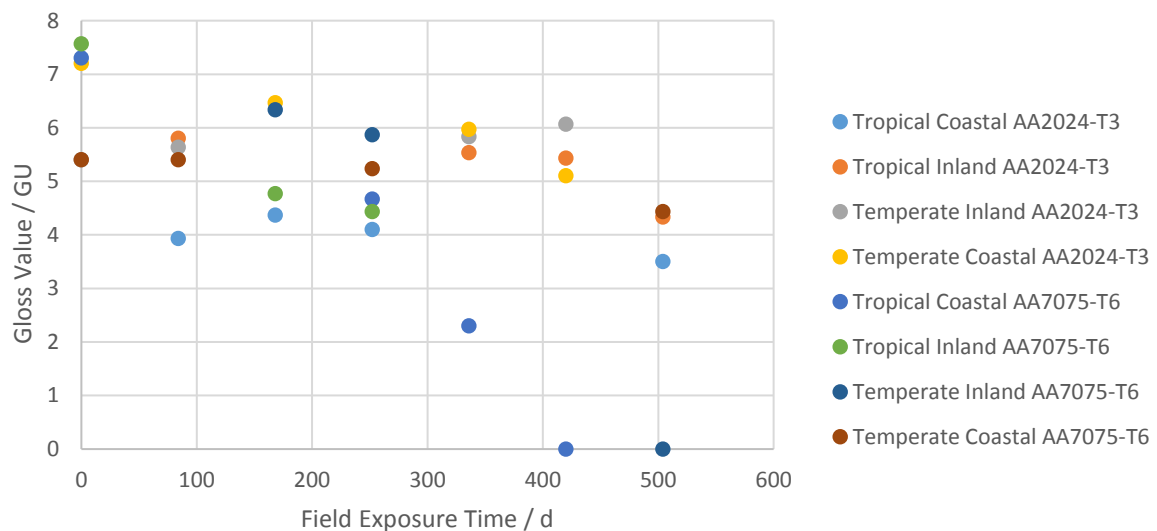


Figure 28: Coating System 4 Topcoat 60 degree gloss vs. exposure time.

Changes in measured gloss are good indicators for changes to the surface of the polymer. Often a decrease in gloss is a response to polymer chain scission. The loss of fidelity of the polymer result in a loss of surface facing extenders. The loss of these extenders increases the surface roughness as a

result of the residual voids, hence decreasing the gloss value [12]. Figure 27 illustrates this trend well, with each of the coupons shows an ever decreasing gloss value for the primer from coating system 3 as exposure length increased. The key point from this work is not the overall trend of decreasing gloss, but instead to note that different field exposures resulted in different rates of gloss change. Coupons expose to the tropical coastal field site showed the fastest decrease in gloss regardless of the substrate in question. It could be perceived that the change in gloss would be a result of a build-up of salt on the surface of the coatings due to the high aerosolised salt levels experienced at a coastal site. However, this can be discounted as prior to gloss measurements being made all samples were washed twice with distilled water. Therefore, the perceived change must be a result of a physical change to the surface of the coating, this could be a build-up of non-soluble corrosion products or polymeric film breakdown.

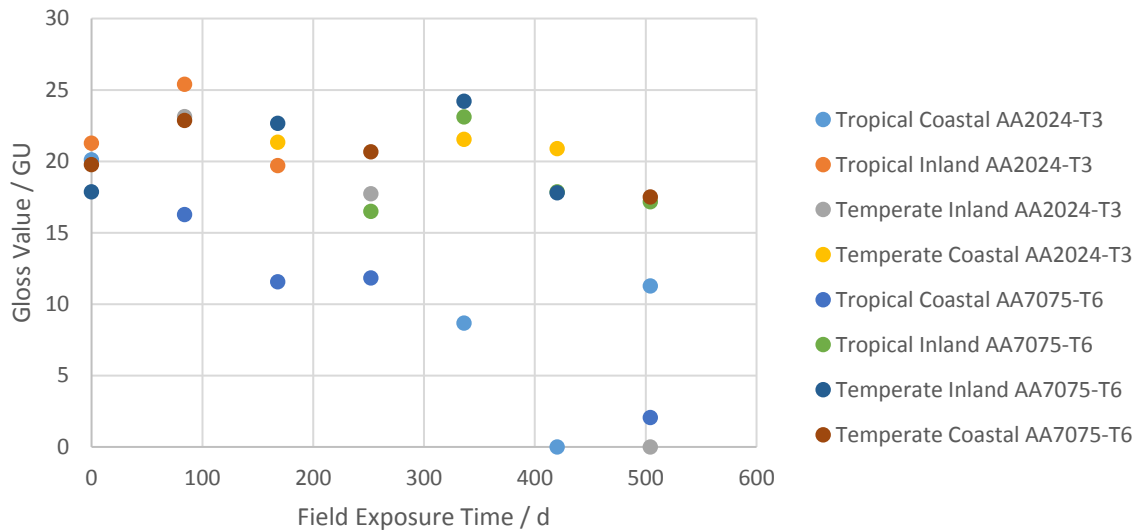


Figure 29: Coating System 5 Topcoat 85 degree gloss vs. exposure time.

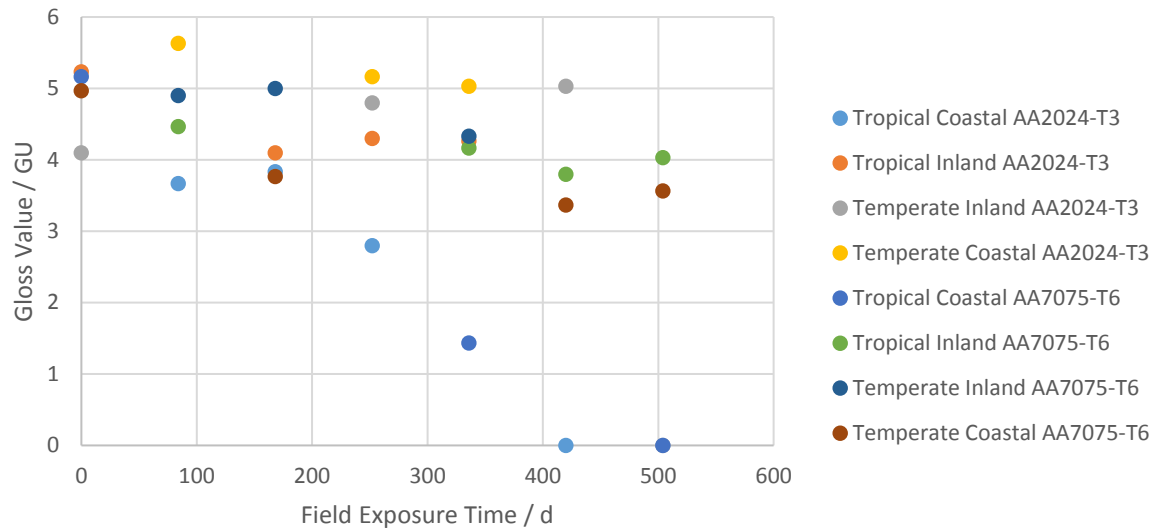


Figure 30: Coating System 6 Topcoat 60 degree gloss vs. exposure time.

3.4.2. Film thickness change with exposure

The primer from coating system 1 imparts cathodic protection to the underlying substrate via the inclusion of magnesium particles. The cathodic protection mechanism is one of preferential reaction, with the more anodic magnesium particles oxidising in favour of the more noble aluminium substrate. Success of the protection mechanism is reliant on electronic connection between the aluminium substrate and all of the magnesium particles, this results in a coating at or near its critical pigment concentration (CPVC). Although imparting the required electronic connection between the magnesium particles, the high PVC also creates a porous matrix which when unprotected by a topcoat allows for rapid solvent ingress. The solvent ingress initiates oxidation of the magnesium particles, and the resultant products can be rinsed away due to lack of protection which would be afforded by a topcoat [88]. The reduction in primer film thickness seen in Figure 31 is a result of dissolution of the magnesium from within the high PVC polymer matrix. The effect is heightened as for the data set illustrated in Figure 31 because there is no protection by a topcoat to prevent the wash off of corrosion products. The rate of film thickness decrease is different on each of the exposure sites, for the primer of coating system 1 the degradation is specific to the exposure.

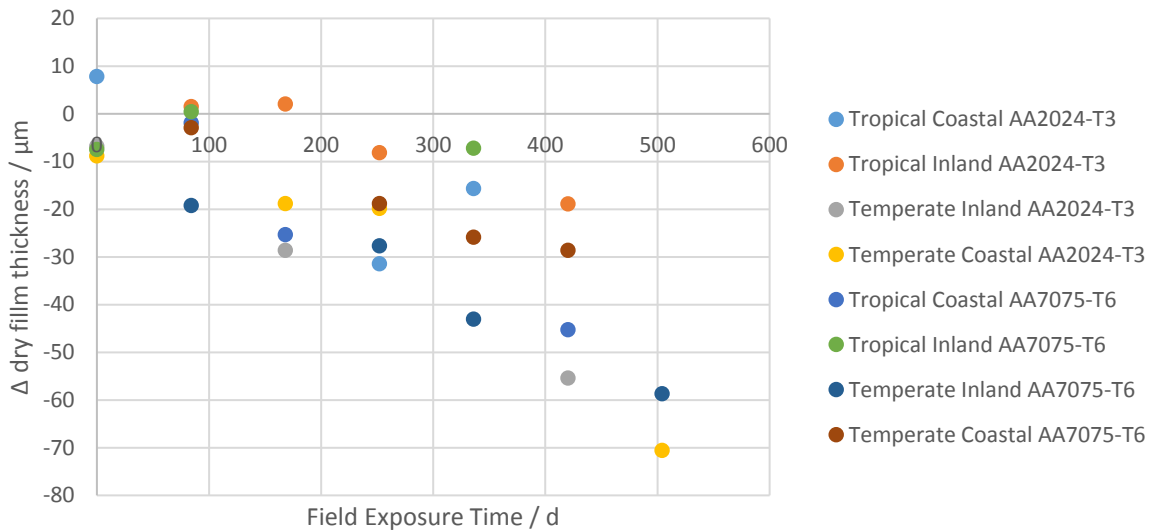


Figure 31: Coating system 1 Primer measured change in film thickness post exposure vs. exposure time.

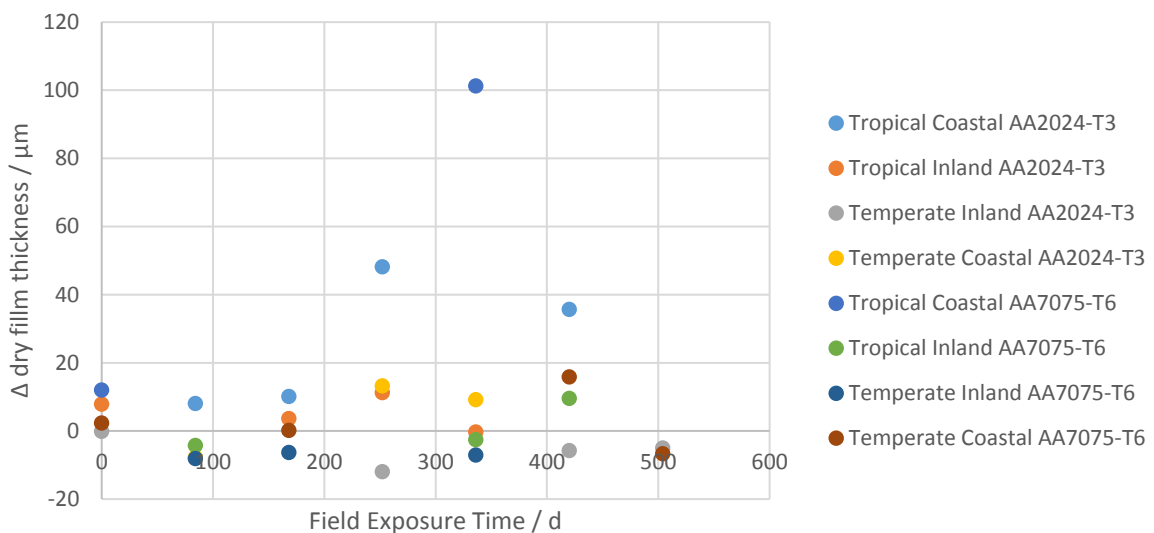


Figure 32: Coating system 6 topcoat measured change in film thickness post exposure vs. exposure time.

The clear trend of decreasing film thickness identified for the primer of coating system 1 is not replicated by other coating systems tested. The change in film thickness witnessed by each section of each of the coating systems is instead defined by the coating sections response to the environment it is exposed to. For example, in Figure 32 the topcoat of coating system 6 shows an increase in film thickness measured when coupons were exposed to tropical coastal sites. The increase is a result in an accumulation of corrosion products under the polymer film. Corrodents and water were able to pass through the topcoat to the unprotected surface underneath. However, the insoluble corrosion

products were unable to pass up through the film and reach the top surface. As a result of this, unlike in the case of the coating system 1 primer whereby the corrosion products were washed away, the corrosion products from system 6 artificially increased the measured film thickness. Once again the performance is different when comparing the different environments, a range of up to 90 μm can be attributed to the effect of the specific exposure.

3.4.3. Colour change with exposure

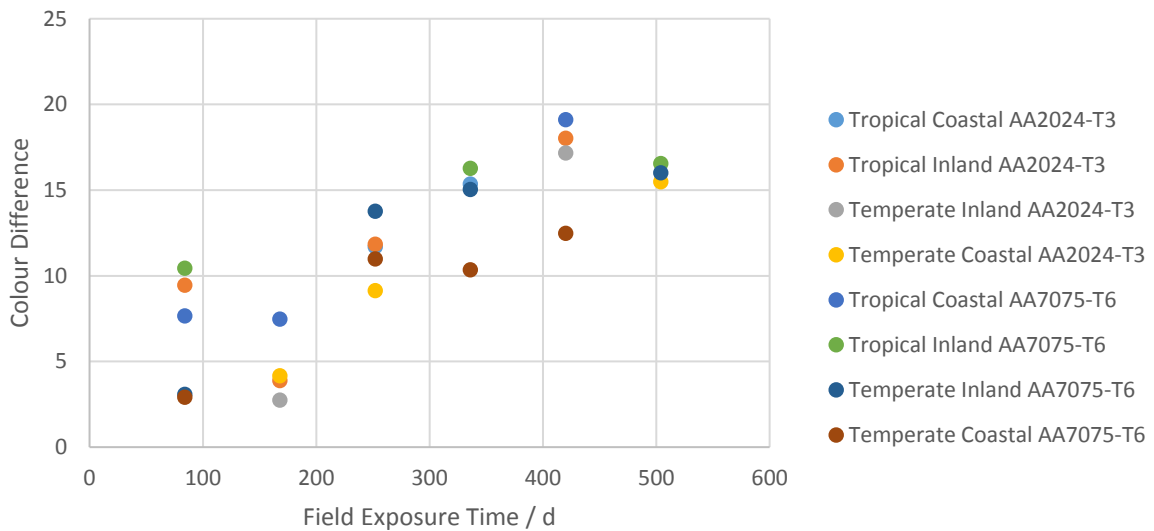


Figure 33: Coating 1 Primer calculated ΔE 2000 colour difference vs. exposure time.

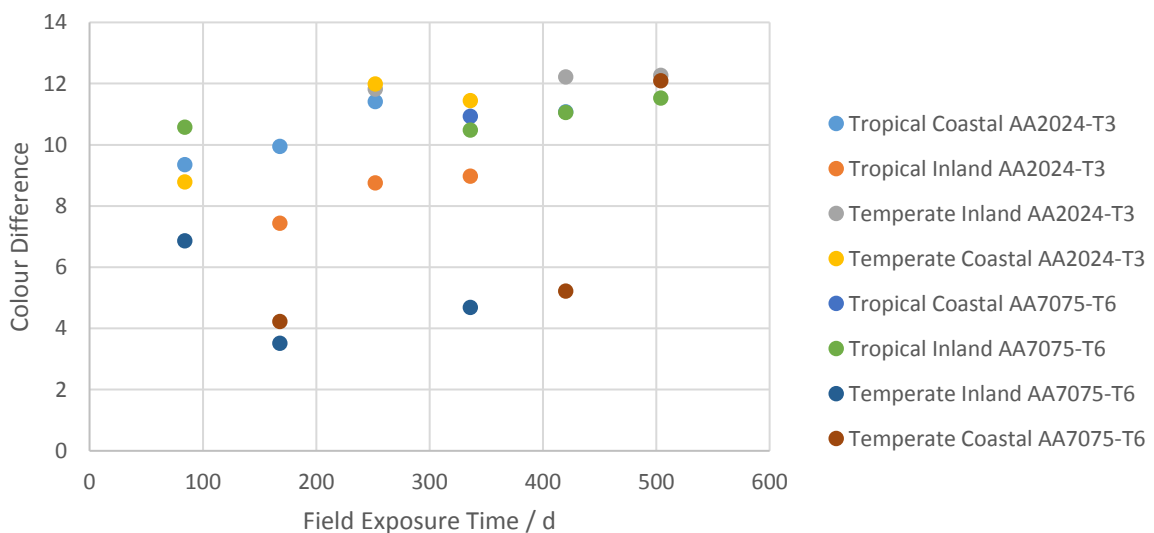


Figure 34: Coating 6 Primer calculated ΔE 2000 colour difference vs. exposure time.

Colour change for primer sections for coating system 1 and coating system 6 are a result of two different mechanisms. The colour change seen for coating system 1 is a result of the sacrificially protecting Mg particles oxidising during exposure. The rate at which this occurred was different dependent upon the specific environment. The colour difference measured for the primer of coating systems 6 is a result of leaching and reacting of the mobile strontium chromate pigment included in the formulation. Although the measured colour change trend is different for each of the coating systems discussed, what is clear is both coatings perform differently when exposure to an array of environments.

3.4.4. Hardness increase with exposure

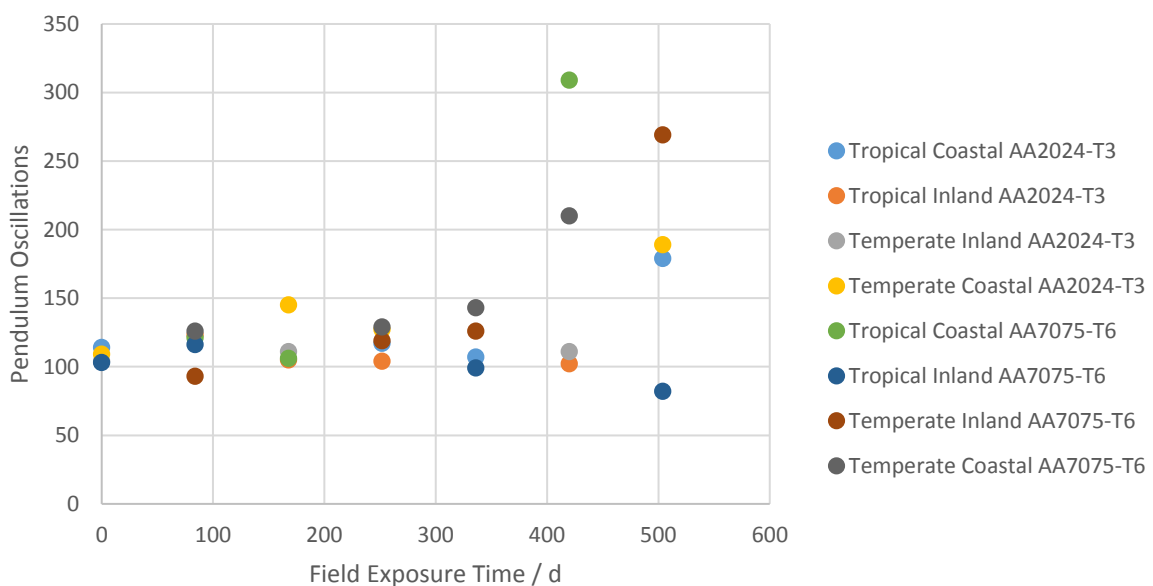


Figure 35: Coating System 1 Primer Konig hardness vs. exposure time.

The general trend for exposure of the primer of coating system 1 to many of the field sites is an increase in the hardness over time. Exposure of coated AA7075-T6 and AA2024-T3 coupons to the tropical coastal, the temperate inland and the temperate coastal site all show this increase. However, both coupon types when exposed to the tropical inland did not experience the same coating hardness increase. Specifically for AA7075-T6 coupons, the key difference between exposure to the three sites that resulted in a hardness increase and the tropical inland site was the level of UV exposure. The tropical inland site was located under the tree canopy (see Figure 36), resulting in a lower level of UV exposure than samples exposed at the three other field sites. Exposure to UV radiation could result in increased crosslink density, which when the exposure to UV is reduced the level of cross linking could have been retarded [71].



Figure 36: Tropical inland field exposure site.

3.4.5. The quantified corroded surface

Comparison of the corroded surface area was used to assess the relative aggressiveness of the exposure environments chosen for the field exposures. To enable the effects of the environmental conditions to be explored, each of the coatings tested was analysed in isolation. The corroded surface area was defined using the pulsed thermographic technique described in Section 3.3.7. Pictorially the effect of exposure environment can be seen in Figure 37, both images are of the same coating system, system 6 applied to the same substrate, i.e., AA2024-T3. The samples exposed to different field exposures for a total of 252 days. The resultant under coating corrosion was evident on the right-hand side of each of the coupons, with corrosion products visible as dark regions on the lighter grey background. The surface area affected was quantified as a percent coverage for each section. The right-hand section of the left image shows a 3 % coverage of corrosion product, whilst the equivalent section of the right image contains 43 % coverage.

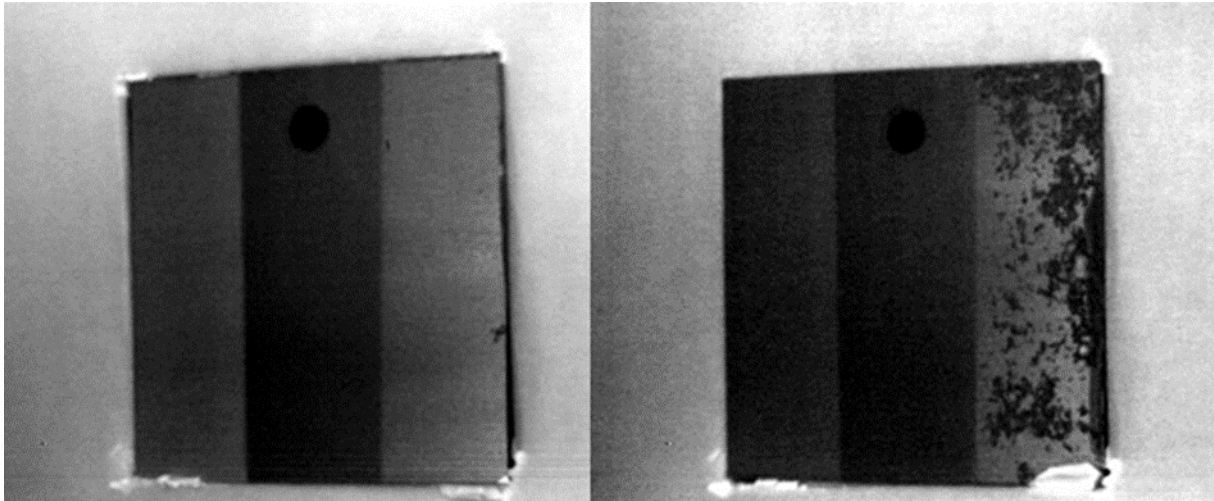


Figure 37: Pulsed infrared thermography frames of coating system 6 on AA2024-T3 exposed for 252 days to either a temperate inland environment (left) or tropical coastal environment (right).

The quantified values when collated provides further evidence for the discussion regarding the effect of exposure environment on the performance of a protective coating. Figure 38 illustrates the progression of undercoating corrosion identified for coating system 1 applied to both AA2024-T3 and AA7075-T6 upon exposure to each of the four field sites. Coating system 1 shows a weakness to tropical coastal systems, with the AA7075-T6 coupons being the most affected by the exposure, reaching 100 % surface corrosion of the right hand topcoat section in 252 days. For AA2024-T3 the coating system appears to provide a little more protection with the maximum corrosion surface coverage being 65 %. The AA7075-T6 coupons also show a heightened response to tropical inland environments compared with AA2024-T3. As a result of the increased corrosion product for both the tropical coastal and tropical inland sites it appears that for coating system 1 a higher temperature is of greater impact than a higher aerosolised salinity level. However, cumulatively high salinity levels and a high temperature has the greatest effect.

Coating system 2 illustrates that the tropical coastal site is most aggressive with regards to corrosion, with AA7075-T6 the most sensitive followed by AA2024-T3. The tropical inland site once again provided the next harshest environment with AA7075-T6 again demonstrating to be a more reactive substrate than AA2024-T3. The weakness of AA7075-T6 over AA2024-T3 when exposed to a tropical coastal environment is in opposition to the performance seen with coating system 1. This could be a result of the protection mechanism associated with coating system 1. The substrate is forced to be noble relative to the Mg particles present in the primer within coating 1.

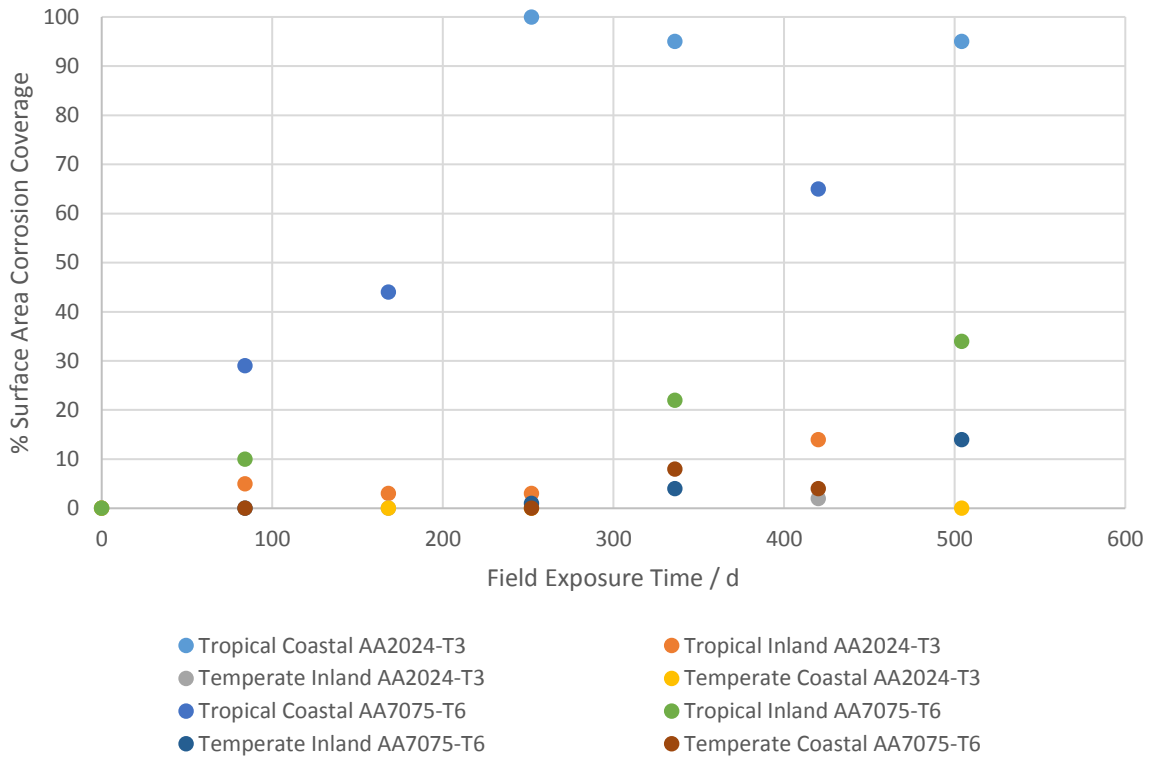


Figure 38: Coating System 1 Topcoat percentage surface area corrosion coverage vs. exposure time.

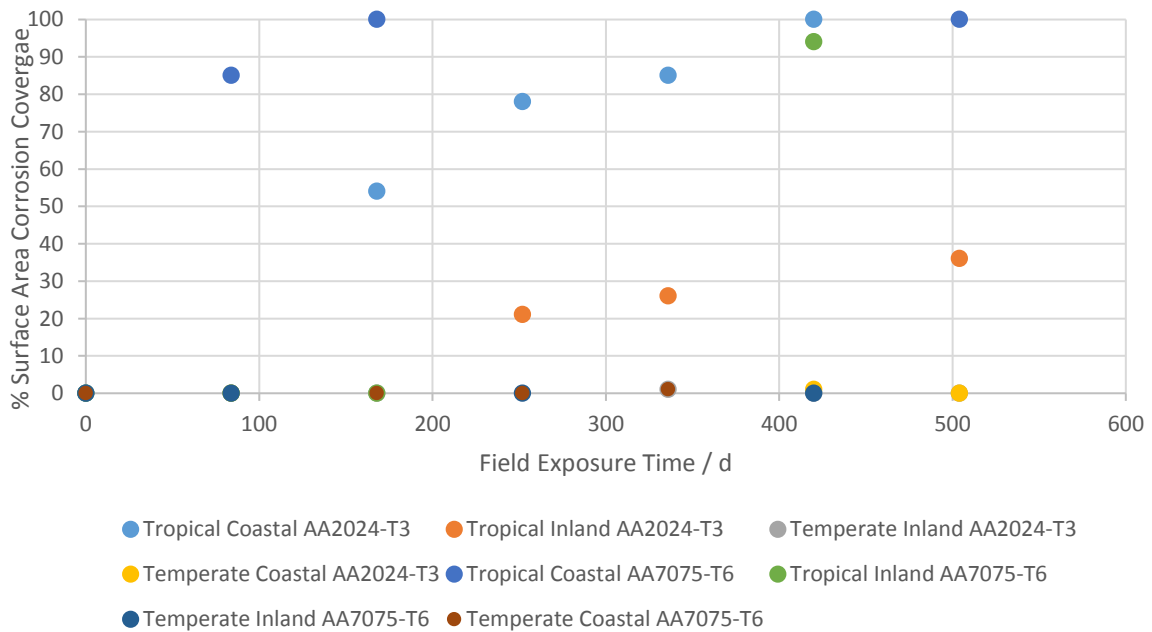


Figure 39: Coating System 2 Topcoat percentage surface area corrosion coverage vs. exposure time.

Coating system 4 provides the singularly best coating system tested. During all field exposures coating system 4 showed very little corrosive response. Only a single coupon showed any signs of corrosion, with 1 % corrosion seen after 336 days exposure of an AA7075-T6 coupon at the tropical coastal site. All other coupons of coating system exposed to the field sites remained intact with no visible corrosion identified. With the ultimate intent of the study being to provide a test that is able to identify the best coating to use in service. It is clear that from the perspective of field exposures, coating system 4 far exceeds the performance of all other coatings studied in the work. What is most unusual regarding the performance of coating system 4 is not the protection afforded by the complete system, but instead the protection of the areas of the coupons that are incomplete with respect to the system as a whole. Together the pre-treatment and topcoat create enough protection to inhibit the formation of surface corrosion even whist exposed to the most aggressive field site.

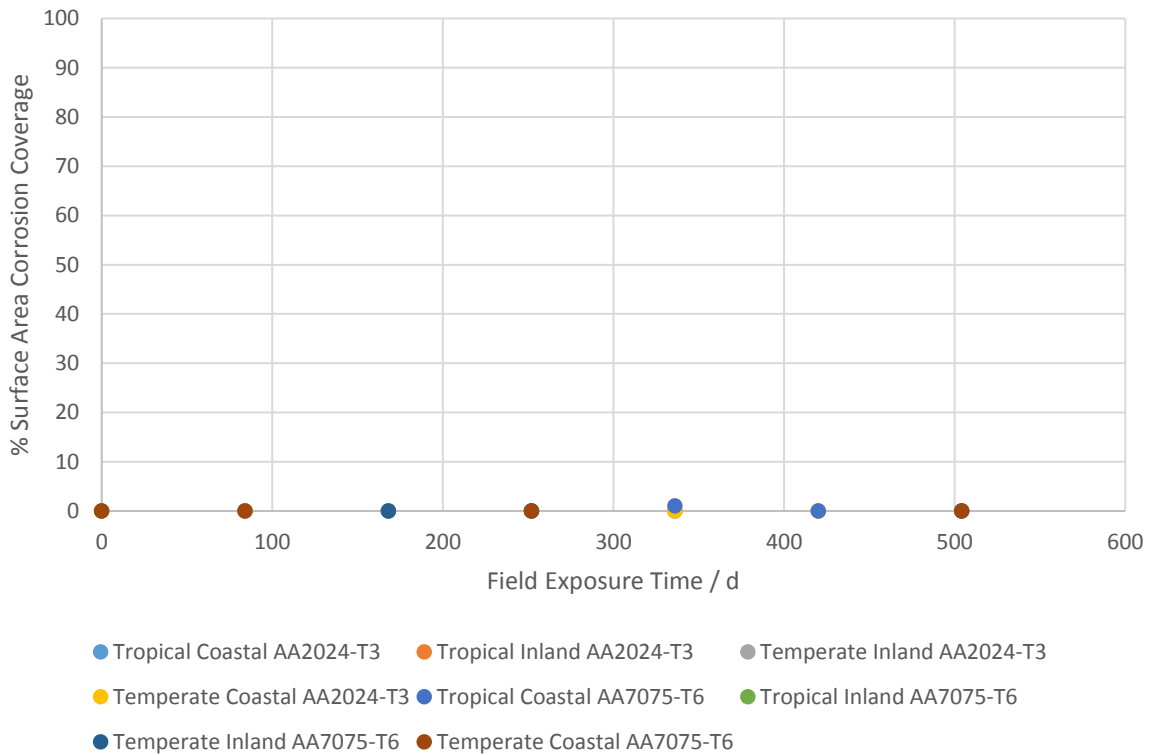


Figure 40: Coating System 4 Topcoat percentage surface area corrosion coverage vs. exposure time.

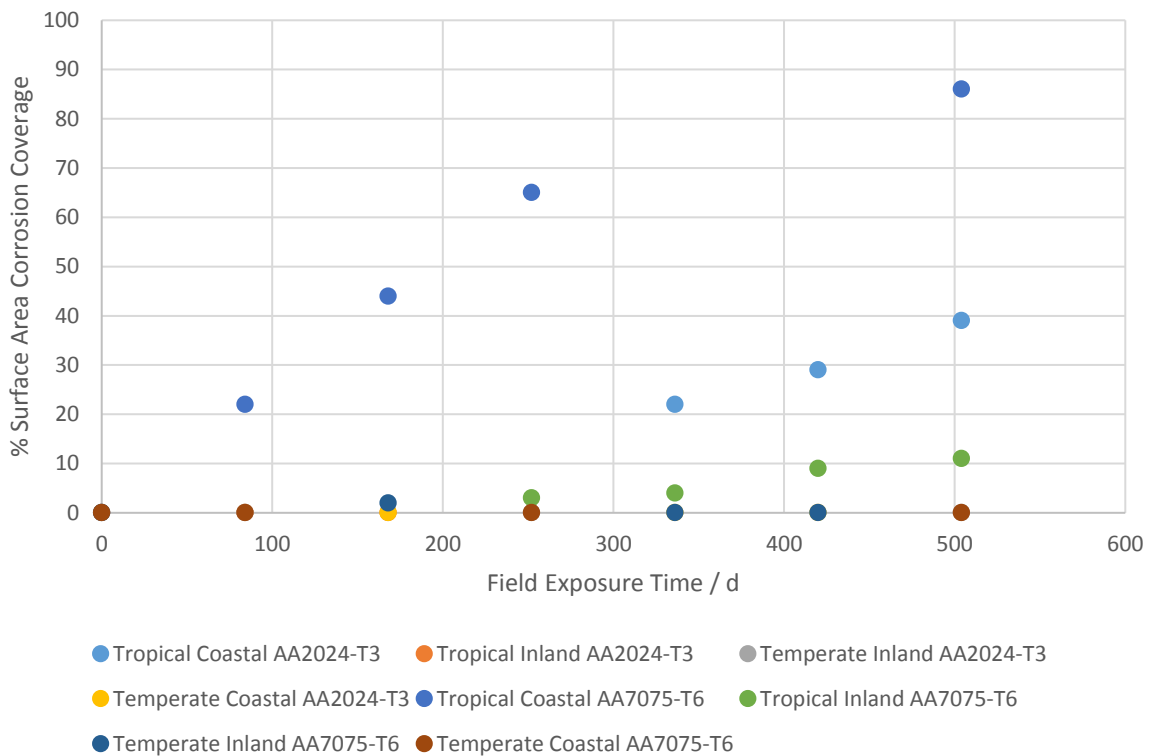


Figure 41: Coating System 5 Topcoat percentage surface area corrosion cover vs. exposure time.

Coating system 5 shows an enhanced performance when compare to coating systems 1 and 2. Similarly to coating system 2, coating system 5 was most affected by the tropical coastal site. The AA7075-T6 corroded faster than the AA2024-T3 coupons. AA7075-T6 coupons exposed to the tropical inland site underwent the greatest surface corrosion after both substrates exposed to the tropical coastal site.

3.5. Summary

The purpose of the chapter was to explore the effects that different in-service environments have on the lifetime of a coating system exposed to them. Fundamentally this identifies if it was possible to create a single accelerated protocol to predict the lifetime of possible coatings when used in-service. This was achieved through examination of the following:

1. In-service locations for UK military aircraft;
2. The frequency of flight for UK military aircraft;
3. The effect of exposure to one of four distinct exposure environments to the set of substrates and coating systems.

To explore a test able to predict the service life of a coating system it was first important to define environments that could influence the service life of military aircraft. This was defined through identification of active UK military bases holding aircraft both in the UK and abroad, as well as sites identified on by the MOD as areas of active military operations. This resulted in a broad spectrum of possible service environments. At a top level the lifetime an aircraft is in-service can be split into two phases, ground based and flight based. It was identified that for military aircraft the balance between the two phases greatly favours time spent on the ground. In response to this and the need to limit the number of environments tested, it was decided that this work would focus on the ground environments possible in-service, as these make up the majority of the service life of aircraft. One point for consideration not included in this research is the transient nature of aircraft. Excluding the actual flight, military aircraft often are held at multiple sites throughout their lifetimes. This work focuses on exposure to single environments only. The potential compounding effects of exposure to multiple environments could be a focus of further research in to the topic of the effects of service on military aircraft coatings.

The identification of the effect to coating degradation different environments have was explored through the use of field exposures. The four sites were selected to provide a variation in temperature, humidity and salinity. The tropical coastal site was identified as being the most damaging to the coating and substrates. The effect of the environment on specific coatings is also different, with coating system 4 showing almost no measureable undercoating corrosion when exposed to any environment. This was not the case for coating system 1 where changes to film thickness, hardness and undercoating corrosion were measured after exposure to a number of the testing environments. The data collected although valuable was limited by the inability to complete chemical analysis on the coatings. If chemical analysis had been possible it may have been conceivable to attribute specific measured changes to chemical processes undertaken as a result of the combination individual exposure environment and specific coating. This could then have informed the later development of the accelerated protocols.

A result of the varied response of coatings exposed to different field sites, the key conclusion to be drawn from this chapter is that a generic test protocol such as the BS EN ISO 9227 would be unable to predict in-service performance of aircraft housed at the numerous sites held by the UK military. It should also be noted that a single exposure site would not be enough detail to predict the lifetime of a coating in-service, unless the aircraft in question were housed only at the specified environment for the entirety of the aircrafts life. It is however the simplest place to begin, hence the purpose of Chapter 5 to explore the potential of acceleration and replication of a specific field exposure.

4. Incompatibility of the Standard BS EN ISO 9227 Performance with Natural Exposures

4.1. Introduction

The performance of a coating and its predicted lifetime is not only a factor of formulation. The effect of the exposure environment for six coating systems and two substrates was explored in the previous chapter. The coating systems were exposed to four distinct environments and a variation in response was measured for most of the coatings when compared between the sites. The tropical coastal site was identified as the most aggressive (CX), and the temperate inland was often the least (C3) [78]. This chapter aims to identify if the BS EN ISO 9227 protocol is representative of any of the exposure environments previously explored.

BS EN ISO 9227 is often used in industry and academia for the development of new coatings, it is used as an iterative step in development prior to natural exposure testing. Industrial manufacturers and academic research groups use the comparative data created from application of the BS EN ISO 9227 to rapidly eliminate poor quality coating formulations, prior to the completion of costly and time consuming natural exposure experiments. As a result of its wide use as a development test, organisations and/or end-users such as DSTL have utilised the BS EN ISO 9227 to bench mark coatings and make selections of preferred coatings for fleet wide use. Hence, the success of a coating is often defined for the end-user by its ability to defend against the BS EN ISO 9227 environment for a specified period of time rather than required service life. This choice can result in end-user requirements detailing performance metrics for BS EN ISO 9227 rather than survival in service. The

difficulty arises when coatings that perform well under BS EN ISO 9227 condition fail prematurely in service. The premature failure being a direct result of assumed performance of a complex heterogeneous coating system in a simplified environment will be matched when exposed to a fluctuating multidimensional environment.

The selection of coatings for service using accelerated corrosion tests rather than natural exposures by the end-user is not without reason. With developments in coating science, new coatings are able to withstand natural service life weathering for many years. With the need for decisions to be made on more rapid timescales, it is clear that analysis using natural exposure tests could become unfeasible.

In this chapter widely used accelerated corrosion tests will be reviewed and their suitability discussed. In addition an overview of corrosion of aluminium alloys and protective coating failure mechanisms will be given prior to the chapter's experimental section. Experimentally a comparison will be made between samples exposed to four different natural exposures and the BS EN ISO 9227 accelerated salt fog test. Using post exposure analysis, multiple coatings across each of the five tests will be compared and success of BS EN ISO 9227 as a replication of service life will be determined. The results will also act as a benchmark for any novel accelerated tests developed as a part of this work. If the novel test provides no better information regarding service-life performance than the BS EN ISO 9227 accelerated test its validity for further development is brought into question.

4.1.1. Accelerated corrosion tests

Although performance of coatings relative to BS EN ISO 9227 will be the focus of this chapter there is a multitude of accelerated corrosion tests available. Tests include static temperature and humidity experiments such as the BS EN ISO 9227, alongside various cyclic protocols [1, 7]. The cyclic protocols can include multiple temperature and humidity hold points as well as atomised pollutants such as NaCl or SO₂ and UV exposure [87, 94]. A number of protocols have been identified and are defined in Table 27.

Table 27: Current Accelerated Test Protocols

Test Regime	Regime Developer	Environmental Description	Temperature	RH	Pollutant	UV
BS EN ISO 9227 [1]	British Standards	Scored coupons are exposed at a 45° incident angle to a constant 5 wt.% NaCl atomised salt water solution with pH between 6.5 and 7.2. The deposition rate of is 1.5 mL h ⁻¹ over 80 cm ² . The chamber is held at 35°C ±2°C.	Static	Uncontrolled	Constant	None
ASTM B117 [6]	ASTM International	Scored coupons exposed to a constant 5 wt.% NaCl atomised salt water solution with pH between 6.5 and 7.2. The deposition rate of is 1.5 mL h ⁻¹ over 80 cm ² . The chamber is held at 35°C ± 2°C.	Static	Uncontrolled	Constant	None
ISO 6270 –CH [95]	International Organization for Standardisation	Coupons exposed at a minimum of 60° incident angle in a constant humidity condensation atmosphere with air temperature of 40°C ± 3°C at 100 % RH. A minimum of 10 mm of water must be present in the base of the chamber throughout testing.	Static	Static	None	None
ISO 6270 – AHT [95]	International Organization for Standardisation	Coupons exposed for 8 h to a 40°C ± 3°C at 100% RH, followed by a cooling period for 16 h with air temperature between 18°C – 28°C and RH approaching ambient. A minimum of 10 mm of water must be present in the base of the chamber throughout testing.	Varied	Varied and uncontrolled	None	None
ASTM G85 Annex A1 – continuous acetic acid salt spray [94]	ASTM International	Scored coupons exposed to a constant 5 wt.% NaCl atomised salt water solution acidified by the addition of acetic acid to a pH between 3.1 and 3.3. The deposition rate of is 1.5 mL h ⁻¹ over 80 cm ² . The chamber is held at 35°C ± 2°C.	Static	Uncontrolled	Constant	Static
ASTM G85 – Annex A2 Cyclic acidified salt spray (MASTMAASI S test) [94]	ASTM International	Coupons exposed to a three stage 6 h cycle. The first stage is a 45 min acidified salt spray. A 5 wt.% NaCl solution is acidified with acetic acid to a pH between 2.8 and 3.0 and is deposited onto the coupons at a rate of 1.0 to 2.0 mL h ⁻¹ 80 cm ² . The second stage is a dry air purge, where the relative humidity of the chamber is driven as low as possible for 2 h. The third stage	Varied	Varied	Varied	None

		is 3.25 h with coupons exposed to 98% RH. All three stages are completed with a fixed temperature of $49^{\circ}\text{C} \pm 2^{\circ}\text{C}$.				
ASTM G85 – Annex A3 Seawater acidified test (SWAAT test) [94]	ASTM International	Coupons exposed to a 2 h varied humidity cycle, with an elevated temperature maintained for the duration of the experiment. When coupons are uncoated this temperature is $49^{\circ}\text{C} \pm 2^{\circ}\text{C}$, when coated the temperature is reduced to between 24°C and $35^{\circ}\text{C} \pm 2^{\circ}\text{C}$. The cycle is defined by two steps. Step 1 is a 30 minutes indirect sea salt spray, the solution replicates the major salt constituents of sea water, acidified with acetic acid to a pH of between 2.8 and 3.0. Step 2 exposes the coupons to 90 minutes at 98 % RH with no sea salt solution spray.	Static	Varied	Varied	None
ASTM G85 - Annex A4-1 SO ₂ Cyclic salt spray test [94]	ASTM International	A constant salt spray is applied to the coupons, with the chamber held at a constant 35°C . The salt spray is 5 wt.% NaCl and has pH between 6.5 and 7.2. In addition to the salt spray the coupons are dosed for 1 h every 6 h with SO ₂ gas at a rate of $35\text{ cm}^3\text{ min}^{-1}\text{ m}^{-3}$ of chamber volume.	Static	Uncontrolled	Constant	None
ASTM G85 - Annex A4-2 SO ₂ Cyclic salt spray test [94]	ASTM International	Coupons exposed to a three stage cycle, stage 1 is a 0.5 h salt spray, the solution is 5 wt.% NaCl with a deposition rate of between 1.0 mL and 2.0 mL h^{-1} over 80 cm^2 . The second stage is a 0.5 h sulfur dioxide (SO ₂) at a rate of $35\text{ cm}^3\text{ min}^{-1}\text{ m}^{-3}$ of chamber volume. The third stage is a 2 h undefined high humidity soak. All three cycles are completed at a fixed temperature of $35^{\circ}\text{C} \pm 2^{\circ}\text{C}$.	Static	Varied	Varied	None
ASTM G85 - Annex A5 Dilute electrolyte cyclic fog/dry test (Prohesion test) [94]	ASTM International	The protocol is a 2 h cycle with two 1 h stages. Stage 1 is completed at ambient conditions (between 21°C and 27°C), with an atomised electrolyte spray depositing at a rate of 1.0 mL to 2.0 mL h^{-1} over 80 cm^2 . The electrolyte is an aqueous solution of 0.05 wt.% NaCl and 0.35 wt.% ammonium sulfate, (NH ₄) ₂ SO ₄ . The second stage is again 1 h and is a constant temperature of $35^{\circ}\text{C} \pm 2^{\circ}\text{C}$ along with a humidity purge and no electrolyte spray.	Varied	Uncontrolled	Varied	None
Hyper test [87]	University of Surrey	Between 1 and 120 minutes exposure to a UV source and ozone (O ₃).	Uncontrolled	Uncontrolled	Static	Static

ASTM D5894 [96]	ASTM International	The ASTM D5894 protocol combines the Prohesion test protocol with a UV condensation exposure. It is completed using two chambers, alternated weekly. The first week is in a cyclic corrosion chamber, coupons are exposed to alternating salt fog and dry air purging at 1 h intervals. The salt solution used is 0.5 wt.% NaCl and 0.05 wt.% (NH ₄) ₂ SO ₄ with a pH 5 to 5.4. The chamber is held at 25°C for the salt spray, the temperature is then increased for a 1 h dry air purge at 35°C. The second week is completed in a QUV chamber. The coupons are irradiated with UV light for 4 h with the chamber held at 60°C, followed by a 4 h pure water condensation stage at 50°C.	Varied	Uncontrolled	Varied	Varied
Thermal cycling method [5]	North Dakota State University	The testing protocol is a varied temperature full immersion test where coupons are cycled through 9 heating and cooling steps. The 9 step cycle is then repeated 3 times followed by a 3 day room temperature soak. The coupons were immersed in a dilute Harrisons solution (0.05 wt.% NaCl and 0.35 wt.% (NH ₄) ₂ SO ₄). The temperature cycle is 24 h in total, and cycles up from room temperature to 85°C and back down to room temperature.	Varied	Full Immersion	Constant	None
ECC1 D172028 [7]	Renault	The testing protocol is a fixed temperature varied humidity test where coupons are also exposed to a salt spray with a pH of 4 for 30 min per day at a deposition rate of 5 mL h ⁻¹ . The chamber environment is then cycled through three humidity stages. The first is 1 h and 35 minutes and the chamber is held a 20 % RH. The stage is 2 h and 40 minutes and the RH is increased to 55 %. Finally the RH is increased once more to 90 % where it is held for 1 h and 20 min. The RH cycle repeats, punctuated by a salt spray deposition once a day for a total of 42 days.	Static	Varied	Varied	None
GM9540P [7]	General Motors	The testing protocol is a varying temperature and humidity experiment with a salt solution deposited four times per day. The salt solution is 0.9 wt.% NaCl, 0.1 % calcium chloride (CaCl ₂) and 0.255 wt.% sodium bicarbonate (NaHCO ₃), the solution pH is held between 6 and 9. The protocol used a 2 step cycle, with a temperature cycle of 50°C and 60°C alongside a	Varied	Varied	Varied	None

		RH cycle from 100 % to 30 %. The total test duration is 40 days.				
PV1210 [7]	Volkswagen	The testing protocol is a varied temperature and humidity experiment. The coupons are exposed to a 5 wt.% NaCl solution with a pH between 6.5 and 7.2, a 1.5 mL h ⁻¹ deposition rate for 4 h per day. The coupons are exposed to a cyclic temperature sequence between 23°C and 40°C and fixed humidity points of 50 % maintained for 4 h and 100 % for 16 h. The total test duration is 42 days.	Varied	Varied	Varied	None
KWT-DC [7]	Daimler - Chrysler	The Daimler Chrysler protocol is a varied temperature and humidity test. Coupons are exposed to a 1 wt.% NaCl solution with a pH between 6.5 and 7.2. The deposition rate is 2 mL h ⁻¹ with the coupons exposed for 2 h, four times per week. The coupons are exposed to a temperature sequence that cycles between -15°C and +50°C with a relative humidity range of 50 % to 100%. The total test duration is 42 days.	Varied	Varied	Varied	None

Static temperature experiments such as the ASTM B117 and G85 tests are not representative of an in-service environments. In-service the temperature and humidity change as a part of the diurnal cycle as well as more long term seasonality. Static tests such as the ASTM B117 do not take this into account and as a result the coatings are not subjected to the changes to water ingress and thermal expansion that would be experienced in-service. Instead when test coatings are held at a constant temperature. The change in temperature would also have an effect on the uptake of water by the polymer [97]. An increase in temperature will increase the rate that water is able to move through the system. In a static temperature and humidity test with a heightened temperature, the uptake will rapidly reach equilibrium with the environment and will only be changed by the addition of further corrodent.

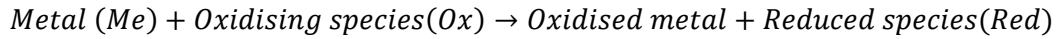
NaCl is often used as the pollutant in accelerated corrosion testing protocols, typically a concentration of 5 wt.% and a deposition rate of $1.5 \text{ mL h}^{-1} 80 \text{ cm}^{-2}$ is used, and wet phase deposition can range from 3.5 h per week to 168 h per week. Meaning the mass of NaCl applied to the coupons ranges between $0.265 \text{ mg } 80 \text{ cm}^{-2} \text{ week}^{-1}$ and $12.726 \text{ mg } 80 \text{ cm}^{-2} \text{ week}^{-1}$. Even when other corrodents are used often they are used in isolation, this limits the possibility of secondary reactions and symbiotic effects from occurring that would naturally occur in service, i.e. the oxidation of the bisulfate ion to the sulfate ion prior to reaction with the metallic substrate, which required the collocation of an atmospheric oxidant [98].

Often accelerated testing protocols have the inclusion of artificial damage to the surface of the coupons. However, the scribing is not representative of in-service damage, and instead is there to provide a gauge of how the coating is able to protect the underlying substrate from direct electrolyte attack [5]. By breaking the intact surface barrier, it makes it unlikely that the coupon will undergo the same degradation as an untouched coupon.

4.1.2. Corrosion

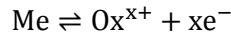
Corrosion is the irreversible interfacial process that results from an electrochemical reaction occurring at the surface of a metal in contact with its surrounding conductive environment [99]. For corrosion to occur the system in question must conform to five conditions: there must be anodic regions, cathodic regions, cathodic reactants, electrical contact between the anodic and cathodic regions and an electrolyte in contact with the anode and the cathode [100]. If all five conditions are met the system is in a position where corrosion is feasible. The occurrence of corrosion is dependent on the thermodynamics of the reaction involved. If the Gibbs energy change (ΔG) of the system is negative then corrosion will spontaneously take place [101]. What Gibbs energy change does not provide is how fast the reaction will occur; this is defined by the reaction kinetics. The corrosion of metals is due to irreversible oxidation-reduction (redox) reactions between the metal and an oxidising species in the environment [101].

Equation 6: Redox corrosion reaction

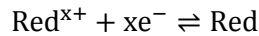


The reactions which occur are dependent on the material and environment the metal is situated within, below are generic forms of oxidative and reductive half-cell reactions [100].

Equation 7: Oxidative half-cell reaction



Equation 8: Reductive half-cell reaction

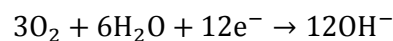


The oxidative reactions are defined by a loss of electrons whilst the reductive reaction gains additional electrons. Oxidation and reduction reactions are symbiotic in nature, one cannot occur without the other. As illustrated by Figure 42, aluminium, and its alloys, in an aerated solution the typical anodic and cathodic reactions are as follows;

Equation 9: Anodic half reaction - metal dissolution



Equation 10: Cathodic half reaction - oxygen reduction reaction



In acidified solutions such as in a pit environment, a result of aluminium ion hydrolysis, hydrogen reduction occurs:

Equation 11: Cathodic half reaction - hydrogen evolution reaction

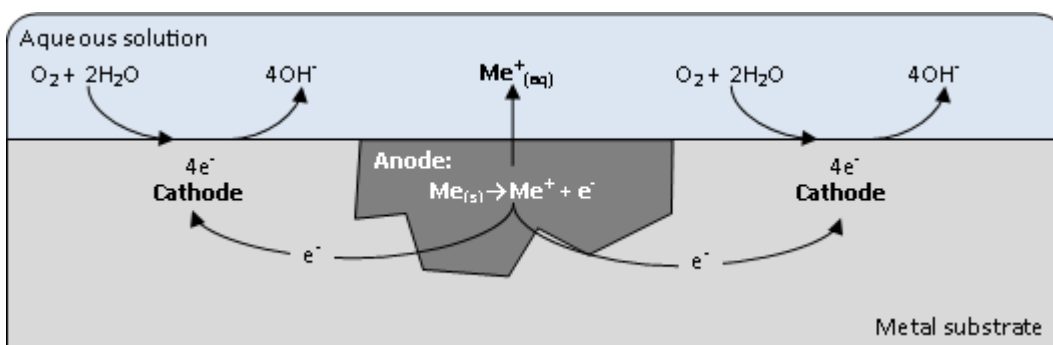
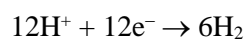


Figure 42: Schematic diagram of aqueous corrosion at metal solution interface.

4.1.3. Atmospheric and bulk solution corrosion

Corrosion measured under thin electrolyte layers in numerous investigations [102-106] has been shown to be very different from that in the bulk solution, this is a result of the ability oxygen to be transported to the surface and its effect on reduction kinetics. Solution film thickness can range from millimetre down to nanometres; when studying atmospheric corrosion the solution depth of interest is most often in micrometres [107].

4.1.4. Corrosion of aluminium and aluminium alloys

Aluminium and its alloys are divided into two main classes, castings and wrought or mechanically worked products. The latter can be further subdivided into heat-treatable and non-heat-treatable alloys, and into various forms produced by mechanical working. Uniform atmospheric corrosion rates for aluminium are typically $0.0 - 0.1 \mu\text{m y}^{-1}$ for rural areas, with marine areas being more corrosive with uniform rates being $0.4 - 0.6 \mu\text{m y}^{-1}$ [85]. Urban environments are the most corrosive because of the high concentrations of sulphate ions, resulting in a corrosion rate of up to being roughly $1 \mu\text{m y}^{-1}$ [85]. The corrosion resistance of aluminium is dependent on a thin protective oxide film (often termed a passive film) [108]. The passive film is formed when aluminium undergoes a rapid redox reaction when in contact with aqueous environments, the resulting film is insoluble and semi-conducting [108]. At room temperature a film thickness of $2 - 4 \text{ nm}$ formed of $\text{Al}_2\text{O}_3 \cdot \text{H}_2\text{O}$ is expected [108]. To achieve thicker films the temperature must be raised ($<100^\circ\text{C}$), with the resultant film formed of two phases. The internal phase is alumina (Al_2O_3) and the external phase is a mixture of boehmite (AlOOH) and bayerite ($\text{Al}(\text{OH})_3$) [108]. The band gap associated with an Al_2O_3 passive film is $\sim 3 \text{ eV}$, whilst the value for bulk (monolithic) Al_2O_3 is $8-9 \text{ eV}$, the larger the band gap the greater the energy requirement to release an outer electron from its nuclear orbit resulting in a mobile charge carrier [109]. Thus, the passive film on aluminium is a better conductor than the same material when in a bulk form.

The thermodynamic stability of the passive film can be graphically represented by a Pourbaix diagram, see Figure 43 [110]. This oxide film (hydrargillite) is thermodynamically stable in aqueous media when the pH is between about 4.0 and 8.5. The passive core is bound on either side by corrosive zones where by the stable chemical compounds are dissolved ions; Al^{2+} , Al^{3+} , or AlO_2^- . The zone whereby Al is stable is referred to as the immunity zone and is where Al is thermodynamically stable in its solid form. The dashed lines are markers for environmental cathodic reactions, the hydrogen evolution reaction (labelled a) and the oxygen reduction reaction (labelled b) [110]. The general consensus for Al and its alloys is that they are resistant towards corrosion in mildly aggressive aqueous environments. The protective oxide layer represents the thermodynamic stability of Al alloys in corrosive environment, the oxide film is known to convert

to its hydrous form in the presence of water or water vapour, the hydrous film is often porous and can lead to activation of the underlying surface [111].

While the passive layer breakdown mechanism by chloride ions is still a matter of some uncertainty and controversy due to the complexity of the process, the general consensus is that localised attack starts by adsorption of aggressive anions and formation of soluble transitional complexes with the cations at the oxide surface [109, 112, 113]. Thermodynamic principles used to explain and predict the passivity phenomenon that controls the corrosion behaviour of Al can be summarised by Pourbaix-type analysis. With respect to atmospheric corrosion, the Figure 43 Pourbaix diagram does not provide any useful information with respect to pitting corrosion, which is characteristic of chloride containing environments [114].

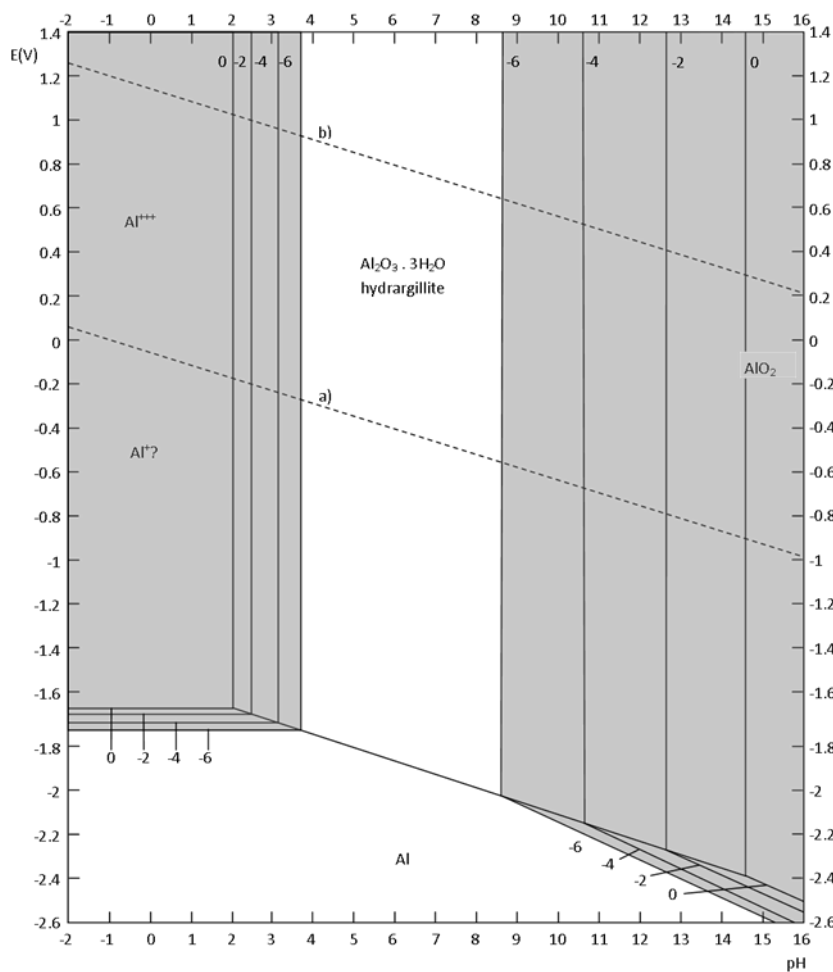


Figure 43: Pourbaix (E-pH) diagram for the aluminium-water system at 25°C (E / V vs. SHE) [9].

The E -pH diagram is an over simplified model of the overall corrosion processes, in actual engineering applications there are several variables that are not considered by Pourbaix. These include: (i) the presence of alloying elements in most engineering metals; (ii) the presence of substances in the electrolyte such as chloride (albeit that this has been addressed in more modern computations); (iii) the operating temperature of the alloy; (iv) the mode of corrosion, and (v) the

rate of reaction. Taking these factors into account is nominally done on a case by case (*i.e.*, alloy by alloy) basis, and a revised version of an E-pH diagram for 5xxx series alloys in 0.5 M sodium chloride is given in Figure 44.

Figure 44 indicates windows where localized attack is highly possible in the supposed passive region. It is also seen that localised attack is possible across the whole range of pH depending on the specific potential. One should therefore not rely solely on the Pourbaix diagram as a direct index to actual corrosion rates, with rates needing to be independently measured for a given alloy-electrolyte combination [115]. Finally, whilst not to be discussed in detail here, it is prudent to indicate that effectively all Al-alloys do not attain practical/empirical immunity as evidence in. Cathodic polarisation tends to contribute to alloy deterioration by two modes. Firstly, the accumulation of hydroxyl ions at the Al-surface will cause chemical dissolution of the Al. Secondly, Al is a very strong hydride former, and hydrogen from the cathodic reaction at such negative potentials will serve combine with Al to form hydrides.

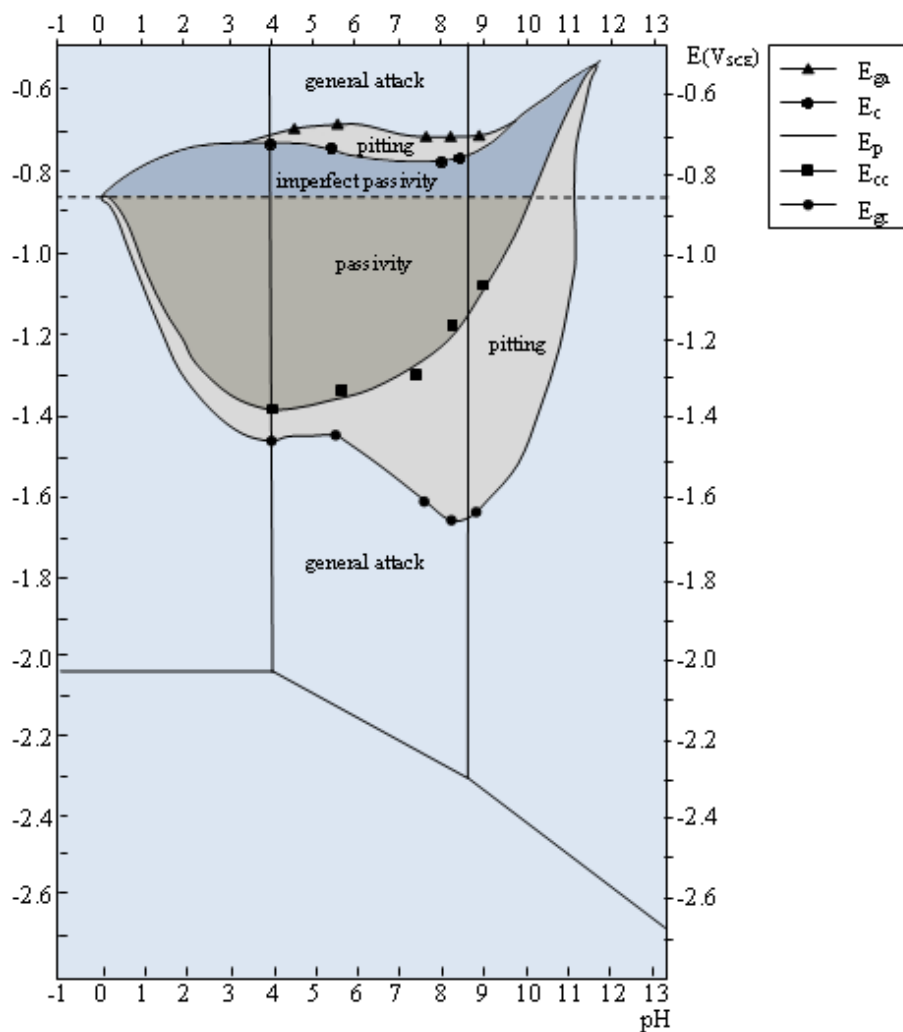


Figure 44: Mode of corrosion based on experimental data for AA5086 in the presence of 0.5 M sodium chloride [116].

Being heterogeneous, age hardened (sometimes referred to as precipitation hardening) alloys are predisposed to localised corrosion due to intrinsic potential differences between the matrix and intermetallic particles. The potential difference between intermetallic particles of AA2024-T3 and their surrounding matrix has been investigated by De Wit, Frankel and Schmutz [117-119]. Scanning Kelvin Probe Microscopy was used by Frankel and Schmutz to simultaneously measure topography and potential distribution of the surface of AA2024-T3 in air. It was identified that in air all surface intermetallic particles are noble with regard to the matrix, a result of passive film formation [117]. If exposed to a NaCl solution or damage to the passive film occurs through *in situ* atomic force microscopy scratching the potential of magnesium containing intermetallic particles shifts to become anodic with respect to the matrix [118]. De Wit identified the potential of known intermetallics of AA2024-T3. The potentials of Al₂CuMg and Al₂Cu were identified as -0.910 V and -0.640 V when measure at room temperature in 53 g L⁻¹ NaCl solution with an additional 3 g L⁻¹ of H₂O₂ using a saturated calomel electrode (SCE) [119]. This can be compared to the average value for AA2024-T3, -0.690 V (SCE) measured under the same conditions [108]. It should be noted that the magnesium containing particle is more anodic than the bulk material. The anodic nature of magnesium containing intermetallic particles is often cited as one of the main causes of localised corrosion. It may seem from the work of Frankel and Schmutz that these conclusions contradict one another. However, the cathodic nature of the magnesium containing particles in air is directly a result of the preparative and testing environments which facilitated the growth of a passive film on the particles in question. These environments are not representative of those experienced by aerospace materials during operation and/or on station. Instead conditions are far closer to those tested which identify magnesium containing intermetallic particles as anodic with respect to the matrix.

In AA7075-T6 it is the anodic magnesium containing Mg₂Si particles which are often identified as the main driving force behind localised corrosive attack. Ryl et al. have identified that under atmospheric conditions (i.e., 22°C and 50% RH) the corrosive resistance of AA7075 actually increases as a result of the formation of a passive film over the Mg₂Si intermetallic particles. The film consists of Mg(OH)₂ and SiO₂ and limits further corrosion of the previously anodic particle [70]. The result is that locally the matrix becomes the anodic constituent

Both AA2024-T3 and AA7075-T6 are specifically susceptible to three types of localised corrosive attack: exfoliation corrosion, filiform corrosion (FFC) and pitting. For aluminium alloys pitting is often associated with a micro-galvanic coupling due to zones of potential difference which occur across the surface of the material as a result of the alloys' intermetallic microstructure. There are four stages associated with the pitting phenomena [109]:

- Reactions occurring on the surface of the passive film which is in contact with the ionic solution;
- Reactions occurring within in the passive film;
- Metastable pitting, where by pits form but quickly repassivate;
- Stable pit growth below the critical pitting potential.

Figure 45 shows the formation of partially soluble aluminium hydroxychloride and hydrogen ions in the base of a pit. The propensity for the pit to propagate is dependent on this layer of aluminium hydroxychloride. A micro-pit ($\phi \sim 0.1 \mu\text{m}$) will result if the aluminium hydroxychlorides solubilise faster than they are produced, meaning no layer forms at the base of the pit. However, if aluminium hydroxychlorides are formed faster than they dissolve, the pit will propagate. The rate of formation of the aluminium hydroxychloride is dependent on the cathodic area associated with the particular pit, if the requirement for electrons is great enough the rate of oxidation of aluminium is fast enough to initiate pit propagation. A result of the formation of the aluminium hydroxychloride is the reduction in pH associated with the formation of hydrogen ions. The increase in pH also acts to drive pit growth. Pit death occurs when the pit current divided by the pit radius (this is often called the pit stability product, ia) decreases to $10^{-2} \text{ A cm}^{-1}$. This results in dissolution of the aluminium hydroxychloride layer and the pit repassivating when in contact with bulk solution.

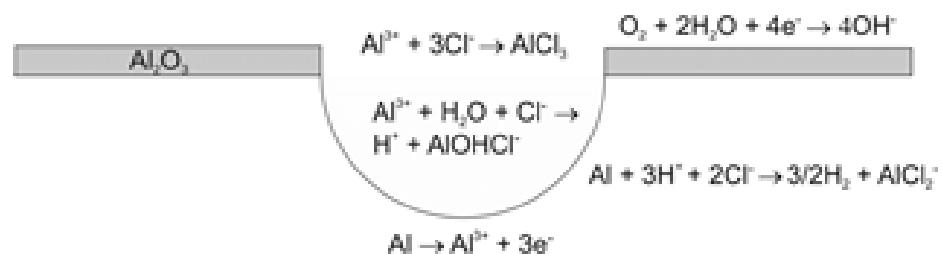


Figure 45: Simplified electrochemical mechanism of pit growth on aluminium showing its autocatalytic self-stimulating nature.

For AA2024-T3 the majority of pitting has been attributed to two classes of intermetallic particles, those which are composed of Al-Cu-Mg, and are anodic with respect to the metal matrix and those which are composed of Al-Cu-Mn-Fe-Si which are cathodic in nature with respect to the metal matrix. The nature of Al-Cu-Mn-Fe-Si particles and their part in pitting is one of general consensus amongst researchers [64, 118, 120]. However, the behaviour of the Al-Cu-Mg particles in the mechanism of pitting of AA2024-T3 is still a subject of much debate. It has been suggested that Al-Cu-Mg particles transition from their initial anodic nature to become cathodic with respect to the matrix. Two opposing theories have been presented to explain the transition; the first suggests preferential dissolution of magnesium and aluminium, whilst the second proposes

deposition of additional copper. Figure 46 shows the mechanism associated with copper deposition.

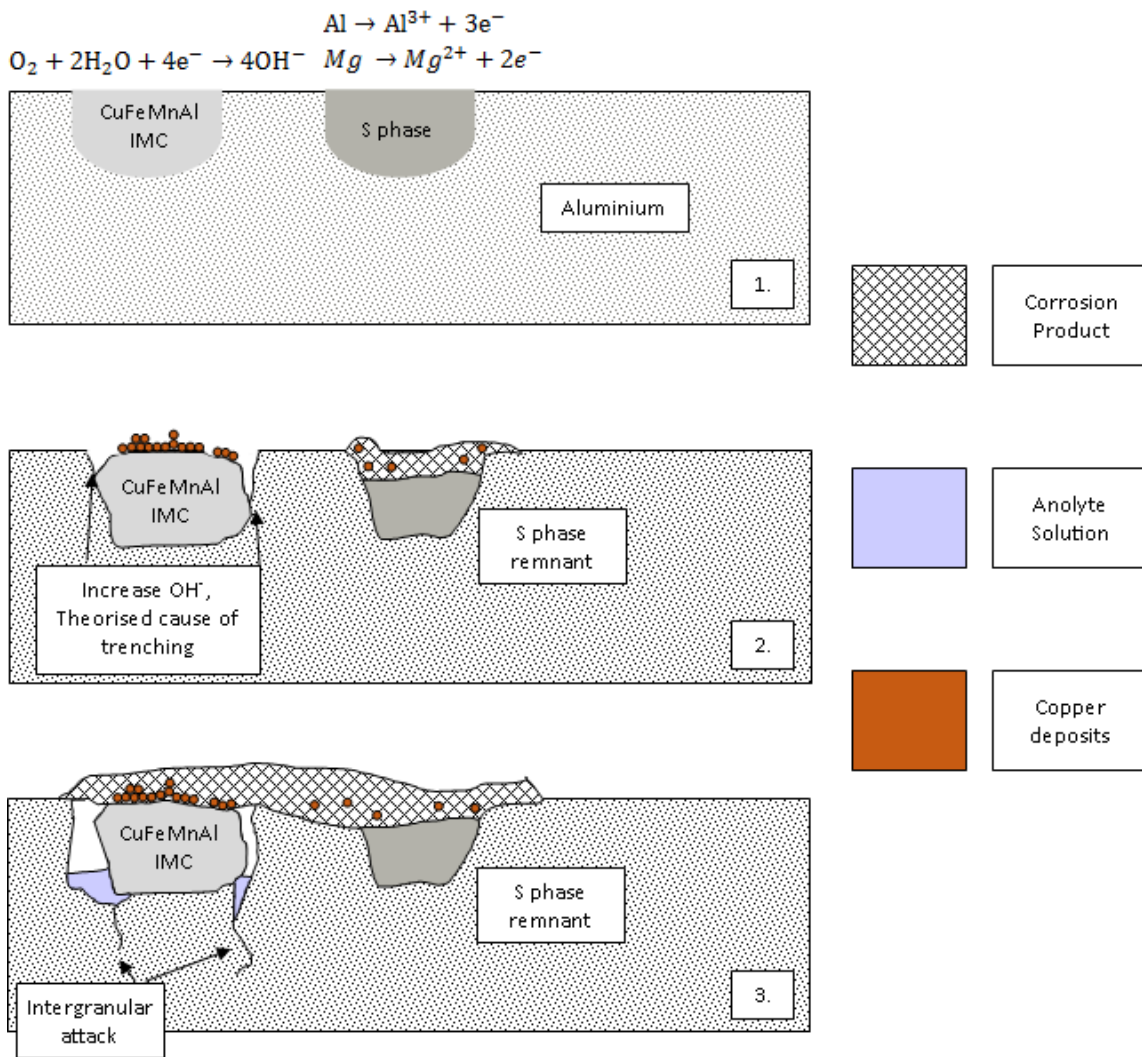


Figure 46: Pitting Schematic: (1) typical exchange current densities, (2) dealloying of s phase and deposition of Cu and (3) trenching of anodic dispersoid free zone around the intermetallic particle.

Aluminium is susceptible to filiform corrosion in the relative humidity range of 75-95%, with temperatures between 20°C and 40°C. Filiforms in aluminium grow most rapidly at 85% RH. Typical filament growth rates average about 0.1 mm day⁻¹ [108]. FFC proceeds due to the formation of a differential aeration cell (oxygen concentration cell), an oxygen deprived anodic head in combination with an oxygen-rich cathodic tail results in a spatially separated active corrosion cell. The differential aeration cell results in a relatively complex chemistry associated with the propagation of the corrosive filament as can be seen in Figure 47. The pure aluminium 1000 series is less prone to filiform corrosion than the alloyed series. The heterogeneous morphology resulting from the alloying elements and the thermo-mechanical treatment of the 2000 to the 8000 series aluminium alloys increases these materials susceptibility towards filiform corrosion. Localised galvanic coupling results when an active filiform head comes into contact with an intermetallic particle, as illustrated in Figure 48. The intermetallic particle can form either

a local cathode or a local anode, if the particle is anodic preferential dissolution of the aluminium can occur; if cathodic there is an increase in corrosion current density [119]. The difference in potential between the head and the tail of the propagating filament can be as much as 0.1 – 0.2 V [108].

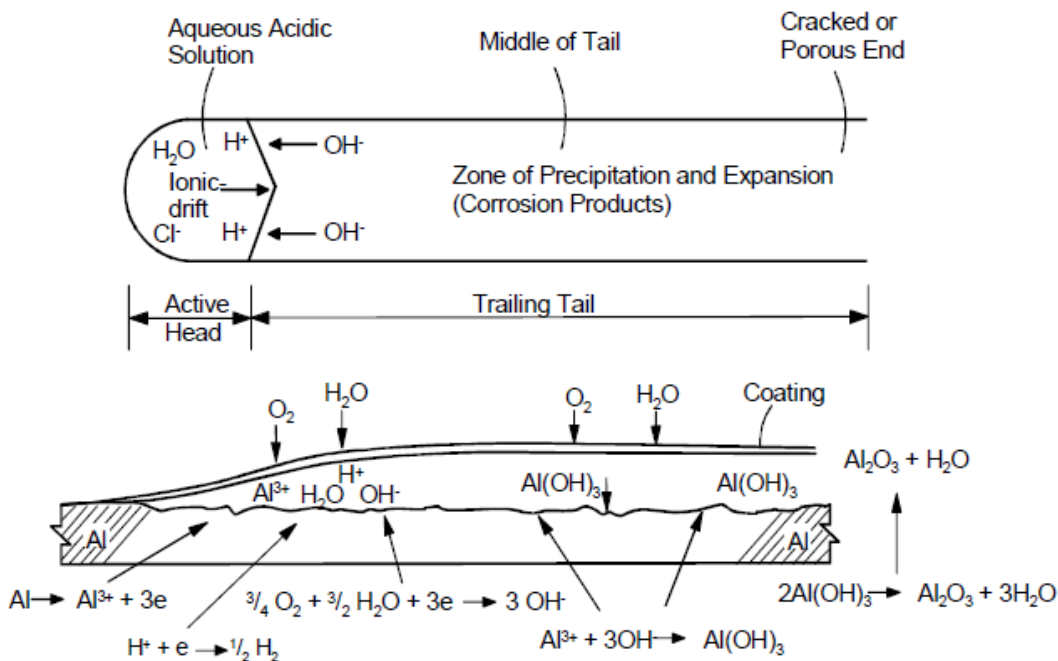


Figure 47: Schematic detailing chemical reactions associated with filiform corrosion [121].

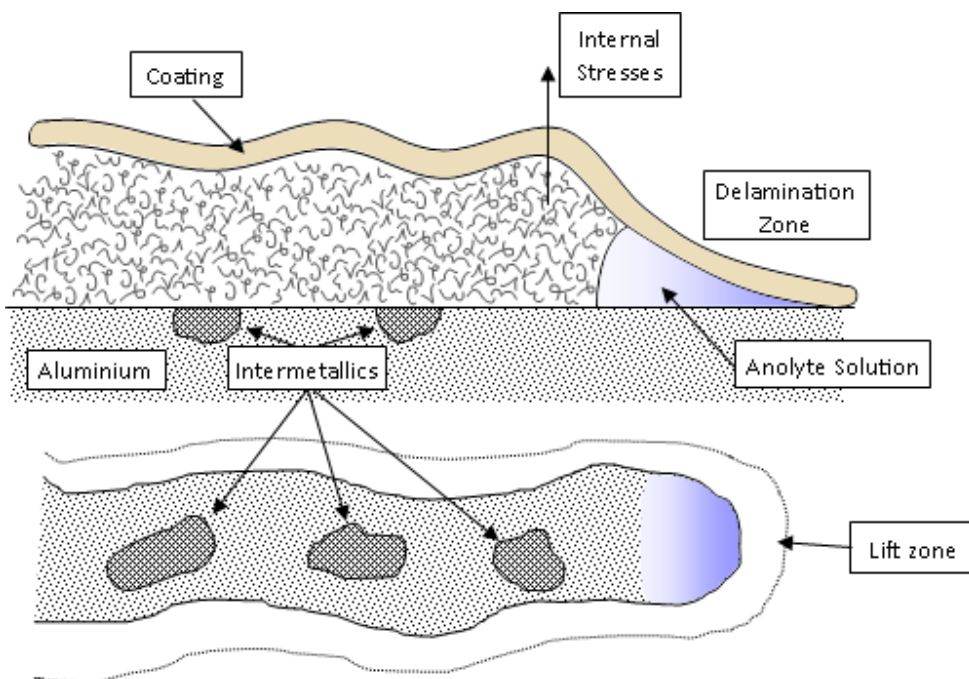


Figure 48: Filiform corrosion: (a) transverse section and (b) plane view.

Exfoliation corrosion is a form of intergranular corrosion. High strength aged aircraft aluminium alloys are particularly prone to this form of corrosion as a result of their heterogeneous microstructures, and the directionality of the microstructures which is a result of the rolling process used for form sheets. Exfoliation corrosion is often seen in the materials when they are operated in environments which are high humidity and high NaCl concentrations [121]. The preferential attack of the grain boundaries associated with intergranular corrosion mechanisms is attributed to micro-galvanic coupling throughout heterogeneous materials. In AA2024-T3 the micro-galvanic couples which are often identified as being responsible for exfoliation corrosion are the copper-rich grain boundaries and the copper depleted precipitation free zones which are adjacent to the grain boundaries. The corrosive behaviour is also heightened by the presence of anodic S-phase particles along the grain boundary [67]. The mechanism by which intergranular corrosion can bring about exfoliation is a result of the corrosion products formed within the grains applying pressure to the remaining material resulting in a leafing effect [121]. This is illustrated schematically in Figure 49. Since the 7000 series alloys are high strength alloys they are also prone to exfoliation corrosion, as can be seen in Figure 50.

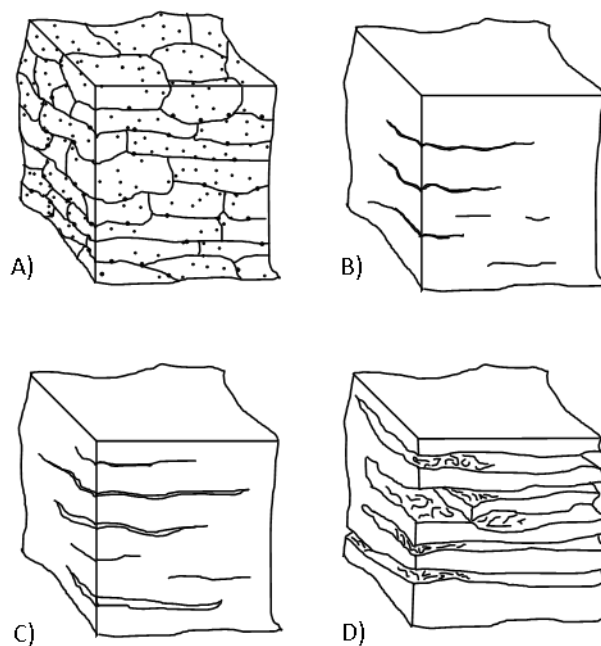


Figure 49: The evolution of exfoliation corrosion: (a) uncorroded microstructure, (b) intergranular corrosion, (c) onset of delamination caused by wedging effect of corrosion products and (d) leafing and loss of structural integrity.

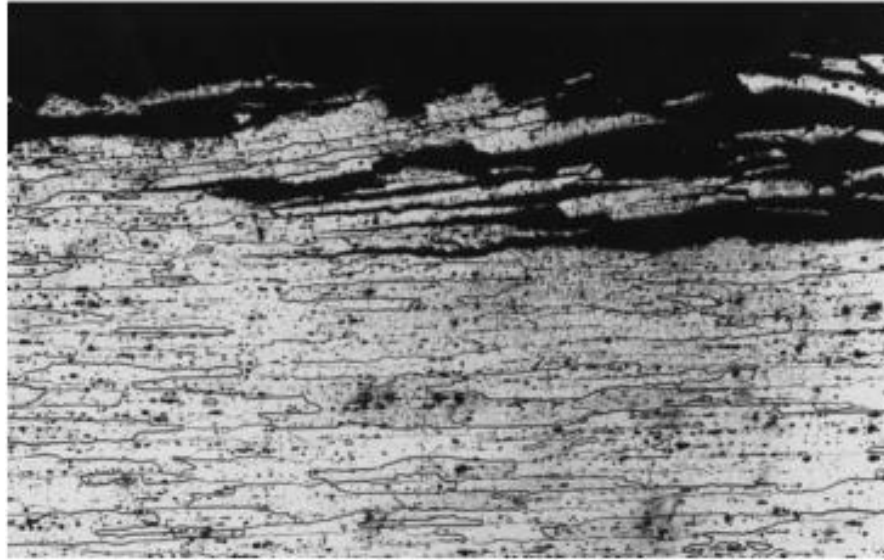


Figure 50: Exfoliation corrosion in a 7000 series aluminium alloy [122].

To protect Al alloy components and structures from the effects of the environment and the risks associated with localised corrosion, multi-layer corrosive resistant coating systems have been developed.

4.2. Experimental Objective

The BS EN ISO 9227 neutral salt spray test is a widely used industry standard accelerated exposure test. It allows for the ranking of coatings performance against that of a neutral salt fog at a fixed heightened temperature. The BS EN ISO 9227 standard reduces the complex phenomena of climate to the control of three environmental variables; temperature, humidity and NaCl concentration. Although controlled with the standard, each of the environmental variables is held at a constant and somewhat unrepresentative level. The objective of this chapter is to compare the performance of a multitude of coatings exposed to a reduced accelerated exposure test alongside natural exposure sites.

4.3. Experimental

4.3.1. Materials

The natural exposure experiments used were the same as those explored in Chapter 3. In line with the natural exposures detailed in Chapter 3 the substrate coating system combinations that were tested were defined using a randomly assigned number, which can also be seen in Table 28.

Coupons of AA2024-T3 and AA7075-T6 were used for the accelerated exposure experiment, BS EN ISO 9227. The coupons source was the same as the coupons used in Chapter 3 with the material composition for both alloys remaining constant for all exposure experiments. The six coating systems defined in Chapter 2 were exposed to the accelerated exposure test. The specific combinations of coatings and substrates tested can be found in Table 28. As a result of the BS EN ISO 9227 accelerated exposure experiment being part of the wider factorial design detailed in Chapter 6 there are a number of substrate and coating combinations that were not tested. The choice to embody all of the experiments within this work within a single factorial design was made as a result of need to examine multiple samples and test protocols (factors). Due to the scale of the endeavour the factorial design also established an experiment approach could allow the study to determine the effects of interactions between factors on the response variable, which may not be immediately apparent. The decision to utilise an incomplete factorial also provided the ability to test a broader range of factors within a manageable data set. However, although the experimental design utilised the aspects to the factorial experiment it was not the singular driver for analysis.

Table 28: BS EN ISO 9227 experimental coupons

Substrate	Coating System	Exposure Length / days						
		0	14	28	42	56	70	84
AA2024-T3	1		393		269		390	
AA7075-T6	1	395		142		263		391
AA2024-T3	2	77	78	79			75	
AA7075-T6	2				105	74		76
AA2024-T3	3			141	17	4		182
AA7075-T6	3	176	288			206	138	
AA2024-T3	4				353	200		202
AA7075-T6	4	231	15	205			224	
AA2024-T3	5	266					264	265
AA7075-T6	5		267	268	290	389		
AA2024-T3	6	140	330	331		326		
AA7075-T6	6	137			332		80	328

4.3.2. Field exposures

The natural exposure experiments defined in Chapter 3 were used to examine the current standard accelerated exposure test; BS EN ISO 9227. The field exposures that will be used for comparison include the tropical inland site, the tropical coastal site, the temperate inland site and the temperate coastal site. The environmental characteristics of each of the exposure sites were detailed in Chapter 3.

4.3.3. Understanding the accelerated exposure environment

To ensure there were no temperature gradients across the chamber prior to its use, and to understand how the chamber responded to rapid changes in the temperature sequence, a chamber scoping experiment was completed.

One sample of AA2024-T3, one of AA7075-T6 and a third of carbon steel, with dimensions 73.5 mm × 73 mm × 0.65 mm were painted with a black polyurethane coating. The three coated samples and two companion aluminium alloy uncoated samples were exposed to sequential changes in humidity and temperature over the course of a 26 h cycle using the Ascott CCT chamber; the sequence can be seen in Figure 52.



Figure 51: University of Southampton cyclic corrosion chamber.

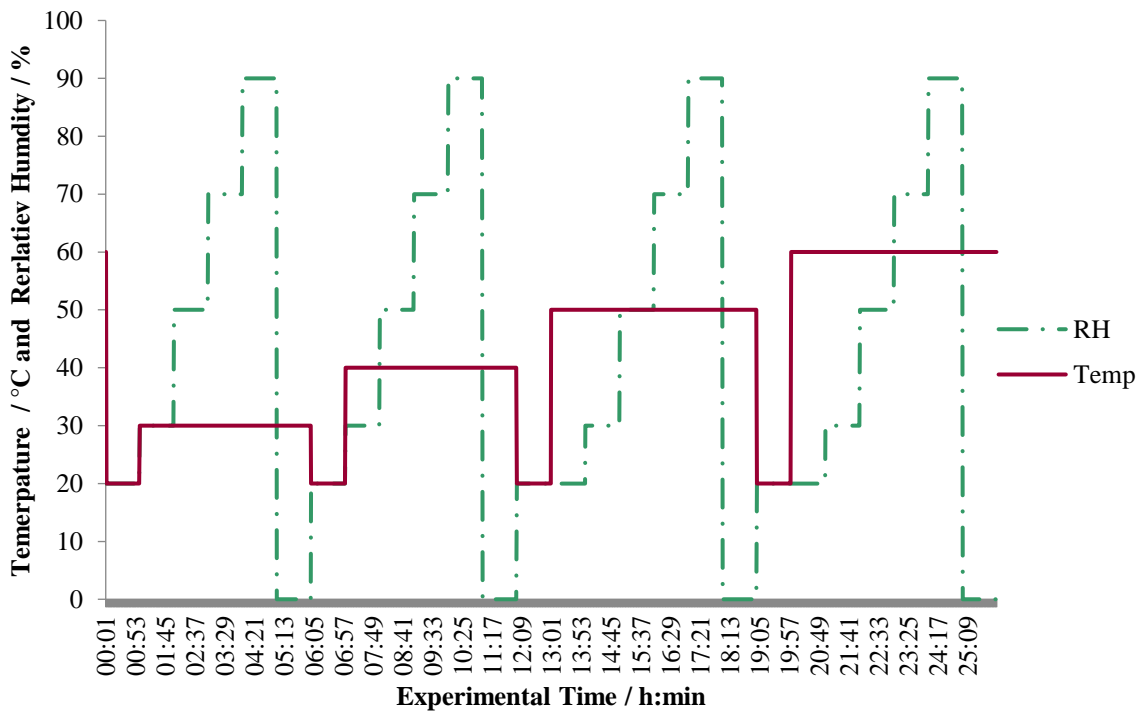


Figure 52: Exposure sequence used in thermocouple study.

The samples were labelled 1 - 5 and were moved throughout the chamber in the sequence illustrated in Figure 53. The full sequence was repeated three times with sample temperature being recorded every 10 s using Omega surface adhesive K type thermocouples with a Pico TC-08 (USB) thermocouple data logger. The data collected from the thermocouples was then compared to see if there were any temperature gradients within the chamber or between different sample types. The experiment also provided information regarding the chambers ability to change temperature as requested by the program.

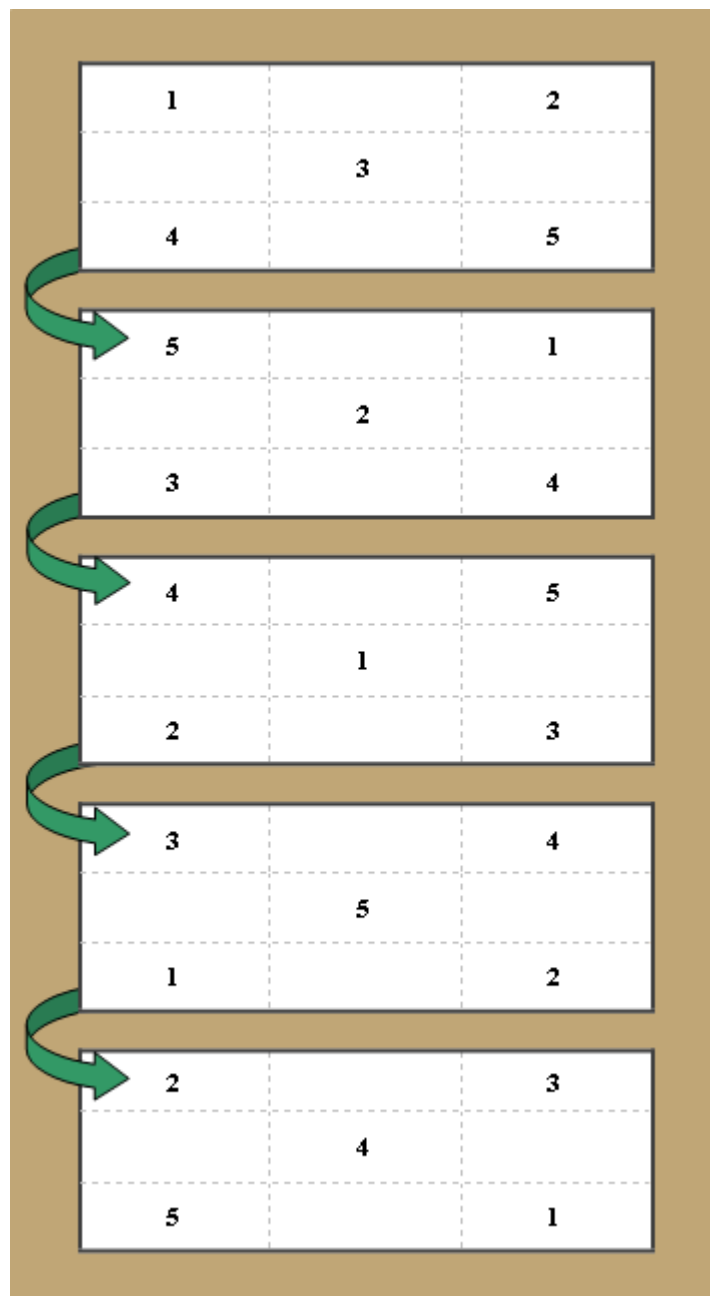


Figure 53: Sample location sequence used in thermocouple study of Ascott CCT Chamber.

The experimental coupon arrangements can be seen in Figure 53, Figure 52 is the temperature humidity sequence used for each cycle. Figure 54 shows the results from the first arrangement of samples, the results gathered for the remaining four cycles and the repeats were similar. The data for the remaining four cycles can be found in the Appendix Section 11.4.

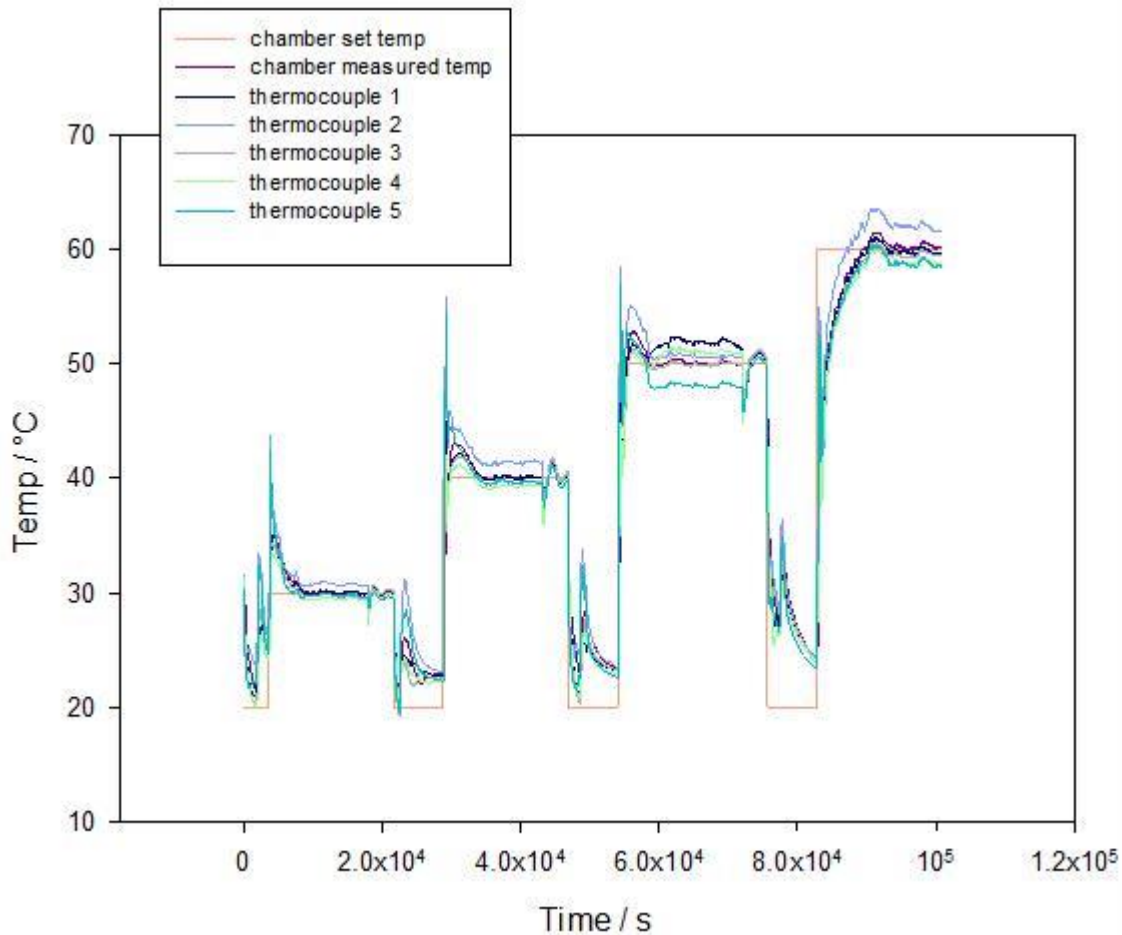


Figure 54: Thermocouple experiment Ascott cyclic corrosion chamber cycle 1 (see Figure 53).

When considering the possibility of chamber temperature gradients Figure 54 shows apparent temperature differences of the thermocouple measurements in the 50°C and 60°C sections of the cycle, however, the largest difference identifiable is within error for the chamber set values. Two features of note can be seen when considering rapid chamber temperature changes. The first is the temperature spike seen at the start of the temperature increase steps. This is a result of the machine attempting to rapidly change the temperature within the chamber, causing an overshoot. If sharp and large temperature changes are needed for testing then it will not be possible to circumvent this error, if a gradual temperature increase is used, this temperature spike should not be seen.

The second feature to note is the temperature spike that occurs in the centre of all low temperature sections. This is most like a result of the test having a RH too high for the temperature in question, as well as the temperature being set too low for ambient conditions. The Ascott chamber uses a

thermal humidifier, which uses a heating element submerged in water to increase the humidity of the chamber. The chamber programming also overrides temperature in favour of humidity. Meaning in the case of novel accelerated tests, not only must the chamber setting be within the available conditions for the machine, but the temperature of the room must be considered when design is created. An example of this would be in the winter months when the ambient conditions are cooler and humidity higher, it would be possible to access lower temperatures with in the chamber than in the summer months.

4.3.4. BS EN ISO 9227

The BS EN ISO 9227 Neutral Salt Spray test is a fixed temperature test, the Ascott cyclic Corrosion Chamber (Figure 51) was held at a constant $35^{\circ}\text{C} \pm 2^{\circ}\text{C}$ [1]. Coupons are then exposed to a constant salt fog for a period of up to 2000 h. The fog was produced through aerosolization of a 5 wt.% NaCl solution with a pH of 6.5 – 7.5 at 25°C [1]. The chamber was calibrated to ensure a collection rate over 80 cm^2 of 1.5 mL h^{-1} , as defined by the standard [1]. The 2000 h exposure equates to 84 days, with coupons removed from exposure every 14 days.

4.3.5. Post exposure analytics

Post exposure coupons were imaged, rinsed twice with distilled water to remove surface contamination, dried with compressed air and imaged a second time. Images were generated using a Canon EDS 550D camera using a 50 mm Canon compact macro lens and a Canon MR-14EX macro ring lite. Once imaged the coupons underwent further analysis to inform the comparison of the different testing methodologies. The methods of analysis used were previously defined in Chapters 1 and 2. The techniques used in this chapter were; gloss measurements and pulsed thermography.

The results from the pulsed thermography analysis will be presented as calculated acceleration factors for BS EN ISO 9227 relative to each of the natural exposures. The acceleration factor (A) was evaluated using Equation 12 [123].

Equation 12: Calculation of acceleration factor

$$A = \frac{r_{\text{SF}}/t_{\text{SF}}}{r_{\text{NE}}/t_{\text{NE}}}$$

A – Acceleration factor

r_{SF} – % thermography result BS EN ISO 9227 Salt Fog

t_{SF} – Exposure length for BS EN ISO 9227 Salt Fog (days)

r_{NE} – % thermography result Natural Exposure

t_{NE} – Exposure length for Natural Exposure (days).

The acceleration factor was calculated for each accelerated time point alongside all available natural exposure time points. The average for each natural exposure was then calculated along with the standard deviation for each data set.

4.4. Results and discussion

The effect BS EN ISO 9227 Accelerated Spray had on a coating surface finish was distinctly different to a natural exposure. The post exposure primer 60° gloss measurements for each of the coatings can be seen in Figure 56 to Figure 60. When coating systems 6, 2, 4 and 5 which are Figure 56, Figure 57, Figure 58, and Figure 55 respectively, were exposed to each of the natural exposure sites, the measured 60° gloss values for the primer section all reduced over time. However, when the same coatings were exposed to BS EN ISO 9227 the measured gloss value did not decrease. The BS EN ISO 9227 data points are differentiated in the figures by triangular series markers. The resistance to change in gloss for coating systems 2, 4, 5 and 6 was also independent of substrate, with both coupons of AA2024-T3 and AA-7075-T6 equally resistant to gloss reduction.

Unlike coating systems 6, 2, 4 and 5, coating system 3 shows in Figure 59 a rapid decrease in primer section 60° gloss measurements for all experiments including the BS EN ISO 9227 accelerated salt fog test. The degradation of the 60° gloss was fastest for the tropical coastal natural exposure and BS EN ISO 9227 accelerated corrosion test. Coating 3 was an experimental primer supplied by AkzoNobel and so the polymer and any active pigmentation was unknown.

Figure 60 shows the post exposure gloss values for coating system 1. Coating system 1 did not mimic the response seen for coating systems 6, 2, 5 and 4. The primer from coating system 1 utilises a sacrificial galvanic protection mechanism meaning it is a high PVC formulation. As a result of the high PVC the primer had a very low gloss prior to exposure. The gloss values did not decrease during exposure, instead, coupons exposed to the tropical coastal exposure showed an increase in gloss when exposed for an extended period of time. The gloss increase was a result of the loss of primer film thickness, and ultimately the reveal of the underlying metallic substrate. Figure 61 shows a coupon of AA7075-T6 exposed to the tropical coastal natural exposure for 420 days. The loss of primer can be seen on the left section of the coupon. There is a 5 mm strip of primer remaining at the top of the coupon section, the remaining area is corroded AA7075-T6 that has been exposed once the primer was reacted.

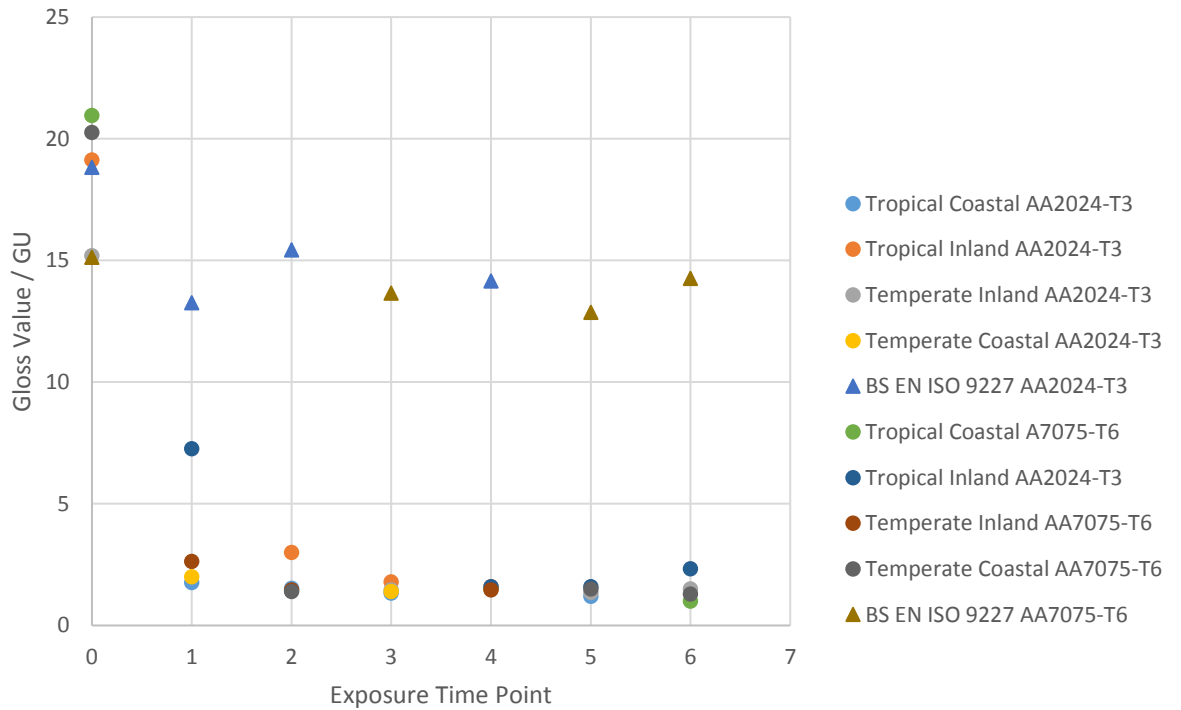


Figure 55: Averaged triplicate 60° gloss measurements post exposure for primer section of coating system 6.

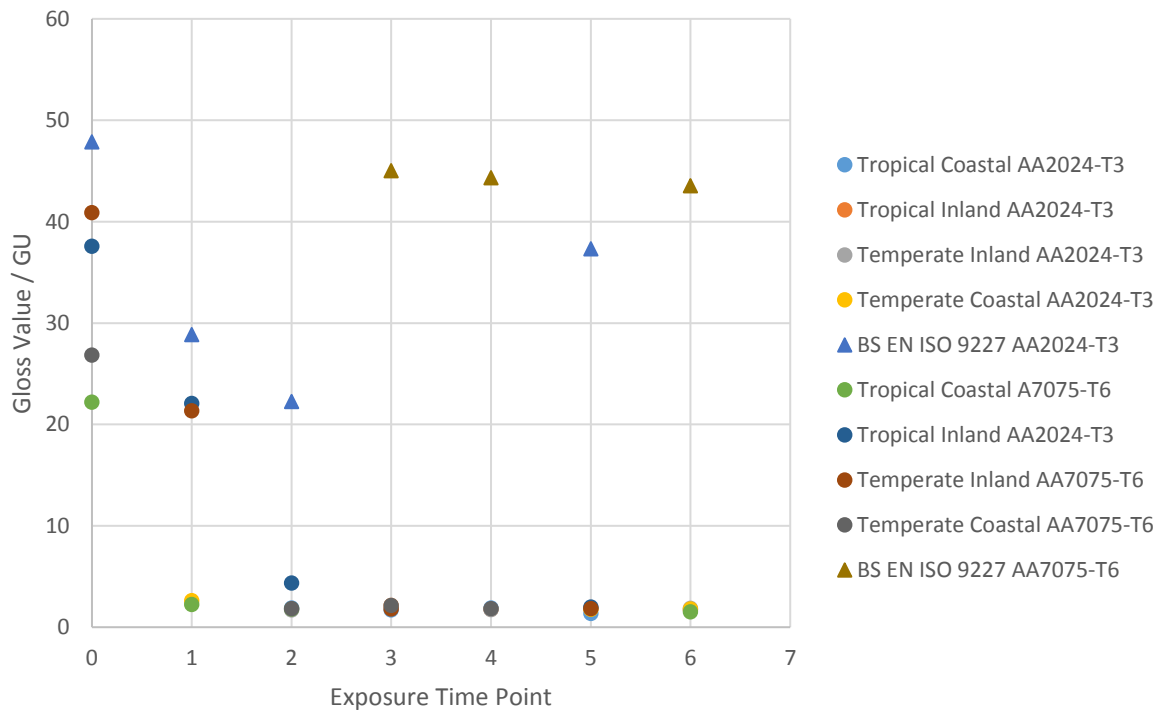


Figure 56: Averaged triplicate 60° gloss measurements post exposure for primer section of coating system 2.

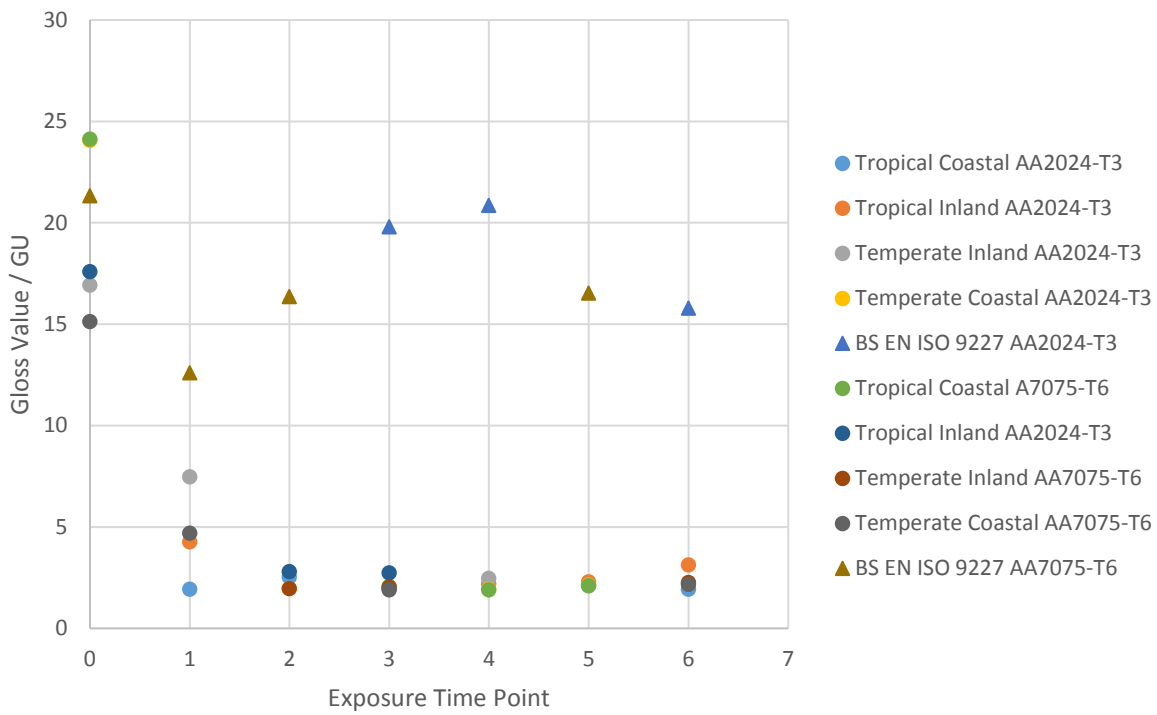


Figure 57: Averaged triplicate 60° gloss measurements post exposure for primer section of coating system 4.

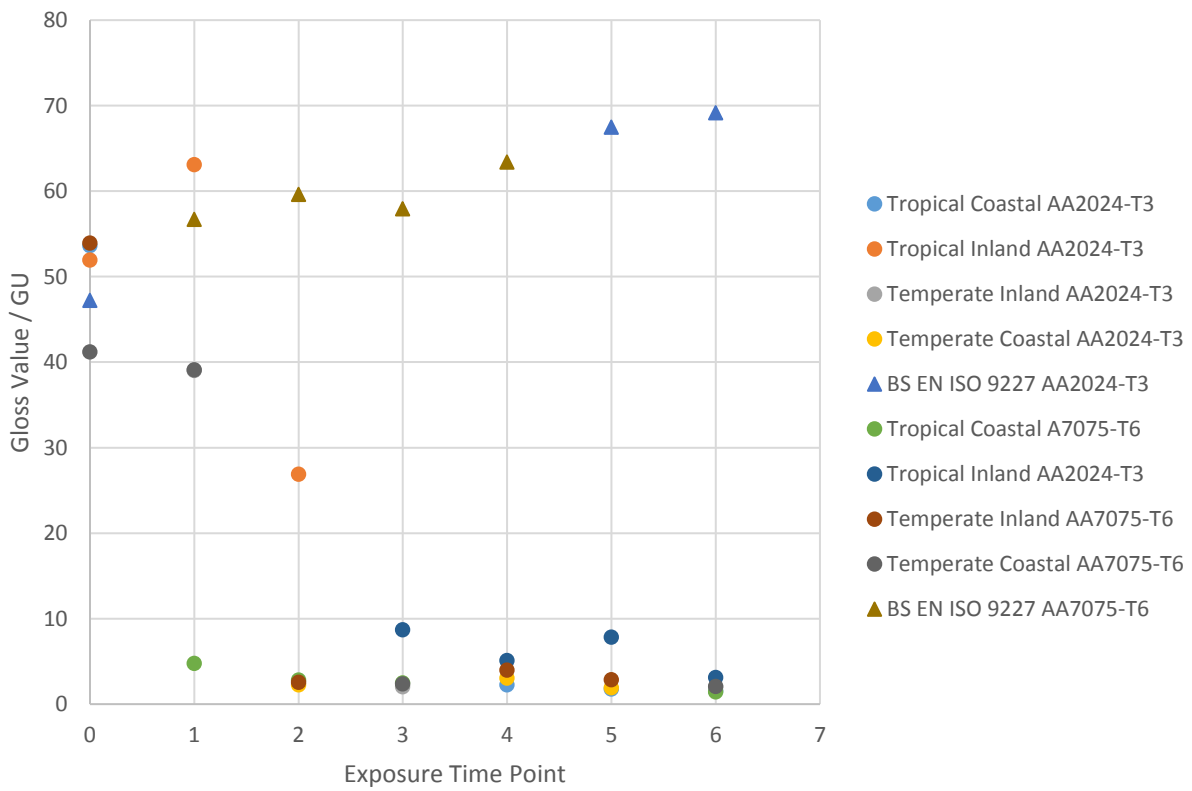


Figure 58: Averaged triplicate 60° gloss measurements post exposure for primer section of coating system 5.

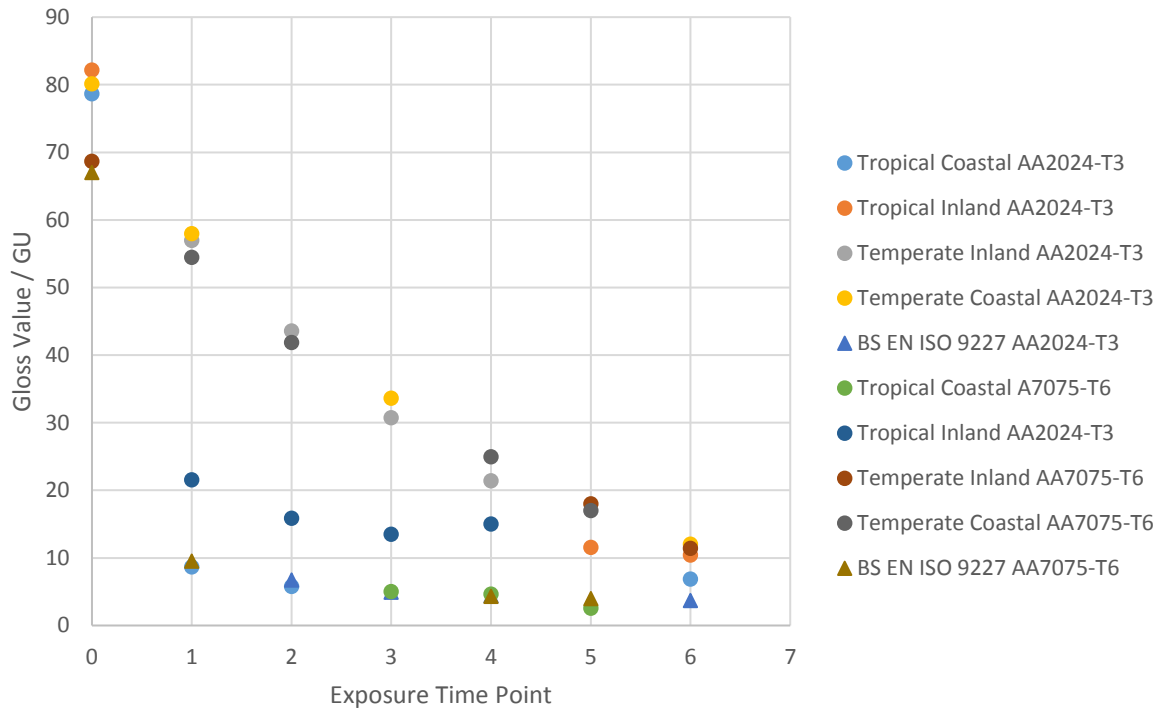


Figure 59: Averaged triplicate 60° gloss measurements post exposure for primer section of coating system 3.

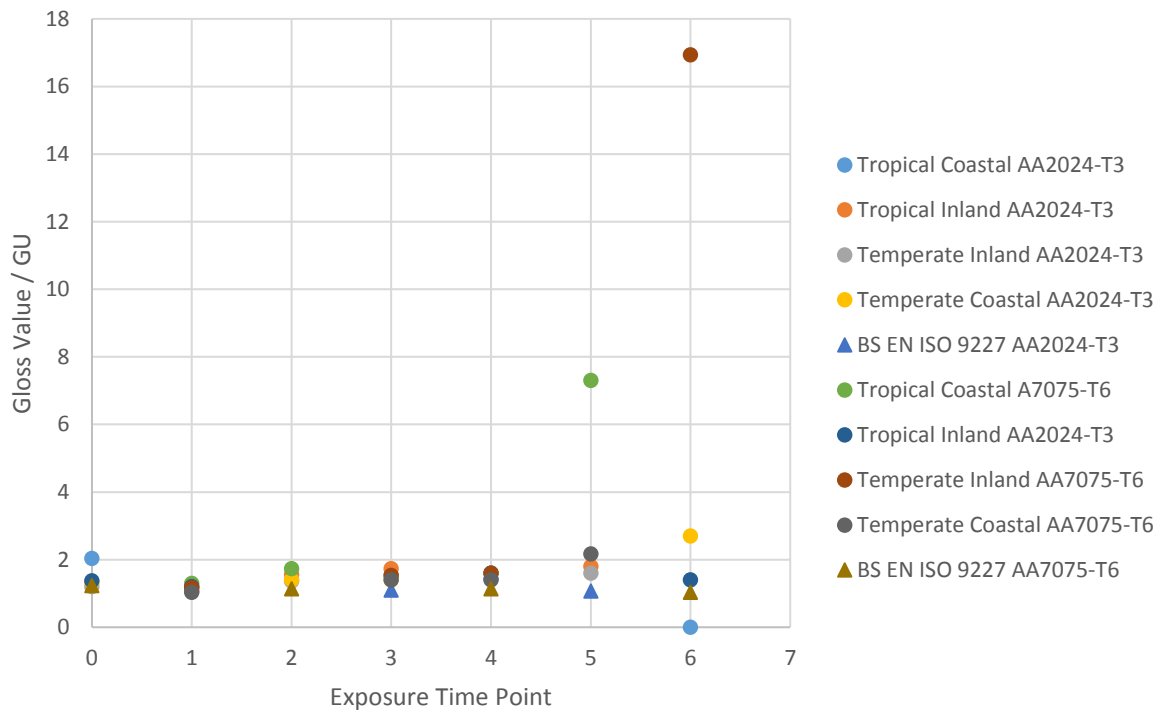


Figure 60: Averaged triplicate 60° gloss measurements post exposure for primer section of coating system 1.



Figure 61: Coating system 1 on AA7075-T6 exposed to tropical coastal natural exposure for 420 days.

One of the ways in which an accelerated corrosion test could be measured as successful would be if it was able to accelerate any coating on any substrate by a consistent factor from a natural exposure. Indicating that all of the key environmental variables related to the natural degradation of the materials had been captured. BS EN ISO 9227 was compared to each of the natural exposure environments and an average acceleration factor was calculated for each coating and substrate combinations.

Acceleration factors have been calculated by a number of research groups, Knudsen et al. compared a range of accelerated tests against a 5 year field exposure at Snorre Oilfield in the southern Norwegian Sea [123]. The average acceleration factor was calculated using scribe creep values and data was quoted for a single coating substrate combination only. The range of acceleration factors for the different tests varied from 14 to 55 and the study identified an inverse relationship between correlation of accelerated test with field exposure and test acceleration [123]. Deflorian et al. identified that when an accelerated salt fog is compared to the humid tropical environment of Daytona Beach the acceleration factor for barrier properties of coated galvanised steel is 13, additional coatings were tested and all provided acceleration factors between 11.5 and 14.5 [124]. An alpine region and Mediterranean beach region were also tested but good correlation was not found with the salt fog test. Alpine regions have lower temperatures and much lower chloride levels, also the Mediterranean site had additional urban pollutants than the salt fog

test. Researchers at the Federal Highway Administration calculated acceleration factors between laboratory corrosion tests and exposures at Sea Isle City, New Jersey with additional sea water applications twice a week. The team concluded similarly to Knudsen et al. that the faster the calculated acceleration factor the lower the correlation between the data sets [125]. For the purpose of this work the acceleration factor was calculated for the percentage area corrosion between each of the field exposure sites and the BS EN ISO 9227 salt spray test.

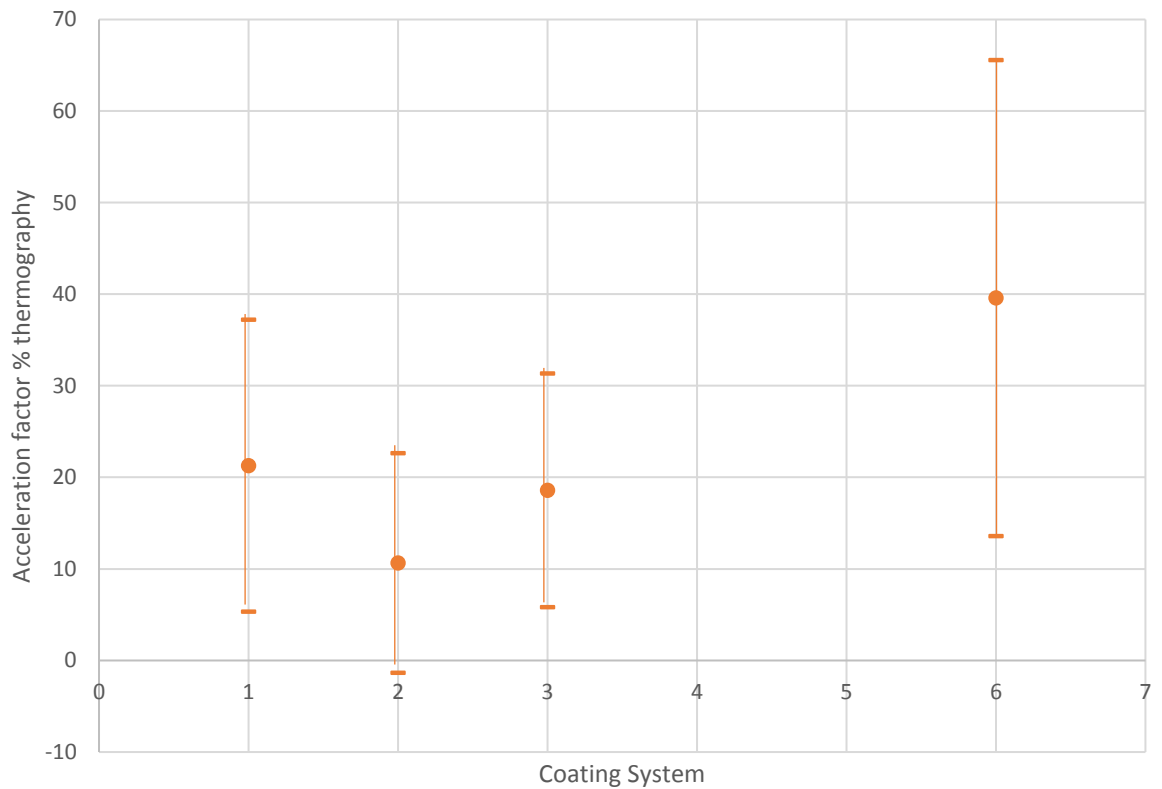


Figure 62: Average acceleration factor bound by standard deviation comparing coating performance when exposed to BS EN ISO 9227 Salt Fog vs. Tropical Inland natural exposure on AA2024-T3, performance measured with % area corrosion beneath topcoat identified using pulsed thermography.

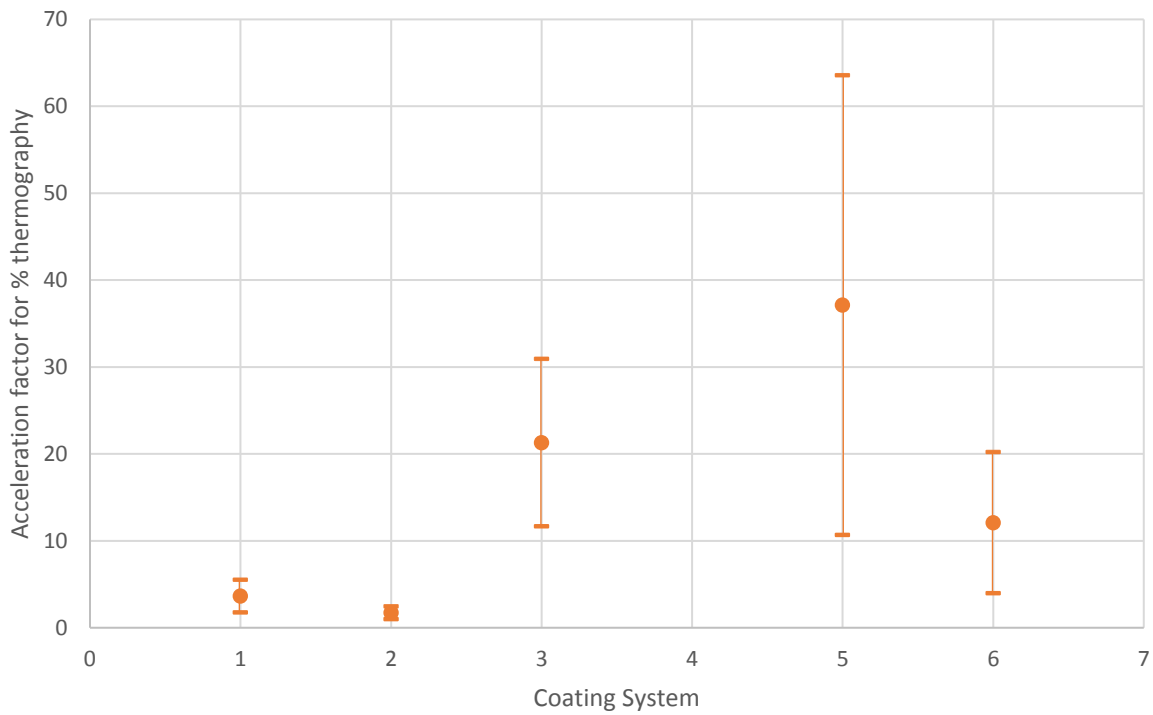


Figure 63: Average calculated acceleration factor bound by standard deviation comparing coating performance when exposed to BS EN ISO 9227 Salt Fog vs. Tropical Inland natural exposure on AA7075-T6, performance measured with % area corrosion beneath topcoat identified using pulsed thermography.

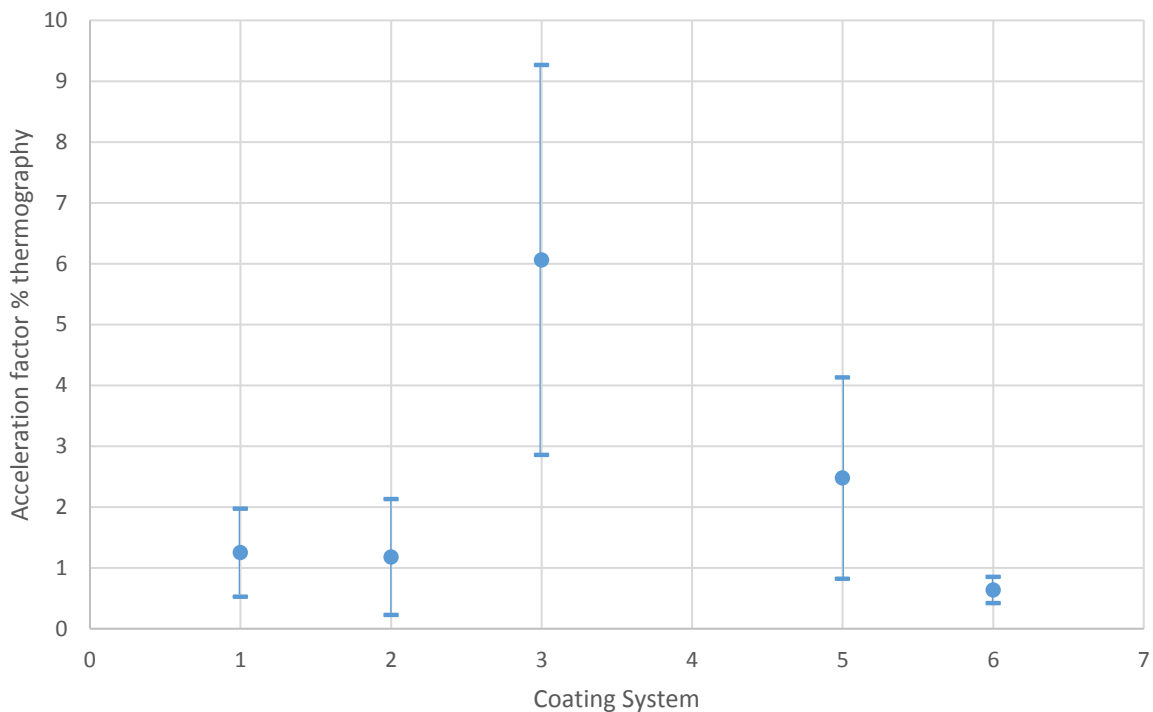


Figure 64: Average calculated acceleration factor bound by standard deviation comparing coating performance when exposed to BS EN ISO 9227 Salt Fog vs. Tropical Coastal natural exposure on AA7075-T6, performance measured with % area corrosion beneath topcoat identified using pulsed thermography.

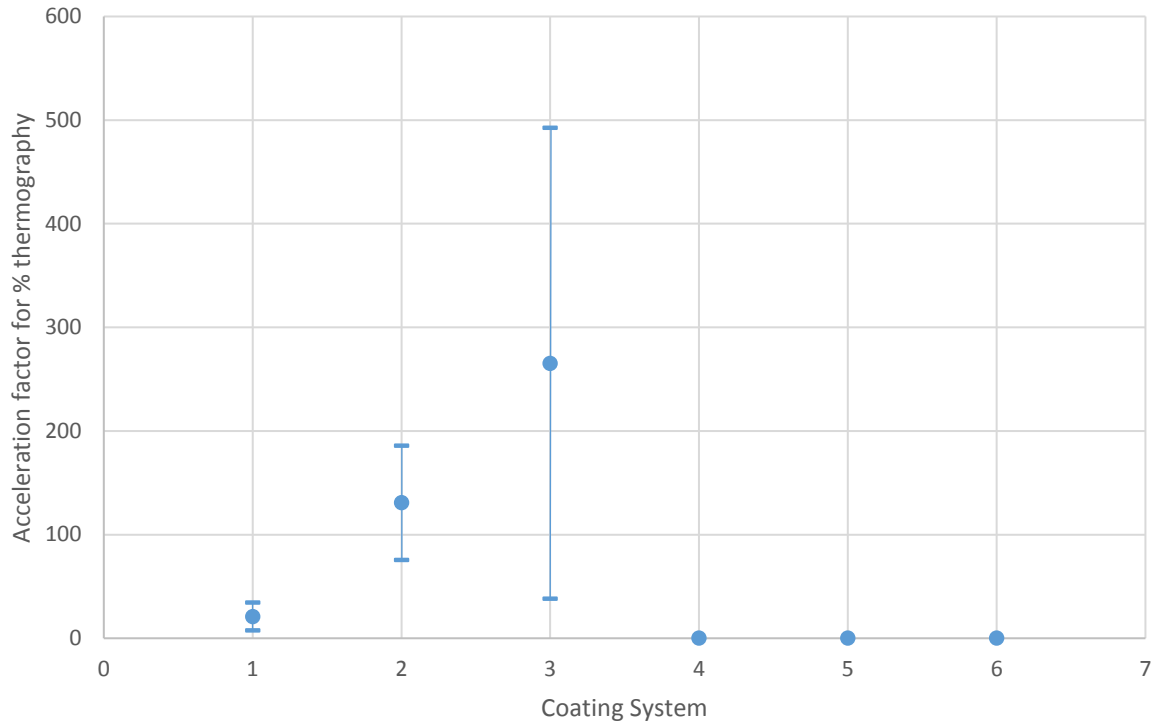


Figure 65: Average calculated acceleration factor bound by standard deviation comparing coating performance when exposed to BS EN ISO 9227 Salt Fog vs. Temperate Coastal natural exposure on AA7075-T6, performance measured with % area corrosion beneath topcoat identified with pulsed thermography.

The calculated acceleration factors provide a simple point of comparison which can be used to identify if the BS EN ISO 9227 salt spray test was able to accelerate any of the given field exposure experiments. Had the calculated acceleration factor for each of the coatings been the same the effect of the BS EN ISO 9227 test would have been replicated at that specified acceleration factor. The BS EN ISO 9227 salt fog test is not an acceleration of the tropical inland field exposure. The range of acceleration factors illustrated in Figure 62 and Figure 63 shows that different coatings degradation processes are effected differently when exposed to the two experiments BS EN ISO 9227 is equally unsuccessful at replicating the tropical inland field exposure regardless of the substrate, with AA2024-T3 (Figure 62) and AA7075-T6 (Figure 63) for each of the coatings showing varied responses in acceleration factor.

Figure 64 shows the acceleration factors for the higher salinity environment of the tropical inland field exposure site, once again the acceleration factors for each of the coatings indicate considerable variation. This shows that some of the coatings are more resilient to the BS EN ISO 9227 than others. The BS EN ISO 9227 has been shown to be unable to accelerate either the tropical field exposures equally across all coatings studied.

Figure 65 illustrates that BS EN ISO 9227 is equally unsuccessful when compared to a temperate environments the acceleration factor calculated for comparison was once again different for each of the coatings tested.

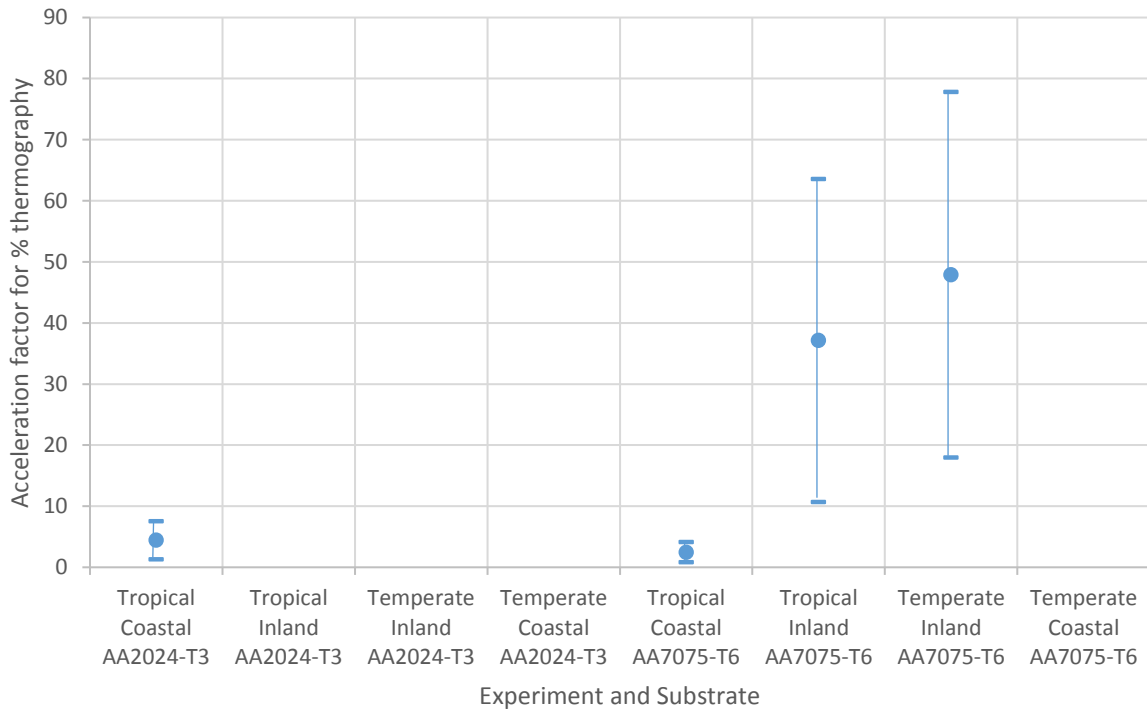


Figure 66: Average calculated acceleration factor bound by standard deviation for coating system 5, comparing performance of exposure to BS EN ISO 9227 Salt Fog and natural exposures on both AA2024-T3 and AA7075-T6. Performance was measured with % area of corrosion beneath the topcoat using pulsed thermography.

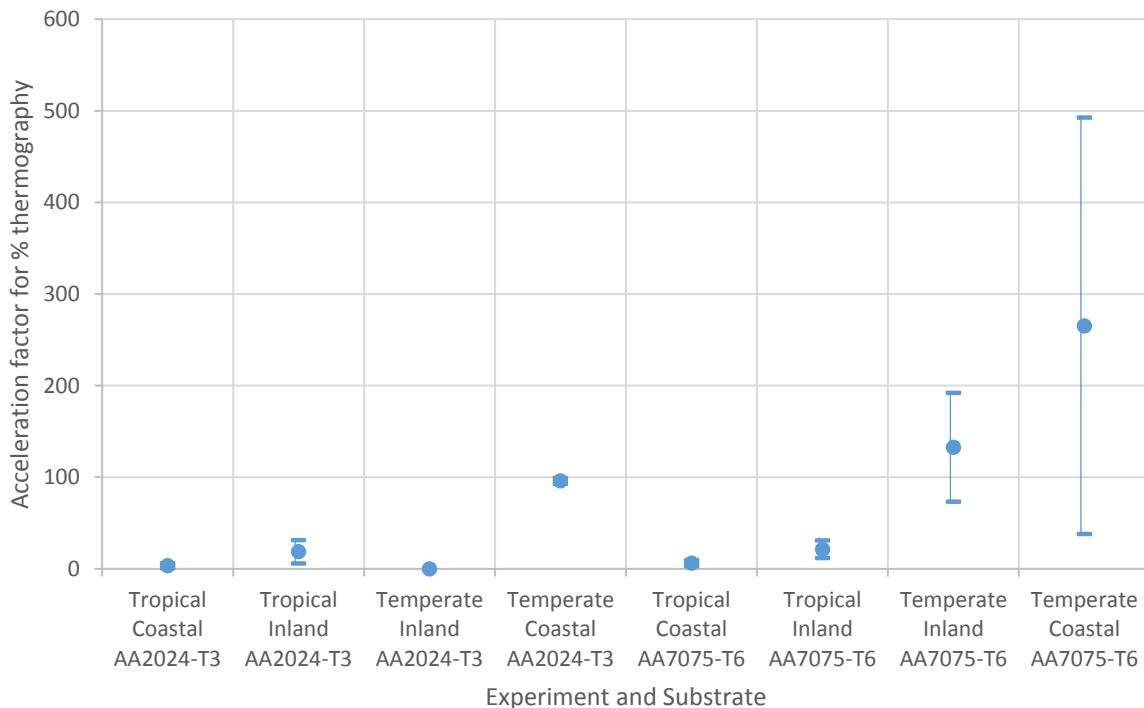


Figure 67: Average calculated acceleration factor bound by standard deviation for coating system 3, comparing performance of exposure to BS EN ISO 9227 Salt Fog and natural exposures on both AA2024-T3 and AA7075-T6. Performance was measured with % area of corrosion beneath the topcoat using pulsed thermography.

The acceleration factor for specific coatings across all environments was also calculated, the data for coating systems 5 and 3 can be seen in Figure 66 and Figure 67, respectively. The calculated acceleration factors allow for easy comparison of BS EN ISO 9227 with a field exposure. If the BS EN ISO 9227 was accelerating the exposure of coupons to the tropical coastal, the tropical inland or the temperate coastal field sites each of the coating systems would be measured as having an equal factor of acceleration for the given field site. The difference in acceleration factor within a single reinforces that a different exposure sites effect coating lifetimes in different ways. The lower the acceleration factor the more aggressive the environments relative to the BS EN ISO9227 test, Any test that was more aggressive than the BS EN ISO 9227 test scored 0 for acceleration factor, meaning it was not easy to compare very aggressive environments using this methodology.

4.5. Summary

The purpose of the chapter was to explore two distinct questions:

1. What is the current state of the art of accelerated corrosion testing used in academia and industry?
2. Does the most widely used testing protocol provide any results representative of a field exposure?

Investigation of the two key chapter questions was achieved through examination of the following topics:

1. Atmospheric aluminium alloy corrosion;
2. Definition of the breath of corrosion testing protocols in industry and academia;
3. Exposure of coupons to BS EN ISO 9927;
4. Comparison of post exposure testing to coupons exposed to field exposures.

The current state of the art for accelerated corrosion testing of coatings is one without a clear direction. Both industry and academia utilise a number of accelerated corrosion test protocols, with some going so far as to specify their own test protocols, i.e., Volvo. With each customer and supplier identifying their own measure of success, a clear link between service and test protocol is not always clear. The UK military typically identify BS EN ISO as the key protocol in spite of a known dissatisfaction with the testing relative to service performance. The dissatisfaction is evident through the request by DSTL for study of a replacement testing protocol that is more representative of actual service.

When BS EN ISO 9227 is compared to other test protocols it is not unsurprising that it is known to underperform. The GM9540P test protocol for instance incorporates multiple temperature and humidity stages, alongside multiple applications of a salt solution. This is in contrast to BS EN ISO 9227 which employs a static temperature control alongside continuous application of aqueous salt spray. Even when compared to the tropical coastal site, which is located on the break line of a Panamanian beach, the diurnal changes in temperature and humidity are not accounted for even if the continuous salt spray could be considered a proxy for the break line location. When exposures were compared between BS EN ISO 9227 and the tropical coastal site the results prove to be ill-matched.

Determination of the inability of BS EN SIO 9227 to replicate service like performance identifies that static temperature and salinity alone do not provide all of the environmental stimulus necessary to degrade coatings as they would be in a field exposure. Meaning any developed test protocol will require control more than the two environmental factors as defined in BS EN ISO 9227. The lack

of direct correlation also acts as a baseline for acceptable accelerated corrosion testing. If the newly developed test provides a result more representative of service conditions than those seen from exposure to BS EN ISO 9227 then some success can be identified within the task set by DSTL.

5. Exploring Replication of a Tropical Coastal Environment

5.1. Introduction

The disparity between the BS EN ISO 9227 testing protocol and service environments was discussed in the previous chapter. One of the key concerns identified was the test protocols unrealistic temperature and relative humidity (RH) set points along with its improbable salt loading. During a natural exposure coupons are exposed to diurnal cycles of temperature and humidity as a result of the transition between day and night. Dependent upon location the coupons may be subjected to seasonal changes in addition to the diurnal cycles.

The BS EN ISO 9227 testing protocol defines a single exposure temperature point and leaves humidity uncontrolled whilst a constant 5 wt.% NaCl aqueous spray is applied to the coupon surfaces at a deposition rate of $1.5 \text{ mL h}^{-1} 80 \text{ cm}^{-2}$. Therefore the coatings undergo no variation in thermal stress and no macroscopic shifts in water concentration within the polymer film. Instead as the polymer is exposed to a steady-state environment it will reach an equilibrium with the exposure environment. The lack of contrast in the exposure protocol could be a factor in the unrepresentative results from BS EN ISO 9227 experiments when compared to natural exposures.

Unrealistic temperature and humidity cycles can result in the appearance of coating failure not seen in service. The unexpected failures a result of alternative pathways of degradation being made available during exposure to environments with no real-world provenance. In response to this, temperature and humidity profiles measured during the natural exposure experiments were used to create the novel cyclic tests described in the remainder of the thesis. The initial experiment

attempted to identify if it was possible to accelerate the effects of an environment through decreased cycle time alone.

The tropical coastal site was the natural exposure environment that was the easiest to replicate within an unmodified cyclic corrosion chamber. Throughout the natural exposure coupons were exposed to a principally wet phase NaCl loading regime along with diurnal but not seasonal cycles of temperature and humidity. The simplicity of the environment lent itself to replication within a test chamber.

The tropical coastal environment provided an envelope of variables that could be created within the confines of the University of Southampton cyclic test chamber. The potential environmental range that could be achieved using the Ascott cyclic corrosion test chamber is defined in Figure 68. The chamber used was the same Ascott cyclic corrosion chamber used for the BS EN ISO 9227 experiment in Chapter 4.

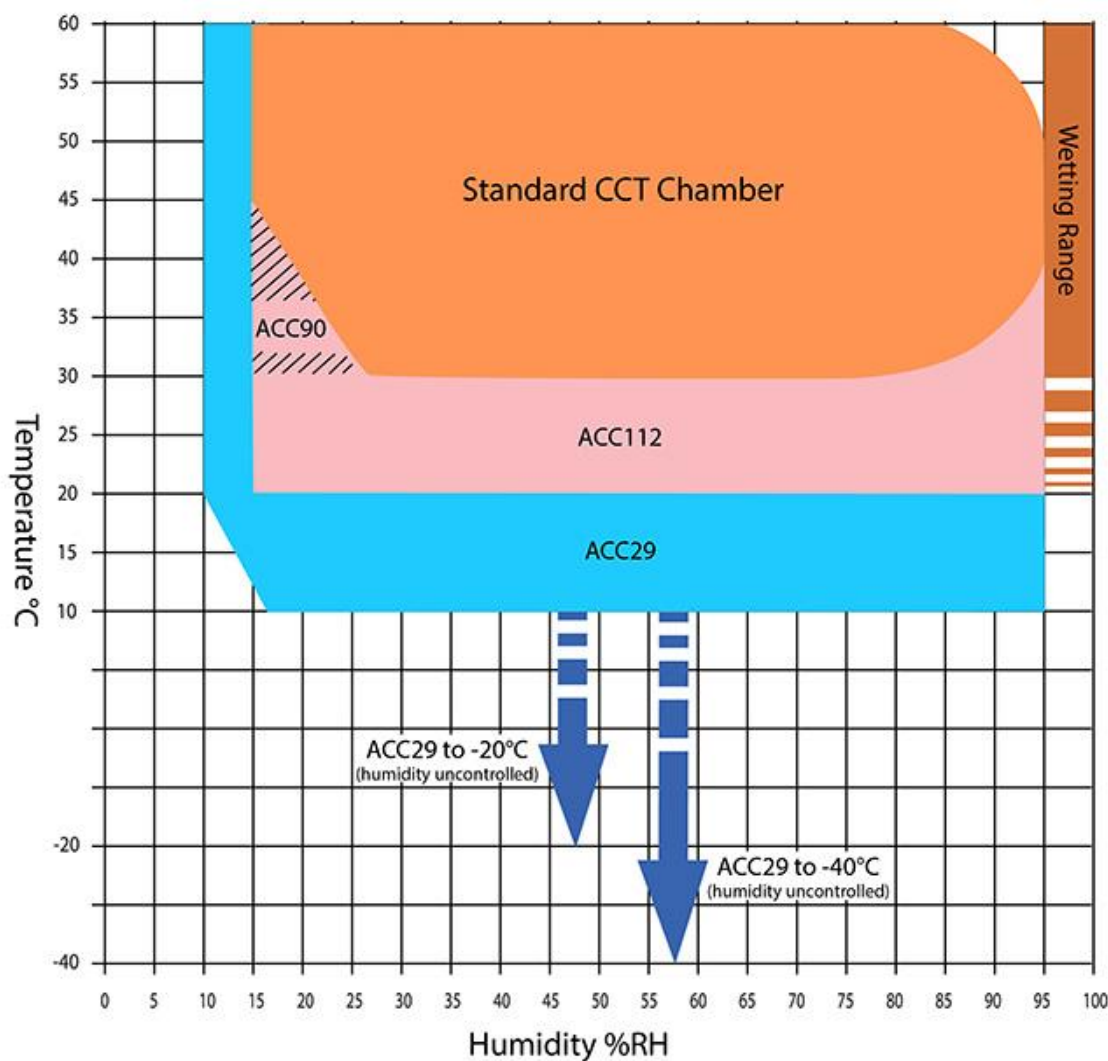


Figure 68: Ascott Analytical graph showing standard range of temperature/humidity control for a CCT chamber and how this may be extended by the addition of optional accessories [126].

5.2. Objective

The objective of this chapter was to identify if whilst using an unmodified cyclic corrosion chamber and without the addition of more environmental parameters, i.e., SO₂ or UV application, it was possible to create a test that more closely replicated the failure seen in a natural exposure test. The standard cyclic corrosion test chamber would allow for variation of temperature, humidity and wet phase NaCl loading. Environmental data was collected from the tropical coastal natural exposure site, and used to create the cyclic corrosion test protocol.

5.3. Experimental

5.3.1. Materials

The coupons illustrated in Table 29 were coated and imaged in preparation for accelerated exposure in the Ascott cyclic corrosion chamber. Coupons of either AA2024-T3 or AA7075-T6 were coated with each of the six coating systems previously defined in Chapter 2. The specific exposures measured for this chapter are detailed in Table 29. The accelerated nature of this experiment in conjunction with the focus of overlapping diurnal like cycles resulted in a total exposure time of 84 day, which was split into seven 14 day time points. The fourteen day subdivision were a result of the increased cycle rate employed within accelerated testing protocol 1 and 2. The fourteen days of exposure provided 84 diurnal like temperature and humidity cycles, with six cycles completed every 24 h. Each of the fourteen day time points provided a pause in exposure protocol whereby the subset coupons defined in Table 29 were extracted from the exposure. Once extracted, coupons were not returned, rather they were washed and photographed before undergoing the analysis detailed in Section.5.3.4.

Table 29: Coupon allocations for Accelerated Test 1

Coating System	Substrate and Time Point													
	AA2024-T3							AA7075-T6						
	1	2	3	4	5	6	7	1	2	3	4	5	6	7
1		29	30			28	27	183			10	25	11	
2	91			94		124			93	86		88		219
3		154		227	151	152		175		157				153
4	89	218	220				359				283	214	215	
5			282	259	277	278		280	281					216
6	343		344		340		342		155	241	178		341	

5.3.2. The field exposure

The natural exposure experiment utilised for the comparison in this chapter was the tropical coastal experiment as defined in Chapter 3.

5.3.3. The accelerated exposure experiment

The accelerated corrosion test was developed using weather and air borne salinity data collected at the tropical breakwater exposure site. The temperature and humidity cycle followed an extreme diurnal cycle as measured at the Panama site and defined in Figure 69. Deposition rates of NaCl solution were based on measured salinity values at the Panama coastal site from May 2014 to May 2015 provided by Luisa de Wong of Trax International in collaboration with DSTL and the DoD. The measured NaCl had an average of $1063 \text{ mg m}^{-2} \text{ d}^{-1}$ and a standard deviation of $810 \text{ mg m}^{-2} \text{ d}^{-1}$, this resulted in a deposition of an 8.5 wt. % NaCl solution at a rate of $1.5 \text{ mL h}^{-1} \text{ 80 cm}^{-2}$ for either 72 minutes or 6 minutes or per day dependent upon cycle. The temperature range identified from the weather data provided by Trax International was from $35 \text{ }^{\circ}\text{C}$ to 28°C , with an accompanying relative humidity range of 95 % to 65 %.

The feature use for acceleration was a decrease in the diurnal cycle time. The coupon were exposed to six extreme temperature and humidity cycles equivalent to the natural diurnal cycles over a 24 h period. Along with the increased cycling of temperature and humidity the deposition rate of NaCl aqueous solution was also increased, thus meaning six times the natural mass of NaCl was applied within each 24 h period. The need to control the humidity was key to the successful replication of a field exposure resulted in a short application of a high concentration NaCl as an initial step in the temperature and humidity cycles as defined in Figure 69. The experiment was completed using the Ascot cyclic corrosion chamber previously described in Section 4.3.3.

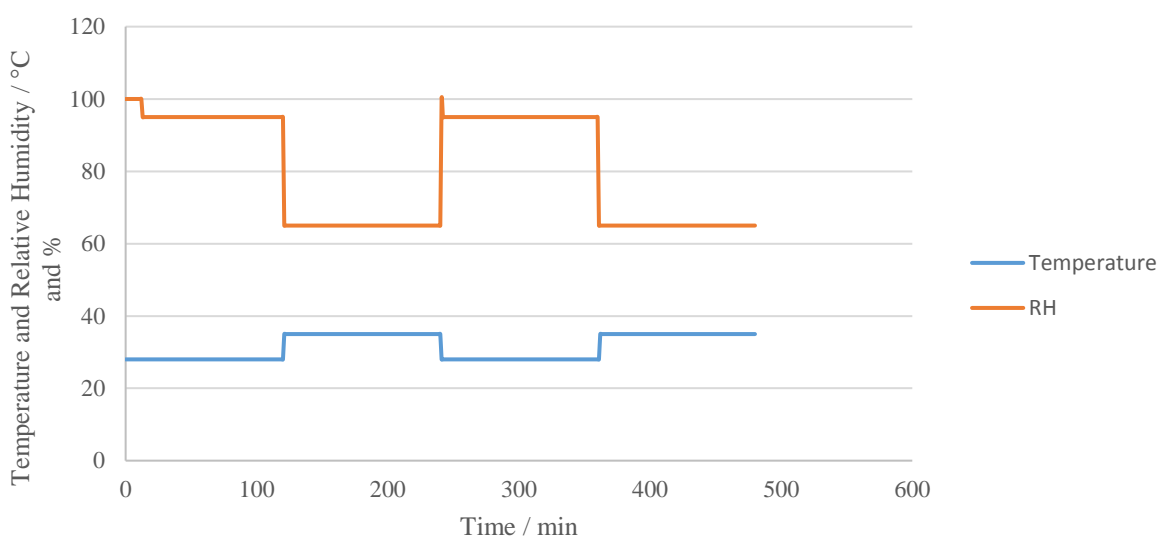


Figure 69: Cycle for accelerated testing protocol 1 – Cycle A from 0 minutes to 240 minutes, Cycle B from 240 minutes to 480 minutes.

The CCT cycle included 2 stages, utilising a ‘real world’ diurnal temperature cycle switching from 28 °C to 35 °C, at 2 hour intervals. The relative humidity cycled through three phases, the 100% RH phase is a result of application of aqueous NaCl solution was completed at 28 °C, the next phase also completed at 28 °C was the condensation phase, where the chamber RH was maintained at 95 %. The final phase was a drying step, where the RH was driven down to 65 % and the temperature increased to 35 °C. The temperature and humidity cycling for this protocol was split into an A and B cycle to encompass the variation in NaCl loading measured at the tropical coastal site. The A cycle was the higher salt loading hence a 12 minute salt spray 4 times per day, whilst the B cycle represented the lower levels of NaCl measured resulting in a brief 1 minute spray 4 times per day.

5.3.4. Post exposure analytics

Post exposure coupons were imaged, rinsed twice with distilled water to remove surface contamination, dried with compressed air and imaged a second time. Images were generated using a Canon EDS 550D camera using a 50 mm Canon compact macro lens and a Canon MR-14EX macro ring lite. Also, once imaged, the coupons underwent further analysis to inform the comparison of the different testing methodologies. The methods of analysis used were previously defined in Chapter 2 and 3. The techniques explored for comparison in this chapter were; gloss measurements and colourimetry.

5.4. Results and discussion

The results presented include 85° gloss measurements of the topcoat sections of coating systems 1, 2, 4 and 5, (Figure 70, Figure 72, Figure 74 and Figure 75) alongside the colourimetry measurements of the primer sections of coating systems 1, 4, 5 and 6 (**Error! Reference source not found.**, Figure 76, Figure 77 and Figure 78). The gloss data was collected after the coupons were exposed to either the tropical coastal site or the accelerated corrosion test that replicated the tropical coastal site. The colorimetry data was calculated using ΔE 2000 protocol with the average 0 point value for each coating system compared to each post exposure measurement [127].

5.4.1. Gloss change

The post exposure 85° gloss values for coating system 1 topcoat sections (Figure 70) are displayed in Figure 70. The measured values did not show a clear distinction between coupons exposed to the field exposure or the accelerated protocol with respect to gloss changes until exposure time point 5 and 6, where a zero measurement was made for both of the field exposure coupons. This was not a result of surface roughness changes to the topcoat, instead it was a result of complete coating failure. The AA2024-T3 coupon exposed to the field site for 504 days image is Figure 71 and the AA7075-T3 coupon image is Figure 61. The AA7075-T6 (Figure 61) coupon underwent complete delamination of the topcoat with little build-up of corrosion materials, while the AA2024-T3 (Figure 71) coupon formed enough corrosion product beneath the surface of the coating to result in the topcoat tearing apart. The failures although different, both prevented measurement of the gloss of the topcoat surface and hence the inclusion of 0 gloss units in the figure. Although not torn apart the AA2024-T3 coupon coated with system 1 did form a large amount of corrosion product across the topcoats section after 84 days exposure with a very different morphology to that seen after exposure to BS EN ISO 9227(see Figure 73).

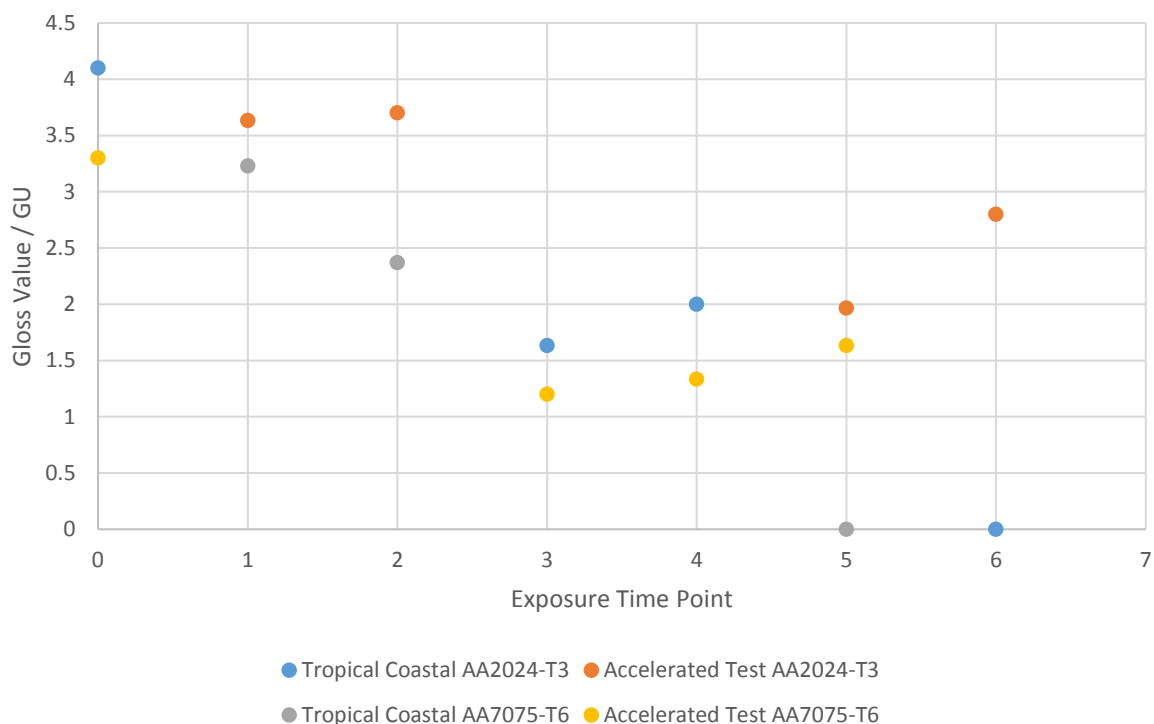


Figure 70: Averaged triplicate 85° gloss measurements post exposure for topcoat section of coating system 1.



Figure 71: Coating System 1 in AA2024-T3 exposed to the tropical coastal site for 504 days (Coupon #58).

The same AkzoNobel topcoat was applied to coating systems 1, 2 and 3, with coating systems 1 and 3 also undergoing the same pre-treatment step, with the application and subsequent washing off of metaflex adhesion promoter. The performance differences between topcoat sections of coating systems 1 and 2 which can be seen in Figure 70 and Figure 72, respectively, was a result of either the inclusion of the pre-treatment step or the ability of the active primer to protect areas where it is not in direct contact with. Coating system 2 (Figure 72) sees a drop in gloss for both the accelerated test and the tropical coastal field exposure site at time point 4. Time point 4 for the tropical field exposure is 252 days of exposure, whilst the accelerated test is 42 days exposure with 252 thermal and humidity cycles were completed.

Coating system 4 (Figure 74) and 5 (Figure 75) both utilise the topcoat supplied by PPG. With coating system 4 showing a decrease in the gloss of the topcoat only applied on AA7075-T6 and exposed to the tropical coastal field exposure. It did not appear to be sensitive in the same way to the subset of environmental variables selected for the accelerated testing protocol.

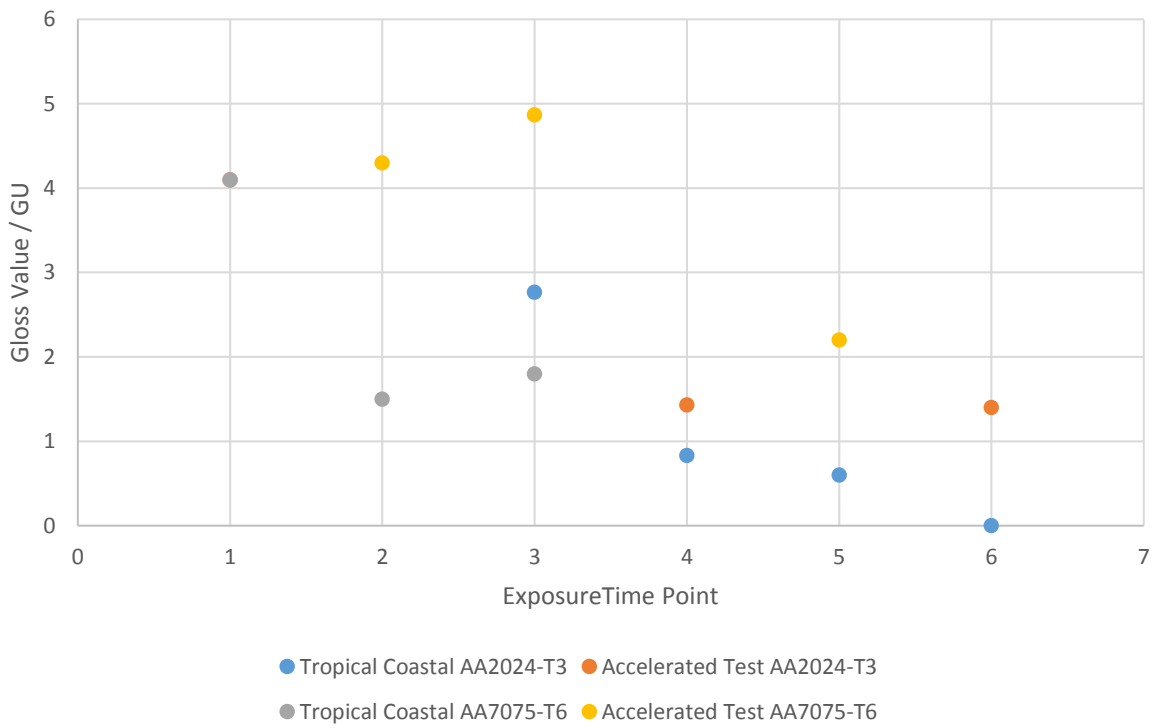


Figure 72: Averaged triplicate 85° gloss measurements post exposure for topcoat section of coating system 2.

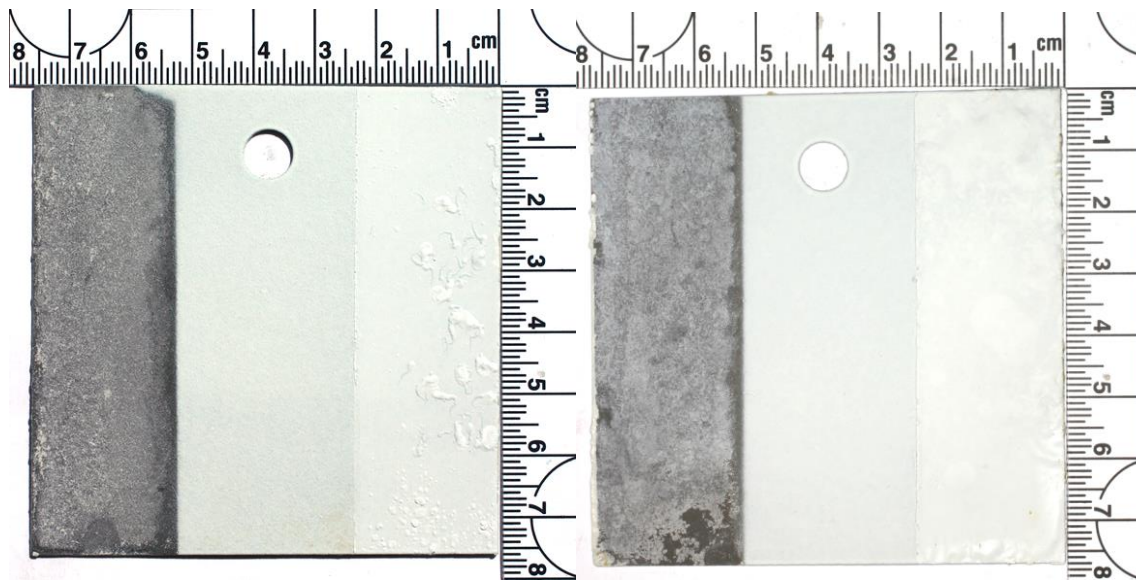


Figure 73: Left - Coating System 1 in AA7075-T6 exposed to the BS EN ISO 9227 for 84 days (Coupon no. 391). Right- Coating System 1 in AA2024-T3 exposed to the accelerated exposure protocol for 84 days (Coupon no. 27).

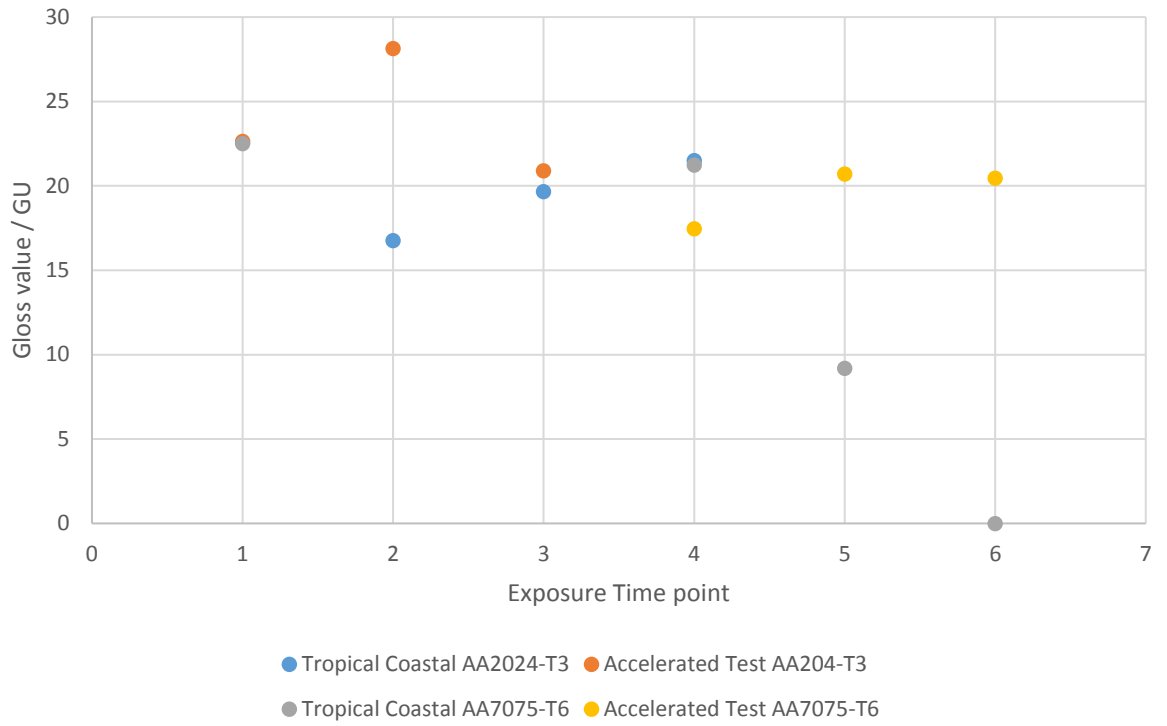


Figure 74: Averaged triplicate 85° gloss measurements post exposure for topcoat section of coating system 4.

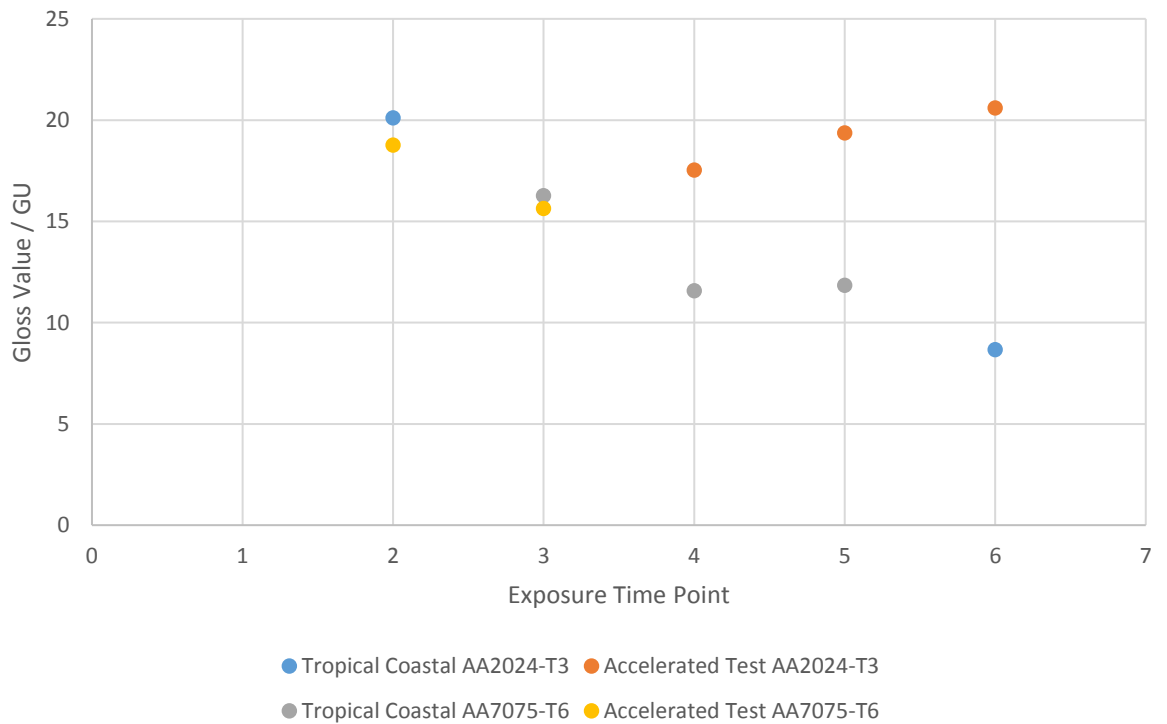


Figure 75: Averaged triplicate 85° gloss measurements post exposure for topcoat section of coating system 5.

5.4.2. Colour change

Colour change can be used to identify chemical changes in coatings upon exposure, reaction of strontium chromate leads to dulling of the green primer over time. The primer from coating system 4 (Figure 76) shows an initial division in colour change between the accelerated testing protocol and the field exposure. The coupons exposed to the field site showed a rapid and sustained change in colour, whilst very little change was evident for coupons exposed to the accelerated protocol. This disparity is most likely a result of a missing parameter within the accelerated testing protocol. Had chemical analysis been available, it may have been possible to identify what the chemical change on the surface was and then identify the environmental variable responsible for the change.

The primer of coating system 5 (Figure 77) also shows a difference in trend of colour change upon exposure to the field exposure or the accelerated testing protocol. Unlike the rapid colour change for coating system 4, the change in colour for coating system 5 was a gradual increase throughout the course of the exposure to the field site. For coupons exposed to the accelerated testing protocol the colour change regardless of substrate remained relatively unchanged. The slow increase in colour change upon exposure to the field site potentially was a result of the accelerated protocol providing no acceleration, instead the coupons may have been following the same degradation path at the same rate, meaning time point 7 for the accelerated protocol was performing as well as the field exposed coupons at time point 1, both of which were after 84 days. The matched pace would align with the work completed on transport of water through coatings, which highlighted the importance of dwell time to enable the coatings to reach equilibrium with the environment [97]

Colour change for the primer of coating system 6 is a result of leeching of strontium chromate pigment from the unprotected primer. Both the field exposure and the accelerated test underwent changes in colour following exposure. AA7075-T6 showed a change in colour after 14 days of accelerated testing equal to that of the 84 days of field exposure. It should be noted that as a result of the selected intervals of 84 days for field exposures it is not possible to identify if this colour change occurred any earlier. Rather unusually when coating system 6 was applied on AA2024-T3 it and exposed to the accelerate test the coating colour change was reduced in comparison to the AA7075-T6 equivalent. This does not align with the performance which was matched for the coupons exposed to the field exposure.

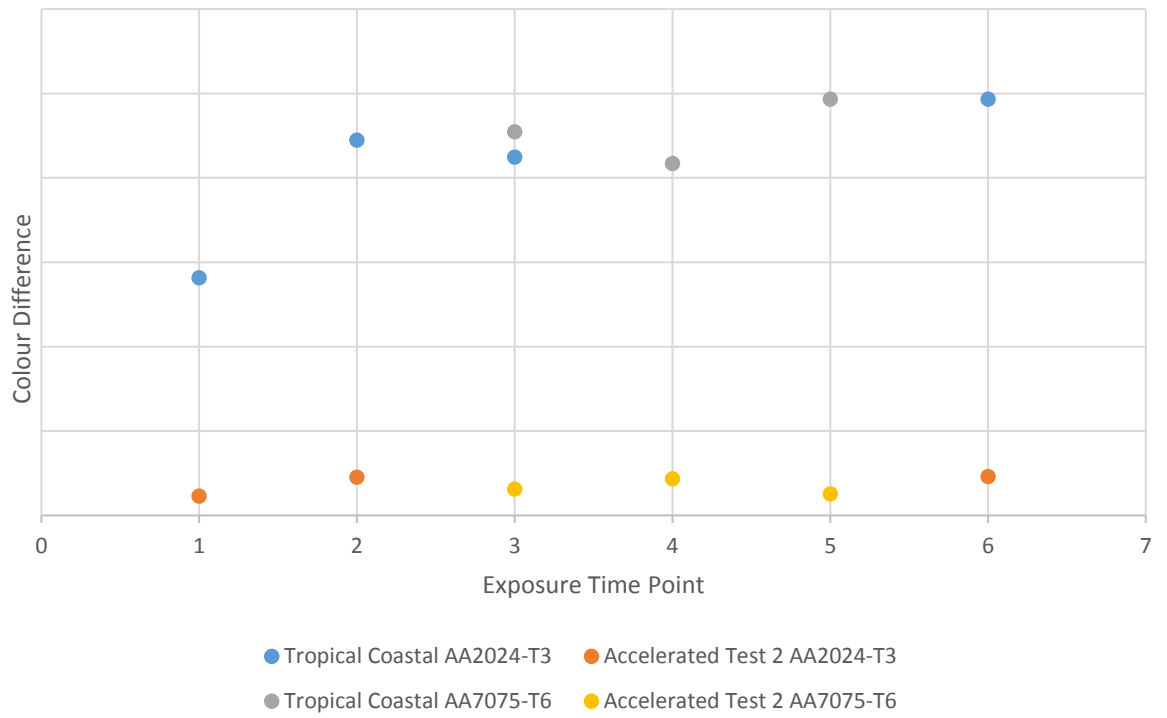


Figure 76: Coating 4 Primer Calculated ΔE 2000 Colour Difference.

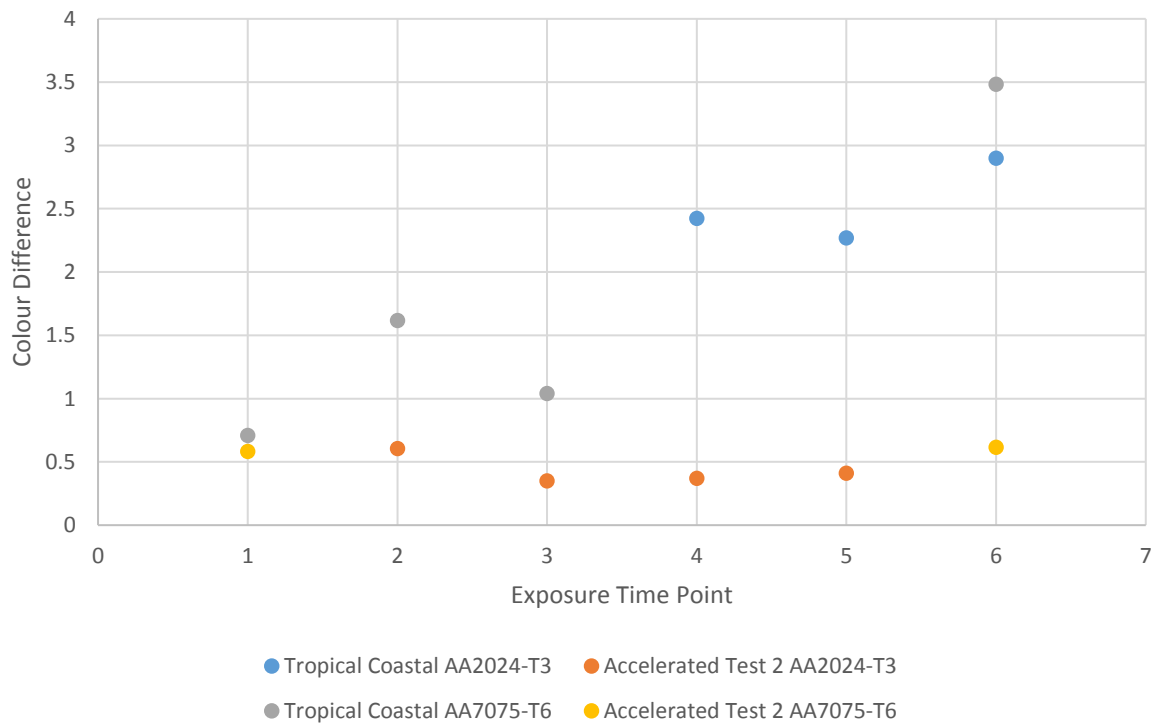


Figure 77: Coating 5 Primer Calculated ΔE 2000 Colour Difference.

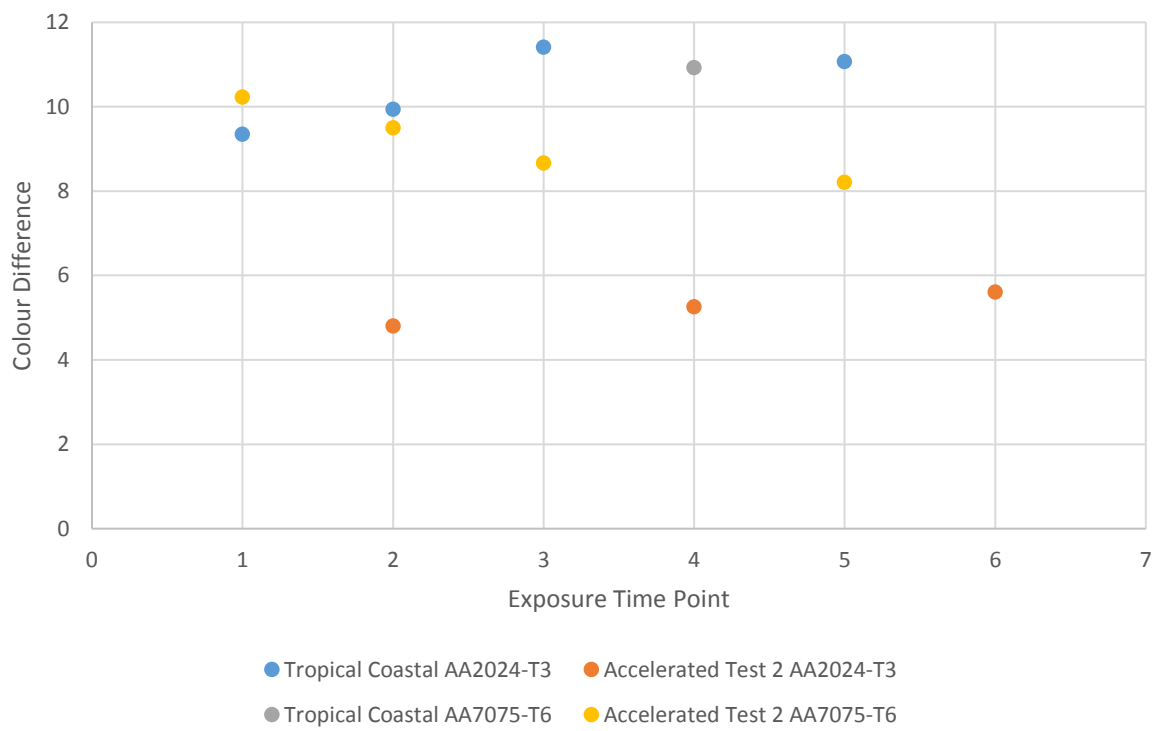


Figure 78: Coating 6 Primer Calculated ΔE 2000 Colour Difference.

5.5. Summary

Chapter 5 asked the question - Is it possible to implement a procedure into a standard CCT chamber that is able to replicate coating performance seen during the tropical coastal field exposure?

The question was asked as a result of the varied response coatings showed upon exposure to different field sites, and the need to create corrosion tests able to predict the service life of a coating. The BS EN ISO 9227, the current testing protocol favoured by the U.K. military has been shown to be unable to meet this need. When compared to the exposure environment most similar, the BS EN ISO 9227 caused dissimilar corrosion and polymer degradation markers to the coupons exposed to the field site. The field site used for comparison in Chapter 4 was the tropical coastal site, an environment that typically has a temperature in the day time of around 35 °C and night time low of 28 °C, the relative humidity is typically between 95 % and 100 % and the salt loading is extreme as a result of the exposure sites location on the break line of a beach. Even this was unable to match the performance seen with coupons exposed to the BS EN ISO 9227 salt spray test.

In response to this inadequacy a novel accelerated CCT protocol was created with the intension of creating a more representative testing protocol that could be implemented directly into a CCT chamber without modification. The protocol was created using weather data measured at the tropical coastal field site along with measured NaCl deposition rates at the site. The program cycled through a diurnal cycle typical of the non-seasonal environment, with coupons spray with a high concentration NaCl solution once every 4 h. The duration of the salt spray was varied to match the range of NaCl deposition data points provided alongside the temperature and humidity data. The intension of this experiment was to replicate performance of coatings exposed to the tropical coastal site in an accelerated time frame, this resulted in a typical diurnal cycle being passed through every 4 hours, and with the NaCl loading to match.

The increase in cycle rate was not able to accelerate all coating system tested at an equal rate, there were some formulation that did not respond to the limited variables applied to the CCT chamber. The corrosion morphology was more representative than that which was created by exposure to BS EN ISO 9227 salt spray. The protocol does not achieve the entirety of the aim of the chapter, but it appears to be a promising starting point for further exploration of this idea to replicate real world conditions within a CCT chamber.

6. Alternative Approaches to Salt Spray

6.1. Introduction

The importance of exposure environment has been highlighted when considering the lifetime of a coating when used in-service. Typically acceleration of corrosion is driven through increases in temperature and humidity, alongside application of aqueous corrodents such as NaCl, SO₂ and Harrison's solution at varying concentrations. Although numerous testing protocols exist, there has yet to be a definitive test or suite of tests that are capable of predicting the service life of any coating within an accelerated time frame. Parameters that have typically been used to accelerated corrosion do not lend themselves to the development of a predictive test. Changes to temperature, humidity and corrodent loading implemented to accelerate all result in the creation of a measurably different environment. For this work only changes to cycle rate were identified as having the potential to accelerate without changing environments inherent qualities. Chapter 5 tested replication of 'real world' environmental conditions within a cyclic corrosion chamber, with the acceleration mechanism employed being an increased cycle rate. The results presented showed an inconsistency on response of different coating systems. Had the increase in cycle rate been able to consistently effect all coatings tested, the potential of a predictive accelerated laboratory test may have been a step closer,

The potential of replicating measured environments in a cyclic corrosion chamber was explored for the temperate inland with the addition of rainfall to the suite of variables testing Chapter 5. The temperate inland environment provided additional challenges for application to a cyclic corrosion

chamber as result of the lower temperature and humidity values necessary then those replicated from the tropical coastal site.

In addition to further exploration of the potential of replication of field exposures within a cyclic corrosion chamber, the potential of accelerating field exposures was also explored. The accelerant of interest was application of an aqueous oxidant. The intent of this was to explore the link between UV, water and atmospheric oxidant loading. The oxidant selected was hydrogen peroxide, the place hydrogen peroxide has within atmospheric corrosion and polymer degradation is explored in Section 6.4.

6.2. Objectives

The objective of the chapter was to explore some previously unexplored alternatives to current approaches to accelerate corrosion testing of coatings. The chapter aimed to answer the following questions:

1. Is it possible to implement a procedure into a cyclic corrosion chamber that is able to replicate coating performance from a temperate field exposure?
2. Does the inclusion of a wash off step create a more presentative accelerated testing protocol?
3. Should UV be consider in isolation or is oxidant important?
4. Is it best to replicate field environments in a cyclic corrosion chamber, or is it better to accelerate the degradation experienced in the field?
5. Could the application of an aqueous oxidant accelerate coating degradation?

6.3. The importance of rain

This question shall be answered by applying seasonal temperature and humidity conditions measured during the first 12 months of exposure at Southampton to the chamber programming. The experiments are synced by time points.

The Southampton exposure time points were as follows:

Start – March – spring exposure

84 days – May – summer exposure

168 days – August – autumn exposure

252 days – November – winter exposure

336 days – February – spring exposure

420 days – April – summer exposure

504 – July - end

The identified seasonal cycle was also described. Due to the large number of variables measured over the course of the first 12 months exposure, it was important to rationalise the parameters to be applied within the chamber. It was decided that four separate cycles would be developed, one to represent each of the seasons. The seasonal cycle was made up of the summer and winter cycle were developed first.

For each month all of the temperature data was plotted in 24 h cycles. Each month was split into three sections, with the data plotted. The highest and lowest days were then identified by eye and extracted from each of the three plots before being plotted together to generate the highest and lowest days for each month. The highest days for each month were plotted together and 7th July was then selected as the day representing summer. The month with the highest temperature day was then further analysed to identify the lowest temperature achieved that month, the day in question then became the second set of variables for the summer cycle. The cycle points in question were:

1. 17 – 30°C and 89 – 45% RH, respectively
2. 13 – 26°C and 96 – 80% RH, respectively

The winter cycle was selected in much the same way, only using coldest days of the month. The resulting cycle did not contain controlled humidity but the temperature cycle was:

1. 0 – 3°C – no RH control
2. 7 – 13°C - 95 – 72 % RH, respectively

The spring and autumn cycles were defined in much the same way the specific values of can be seen in Figure 79.

All of the accelerated testing protocols created within this work were completed after 84 days of exposure. This was a result of the decision to focus on accelerated through increased cycling rate of diurnal cycles. Specifically for accelerated testing protocol 2 which aimed to accelerate the performance measured during the temperate field exposure, the diurnal cycle rate was increased six fold. A six fold increase was used as it was the fastest that the exposure chamber was able to travel between the extremes of temperature and humidity required. The increase in cycle rate combined with the 14 day removal of coupons resulted in each 14 day time point equalling the 84 diurnal cycles of temperature and humidity were experience in the field with respect to temperature and humidity cycles. The decreased cycle time in the accelerated testing protocol resulting in the typical three month seasonal cycles defined above reduce to a total of 14 days. The 14 day pseudo seasons within the accelerated testing protocol resulted in the coupons being exposed within the laboratory to the equivalent of 18 months field exposure meaning the protocol included two spring

14 days seasons, two summer seasons, a single autumn season and a single winter season. This was selected to match the spring start of the temperate inland field exposure.

6.3.1. Materials

The aluminium alloy coupons defined in Table 30 were coated and imaged in preparation for accelerated exposure in the Weiss WVC340-40 environmental chamber. Coupons of either AA2024-T3 or AA7075-T6 coated with each of the six coating systems previously defined in Chapter 2.

Table 30: Coupon allocations for accelerated testing protocol 2

Coating System	Substrate and Time Point													
	AA2024-T3							AA7075-T6						
	1	2	3	4	5	6	7	1	2	3	4	5	6	7
1	23	22			396					212	24		19	20
2		295	149				83	85			87	81	84	
3			163		12	145	146	147	18		150			
4		92	310	213		26		234	211			207		335
5	273			276	270				337	275			271	272
6	336			327		334	321		21	338	368	333		

6.3.2. Experimental procedure

The coupons were exposed at a 45° angle to the seasonal temperature and humidity cycles defined in Figure 79 starting with spring variant and following the seasons as they would occur in the field. Step changes in temperature and humidity were made at 2 h intervals meaning there were six diurnal type changes per 24 h. Along with the temperature and humidity cycles the coupons were also exposed to a wash off sequence using a fine rose on watering can representative of the rain fall events measured at the temperate inland field site, see Table 31. Once the coating surfaces were ‘washed off’ with deionised water the coupons were reloaded with 1 mL of NaCl solution using a spray bottle, the concentration of NaCl varied dependent upon the seasonal cycle. The concentration of the NaCl solution was modified to ensure the total loading of NaCl remained constant. The individual seasonal cycles were maintained for 14 days, resulting in a match between number of diurnal cycles experienced during the temperate inland field exposure and the accelerated protocol

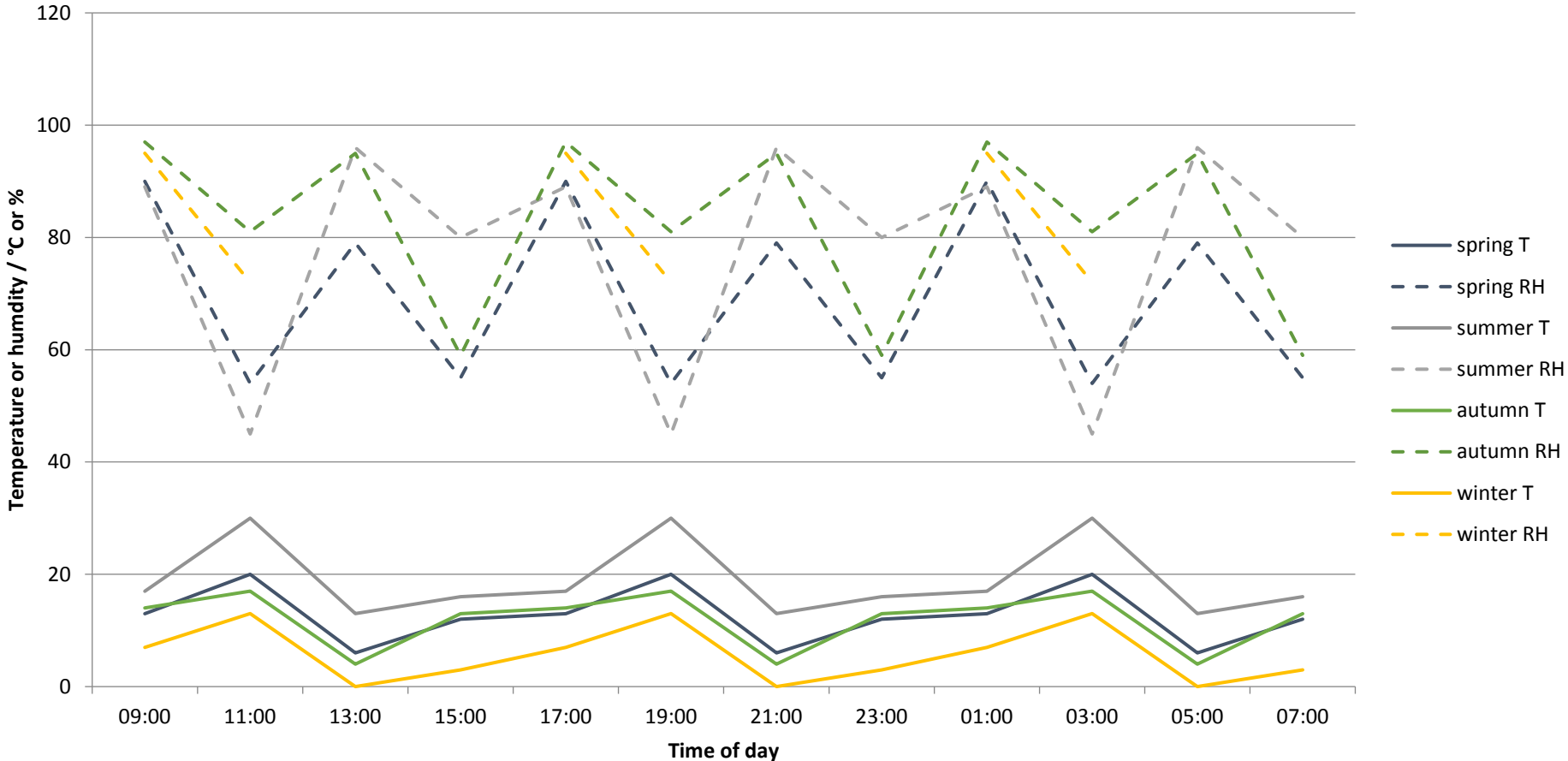


Figure 79: Temperature and humidity cycle for seasonal accelerated protocol.

The concentration of NaCl solution was varied depending upon the season of exposure; spring and winter cycles utilised a concentration of 0.668 g L^{-1} , the summer cycle used a concentration of 1.336 g L^{-1} and autumn which had the greatest number of rain events utilised a concentration of 0.444 g L^{-1} . The average volume of water used for the wash off step of each coupon was $25 \pm 9 \text{ ml}$.

Table 31: Seasonal wash off and corrodent loading events

Season	Time of Day			
	9:00	13:00	16:00	17:00
spring	Rain / NaCl	-	Rain / NaCl	-
summer	Rain / NaCl	-	-	-
autumn	Rain / NaCl	Rain / NaCl	-	Rain / NaCl
winter	Rain / NaCl	-	Rain / NaCl	-

The coupons were exposed for up to a total of 84 days with subsets of coupons removed every 14 days. This ensured that at each time point the coupons exposure was matched in number of cycles to that of the temperate inland field exposure.

6.4. Trials with oxidants

Typically metallic atmospheric corrosion is accelerated in a laboratory through the application of additional mass of a corroding species alongside exposure to an elevated temperature and increased humidity environment. The corrosion species of choice is often NaCl, as illustrated by its use in standards such as BS EN ISO 9227 and ASTM B117 [1, 6]. NaCl should not be considered as the only atmospheric species of interest industrially, other species have been included in standardised testing. One example is sulfur dioxide (SO_2), copper and zinc substrates are both sensitive to SO_2 exposure [98, 128]. This sensitivity is reflected by its place in standard acceleration tests such as ASTM G85-Annex A4-1 [94].

Atmospheric oxidants have a key role in corrosion of metallic substrates but often are not considered in accelerated tests. Oxidants identified as having a role in the atmospheric corrosion of metallic substrates include ozone (O_3) and hydrogen peroxide (H_2O_2) [85]. Atmospheric oxidants can react directly and indirectly with the metallic surface, with direct reaction resulting in direct oxidation of the surface, i.e., the formation of silver(I) oxide (Ag_2O) through direct oxidation of silver by ozone in a dry environment [129]. Hydrogen peroxide and its related photoactive radicals are also able to create direct oxidation, their reaction with the ferrous cation (Fe^{2+}) ion is well documented [130]. The oxidation of Fe^{2+} identified a diurnal relationship between H_2O_2 and its

photoactive radicals with respect to the dominant reaction species, with H_2O_2 dominant in the bulk oxidation of Fe^{2+} by night and the hydroxyl (OH) and hydroperoxyl (HO_2) radicals dominant by day [130].

For the purpose of developing an accelerated corrosion test, a solution based atmospheric oxidant is best, as it is possible to simply control the application of the oxidant to the substrate. Application of ozone has been explored academically but does require rather dramatic modification of traditional corrosion chamber [131]. As gaseous loading of oxidant would have increased the complexity of the task at hand, an aqueous phase reactant was sought.

H_2O_2 is a naturally occurring atmospheric oxidant, formed outside via reactions in smog, as well as it is also documented as a constituent species in precipitation [132]. Dry phase and wet phase deposition of H_2O_2 occurs on surfaces exposed outside. H_2O_2 provided the opportunity for a naturally occurring aqueous phase oxidant. H_2O_2 is found in the gaseous phase in levels of parts per billion or less, however, when found in solution micro molar concentrations are the norm, Vione et al. quoted a range of international concentrations from 0.1 μM and 180 μM [133].

Aluminium is often defined as being the metal most resistant to hydrogen peroxide, as a result of no identified primary reaction with H_2O_2 in all of the known atmospheric corrosion reactions [85]. However, H_2O_2 does still have a role to play in the corrosion of aluminium, and its alloys, and of many other metallic materials in the form of a reactant in secondary reactions necessary to transform atmospheric species into viable corrosion reactants. H_2O_2 has been identified as one of a set of possible atmospheric oxidants which are pivotal in sulfate containing corrosion mechanisms. The oxidants are responsible for oxidation of the bisulfate ion (HSO_3^-) to the sulfate ion (SO_4^{2-}) which is then able to react with the metallic substrate [128]. Nickel, aluminium and zinc are all known to react with sulfate (SO_3^{2-}) ions when examined after atmospheric exposure [85, 134, 135].

6.4.1. Materials

Two sets of field exposures were completed to explore the possibility of hydrogen peroxide as an accelerating agent. The specific coupons tested are defined in Table 32 and Table 33. The difference between the experimental procedures is detailed in Section 6.4.2. As with all previously defined exposures, the two campaigns appear incomplete as they were created as a part of the larger factorial design detailed in Chapter 7.

Table 32: Coupon allocations for accelerated testing protocol 3 coupon definitions

Coating System	Substrate and Time Point													
	AA2024-T3							AA7075-T6						
	1	2	3	4	5	6	7	1	2	3	4	5	6	7
1		13			8	33	160	35		37	38			
2	98		100		95		113		99		101		96	97
3	350	162		164		159				226		158		181
4	203		349	250	221				225				222	223
5		2		360			286	287		289		284	285	
6			352			348	361	210	351		34	143		

Table 33: Coupon allocations for accelerated testing protocol 4

Coating System	Substrate and Time Point													
	AA2024-T3							AA7075-T6						
	1	2	3	4	5	6	7	1	2	3	4	5	6	7
1			44	45	39		41	42	43				40	230
2	126	274		108						107		102	292	104
3	168		170		6	103			*469		171			167
4	14			346		229	251		232	233		228		
5		296	303			294	293	106			297	291	208	
6		358			354	355	356	357		9	339			

6.4.2. Experimental procedure

The coupons were exposed externally at the temperate inland site beginning in spring of 2016. The racking used was the same as that detailed in Section 3.3.2. In addition to the natural exposure conditions coupon were individually exposed to a 1 mL spray H₂O₂ at either a high or low concentration twice per week. The original intention was to apply then spray once per day, but the results for the high concentration were so immediate that the frequency of application was lowered to try and ensure coupons would be viable for the entirety of the exposure. The lower H₂O₂ concentration used is 0.03 wt. % and the higher concentration was 100 time stronger at 3 wt.%. The total exposure time was up to 84 with coupon subsets removed every 14 days.

6.5. Results and discussion

The results and discussion for studying the effect of rain shall be discussed first, the results and discussion from the work exploring the effect of addition of oxidant will then follow.

6.5.1. Studying the effect of rain

Coating system 1 after 84 days exposure at time point 7 (see Figure 80) to accelerated testing protocol 2 the coupon exhibited micro blistering of the topcoat section and discolouration of the magnesium primer. When compared to time point 7 (504 days) of the temperate inland exposure (see Figure 81) the micro blisters (area <math>< 3 \text{ mm}^2</math>) present have progressed further leading to the blistering events on the bottom of the topcoat section. The location of the blisters at the edge of the coupon identifies that the edge of the coupon may have the location for ingress of corrosives rather than permeation through the coating. The primer section also shows a deviation in behaviour between the field exposure (Figure 81) and the accelerated testing protocol (Figure 80), when exposed to the field exposure all open primer has reacted leaving the bare metal, whilst in the surface level reaction has occurred. The difference illustrates that the sacrificial reaction of the Mg primer is not driven only by the number of diurnal cycles, instead the length of exposure cannot be ignored.

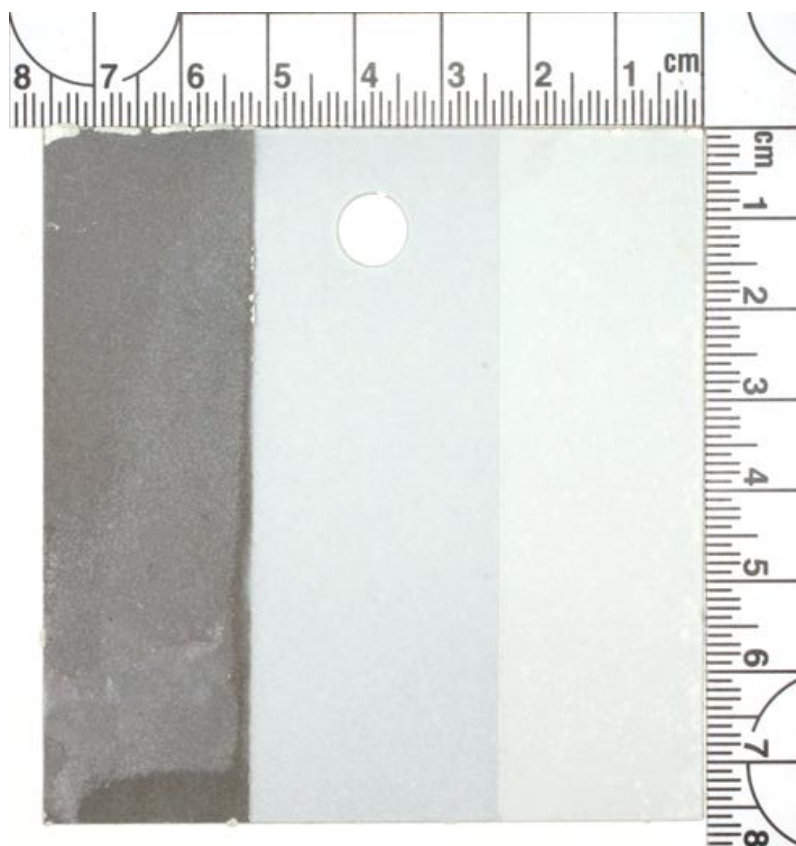


Figure 80: Post exposure image of Coating System 1 (Coupon #20) applied to AA7075-T6 exposed for 84 days to the laboratory based accelerated test protocol 2; temperature range of 30 °C to 0 °C, Relative Humidity range of 95 % to 45 %, [NaCl] range of 0.444 g L⁻¹ to 1.333 g L⁻¹ and wash off volume of 25 ML per coupon.



Figure 81: Post exposure image of Coating System 1 (Coupon #62) applied to AA7075-T6 exposed for 504 days to the temperate inland field exposure.

The difference in progression of coating failure for coating system 1 between the field exposure and the accelerated test, the increase in cycle rate is not the complete picture regarding acceleration of an environment. However, when the time point 7 coupon for the accelerated test is compared to some of the earlier the time point of the temperate inland exposure it is possible to see the progression of the degradation passing through a point similar to that seen in the accelerated test. Figure 82, Figure 83 and Figure 84 illustrate the progression of coating failure for coating system 1 at 84 days, 252 day and 336 days exposure to the temperate inland site. The progression for the topcoat is the initiation of micro blisters visible on the surface of the topcoat and the reaction of the primer towards complete removal.

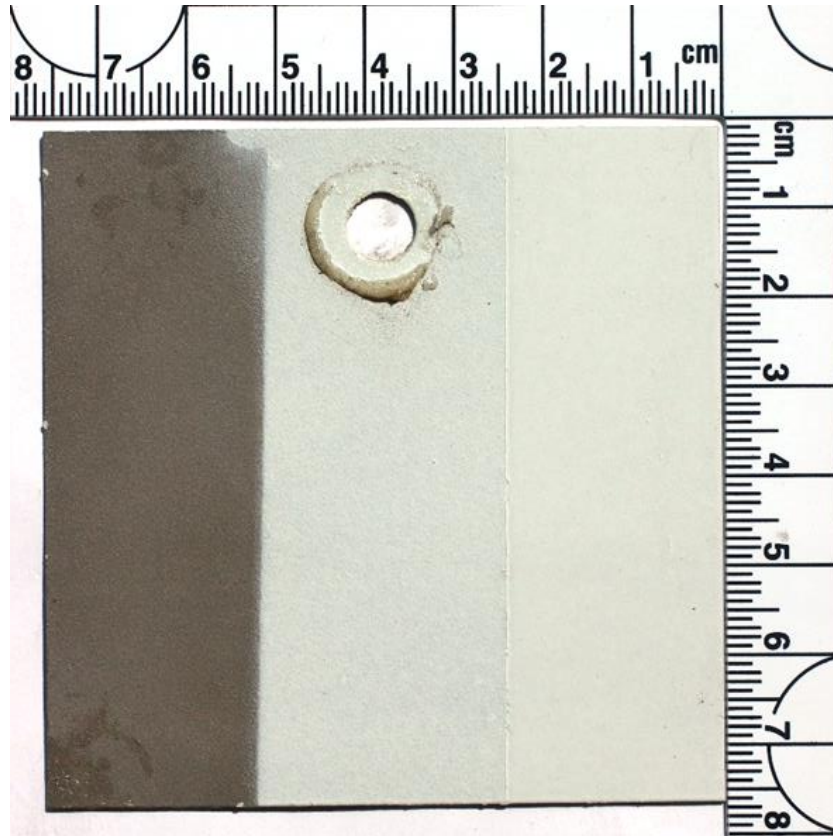


Figure 82: Post exposure image of Coating System 1 (Coupon #379) applied to AA7075-T6 exposed for 84 days to the temperate inland field exposure.

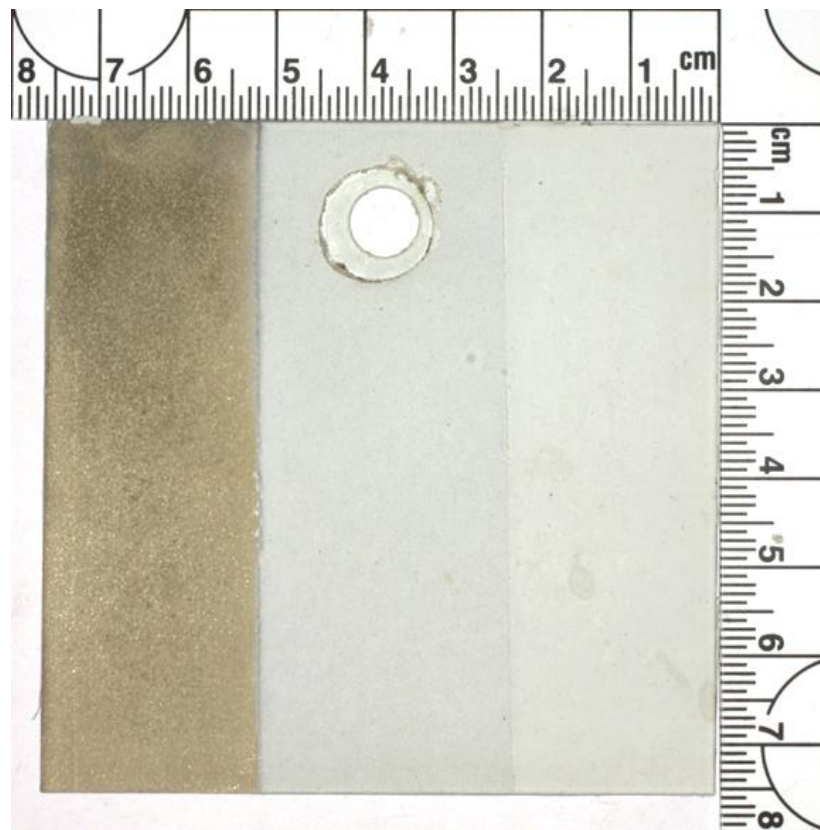


Figure 83: Post exposure image of Coating System 1 (Coupon #381) applied to AA7075-T6 exposed for 252 days to the temperate inland field exposure.

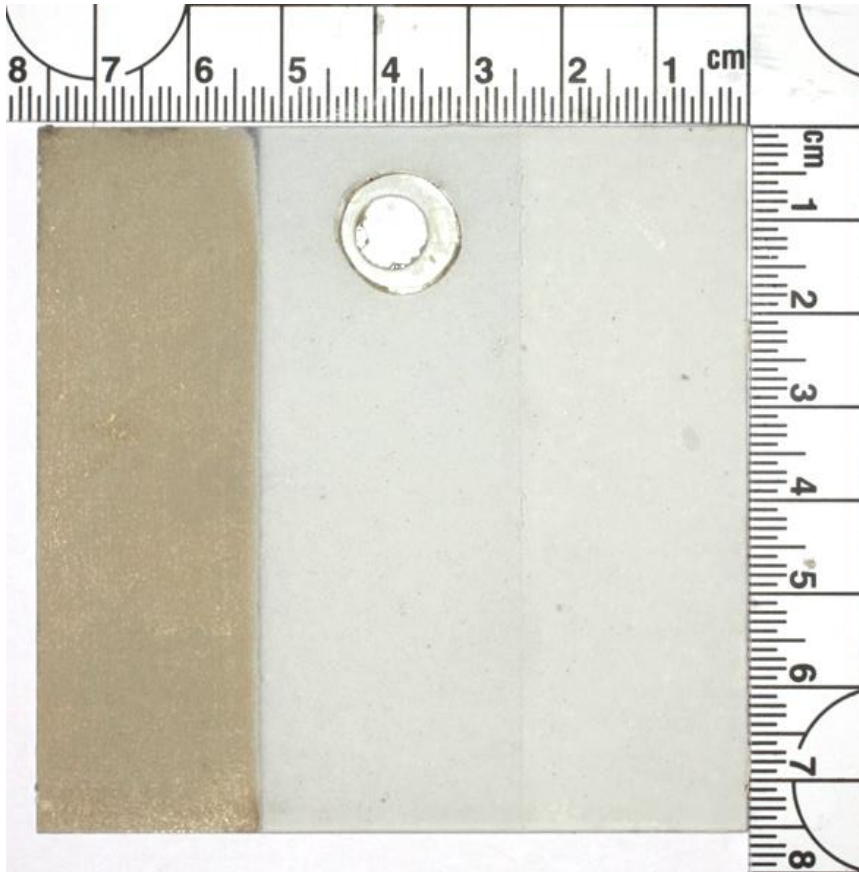


Figure 84: Post exposure image of Coating System 1 (Coupon #60) applied to AA7075-T6 exposed for 336 days to the temperate inland field exposure.

Continuing comparisons between accelerated test protocol 2 and the temperate inland field exposure using coating system 6 after 84 days exposure at time point 7 shows a similar pattern. Micro blisters although more frequent on the accelerated exposure experiment are of the same scale seen post temperate inland field exposure and of those seen on coating system 1. The decrease in gloss was not as pronounced in the accelerated test for coating system 6, but this could be indicative of a lack of UV exposure.

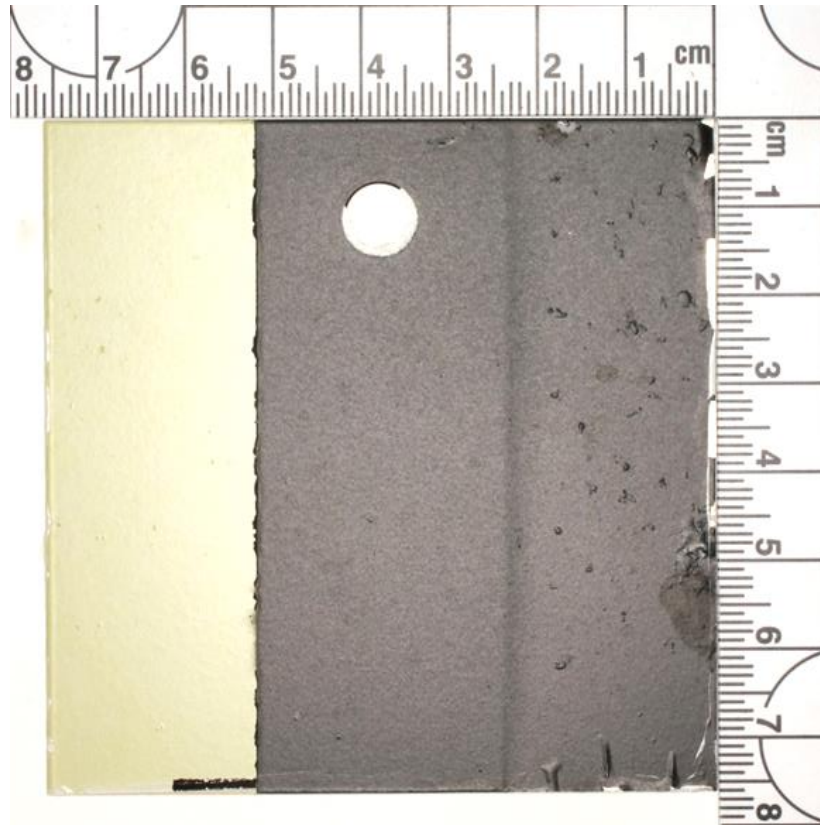


Figure 85: Post exposure image of Coating System 6 (Coupon #321 applied to AA2024-T3 exposed for 84 days to the laboratory based accelerated test protocol 2; temperature range of 30 °C to 0 °C, Relative Humidity range of 95 % to 45 %, [NaCl] range of 0.444 g L⁻¹ to 1.333 g L⁻¹ and wash off volume of 25 ML per coupon.



Figure 86: Post exposure image of Coating System 6 (Coupon #377) applied to AA2024-T3 exposed for 504 days to the temperate inland field exposure.

Disregarding the increased cycle rate and comparing exposures in time rather than the number of transitions in temperature and humidity shows that the decrease in gloss of the primer section occurs rapidly during outside exposure. Figure 87 shows coating system 6 coupon after 84 days exposure to the temperate inland field site, and unlike Figure 86, the field exposure coupon shows strontium chromate leaching stains. It appears in the case of the accelerated test that the primer remained relative intact. Highlighting that although the topcoat breakdown is showing similar features, there is a variable missing from the exposure that is driving the leaching of the active pigment found in coating system 6 when exposed at a field site. It should be noted that although the accelerated protocol is not a complete story it does hold promise, when compared to a coupon exposed to BS EN ISO 9227 (Figure 88). The coupon exposed to BS EN ISO 9227 for 84 days shows little loss of chromate pigment, as well as a very different style of blister to coupons exposed either externally in a field site or to accelerated test protocol 2. As a result of the shortened experimental campaign in the accelerated tests it is difficult to identify if the accelerated test was completely successful.



Figure 87: Post exposure image of Coating System 6 (Coupon #316) applied to AA7075-T6 exposed for 168 days to the temperate inland field exposure.

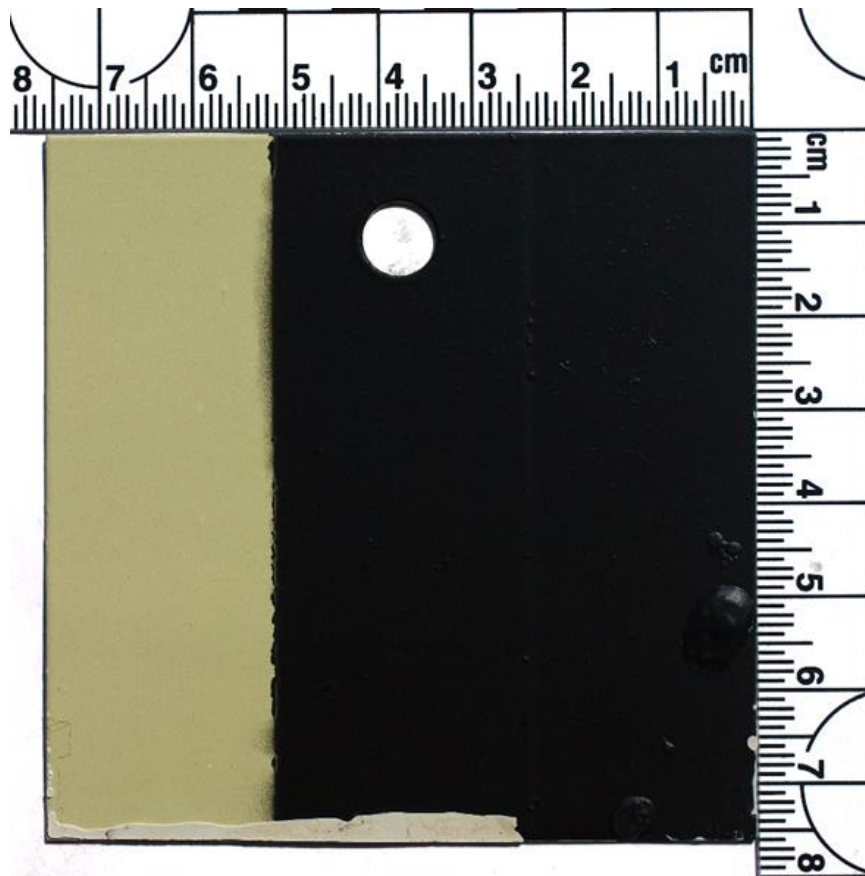


Figure 88: Post exposure image of Coating System 6 (Coupon #328) applied to AA7075-T6 exposed for 84 days to the BS EN ISO 9227 salt spray test, exposure temperature 35 °C with a continuous 5 wt.% NaCl solution deposited at a rate of 1.5 mL h⁻¹ 80 cm².

6.5.2. Studying the effect of oxidants

The application of an oxidant to accelerate a field exposure provided an opportunity to explore the potential of the approach rather than create a fully defined exposure protocol that could be used for ongoing coating research. This preliminary exploration aimed to answer a number of questions related to the potential of aqueous application H₂O₂ as a natural exposure accelerant. The questions were as follows:

1. Over the course of a field exposure does the application of aqueous H₂O₂ have a measurable effect on the degradation of polymeric coatings?
2. Do different concentrations of oxidant loading result in measurable differences in coating performance?
3. Does the application of H₂O₂ affect all coating types tested?
4. What was the effect on the substrate?
5. How do the results compare to the chamber acceleration previously performed in Section 6.5.1?
6. Which coating system was most resistant to the additional oxidant loading?

In response to Question 1, the ability of H_2O_2 to have an effect on the degradation of a polymeric coating upon exposure to a given environment was tested using the higher concentration (0.03 wt. %) application of aqueous H_2O_2 to each of the coating systems. The effect the application had on each of the coating system types below in Figure 89 to Figure 94.

Coating system 1 showed clear evidence of reactivity with H_2O_2 , the rate of reaction of the primer appeared to be accelerated by the application of H_2O_2 illustrated by the colour change (labelled 'a') at the bottom of the primer section (Figure 89). The change in colour of the primer was documented in Section 6.5.1 with the progression of primer degradation upon exposure illustrated by Figure 82, Figure 83, Figure 84 and Figure 81. The primer first changes from a deep matte grey colour (Figure 82) to include localised lightening of the panel (Figure 83), before an all over beige shade (Figure 84) is seen prior to the loss of the coating and revelation of the uncorroded Al substrate (Figure 81). The topcoat section of coating system 1 also saw faster degradation upon application of H_2O_2 . After 84 days exposure to the temperate inland field site augmented with the addition of 3 wt. % H_2O_2 a number of osmotic blisters (labelled b) were identified across the surface of the topcoat (see Figure 89). The identification of the blisters as being osmotic in nature will be defined later within this section whilst discussion the effect H_2O_2 had on the aluminium substrates tested.

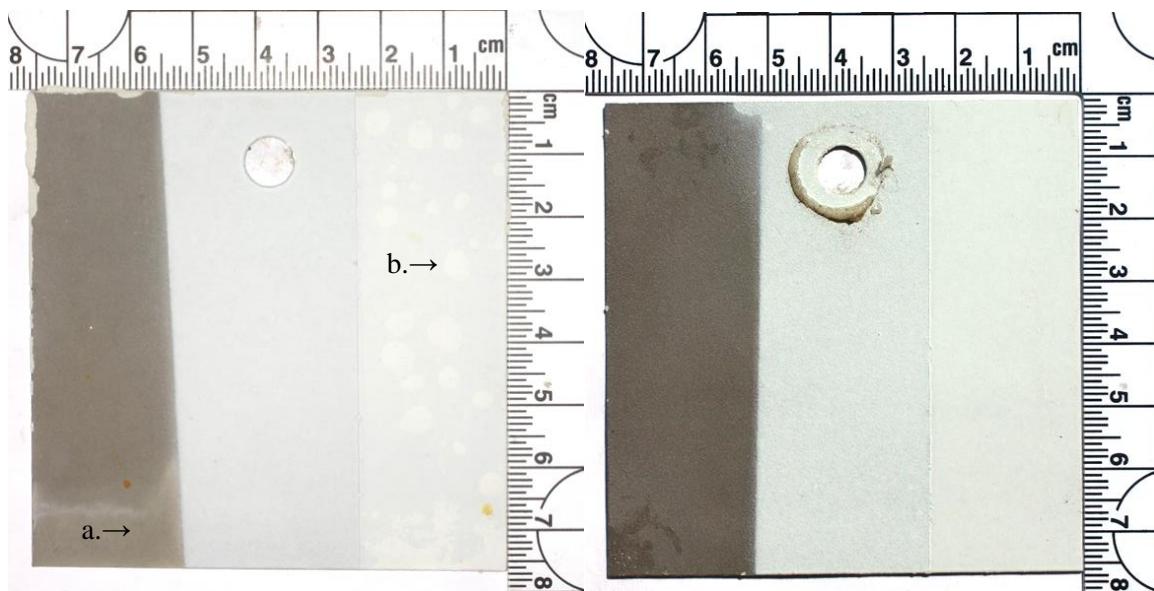


Figure 89: Coating system 1 coupon number 230 (left) and 379 (right) post 84 days exposure to temperate inland site, coupon 230 exposure augmented with the addition of 1 mL of 3 wt. % H_2O_2 solution twice per week.

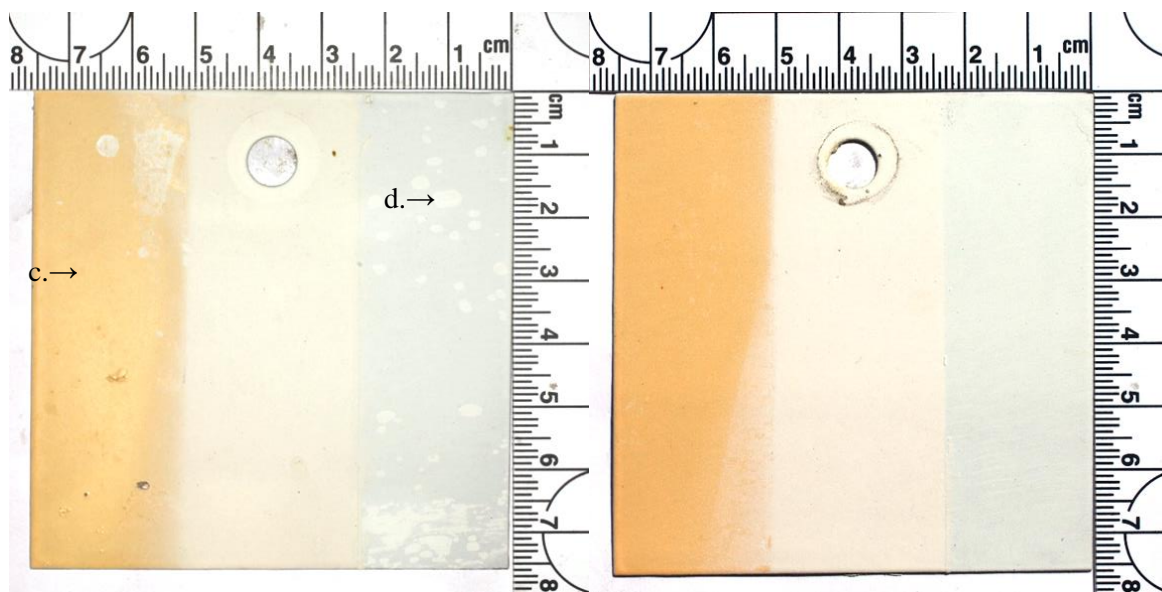


Figure 90: Coating system 2 coupon number 104 (left) and 82 (right) after 84 days exposure to temperate inland site, coupon 104 exposure augmented with the addition of 1 mL 3 wt. % H_2O_2 solution twice per week.

Coating system 2 displayed a varied response to the application of H_2O_2 ; the measured gloss of the primer section was more effected than that of the coupons exposed to the unaugment temperate inland field site. The coupon exposed to the temperate inland site for 84 days (Figure 90 - Coupon 82) had a measured gloss profile of the primer post exposure of 5 GU, 22 GU and 8 GU at 20° , 60° , and 85° , whilst the coupon exposed to the temperate inland site with the addition of H_2O_2 had a primer gloss profile (labelled c) of 2 GU, 10 GU and 16 GU respectively. Prior to exposure the average gloss measurements for the primer of coating system 2 coupons were 9 GU, 36 GU and 22 GU. Early degradation of polymer chains in coatings has been documented as manifesting as a change in measured gloss, providing weight to the argument that application of H_2O_2 has an effect to the stability of the polymeric chains present in the coating [136]. Had chemical analysis been permitted further exploration of this would have been possible, unfortunately this was prohibited by the coating supplier.

Coating system provides a second feature of interest upon exposure with H_2O_2 . The blistering observed for coating system 2 (labelled d on Figure 90) is of a different morphology than those seen in the topcoat of coating system 1 and 3, coating system 3 is illustrated in Figure 91. This was unexpected as all of the topcoats for coating systems 1, 2 and 3 were the same formulation applied at the same time using the same batch of paint. The only difference between the three topcoat sections is that Metaflex pre-treatment was used for coating systems 1 and 3, but not for 2. Due to the small scale of blistering seen on coating system 2, it is hypothesised that the interlayer between the Mexaflex adhesion promotor and the substrate is more sensitive to the application of H_2O_2 than

the topcoat metallic interface found on system2. Separate analysis of the effect H_2O_2 has on the Metaflex pre-treatment could be completed as a part of future studies.

Coating system 3 (Figure 91) showed one of the more dramatic responses to the application of H_2O_2 . The primer section (labelled e) the primer topcoat (labelled g) and the topcoat (labelled f) all showed osmotic blistering as a result of localised loss of adhesion between the coating and substrate. After 84 days both the primer and the topcoat (f) showed widespread blistering across the entirety of the sections surface. The primer topcoat was more sparsely affected, nevertheless damage did occur. The blistering must be attributed to the inclusion of H_2O_2 , see coupon no.127 (Figure 91) which was exposed to the same environment, just without the addition of H_2O_2 showed no identifiable blistering.

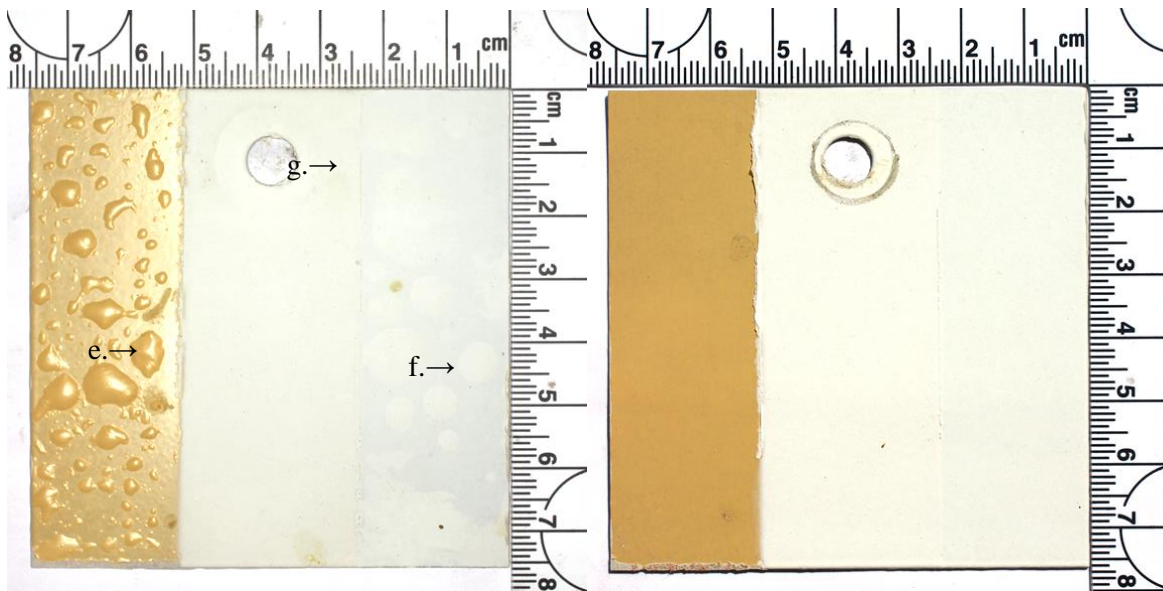


Figure 91: Coating system 3 coupon number 167 (left) and 127 (right) after 84 days exposure to temperate inland site, coupon 167 exposure augmented with the addition of 1 mL of 3 wt. % H_2O_2 solution twice per week.

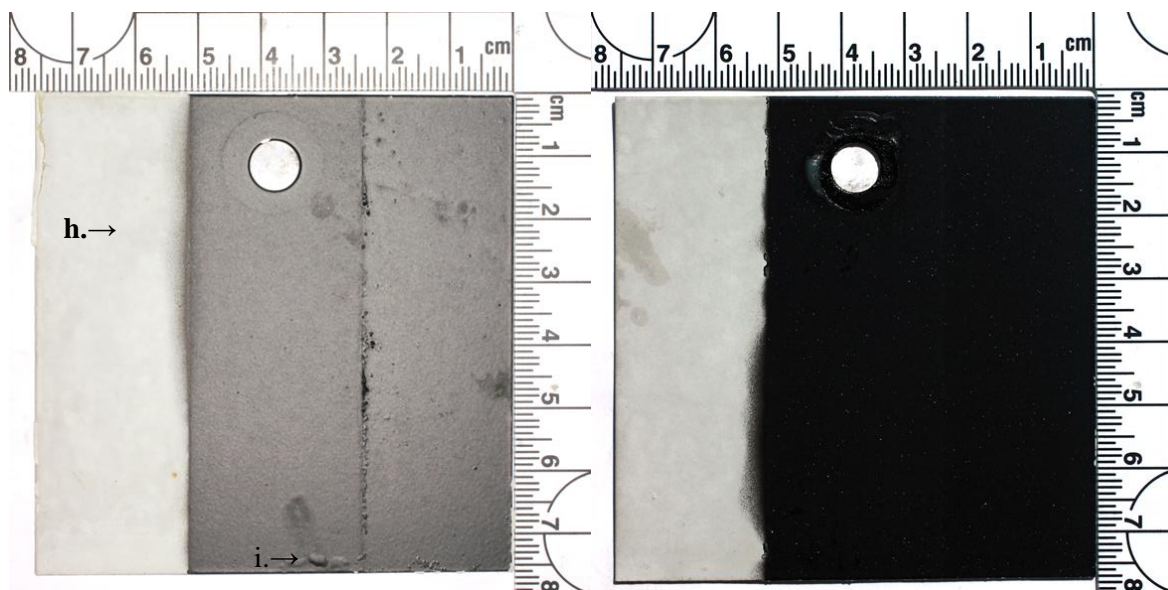


Figure 92: Coating system 4 coupon number 251 (left) and 190 (right) after 84 days exposure to temperate inland site, coupon 251 exposure augmented with the addition of 1 mL 3 wt. % H_2O_2 solution twice per week.

Coating system 4 (Figure 92) showed the most resistance to H_2O_2 with only a slight dappling showing on the surface of the primer section. The topcoat proved to be unaffected by the application of H_2O_2 unlike the topcoat for coating systems 5 and 6 which utilised the same coating but which did not prove to perform as well. The primer topcoat section shows a small amount of blistering labelled I, this was attributed to corrosion ingress from the edge of the coupon rather than as a result of coating failure on the weathering face.

The primer of coating system 5 (Figure 93) appeared relatively unaffected by the application of H_2O_2 to the surface no visible change in gloss resulted and the coating remained resistant to any chalking. The primer topcoat section did show some localised blistering (labelled j), it was postulated that the sol-gel pre-treatment was not as resistant to the application of H_2O_2 as the Desoprime 7530 pre-treatment used on coating system 4. The resistance of the topcoat of coating system 4 and 5 cannot be attributed to the topcoat alone, the pre-treatment which was applied across the entire surface prior to priming likely is responsible for any identifiable differences in performance of the topcoat.

The success of both pre-treatments can be identified through the examination of coating system 6 (Figure 94) after exposure to the temperate inland field site with the addition of H_2O_2 . The exposure resulted in large osmotic blistering on the topcoat section (labelled k) which were unlike the performances seen for the topcoat on the coating systems 4 and 5. The primer section of coating system 6 also showed a reduced resistance to H_2O_2 . The colour shifted from a vibrant green similar to that seen after exposure to the temperate inland environment (Coupon 316 in Figure 94) to the pale greenish grey labelled l on Figure 94. The green colour in Cr(VI) coatings is

a result of the inclusion of the active pigment strontium chromate and the reduction of colour was a result of pigment leeching from the coating and being rinsed from the surface. The reactivity of the primer was great enough that the primer was removed in localised spots across the surface (labelled m). The areas that the coating were removed from left uncorroded substrate visible, with the residual primer protecting the exposed substrate. The loss of primer coverage was thought to be a result of the release of the strontium chromate pigment from a high PVC matrix.

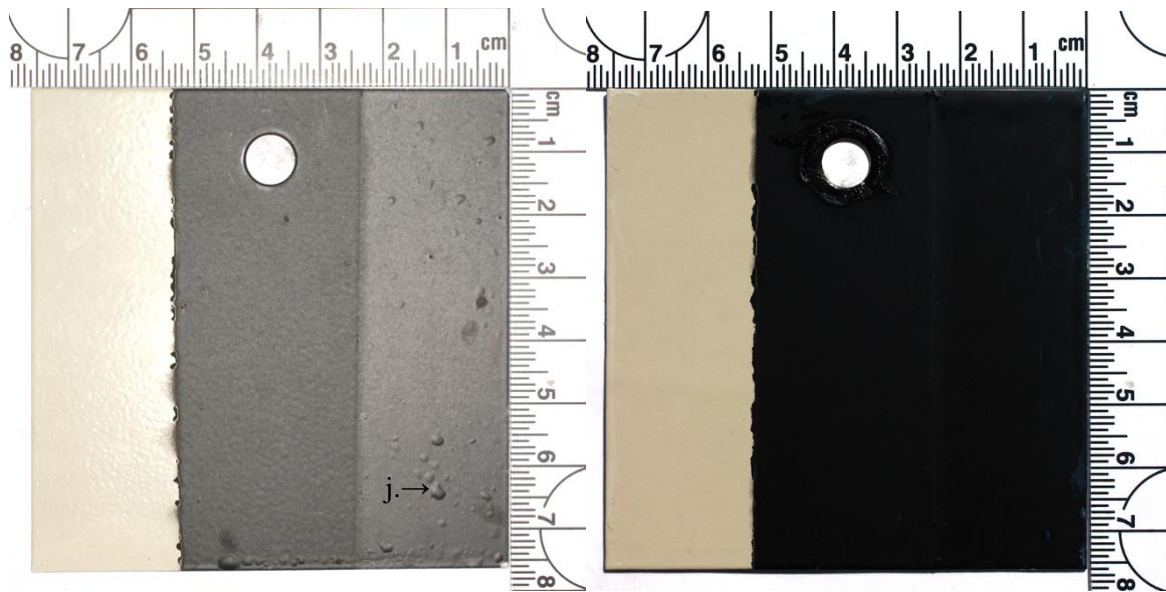


Figure 93: Coating system 5 coupon number 293 (left) and 253 (right) after 84 days exposure to temperate inland site, coupon 293 exposure augmented with the addition of H₂O₂.

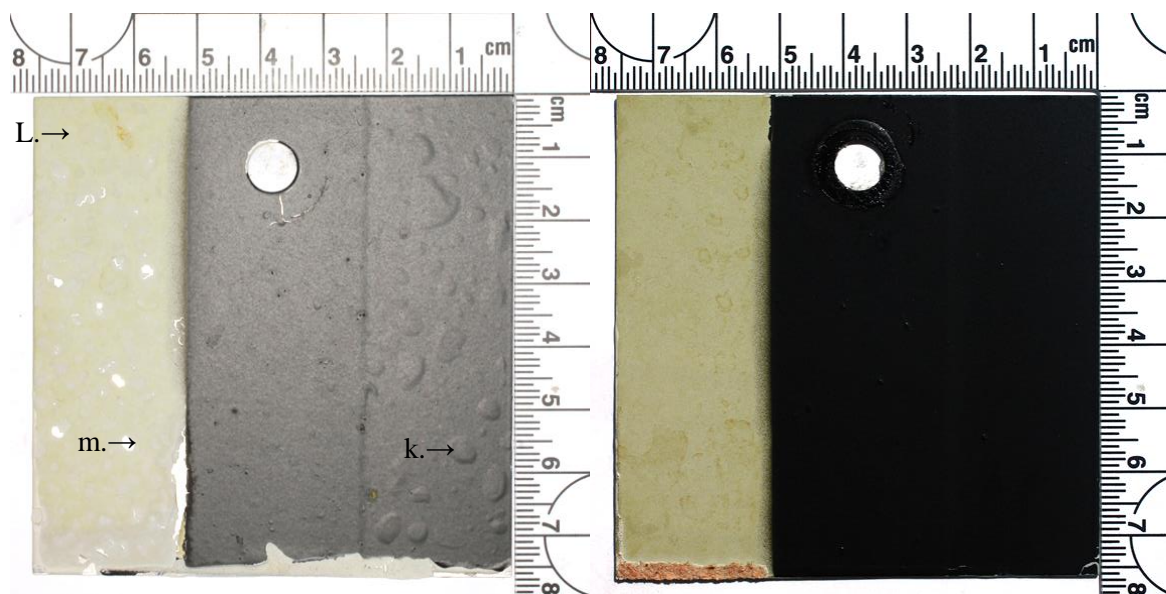


Figure 94: Coating system 6 coupon number 356 (left) and 316 (right) after 84 days exposure to temperate inland site, coupon 356 exposure augmented with the addition of 1 mL 3 wt. % H₂O₂ solution twice per week.

Question 2 required the comparison of matching coupon types exposed to both the high and low concentration of H_2O_2 . Figure 95 to Figure 100 provide a comparison of the effect of the two peroxide concentrations for each of the six coating systems. Coating system 1 (Figure 95) showed a clear reaction to the application of 3 wt. % H_2O_2 with both blistering of the top coat and a loss of Mg particles in the primer. The lower concentration 0.03 wt. % H_2O_2 showed a lesser reaction, no blistering was visible on the topcoat section but there was some evidence of loss of Mg particles resulting in a beige hue (labelled n) across the primer section. Coating system 2 (Figure 96) showed a measurable y different response to the two different concentration of oxidant loading. The blistering that was evident after exposure to the high concentration H_2O_2 solution was not present when the concentration of H_2O_2 was reduced by a factor of 100. Coating system 3 (Figure 97) similarly showed no evidence of the blistering that was present at the high concentration of H_2O_2 when the concentration was reduced.

When different concentrations of H_2O_2 were applied to coating system 4 (Figure 98) a measurable difference in performance was not identified. However, this is in line with what has been measured for coating system 4 throughout the other exposure experiment, even when exposed to an environment qualified as extreme such as the tropical coastal field exposure for 504 days, very little effect was seen. Thus although there was no measured difference in performance for coating system 4 between the two concentrations of H_2O_2 , it was the performance that was expected.

Coating system 5 showed a measurable difference in performance between the top coat section, with application of the higher concentration (3 wt. %) H_2O_2 blisters were identified across the surface (Figure 99 labelled p). When the lower concentration was applied (Figure 99) no blisters were identified. Coating system 6 (Figure 100) also showed a measurable difference with heavy blistering evident on the topcoat and loss of protective pigment and primer coverage upon exposure to the higher concentration of H_2O_2 . When the lower concentration was applied the blistering of the topcoat was not seen, but some loss of pigment was evident in the primer section, however the loss was reduced relative to the higher concentration H_2O_2 application.

The two concentrations of H_2O_2 have been shown to effect coating degradation in a measurably different way. It should be noted that the concentration were not optimised, and so the optimum concentration to best effect all coatings has yet to be defined.

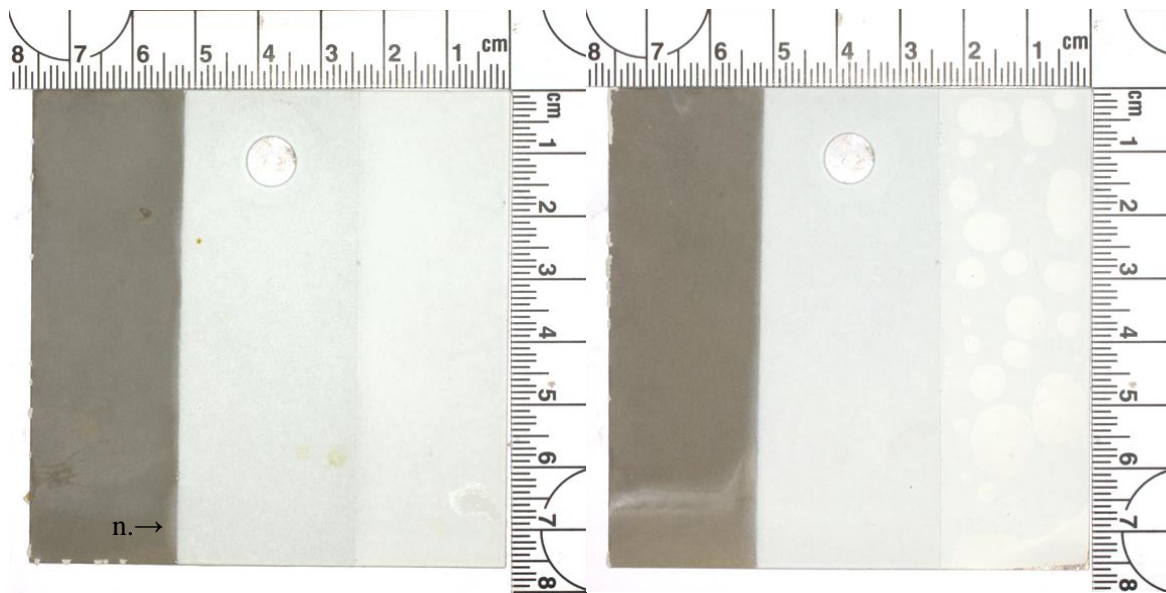


Figure 95: Coating system 1, coupon 160 (left) exposed to temperate inland site after 84 days with addition of 1 mL 0.03 wt. % H_2O_2 solution twice per week, coupon 41 (right) exposed to temperate inland site for 84 days with addition of 1 mL 3 wt. % H_2O_2 solution twice per week.

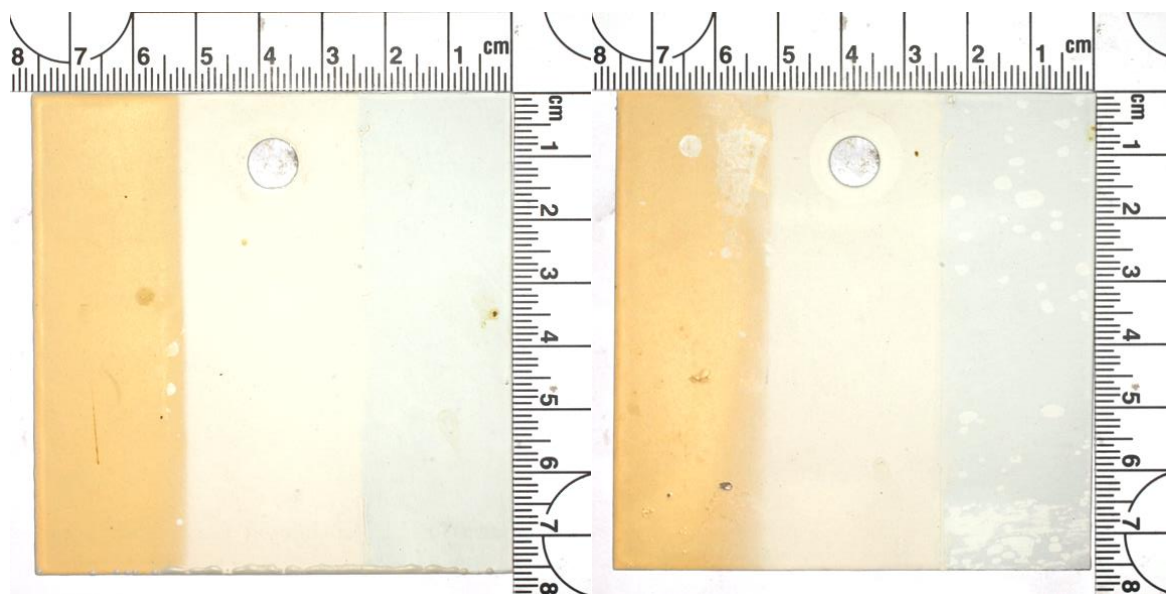


Figure 96: Coating system 2, coupon 97 (left) exposed to temperate inland site after 84 days with addition of 1 mL 0.03 wt. % H_2O_2 solution twice per week, coupon 104 (right) exposed to temperate inland site for 84 days with addition of 1 mL 3 wt. % H_2O_2 solution twice per week.

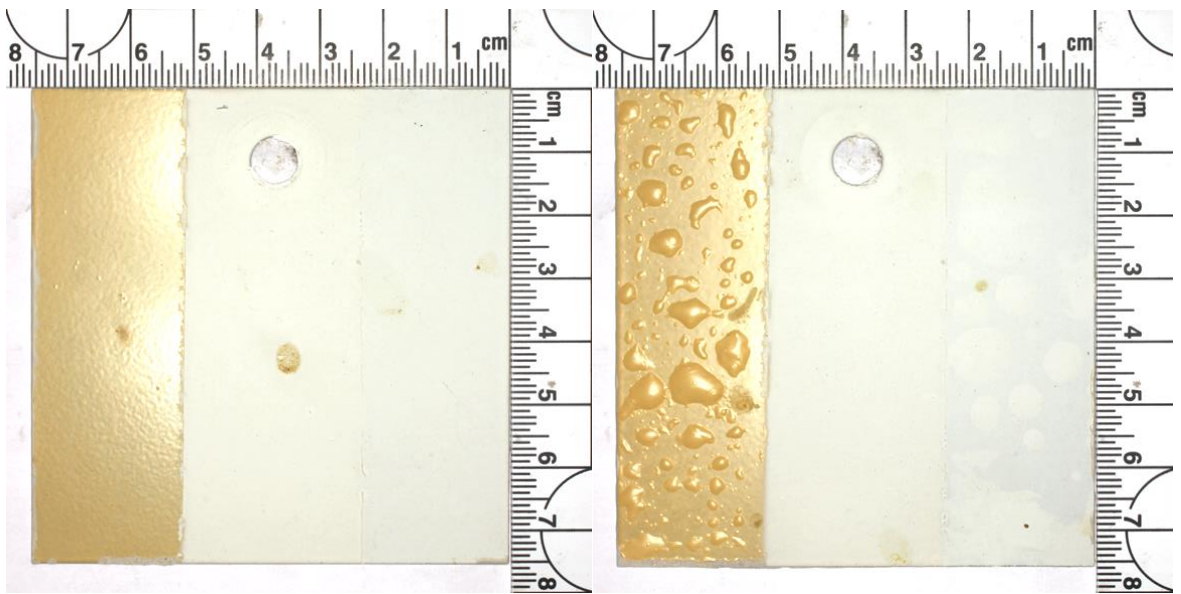


Figure 97: Coating system 3, coupon 181 (left) exposed to temperate inland site after 84 days with addition of 1 mL 0.03 wt. % H_2O_2 solution twice per week, coupon 167 (right) exposed to temperate inland site for 84 days with of 1 mL 3 wt. % H_2O_2 solution twice per week.

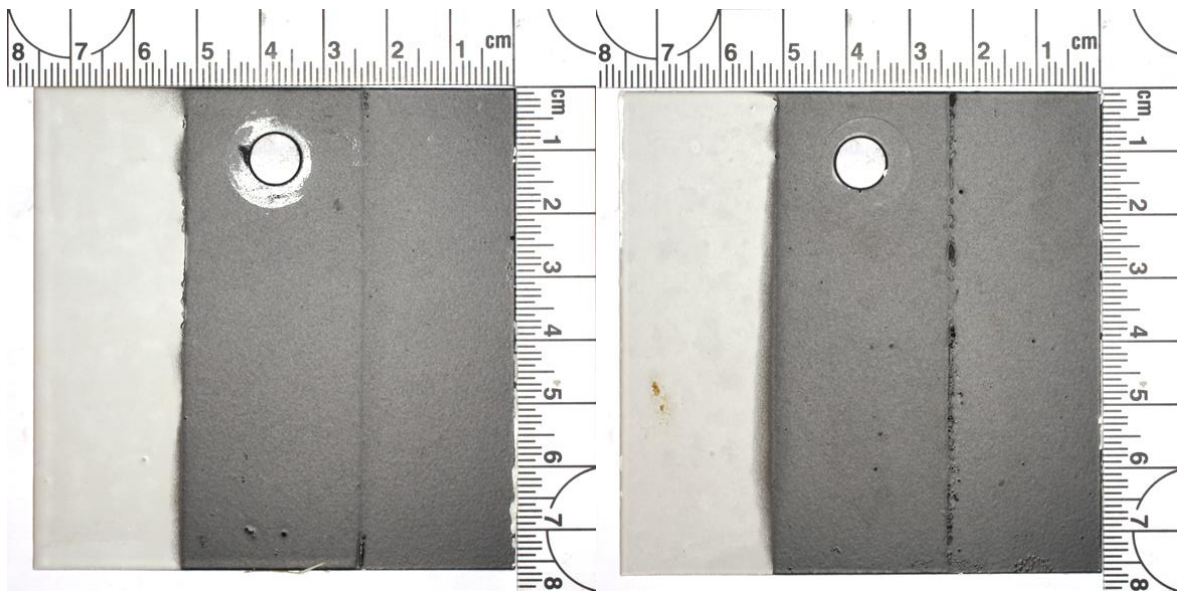


Figure 98: Coating system 4, coupon 250 (left) exposed to temperate inland site after 42 days with addition of 1 mL 0.03 wt. % H_2O_2 solution twice per week, coupon 346 (right) exposed to temperate inland site for 42 days with of 1 mL 3 wt. % H_2O_2 solution twice per week.



Figure 99: Coating system 5, coupon 286 (left) exposed to temperate inland site after 84 days with addition of 1 mL 0.03 wt. % H_2O_2 solution twice per week, coupon 293 (right) exposed to temperate inland site for 84 days with addition of 1 mL 3 wt. % H_2O_2 solution twice per week.

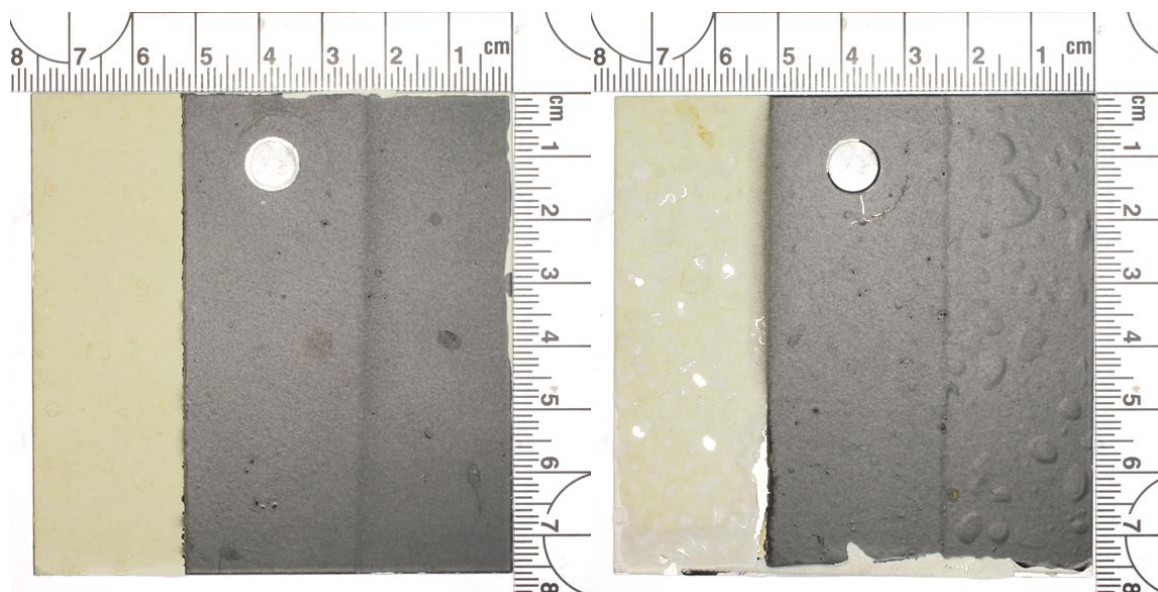


Figure 100: Coating system 6, coupon 361 (left) exposed to temperate inland site after 84 days with addition of 1 mL 0.03 wt. % H_2O_2 solution twice per week, coupon 356 (right) exposed to temperate inland site for 84 days with addition of 1 mL 3 wt. % H_2O_2 solution twice per week.

In response to Question 3, H₂O₂ has been shown to effect all coating systems to varying degrees, from large blisters to a surface level damage.

Question 4 was focused on identifying if the application of H₂O₂ had any measureable effect on the corrosion of either of the two aluminium alloys tested, AA2024-T3 and AA7075-T6. This was tested using pulsed thermography data collected post exposure. Pulsed thermography was used to identify in two dimension the undercoating corrosion as result of differing emissivities of the substrate and built up corrosion products. Figure 101 shows a thermography frame captured of coupon no. 172 after exposure to the tropical coastal site. Coupon no. 172 was unique because of the delamination that was experienced during transport, the topcoat began to peel away from the substrate, the curled coating is labelled with an 's' on Figure 101. The peeling back provided an opportunity to identify the source of the change in emissivity under the other imaged coupons where the coatings have remained intact. The darker features labelled 'r' and 'q' are a result of corrosion product building up on the surface, which was confirmed on the section of coupon labelled 'r' where the coating was peeled back revealing the underlying substrate. When coupon no. 172 (Figure 101) was then compared with the pulsed thermography frame of coupon no. 352 (Figure 102), an AA2024-T3 coupon exposed to the temperate inland field site but augmented with the addition of 3 wt. % H₂O₂, there is a visible difference in response to the thermal stimuli used for pulsed thermography measurements. The blisters (labelled 't' on Figure 102) which formed as a result of coupon no. 352 being exposed to the augmented field site have a lighter relief 100 frames after the flash than the surrounding substrate which is unlike the dark patterning seen for the other experiments. The areas which provided the brightest relief (labelled 'u' on Figure 102) on the primer section of coupon no. 356 where as a result of localised sites of coating loss which revealed the underlying uncorroded substrate.

The blisters identified in Figure 102 (labelled 't') and on Figure 103 (labelled 'v') both formed upon exposure to the H₂O₂ augmented temperate inland field exposure. The thermal images showed no signs of obvious corrosion product, the lack of corrosion product was confirmed with the small area of delamination labelled as 'w' in Figure 103, where no surface corrosion product was visible. Without a build-up of undercoating corrosion product the blisters were deemed osmotic in nature, and forming due to the combination of loss of adhesion and polymer swelling from water ingress [137]. It is postulated that the permeation of H₂O₂ at the higher concentration helped to disrupt the coating adhesion to the underlying substrate, resulting in the wide spread osmotic blistering seen across many of the coating systems. As was expected the ingress of H₂O₂ had a greater effect on the adhesion of the coating to the substrate than the corrosion rate of the AA substrates.

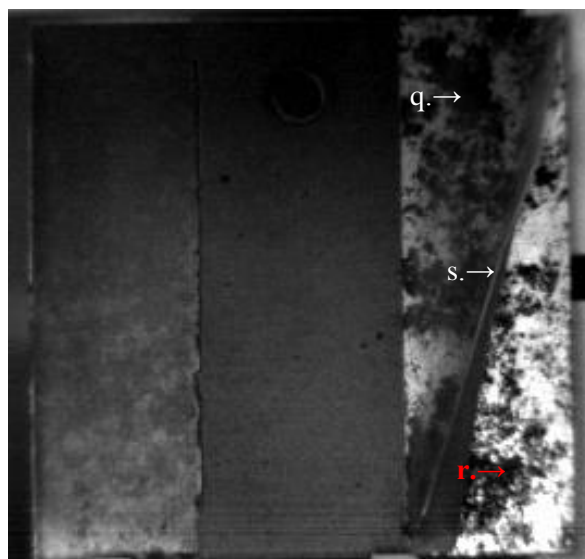


Figure 101: Pulsed thermography frame of coupon 172, coating system 3, AA7075-T6 exposed for 336 days at the tropical coastal site. Image extracted 100 frames after camera flash.

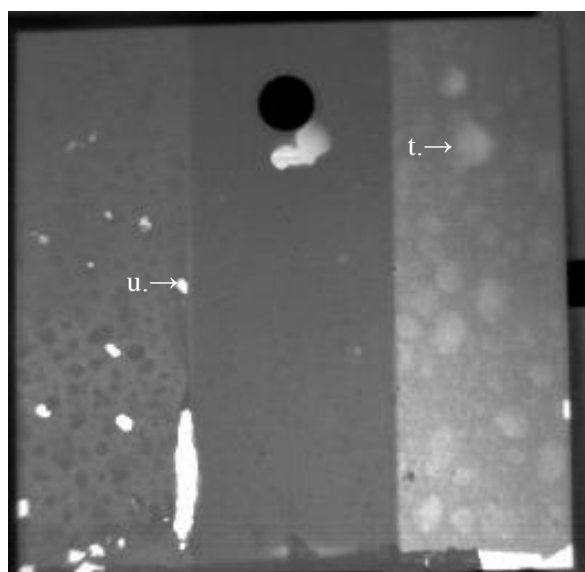


Figure 102: Pulsed thermography frame of coupon 356, coating system 6, AA2024-T3 exposed for 84 days at the temperate inland site with addition of 1 mL 3 wt. % H₂O₂ solution applied twice per week. Image extracted 100 frames after camera flash.

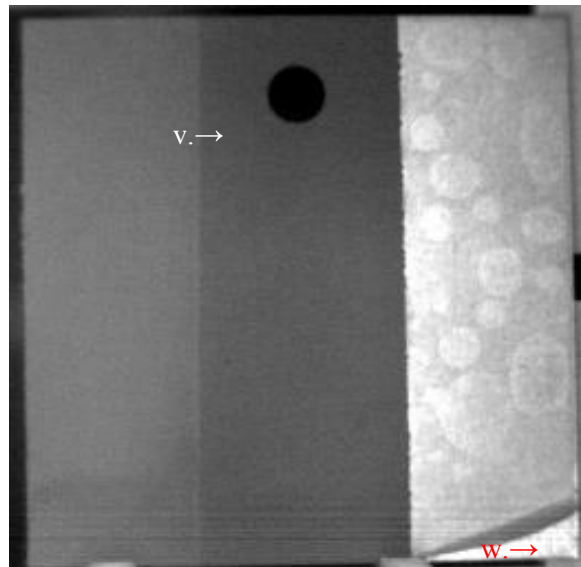


Figure 103: Pulsed thermography frame of coupon 41, coating system 1, AA2024-T3 exposed for 84 days to the temperate inland site with addition of 1 mL 3 wt. % H_2O_2 solution applied twice per week. Image extracted 100 frames after camera flash.

Question 5 aimed to provide a point of comparison between the acceleration achieved through application of H_2O_2 during a field exposure and the acceleration achieved by increased cycle rate coupled with the use of realistic environmental within a CCT chamber. The comparison was made between coupons exposed to the temperate inland field site with the addition of 0.03 wt. % H_2O_2 (Figure 104 coupon no. 96) and the accelerated testing protocol (Figure 104 coupon no. 84) replicating the temperate inland field site (testing detailed in Section 6.3). Coating system 2 was explored through comparison of two coupons each exposed for a total of 70 days, resulting in 20 application for H_2O_2 coupon no. 96 and 420 diurnal cycles for coupon no. 84. Post exposure neither environment resulted in visible signs of degradation of the topcoat sections. However, there was a measurable difference on the primer sections. Coupon no. 96 showed a measureable decrease in gloss after exposure to the augmented field exposure. The gloss values pre exposure were 9 GU's, 36 GU's and 27 GU's measured at 20 °, 60 ° and 85 ° respectively, post exposure the values were 1 GU, 4 GU's and 2 GU's. The decrease in gloss is attributed to polymeric chain damage on the surface of the primer. Coupon no. 84 which was exposed to the laboratory based protocol, showed an increase in gloss values post exposure, the measured values were 12 GU's 60 GU's and 62 GU's once again measured at 20 °, 60 ° and 85 ° in turn. The increase in gloss highlight the incomplete nature of the CCT type tests when the trends of the two experiments are compared with a coupon exposed to the standard temperate inland field site. The temperate field site causing a decrease in gloss without the addition of H_2O_2 . Coating system 3 (Figure 105) showed no visible change post exposure to either the augmented field site or the laboratory replication study.

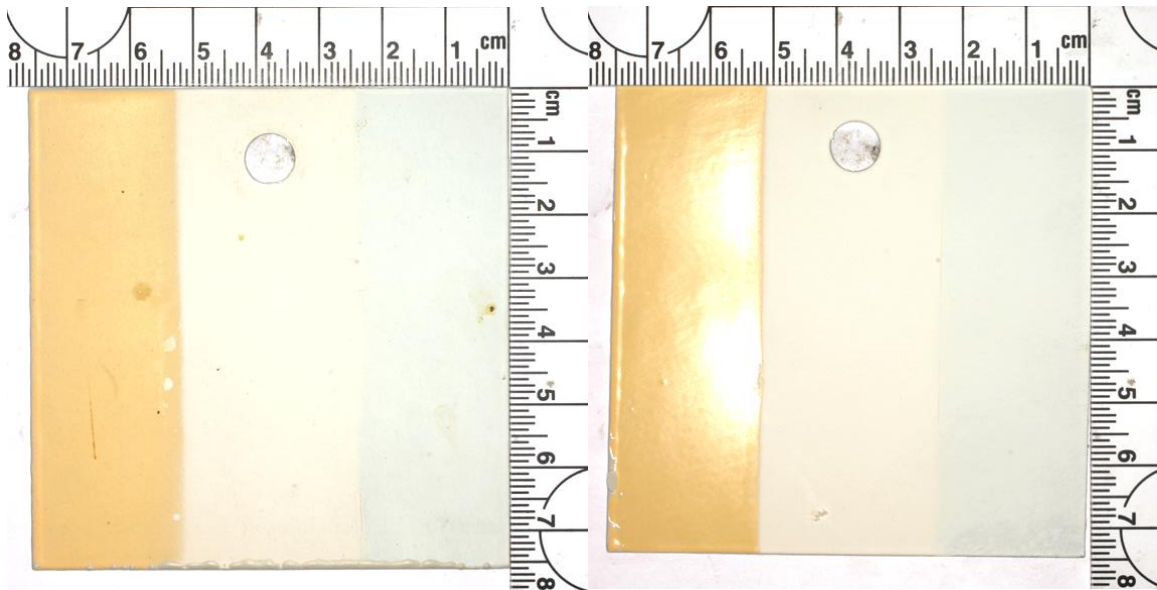


Figure 104: Coating system 2, coupon 96 (left) exposed to temperate inland site for 70 days with addition of 1 mL 0.03 wt. % H₂O₂ solution applied twice per week, coupon 84 (right) exposed for 70 days to the novel accelerated protocol 2 (Section 6.3).

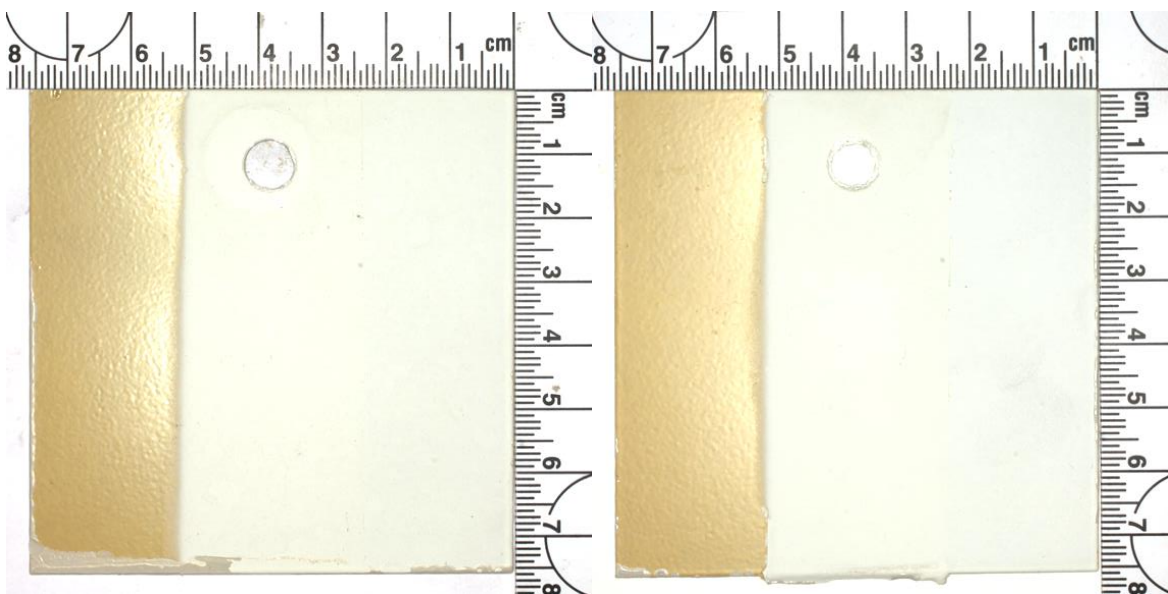


Figure 105: Coating system 3, coupon 159 (left) exposed to temperate inland site for 70 days with addition of 1 mL 0.03 wt. % H₂O₂ solution applied twice per week, coupon 145 (right) exposed for 70 days to the novel accelerated protocol 2 (Section 6.3)

Coating system 4 (Figure 106) showed a greater change when exposed to the field site augmented with the addition of 0.03 wt. % H_2O_2 , the coupons exposed to the CCT temperate inland replication study. The effect proved difficult to capture using the testing methodologies employed in this work. When exposed to the augmented field exposure, the primer section became mottled on the surface, this mottling was not identified post exposure in the laboratory, but was seen after field exposures with no augmentation. As a result of surface modification of the primer being present on both of the augment and non-augmented field exposures but not the laboratory experiment, it is most likely an effect of one or a number of atmospheric chemicals in combination with UV exposure. As chemical analysis was prohibited it was not possible to provide any further analysis regarding the phenomenon.

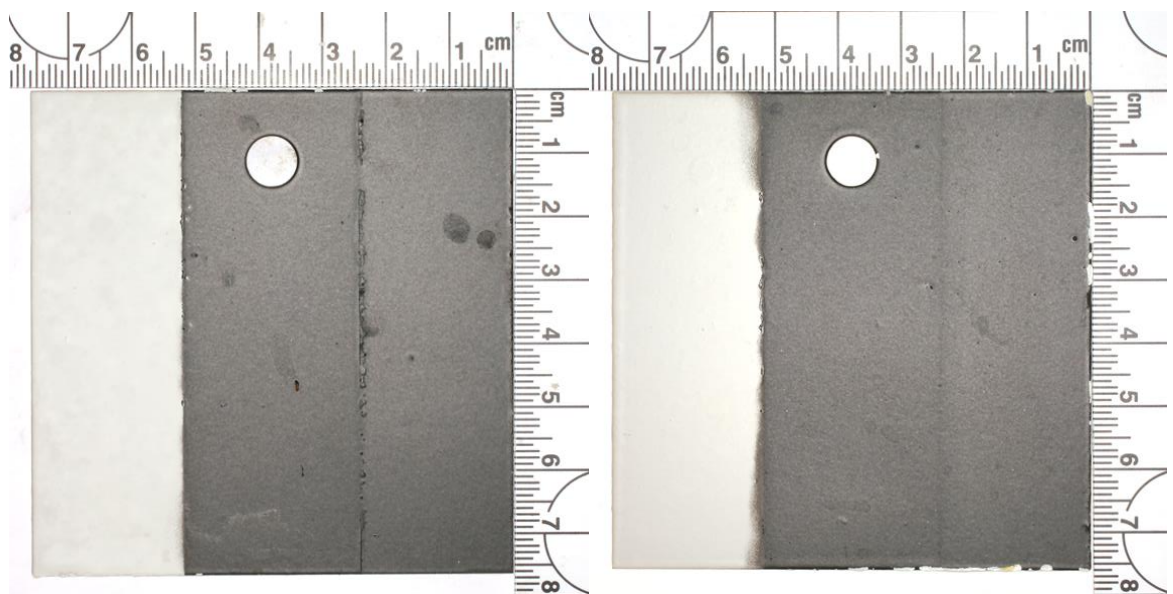


Figure 106: Coating system 4, coupon 223 (left) exposed to temperate inland site for 84 days with addition of 1 mL 0.03 wt. % H_2O_2 solution applied twice per week, coupon 335 (right) exposed for 84 days to the novel accelerated protocol 2 (Section 6.3).

The topcoats of coating systems 5 (Figure 107) and coating system 6 (Figure 108) were more greatly affected by the laboratory based CCT experiments than the augmented field exposure. The onset of micro blisters on the topcoat is the key link to the temperate inland field experiment, identifying that UV did not play a key role in all of the failure mechanisms witnessed during field exposures. The distinction of similarity in response between the two experiments relative to the original field exposure highlights the importance replication of an entire environment when developing a standardised laboratory test, to ensure the failures seen in CCT chambers match those measured in-service.

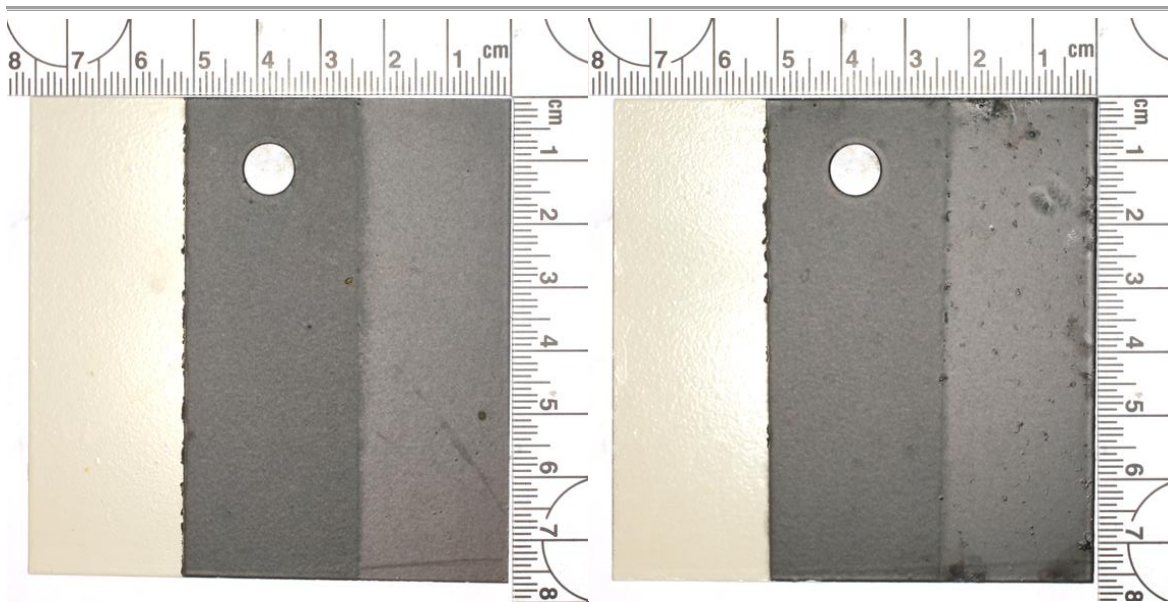


Figure 107: Coating system 5, coupon 285 (left) exposed to temperate inland site for 70 days with addition of 1 mL 0.03 wt. % H₂O₂ solution applied twice per week, coupon 271 (right) exposed for 70 days to the novel accelerated protocol 2 (Section 6.3).

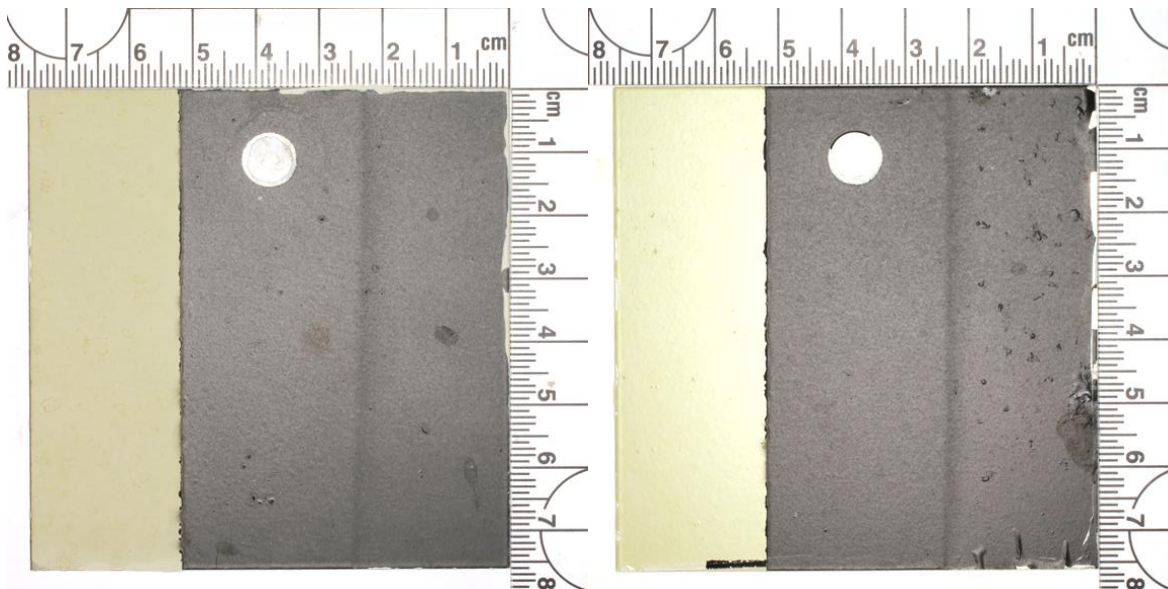


Figure 108: Coating system 6, coupon 361 (left) exposed to temperate inland site for 84 days with addition of 1 mL 0.03 wt. % H₂O₂ solution applied twice per week, coupon 321 (right) exposed for 84 days to the novel accelerated protocol 2 (Section 6.3).

6.6. Summary

The purpose of this chapter was to explore a number of questions related to furthering the development of realistic and predictive accelerated corrosion tests. The questions devised were as follows:

1. Is it possible to implement a procedure into a cyclic corrosion chamber that is able to replicate coating performance from a temperate field exposure?
2. Does the inclusion of a wash off step create a more representative accelerated testing protocol?
3. Should UV be consider in isolation?
4. Is it best to replicate field environments in a cyclic corrosion chamber, or is it better to accelerate the degradation experienced in the field?
5. Could the application of an aqueous oxidant accelerate coating degradation?

Investigations into the questions was achieved through creation of two distinct experimental protocols. The first, a new CCT protocol replicated a seasonal temperate inland environment, utilising measured weather data to create a representative four season cycle, it also considered natural NaCl loading and the frequency of rain events experienced. The second experiment, approached the requirements of an accelerated corrosion test from a new point of view.

Traditionally the focus being acceleration of the substrates corrosion. Through augmentation of a field exposure experiment via application of an aqueous oxidant, the intention was the inherent weaknesses of the polymers could be intensified. The intensification would then lead to acceleration of any active protection mechanisms to become engaged in protecting the substrate from the selected environment.

The CCT cycle specifically was attempting to answer questions 1 and 2. The first was a feasibility question, which upon initial trials it was identified that the Ascott CCT chamber was not able to cope with the lower temperatures required to replicate a temperate environment. It was possible to implement the cycle into an alternate environmental chamber, however, the application of NaCl and water had to be completed outside of the chamber. Meaning in broad terms it is absolutely possible to replicate temperate environments within a chamber, but care must be taken in selecting the specific chamber in question.

The second question is one regarding the inclusion of a rain or wash off step, and if it made for a more representative of service response. The experiment did prove to produce degradation morphologies that were more repetitive of the natural progression of coating degradation seen during relevant field exposures than static temperature experiments such as the BS EN ISO 9227.

However, the effect of cycle rate was not as pronounced as was desired, with the degradation measured not driven singularly via the transitions experienced during the diurnal like cycles. The dwell time appears to play a role in the degradation reactions as was evident by the complete removal of the Mg primer (coating system 1) after 504 days exposure, but it remaining intact after 504 accelerated cycles.

The oxidant loading experiment aimed to answer three of the questions raised for the chapter, the question asking if UV should be considered in isolation was answered through comparison of each of the coating systems post exposure to either the temperate field exposure or the augmented field exposure with application of 3 wt. % H_2O_2 . The experiment showed widespread damage to 5 of the 6 coating systems tested with the addition of H_2O_2 . However, to identify if it the combination of UV and H_2O_2 is necessary to provide this response, an experiment with H_2O_2 and no UV would need to be completed as a part of the future work.

To identify which is best the augmented field exposure or a controlled CCT type protocol, coupons exposed to either the field exposure with 0.03 wt. % H_2O_2 or the CCT protocol were compared. The response was divisive, as for some of the coating formulations (coating systems 1, 2 and 3) they performed more closely to the standard field exposure in the augmented experiment, whilst others (coating systems 5 and 6) more closely replicated the field exposure in the CCT protocol and for coating system 4 it appeared to make little difference other than some slight mottling of the colour of the primer section.

The final question was to see if the application of an aqueous oxidant could accelerated coating degradation. What is clear from the high concentration H_2O_2 application it is possible to increase the rate of coating degradation through application of aqueous oxidant. What the two experiments (high and low concentrations of H_2O_2) have not been able to identify is what the best concentration would be to try and do this. Keeping the outcome of these experiments in mind it appears that the high concentration is too high and the low concentration is too low. This do not affect the possibility that somewhere between the two concentrations is the perfect concentration, which potentially could be identified as a part of future work.

In addition to answering the questions these experiments raised a number of additional points, the first being the need for oxidant studies to be trialled at other sites to see if differing intensities of UV and other contaminants result in a different responses. This should also include an attempt to move this into a controlled CCT environment to identify if the response is truly a result of the combination of H_2O_2 and UV or if there is another parameter from the field exposure that is being overlooked.

In totality this chapter has provided early insight into two potential techniques that could be used for a new accelerated corrosion test protocol. The suggestions could be used in isolation or combined to create a more representative CCT protocol. It has also provided further evidence for

the need to begin long term field exposure experiments that can be used to study the next generation of accelerated tests. The work provides a spring point for further testing to be developed and help identify if the path that was devised with this work is the correct way forward to create a set of representative and predictive accelerated corrosion tests.

7. The Factorial Design

7.1. Introduction

The factorial design was utilised to enable the breath of environments explored to as expansive as possible without sacrificing in depth. Factorial designs have been used in a number of studies exploring the effects of atmospheric corrosion and the weathering of coatings [138-141].

7.2. Objectives

The factorial design was utilised to compare different experiments and to identify the importance of each of the factors when considering the development of a new test. As well as answer the overarching thesis question (see Section 1.4); can further information be extracted through the use of a factorial design?

7.3. The factorial design

All exposure experiments completed within the scope of this research were planned as a part of an overarching partial factorial design. The design was created by Dr Kalliopi Mylona of the University of Southampton's Mathematical Sciences Department. The random partial factorial design was created using JMP Pro 13 statistical software [142]. The design included four categorical factors each with a specified number of levels, as defined by Table 34. The design was optimise for the time factor and the substrate factor was equally spaced. The equal spacing of the substrate levels and the total number of coupons created were both limitations set upon the design prior to its creation as a result of agreements made with 1710 Naval Air Squadron regarding the number of coupons that could be processed.

Table 34: Overview of factorial design factors and levels

Factor	Number of levels
Substrate	2
Coating system	6
Experiment	9
Time point	7

Potentially a full factorial design encompassing all of the combinations of factors and levels would result in 708 possible combinations. This was more coupons than could be created with 1710 Naval Air Squadron and too many to manage singlehandedly throughout the study. By limiting the factorial design to only 396 coupons meaning it was only 56% complete, the possibility of successful management through testing become greater. Each of the 396 coupons created and tested were defined by the experimental design, the coupons were also randomly assigned an identification number by the factorial design, and the random nature of the design is shown in section 11.5.

The design considered the difference in performance associated with the two most prolifically used historic aircraft aluminium alloys AA2024-T3 and AA7075-T6 and the interaction of those substrates with a total of six coating systems. Multiple coatings were used in the design as any conclusions regarding testing must be able to predict performance of novel coatings as well as typical in-service coatings. The design included a total of nine experiments; four field exposures, four novel accelerated exposures and the British Standard 9227 Salt Fog experiment [1]. The progress of the nine experiments was probed using the time optimised factor made up of seven levels. The levels corresponded to seven equal time slices with sets of samples being removed from exposure at each time point. The natural exposure tests were 504 days in length, with samples removed every 84 days. The accelerated tests were 2000 h or 84 days in length, with samples being removed every 14 days. The length of the accelerated tests was defined by the increased cycle rate used for accelerated tests 1 and 2, with the replication of the natural diurnal cycle changes reduced from 24 hours to 4 hours, meaning a six fold increase in cycle rate. This resulted in the total number of pseudo diurnal cycles for accelerated protocols matching that the natural diurnal cycles of the field exposures.

An unavoidable weakness of the natural exposure tests is their short duration; typical outdoor exposures can last 16 years [143]. The 18 month duration of the field exposures was an inescapable weakness which is a direct result of the time limitations of a PhD. It was anticipated that although the data collected would not be a complete data set for the degradation of the chosen

coatings, it would be able to validate early stage breakdown measurements made during accelerated testing.

7.4. Data collection

Once exposure was complete each of the coupons underwent a number of post exposure tests to collect quantitative information regarding the coatings performance. Each of the three coupon sections previously defined in Section 2.5.1. In total 21 quantitative data sets were collected from the coupons post exposure, with seven distinct measurements (see Table 35) made for each of the three sections.

Table 35: Post exposure data collection

Data Sets collected for each section
Average 20 ° gloss
Average 60 ° gloss
Average 85 ° gloss
Average Δ E 2000
Average film thickness
Hardness
% area corrosion measured with pulsed thermography

7.5. Analysis

A subset of collected data was submitted to Dr Kalliope Mylona for analysis. The full data set submitted for analysis to Dr Mylona can be found in the Appendix Section 11.5. The conclusion made were based upon the analysis of the following data set (Table 36)

Table 36: Factorial design data set

Reference	Data set
R1	% area corrosion of the topcoat section
R2	85° gloss of the primer section
R3	ΔE 2000 of the primer section
R4	Konig Hardness of the primer/topcoat section
R5	60° Gloss of the primer/topcoat section

Along with the submission of the data set (section 11.5), a number of research question (Table 37) were created to focus the statistical analysis. The results from the analysis shall be discussed in relation to the specific research questions.

The r^2 values for data sets R1, R2, R4 and R5 were deemed acceptable, R3 did not have a good enough r^2 until the log of the values was used where the r^2 was identified as not be ideal but good enough to continue.

Table 37: Factorial design research questions

Reference	Research question
Q1	With respect to experiment do the field exposures create different results?
Q2	With respect to experiment factor is BS EN ISO 9227 more similar to any of the other experiments?
Q3	With respect to substrate is there difference between the performance of AA2024-T3 and A7075-T6?

7.5.1. Factorial design response to Q1

Although requested data related to Q1 was not explored in the initial assessment of the data set and the factorial design.

7.5.2. Factorial design response to Q2

For 85° gloss of the primer section the results from the BS EN ISO 9227 are similar to the tropical inland field exposure site and the 4 novel accelerated tests it is only significantly different to the tropical coastal and the temperate inland site.

The % corrosion results show statistically BS EN ISO 9227 is similar to accelerated corrosion test 2 and to the tropical inland field exposure.

When considering the 60° gloss of the primer topcoat section results of the BS EN ISO 9227 test are statistically similar to all of the experiments except for the tropical coastal field exposure.

7.5.3. Factorial design response to Q3

When comparing each of the % thermography data set, substrates was deemed statistically insignificant. The degradation of the 85° gloss value of the primer they substrate does not affect the outcome of the degradation across any of the experiments.

7.5.4. Additional analysis

The measured hardness value was only related to the coating selected, none of the other variables; substrate, experiment or time had a bearing on the hardness value measured for the primer topcoat sections of the coupons.

Individually 85° gloss of the primer section is not significantly affected by the coating or the experiment, however coating multiplied by experiment is statistically significant.

The effect of substrate is only statistically significant when considering the 60° gloss of the primer top coats section.

7.6. Summary

The analysis completed by Dr Kaliopé Mylona on a subset of the data collected, illustrated that it is possible to analyse corrosion testing data using a factorial design. In answer to the key question of the chapter the use of a factorial design did go on to provide information that was in addition to what was found using more conventional methods of analysis, for example dismissing the need to test both AA7075-T6 and AA2024-T3, as the substrate often plays little role in the performance of the coatings upon exposure.

The analysis also provided a steer for future work, as an additional 16 data sets were available for analysis with many more combinations of the 21 total data sets. Further analysis of additional data sets did not seem appropriate to the focus of this thesis as it was at this time completed by another. Nevertheless, this factorial design may be able to produce greater analysis of the dataset in the future.

8. Conclusions

8.1. Response to Thesis Questions

The purpose of this thesis was to explore a number of questions related to furthering the development of realistic and predictive accelerated corrosion test. To provide organisation to a broad topic of research a number of questions were posed, these questions, defined in Table 2 formed the basis of the thesis structure. The conclusions aim to summarise the answers each of the questions and detail any additional insights made throughout the course of this research.

Question 1 was questioning the rationale for a new accelerate corrosion test. The need for a new test was a combination of the sunset date for use of Cr(VI) in military coatings and the inability of the accelerated corrosion tests favoured by the UK military to predict the in-service performance of Cr(VI) replacements. The range of replacement materials form the basis for question 2. A range of Cr(VI) replacement technologies and the current Cr(VI) coating used in service were sourced from two multinational coating manufacturers; AkzoNobel and PPG. Six coating systems were tested in all, the need for a wide range of technologies was a driving force in the total number of coating systems selected, as any newly designed test needed to be applicable to any replacement technology with no biased towards one system over another, as with the BS EN ISO 9227 Salt spray test. The coatings were applied to two commonly used aluminium alloys used in the structure of the military aircraft. It was important to test with both AA2024-T3 and AA7075-T6 as the differing composition had the potential to perform differently with the coatings selected.

The next question to answer was whether different environments resulted in varied performance for coatings. This was tackled using 4 field exposure experiments each in a distinctly different

environment, a tropical coastal site, a tropical inland site, a temperate coastal site and a temperate inland site. Together the experiments were able to prove that when exposed to different environments a coating will perform differently over the course of the exposure. The series of experiments highlighted that the tropical coastal site was the most aggressive and that coating system 4 was the most resistant to any of the tested field exposure environments.

The current state of the art for accelerated corrosion testing used in academia and industry defined through a literature review, with the preference for use of BS EN ISO 9227 by DSTL and the Royal Navy. This preference highlighted as a result of a lack of industry consensus on the most representative testing protocol to use when testing novel coatings prior to selection for service. The inability of BS EN ISO 9227 to represent failure mechanisms seen in service was then explored in Chapter 4. BS EN ISO 9227 was compared with the tropical coastal field exposure as the site with the most similar environmental conditions. The degradation identified after exposure to the BS EN ISO 9227 was typically of a different morphology to that identified after exposure to the field site. BS EN ISO 9227 was also unable to create uniform acceleration factors for each of the coating systems, meaning it was having a greater effect to some of the coatings than others. This could have been a result of the over simplification of environmental features in comparison to a field exposure. In the field it is conceivable that an environmental variable present wither in isolation or in combination with others created an effect within a subset of the coatings that was not captured in the BS EN ISO 9227 protocol.

A step change was made in design of accelerated CCT protocols in Chapter 5, rather than selection of unrelated environmental variables or even selection of somewhat representative values. The replication study completed in chapter 5 implemented measured temperatures, relative humidity values and NaCl levels from a field exposure site to create a cyclic corrosion test. The viability of integration of real world environmental variables in a CCT chamber was the success from this chapter. The variables were on the edges of the working envelope of the machine, nevertheless they were implemented along with application of the far more concentrated NaCl solution. It did prove possible to implement real world weather data into a CCT chamber, however, the results did not replicate the field exposure performance for all of the coating system. It nevertheless, provided a starting point for expansion of the concept in Chapter 6.

Replication of the temperate inland field site with a laboratory test chamber proved that it was possible to implement a procedure into a cyclic corrosion chamber that is able to replicate a temperate field exposure. Upon exposure to these protocols a number of coatings did degrade with similar features as were experienced in the field site. Due to the shortened exposure time it was not possible to identify if the laboratory study provided any acceleration to the testing. This may be possible if the exposures were repeated but for longer periods of time. What was once again drawn into question was the effectiveness of the increased cycle rate. Neither of the two experiments

completed within this work which utilised the concept of increased cycle rate produced any strong evidence for its success in accelerating the degradation measured.

The oxidant augmented field exposure detailed in Chapter 6, showed that it was possible to accelerate the degradation of many coating systems through application of an aqueous oxidant, in the form of H_2O_2 . When compared to its equivalent CCT protocol also detailed in Chapter 6, it was clear that how representative a response was dependent upon formulation, with some coatings favouring the augmented field exposure whilst others performed more as expected within the CCT environment. As a result of the disparity between the two sites, moving forward a combination would seem to be the most pragmatic approach. Possibly the addition of H_2O_2 and a UV source to a CCT protocol similar to the one devised in Chapter 6. This would provide greater repeatability than a variable field exposure, but working to create a more representative environment. The final question for chapter six regarding the testing with UV in isolation was not definitively answered within this study, as a number of unanswered questions came to light. Such as the effect of H_2O_2 without UV exposure.

8.2. Wider learnings

The choice to try and accelerate atmospheric corrosion and polymer degradation through increased cycle time was made in response to the need to create a testing response that was representative of service and able to predict coating lifetime. This resulted in the need to define what variables specify distinct environments. For this work it was decided that temperature, relative humidity and chemical components i.e. NaCl concentration, in combination are specific to an environment. Therefore in the context of a CCT protocol only the rate of change between these variables could be altered without fundamentally changing the environment of interest. It was hypothesised that if the other environmental variables all remained the same but the speed of cycling was increased, no alternative degradation reaction would be made available but the rate of stress build up would increase. Throughout the testing completed for this work, this did not appear to be the case. Hence the key question of this study was identified – To accelerate you must change something, i.e. the addition of aqueous H_2O_2 , but in changing something do you create something different entirely. The viability of decreased cycle time to accelerated degradation was not proven as a concept through this experimental work. Meaning if it is not possible to alter the cycle time without effecting the result and so it may not be possible to create a true accelerated test, as no variable can be altered without departure from the intended environment. Then can it not be concluded that it is not and will not be possible to precisely accelerate the degradation of a material within the laboratory environment relative to a specific exposure site.

9. Future Work

9.1. The factorial design

The factorial design detailed in Chapter 7, provides a number of opportunities for further analysis. The design was created to analyse 5 data sets created from the post exposure analytical work, however 21 data sets were created. Meaning there is plenty of scope for further analysis, comparing many combinations of data sets. It would also be possible to analyse the coating sections on the coupons in isolation, identifying for example trends regarding primer performance without considering the topcoat of the system.

9.2. The current data set

The pulse thermography processing provides additional opportunities for the analysis of morphology of corrosion products, the close up lens could also be used to gain a better resolution image of the undercoating corrosion. A number of other techniques could be applied to the data sets which could provide data that is directly comparable with literature. Micro indentation measurements and surface roughness could both strengthen the argument regarding coating aging vs. weathering.

9.2.1. With permission for chemical analysis

Given more time it may be possible to negotiate the chance to perform some chemical analysis on the coupons. Information such as XPS and IR spectroscopy could prove useful in understanding

the underlying mechanisms effecting the changes measured at the macroscale. Without permission from the coating manufacturers this would not be a possible direction of enquiry.

9.3. Future experiments

Identify and implement oxidant loading laboratory tests exploring the importance dry phase application verses wet phase application of corrodents. In addition to this experiments should be completed both with and without a source of UV to identify if the effects are cumulative or if they are a result of just the addition of oxidant. If the testing proves positive, further oxidant testing should then be optimised to identify the most desirable concentration of oxidant and the best frequency of application.

Repetition of the temperate exposure tests for an extended period of time, both externally and within the laboratory. Due to time limitations of the project it was not possible to expose coupons to the temperate environments until corrosion was initiated, making the comparison between each of the coating systems reliant upon surface changes associated with early stage weathering i.e. changes to gloss and colour. If the experiments were extended the data created would make for a stronger comparison.

It would be beneficial as a part of the future work to explore a number of additional service environments potentially matching them to Koppen definitions environments. This work to build an understanding of the variability of all potential environments, with a subset then being defined for use in the creation of a suite of accelerated tests.

The pulsed thermography technique could be applied to service aircraft which overtime could be used to optimise the need to for costly resprays, for this to be possible the equipment would need to be made portable and the measured pixel size would have to be optimised. Further clarity regarding the morphology of undercoating corrosion could be gained through application of the more complex technique of pulsed phase thermography where the data output from the entirety of the process is analysed pixel by pixel through the application of a Fourier transform operation. The potential of this was explored in conjunction with Dr. Rachael Tigre of the University of Southampton. The resultant image can be seen in Figure 109, the benefit of the more complex task is something that would need to be explored.

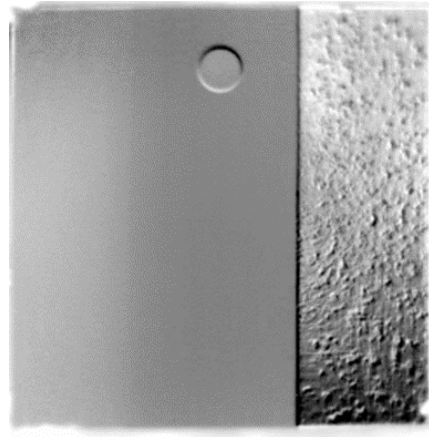


Figure 109: Post pulsed phase thermography analysis of exposed coupon.

10. Bibliography

- [1] BSI, "BS EN ISO 9227 - Corrosion tests in artificial atmospheres - Salt spray tests," 2012, p. 30.
- [2] BSI, "BS EN ISO 11474 - Corrosion of metals and alloys - corrosion tests in artificial atmosphere - accelerated outdoor test by intermittent spraying of a salt solution (scab test)," 2014.
- [3] L. Brooke-Holland, and C. Mills, "The 2015 Strategic Defence and Security Review," 22 January 2016.
- [4] *Active Protective Coatings*: Springer, 2016.
- [5] G. P. Bierwagen, L. He, J. Li, L. Ellingson, and D. E. Tallman, "Studies of a new accelerated evaluation method for coating corrosion resistance — thermal cycling testing," *Progress in Organic Coatings*, vol. 39, no. 1, pp. 67-78, 2000.
- [6] ASTM International, "ASTM B117 - Standard practice for operating salt spray (fog) apparatus," 2011.
- [7] N. LeBozec, N. Blandin, and D. Thierry, "Accelerated corrosion tests in the automotive industry: A comparison of the performance towards cosmetic corrosion," *Materials and Corrosion*, vol. 59, no. 11, pp. 889-894, 2008.
- [8] C. J. Smith, S. Higgs, and K. R. Baldwin, *Advances in Protective Coatings and Their Application to Ageing Aircraft*, Farnborough: Defense Technical Information Center, 2000.
- [9] "Aluminum 2024-T3 Material Specification," Aerospace Specification Metals, 17th July 2014, [Online].
Available: <http://asm.matweb.com/search/SpecificMaterial.asp?bassnum=MA2024T3>.
- [10] J. P. Immarigeon, R. T. Holt, A. K. Koul, L. Zhao, W. Wallace, and J. C. Beddoes, "Lightweight materials for aircraft applications," *Materials Characterization*, vol. 35, no. 1, pp. 41-67, 1995.
- [11] ASM Aerospace Specification Metals Inc., "Aluminum 7075-T6 Material Specification," ASM Aerospace Specification Metals Inc., 17th June, 2014, [Online].
Available: <http://asm.matweb.com/search/SpecificMaterial.asp?bassnum=MA7075T6>.
- [12] R. J. Varley, E. K. Simmonds, J. E. Seebergh, and D. H. Berry, "Investigation of factors impacting the in-service degradation of aerospace coatings," *Progress in Organic Coatings*, vol. 74, no. 4, pp. 679-686, 2012.
- [13] J. Sinko, "Challenges of chromate inhibitor pigments replacement in organic coatings," *Progress in Organic Coatings*, vol. 42, no. 3-4, pp. 267-282, 2001.

-
- [14] T. J. Harrison, B. R. Crawford, M. Janardhana, and G. Clark, "Differing microstructural properties of 7075-T6 sheet and 7075-T651 extruded aluminium alloy," *Procedia Engineering*, vol. 10, pp. 3117-3121, 2011.
- [15] PPG Aerospace, "Technical data sheet PR205 HS Epoxy Primer," p. 6.
- [16] PPG Aerospace, "Technical data sheet Wash Primer P99," pp. 1.
- [17] R. G. Buchheit, H. Guan, S. Mahajanam, and F. Wong, "Active corrosion protection and corrosion sensing in chromate-free organic coatings," *Progress in Organic Coatings*, vol. 47, no. 3-4, pp. 174-182, 2003.
- [18] G. M. Brown, and K. Kobayashi "Nucleation and Growth of a Chromate Conversion Coating on Aluminum Alloy AA 2024-T3," *Journal of The Electrochemical Society*, vol. 148, no. 11, pp. B457-B466, 2001.
- [19] J. Zhao, G. Frankel, and R. L. McCreery, "Corrosion Protection of Untreated AA-2024-T3 in Chloride Solution by a Chromate Conversion Coating Monitored with Raman Spectroscopy," *Journal of The Electrochemical Society*, vol. 145, no. 7, pp. 2258-2264, 1998.
- [20] R. L. Twite, and G. P. Bierwagen, "Review of alternatives to chromate for corrosion protection of aluminum aerospace alloys," *Progress in Organic Coatings*, vol. 33, no. 2, pp. 91-100, 1998.
- [21] P. Campestrini, H. Terryn, J. Vereecken, and J. H. W. de Wit, "Chromate Conversion Coating on Aluminum Alloys: II: Effect of the Microstructure," *Journal of The Electrochemical Society*, vol. 151, no. 6, pp. B359-B369, 2004.
- [22] G. P. Bierwagen, "Reflections on corrosion control by organic coatings," *Progress in Organic Coatings*, vol. 28, no. 1, pp. 43-48, 1996.
- [23] X. F. Yang, J. Li, S. G. Croll, D. E. Tallman, and G. P. Bierwagen, "Degradation of low gloss polyurethane aircraft coatings under UV and prohesion alternating exposures," *Polymer Degradation and Stability*, vol. 80, no. 1, pp. 51-58, 2003.
- [24] E. Akiyama, A. J. Markworth, J. K. McCoy, G. S. Frankel, L. Xia, and R. L. McCreery, "Storage and Release of Soluble Hexavalent Chromium from Chromate Conversion Coatings on Al Alloys: Kinetics of Release," *Journal of The Electrochemical Society*, vol. 150, no. 2, pp. B83-B91, 2003.
- [25] M. C. M. Kendig, L. Warren, S. Jeanjaquet, . p. 1.
- [26] L. Li, D. Y. Kim, and G. M. Swain, "Transient Formation of Chromate in Trivalent Chromium Process (TCP) Coatings on AA2024 as Probed by Raman Spectroscopy," *Journal of The Electrochemical Society*, vol. 159, no. 8, pp. C326-C333, 2012.
- [27] Y. Guo, and G. S. Frankel, "Characterization of trivalent chromium process coating on AA2024-T3," *Surface and Coatings Technology*, vol. 206, no. 19-20, pp. 3895-3902, 2012.
- [28] O. Lopez-Garrity, and G. S. Frankel, "Corrosion Inhibition of Aluminum Alloy 2024-T3 by Sodium Molybdate," *Journal of The Electrochemical Society*, vol. 161, no. 3, pp. C95-C106, 2014.
- [29] S. B. Madden, and J. R. Scully, "Inhibition of AA2024-T351 Corrosion Using Permanganate," *Journal of The Electrochemical Society*, vol. 161, no. 3, pp. C162-C175, 2014.
- [30] K. D. Ralston, S. Chrisanti, T. L. Young, and R. G. Buchheit, "Corrosion Inhibition of Aluminum Alloy 2024-T3 by Aqueous Vanadium Species," *Journal of The Electrochemical Society*, vol. 155, no. 7, pp. C350-C359, 2008.
- [31] K. D. Ralston, T. L. Young, and R. G. Buchheit, "Electrochemical Evaluation of Constituent Intermetallics in Aluminum Alloy 2024-T3 Exposed to Aqueous Vanadate Inhibitors," *Journal of The Electrochemical Society*, vol. 156, no. 4, pp. C135-C146, 2009.
- [32] M. Kendig, and C. Yan "Critical Concentrations for Selected Oxygen Reduction Reaction Inhibitors," *Journal of The Electrochemical Society*, vol. 151, no. 12, pp. B679-B682, 2004.
- [33] A. C. Balaskas, M. Curioni, and G. E. Thompson, "Evaluation of Inhibitor Performance by Electrochemical Methods: Comparative Study of Nitrate Salts on AA 2024-T3," *Journal of The Electrochemical Society*, vol. 161, no. 9, pp. C389-C394, 2014.

- [34] N. C. Rosero-Navarro, M. Curioni, R. Bingham, A. Durán, M. Aparicio, R. A. Cottis, and G. E. Thompson, "Electrochemical techniques for practical evaluation of corrosion inhibitor effectiveness. Performance of cerium nitrate as corrosion inhibitor for AA2024T3 alloy," *Corrosion Science*, vol. 52, no. 10, pp. 3356-3366, 2010.
- [35] K. Aramaki, "Treatment of zinc surface with cerium(III) nitrate to prevent zinc corrosion in aerated 0.5 M NaCl," *Corrosion Science*, vol. 43, no. 11, pp. 2201-2215, 2001.
- [36] F. Mansfeld, C. Chen, C. B. Breslin, and D. Dull, "Sealing of Anodized Aluminum Alloys with Rare Earth Metal Salt Solutions," *Journal of The Electrochemical Society*, vol. 145, no. 8, pp. 2792-2798, 1998.
- [37] V. Palanivel, Y. Huang, and W. J. van Ooij, "Effects of addition of corrosion inhibitors to silane films on the performance of AA2024-T3 in a 0.5 M NaCl solution," *Progress in Organic Coatings*, vol. 53, no. 2, pp. 153-168, 2005.
- [38] G. Bierwagen, R. Brown, D. Battocchi, and S. Hayes, "Active metal-based corrosion protective coating systems for aircraft requiring no-chromate pretreatment," *Progress in Organic Coatings*, vol. 67, no. 2, pp. 195-208, 2010.
- [39] A. Simões, D. Battocchi, D. Tallman, and G. Bierwagen, "Assessment of the corrosion protection of aluminium substrates by a Mg-rich primer: EIS, SVET and SECM study," *Progress in Organic Coatings*, vol. 63, no. 3, pp. 260-266, 2008.
- [40] K. N. Allahar, D. Battocchi, G. P. Bierwagen, and D. E. Tallman, "Transmission Line Modeling of EIS Data for a Mg-Rich Primer on AA 2024-T3," *Journal of The Electrochemical Society*, vol. 157, no. 3, pp. C95-C101, 2010.
- [41] K. N. Allahar, D. Battocchi, M. E. Orazem, G. P. Bierwagen, and D. E. Tallman, "Modeling of Electrochemical Impedance Data of a Magnesium-Rich Primer," *Journal of The Electrochemical Society*, vol. 155, no. 10, pp. E143-E149, 2008.
- [42] D. Wang, and G. P. Bierwagen, "Sol-gel coatings on metals for corrosion protection," *Progress in Organic Coatings*, vol. 64, no. 4, pp. 327-338, 2009.
- [43] D. Battocchi, A. M. Simões, D. E. Tallman, and G. P. Bierwagen, "Comparison of testing solutions on the protection of Al-alloys using a Mg-rich primer," *Corrosion Science*, vol. 48, no. 8, pp. 2226-2240, 2006.
- [44] D. Battocchi, A. M. Simões, D. E. Tallman, and G. P. Bierwagen, "Electrochemical behaviour of a Mg-rich primer in the protection of Al alloys," *Corrosion Science*, vol. 48, no. 5, pp. 1292-1306, 2006.
- [45] D. Wang, D. Battocchi, K. N. Allahar, S. Balbyshev, and G. P. Bierwagen, "In situ monitoring of a Mg-rich primer beneath a topcoat exposed to Prohesion conditions," *Corrosion Science*, vol. 52, no. 2, pp. 441-448, 2010.
- [46] M. Nanna, and G. Bierwagen, "Mg-rich coatings: A new paradigm for Cr-free corrosion protection of Al aerospace alloys," *JCT Research*, vol. 1, no. 2, pp. 69-80, 2004.
- [47] J. H. Osborne, K. Y. Blohowiak, S. R. Taylor, C. Hunter, G. Bierwagon, B. Carlson, D. Bernard, and M. S. Donley, "Testing and evaluation of nonchromated coating systems for aerospace applications," *Progress in Organic Coatings*, vol. 41, no. 4, pp. 217-225, 2001.
- [48] N. Voevodin, C. Jeffcoate, L. Simon, M. Khobaib, and M. Donley, "Characterization of pitting corrosion in bare and sol-gel coated aluminum 2024-T3 alloy," *Surface and Coatings Technology*, vol. 140, no. 1, pp. 29-34, 2001.
- [49] R. L. Parkhill, E. T. Knobbe, and M. S. Donley, "Application and evaluation of environmentally compliant spray-coated ormosil films as corrosion resistant treatments for aluminum 2024-T3," *Progress in Organic Coatings*, vol. 41, no. 4, pp. 261-265, 2001.
- [50] N. N. Voevodin, N. T. Grebasch, W. S. Soto, L. S. Kasten, J. T. Grant, F. E. Arnold, and M. S. Donley, "An organically modified zirconate film as a corrosion-resistant treatment for aluminum 2024-T3," *Progress in Organic Coatings*, vol. 41, no. 4, pp. 287-293, 2001.
- [51] D. Zhu, and W. J. van Ooij, "Corrosion protection of AA 2024-T3 by bis-[3-(triethoxysilyl)propyl]tetrasulfide in neutral sodium chloride solution. Part 1: corrosion of AA 2024-T3," *Corrosion Science*, vol. 45, no. 10, pp. 2163-2175, 2003.
- [52] D. Zhu, and W. J. van Ooij, "Corrosion protection of AA 2024-T3 by bis-[3-(triethoxysilyl)propyl]tetrasulfide in sodium chloride solution.: Part 2: mechanism for corrosion protection," *Corrosion Science*, vol. 45, no. 10, pp. 2177-2197, 2003.

-
- [53] D. Zhu, and W. J. v. Ooij, "Enhanced corrosion resistance of AA 2024-T3 and hot-dip galvanized steel using a mixture of bis-[triethoxysilylpropyl]tetrasulfide and bis-[trimethoxysilylpropyl]amine," *Electrochimica Acta*, vol. 49, no. 7, pp. 1113-1125, 2004.
- [54] V. Palanivel, D. Zhu, and W. J. van Ooij, "Nanoparticle-filled silane films as chromate replacements for aluminum alloys," *Progress in Organic Coatings*, vol. 47, no. 3-4, pp. 384-392, 2003.
- [55] G. Pan, D. W. Schaefer, W. J. van Ooij, M. S. Kent, J. Majewski, and H. Yim, "Morphology and water resistance of mixed silane films of bis[3-(triethoxysilyl)propyl]tetrasulfide and bis-[trimethoxysilylpropyl]amine," *Thin Solid Films*, vol. 515, no. 4, pp. 2771-2780, 2006.
- [56] J. G. Kaufman, *Introduction to Aluminium Alloys and tempers*, OH, USA: ASM International, 2000.
- [57] R. G. Buchheit, R. P. Grant, P. F. Hlava, B. Mckenzie, and G. L. Zender, "Local Dissolution Phenomena Associated with S Phase (Al₂CuMg) Particles in Aluminum Alloy 2024-T3," *Journal of The Electrochemical Society*, vol. 144, no. 8, pp. 2621-2628, 1997.
- [58] A. E. Hughes, C. MacRae, N. Wilson, A. Torpy, T. H. Muster, and A. M. Glenn, "Sheet AA2024-T3: a new investigation of microstructure and composition," *Surface and Interface Analysis*, vol. 42, no. 4, pp. 334-338, 2010.
- [59] A. Boag, A. E. Hughes, N. C. Wilson, A. Torpy, C. M. MacRae, A. M. Glenn, and T. H. Muster, "How complex is the microstructure of AA2024-T3?," *Corrosion Science*, vol. 51, no. 8, pp. 1565-1568, 2009.
- [60] J. E. Hatch, *Aluminium: Properties and physical metallurgy*: ASM International, 1984.
- [61] S. P. Ringer, and K. Hono, "Microstructural Evolution and Age Hardening in Aluminium Alloys: Atom Probe Field-Ion Microscopy and Transmission Electron Microscopy Studies," *Materials Characterization*, vol. 44, pp. 101-131, 2000.
- [62] M. V. Lancker, *Metallurgy of Aluminium Alloys*, p. 209, London: Chapman and Hall Ltd, 1967.
- [63] Z. Zhao, and G. S. Frankel, "On the first breakdown in AA7075-T6," *Corrosion Science*, vol. 49, no. 7, pp. 3064-3088, 2007.
- [64] N. Birbilis, and R. G. Buchheit, "Electrochemical Characteristics of Intermetallic Phases in Aluminum Alloys: An Experimental Survey and Discussion," *Journal of The Electrochemical Society*, vol. 152, no. 4, pp. B140-B151, 2005.
- [65] R. Ayer, J. Y. Koo, J. W. Steeds, and B. K. Park, "Microanalytical study of the heterogeneous phases in commercial Al-Zn-Mg-Cu alloys," *Metallurgical Transactions A*, vol. 16, no. 11, pp. 1925-1936, 1985.
- [66] Z. Zhao, and G. S. Frankel, "The effect of temper on the first breakdown in AA7075," *Corrosion Science*, vol. 49, no. 7, pp. 3089-3111, 2007.
- [67] A. E. Hughes, N. Birbilis, J. M. C. Mol, S. J. Garcia, X. Zhou, and G. E. Thompson, "High Strength Al-Alloys: Microstructure, Corrosion and Principles of Protection " *Recent Trends in the Processing and Degredation of Aluminium Alloys*, P. Z. Ahmad, ed.: InTech 2011.
- [68] M. Gao, C. R. Feng, and R. Wei, "An analytical electron microscopy study of constituent particles in commercial 7075-T6 and 2024-T3 alloys," *Metallurgical and Materials Transactions A*, vol. 29, no. 4, pp. 1145-1151, 1998.
- [69] J. Wloka, and S. Virtanen, "Detection of nanoscale η -MgZn₂ phase dissolution from an Al-Zn-Mg-Cu alloy by electrochemical microtransients," *Surface and Interface Analysis*, vol. 40, no. 8, pp. 1219-1225, 2008.
- [70] J. Ryl, J. Wysocka, M. Jarzynka, A. Zielinski, J. Orlikowski, and K. Darowicki, "Effect of native air-formed oxidation on the corrosion behavior of AA 7075 aluminum alloys," *Corrosion Science*, no. 0.
- [71] J. F. Larché, P. O. Bussière, S. Thérias, and J. L. Gardette, "Photooxidation of polymers: Relating material properties to chemical changes," *Polymer Degradation and Stability*, vol. 97, no. 1, pp. 25-34, 2012.
- [72] Air Command Serectariat, "FOI request total flying hours for typhoon in 2014," U.K. Government, 8th August, 2017, [Online].

- Available:https://www.gov.uk/government/uploads/system/uploads/attachment_data/file/466740/20150915-FOI-Typhoon-Flying-Training-Hours-O.pdf.
- [73] Air Command Serectariat, "FOI request for details of the servicability of the RAF's aircraft fleet.," U.K. Government 8th August,2017, [Online]. Available:https://www.gov.uk/government/uploads/system/uploads/attachment_data/file/489644/20150106-Military_aircraft_numbers_and_availability.pdf.
- [74] R. A. F. Webmaster., "RAF Stations," RAF Organisation, 15th December,2015, [Online]. Available:<https://www.raf.mod.uk/organisation/stations.cfm>.
- [75] R. A. F. Webmaster., "Current Operations," Royal Air Force, 26th November 2015, [Online]. Available:<https://www.raf.mod.uk/currentoperations/>.
- [76] British Army MOD, "British army operations and deployment " British Army 26th November,2015, [Online]. Available:<http://www.army.mod.uk/operations-deployments/operations-deployments.aspx>.
- [77] Royal Navy MOD, "Royal Navy Current Operations," 26th November,2015, [Online]. Available:<http://www.royalnavy.mod.uk/news-and-latest-activity/operations>.
- [78] BSI., "BS EN ISO 9223 - Corrosion of metals and alloys - Corrosivity of atmospheres - Classification, determination and estimation," 2012.
- [79] D. Chen, and H. W. Chen, "Using the Köppen classification to quantify climate variation and change: An example for 1901–2010," *Environmental Development*, vol. 6, pp. 69-79, 2013.
- [80] BSI., "BS EN ISO 9224 - Corrosion of metals and alloys - Corrosivity of atmospheres - Guiding values for the corrosivity categories," 2012.
- [81] BSI., "BS EN ISO 9225 - Corrosion of metals and alloys - corrosivity of atmospheres - measurements of environmental parameters affecting corrosivity of atmospheres," 2012.
- [82] BSI., "BS EN ISO 9226 - Corrosion of metals and alloys - Corrosivity of metals - Determination of corrosion rate of standard specimens for the evaluation of corrosivity ", 2012.
- [83] BSI., "BS EN ISO 8565 - Metals and alloys - Atmospheric corrosion testing - General requirements," 2011.
- [84] BSI., "BS EN ISO 8407 - Corrosion of metals and alloys - Removal of corrosion products from corrosion test specimens," 2014.
- [85] C. Leygraf, and T. E. Graedel, "Appendix C : The Atmospheric Corrosion of Aluminum," *Atmospheric Corrosion*: John Wiley and Sons, 2000.
- [86] X. F. Yang, D. E. Tallman, G. P. Bierwagen, S. G. Croll, and S. Rohlik, "Blistering and degradation of polyurethane coatings under different accelerated weathering tests," *Polymer Degradation and Stability*, vol. 77, no. 1, pp. 103-109, 2002.
- [87] T. B. Moghim, M.-L. Abel, and J. F. Watts, "A novel approach to the assessment of aerospace coatings degradation: The HyperTest," *Progress in Organic Coatings*, vol. 104, pp. 223-231, 2017.
- [88] M. E. Nanna, and G. P. Bierwagen, "Mg-rich coatings: A new paradigm for Cr-free corrosion protection of Al aerospace alloys," *JCT Research*, vol. 1, no. 2, pp. 69-80, 2004.
- [89] BSI., "BS EN ISO 4628-1:2016 Paints and varnishes. Evaluation of degradation of coatings. Designation of quantity and size of defects, and of intensity of uniform changes in appearance. General introduction and designation system," BSI, 2016.
- [90] BSI., "BS EN ISO 4628-2 - Designation of quantity and size of defects, and of intensity of uniform changes in appearance. Assessment of degree of blistering," *Paints and varnishes. Evaluation of degradation of coatings. Designation of quantity and size of defects, and of intensity of uniform changes in appearance. Assessment of degree of blistering*, BSI., 2016.
- [91] J. Alcántara, B. Chico, I. Díaz, D. de la Fuente, and M. Morcillo, "Airborne chloride deposit and its effect on marine atmospheric corrosion of mild steel," *Corrosion Science*, vol. 97, pp. 74-88, 2015.
- [92] BSI., "BS EN ISO 5466 - CorroionTesting of Metallic Coatings - Guidance on stationary outdoor exposure corrosion tests," 2013.

-
- [93] G. Sharma, W. Wu, and E. N. Dalal, "Supplemental test data and excel and matlab implementations of the CIEDE2000 color difference formula.," 22nd July,2016, [Online]. Available:<http://www.ece.rochester.edu/>.
- [94] ASTM International, "ASTM G85 - Standard Practice for Modified Salt Spray (Fog) Testing," 2011.
- [95] International Organization for Standardization, "ISO 6270 - 2 - 2005 (en) Paints and Varnishes - Determination of resistance to humidity," ISO/TC 35/SC 9., 2005-2007.
- [96] ASTM International, "ASTM D5894-16, Standard Practice for Cyclic Salt Fog/UV Exposure of Painted Metal, (Alternating Exposures in a Fog/Dry Cabinet and a UV/Condensation Cabinet)," 2016.
- [97] V. Baukh, H. P. Huinink, O. C. G. Adan, and L. G. J. van der Ven, "Natural versus accelerated weathering: Understanding water kinetics in bilayer coatings," *Progress in Organic Coatings*, vol. 76, no. 9, pp. 1197-1202, 2013.
- [98] C. Leygraf, and T. E. Graedel, "The Atmospheric Corrosion of Copper - Chemical Mechanisms of Copper Corrosion," *Atmospheric Corrosion*.
- [99] P. Schweitzer, *Fundamentals of metallic corrosion*, p.^pp. 46: CRC Press, 2006.
- [100] W. D. Callister, and D. G. Rethwisch, "Materials Science and Engineering," pp. 108-109, Asia: John Wiley and Sons, 2011.
- [101] C. E. C. Housecroft, E.C., *Chemistry*, 3 ed., p.^pp. 547, England: Pearson Education, 2006.
- [102] G. Song, B. Johannesson, S. Hapugoda, and D. StJohn, "Galvanic corrosion of magnesium alloy AZ91D in contact with an aluminium alloy, steel and zinc," *Corrosion Science*, vol. 46, no. 4, pp. 955-977, 2004.
- [103] M. Yamashita, H. Nagano, and R. A. Oriani, "Dependence of corrosion potential and corrosion rate of a low-alloy steel upon depth of aqueous solution," *Corrosion Science*, vol. 40, no. 9, pp. 1447-1453, 1998.
- [104] X. G. Zhang, and E. M. Valeriote, "Galvanic protection of steel and galvanic corrosion of zinc under thin layer electrolytes," *Corrosion Science*, vol. 34, no. 12, pp. 1957-1972, 1993.
- [105] A. P. Yadav, H. Katayama, K. Noda, H. Masuda, A. Nishikata, and T. Tsuru, "Surface potential distribution over a zinc/steel galvanic couple corroding under thin layer of electrolyte," *Electrochimica Acta*, vol. 52, no. 9, pp. 3121-3129, 2007.
- [106] Y. L. Cheng, Z. Zhang, F. H. Cao, J. F. Li, J. Q. Zhang, J. M. Wang, and C. N. Cao, "A study of the corrosion of aluminum alloy 2024-T3 under thin electrolyte layers," *Corrosion Science*, vol. 46, no. 7, pp. 1649-1667, 2004.
- [107] A. d. Rooij, and L. Cavalli, "Bimetallic compatibility for space applications," in Proc. of the 10th ISMSE & 8th ICPMSE, Collioure, France, 2006.
- [108] *Uhlig's Corrosion Handbook 3rd Edition*, p.^pp. 726, Hoboken, NJ.: John Wiley and Sons, 2011.
- [109] Z. Szklarska-Smialowska, "Pitting corrosion of aluminum," *Corrosion Science*, vol. 41, no. 9, pp. 1743-1767, 1999.
- [110] M. Pourbaix, *Atlas of electrochemical equilibria in aqueous solutions*, Oxford: Pergamon, 1966.
- [111] C. G. Leygraf, T. , *Atmospheric Corrosion*, p.^pp. 252, New York: John Wiley & Sons, 2000.
- [112] E. McCafferty, "Passivity," *Introduction to Corrosion Science*, pp. 209-262: Springer New York, 2010.
- [113] N. Sato, "An overview on the passivity of metals," *Corrosion Science*, vol. 31, no. 0, pp. 1-19, 1990.
- [114] C. G. Leygraf, T., *Atmospheric corrosion* p.^pp. 253, New York: John Wiley & Sons, 2000.
- [115] R. Ambat, and E. S. Dwarakadasa, "The influence of pH on the corrosion of medium strength aerospace alloys 8090, 2091 and 2014," *Corrosion Science*, vol. 33, no. 5, pp. 681-690, 1992.
- [116] P. Gimenez, and J. J. Rameau, "Experimental pH potential diagram of aluminium for seawater," *Corrosion*, vol. 37, pp. 673-682, 1981.

- [117] P. Schmutz, and G. S. Frankel, "Characterization of AA2024-T3 by Scanning Kelvin Probe Force Microscopy," *Journal of The Electrochemical Society*, vol. 145, no. 7, pp. 2285-2295, 1998.
- [118] P. Schmutz, and G. S. Frankel, "Corrosion Study of AA2024-T3 by Scanning Kelvin Probe Force Microscopy and In Situ Atomic Force Microscopy Scratching," *Journal of The Electrochemical Society*, vol. 145, no. 7, pp. 2295-2306, 1998.
- [119] J. H. W. de Wit, "New knowledge on localized corrosion obtained from local measuring techniques," *Electrochimica Acta*, vol. 46, no. 24-25, pp. 3641-3650, 2001.
- [120] A. Boag, R. J. Taylor, T. H. Muster, N. Goodman, D. McCulloch, C. Ryan, B. Rout, D. Jamieson, and A. E. Hughes, "Stable pit formation on AA2024-T3 in a NaCl environment," *Corrosion Science*, vol. 52, no. 1, pp. 90-103, 2010.
- [121] M. Posada, L. E. Murr, C. S. Niou, D. Roberson, D. Little, R. Arrowood, and D. George, "Exfoliation and related microstructures in 2024 aluminum body skins on aging aircraft," *Materials Characterization*, vol. 38, no. 4-5, pp. 259-272, 1997.
- [122] E. L. Colvin, "Aluminum Alloys: Corrosion," *Encyclopedia of Materials: Science and Technology (Second Edition)*, K. H. J. Buschow, R. W. Cahn, M. C. Flemings, B. Iilschner, E. J. Kramer, S. Mahajan and P. Veyssi re, eds., pp. 107-110, Oxford: Elsevier, 2001.
- [123] O. O. Knudsen, U. Steinsmo, M. Bjordal, and S. Nijjer, "Accelerated Testing: Correlation between four accelerated tests and five years of offshore field testing" *Journal of Polymer Coating and Linings*, vol. March pp. 52-56, 2001.
- [124] F. Deflorian, S. Rossi, and M. Fedel, "Organic coatings degradation: Comparison between natural and artificial weathering," *Corrosion Science*, vol. 50, no. 8, pp. 2360-2366, 2008.
- [125] S. Chong, "A comparison of accelerated tests for steel bridge coatings in marine environments," *Journal of Protective Coatings and Linings*, vol. March, pp. 20-33, 1997.
- [126] Ascott Analytical, "Graph showing standard range of temperature/humidity control for a CCT chamber and how this may be extended by the addition of optional accessories."
- [127] British Standard Institution, "BS EN ISO 11664-6:2016 Colorimetry" *Part 6 : CIEDE2000 Colour-difference formula*, BSI, 2016.
- [128] C. Leygraf, and T. E. Graedel, "The Atmospheric Corrosion of Zinc - Chemical Mechanisms of Zinc Corrosion," *Atmospheric Corrosion*, 2000.
- [129] R. Wiesinger, I. Martina, C. Kleber, and M. Schreiner, "Influence of relative humidity and ozone on atmospheric silver corrosion," *Corrosion Science*, vol. 77, no. Supplement C, pp. 69-76, 2013.
- [130] C. Leygraf, and T. E. Graedel, "The Atmospheric Corrosion of Iron and Low Alloy Steels - Chemical Mechanisms of Iron and Steel Corrosion," *Atmospheric Corrosion*: John Wiley and Sons, 2000.
- [131] D. Liang, H. C. Allen, G. S. Frankel, Z. Y. Chen, R. G. Kelly, Y. Wu, and B. E. Wyslouzil, "Effects of Sodium Chloride Particles, Ozone, UV, and Relative Humidity on Atmospheric Corrosion of Silver," *Journal of The Electrochemical Society*, vol. 157, no. 4, pp. C146-C156, 2010.
- [132] C. Leygraf, and T. E. Graedel, "The Atmospheric Corrosion of Silver - Chemical Transformation Sequences," *Atmospheric Corrosion*, 2000.
- [133] D. Vione, V. Maurino, C. Minero, and E. Pelizzetti, "The atmospheric chemistry of hydrogen peroxide: A review," *Annali di Chimica*, vol. 93, pp. 477-88, 2003.
- [134] T. E. Graedel, "Corrosion Mechanisms for Zinc Exposed to the Atmosphere," *Journal of The Electrochemical Society*, vol. 136, no. 4, pp. 193C-203C, 1989.
- [135] C. Leygraf, and T. E. Graedel, "The Atmospheric Corrosion of Nickel - Chemical Mechanisms of Nickel Corrosion," *Atmospheric Corrosion*, 2000.
- [136] K. N. S. Adema, H. Makki, E. A. J. F. Peters, J. Laven, L. G. J. van der Ven, R. A. T. M. van Benthem, and G. de With, "The influence of the exposure conditions on the chemical and physical changes of polyester-urethane coatings during photodegradation," *Polymer Degradation and Stability*, vol. 123, no. Supplement C, pp. 13-25, 2016.
- [137] B.-s. Liu, Y.-h. Wei, W.-y. Chen, L.-f. Hou, and C.-l. Guo, "Blistering failure analysis of organic coatings on AZ91D Mg-alloy components," *Engineering Failure Analysis*, vol. 42, pp. 231-239, 2014.

- [138] S. Caines, F. Khan, J. Shirokoff, and W. Qiu, "Experimental design to study corrosion under insulation in harsh marine environments," *Journal of Loss Prevention in the Process Industries*, vol. 33, no. Supplement C, pp. 39-51, 2015.
- [139] S. G. Croll, B. R. Hinderliter, and S. Liu, "Statistical approaches for predicting weathering degradation and service life," *Progress in Organic Coatings*, vol. 55, no. 2, pp. 75-87, 2006.
- [140] R. I. Trezona, M. J. Pickles, and I. M. Hutchings, "A full factorial investigation of the erosion durability of automotive clearcoats," *Tribology International*, vol. 33, no. 8, pp. 559-571, 2000.
- [141] R. L. De Rosa, D. A. Earl, and G. P. Bierwagen, "Statistical evaluation of EIS and ENM data collected for monitoring corrosion barrier properties of organic coatings on Al-2024-T3," *Corrosion Science*, vol. 44, no. 7, pp. 1607-1620, 2002.
- [142] "JMP Pro 13," Windows, North Carolina: SAS, 2018,
- [143] C. G. Leygraf, T, "Atmospheric Corrosion," p. 94, New York: John Wiley & Sons, 2000.

11. Appendix

11.1. Coating systems supplied by AkzoNobel

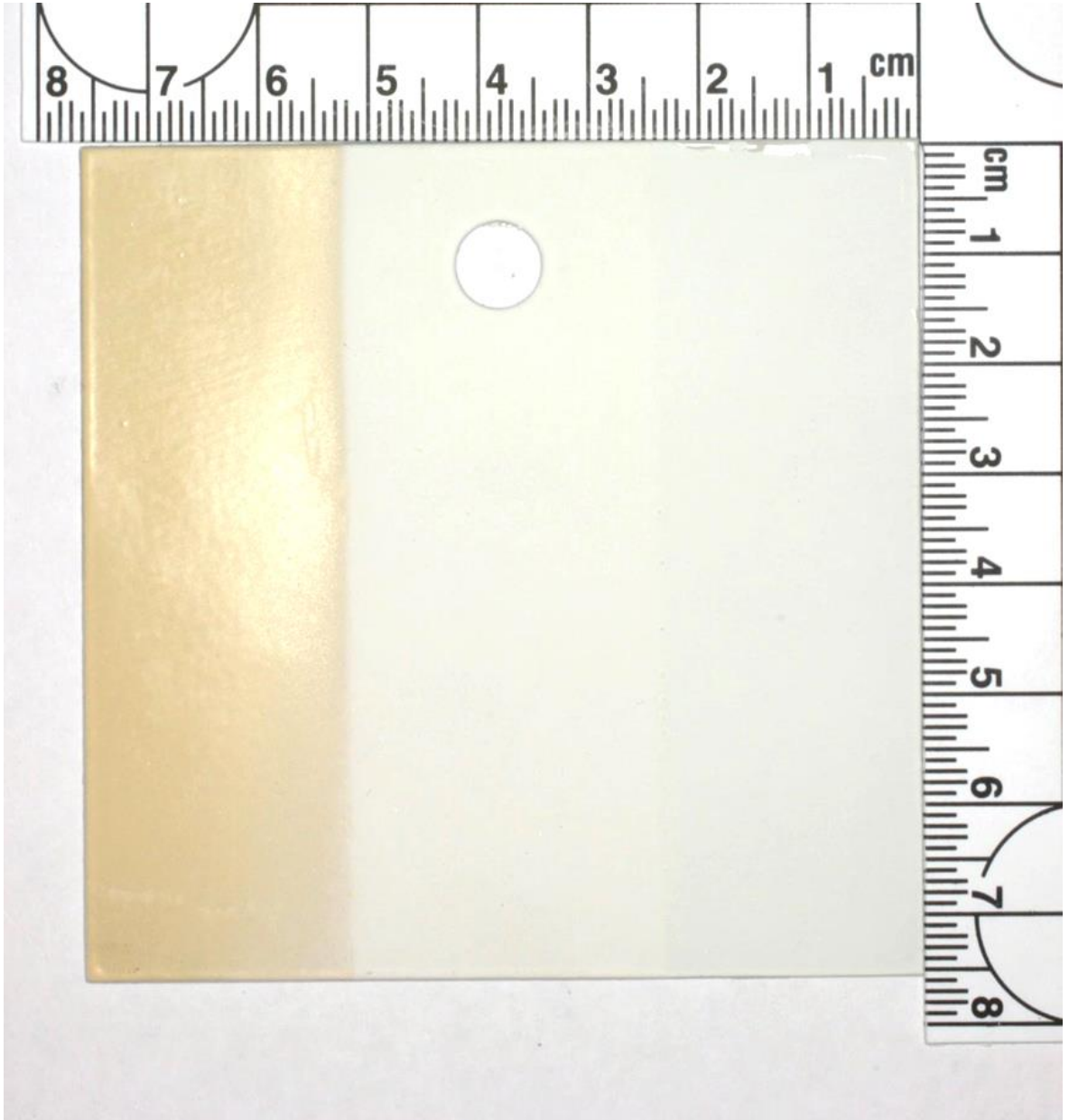


Figure 110: Example of an as-coated AkzoNobel coating system 2 – Coupon # 122 (AA2024-T3 substrate).

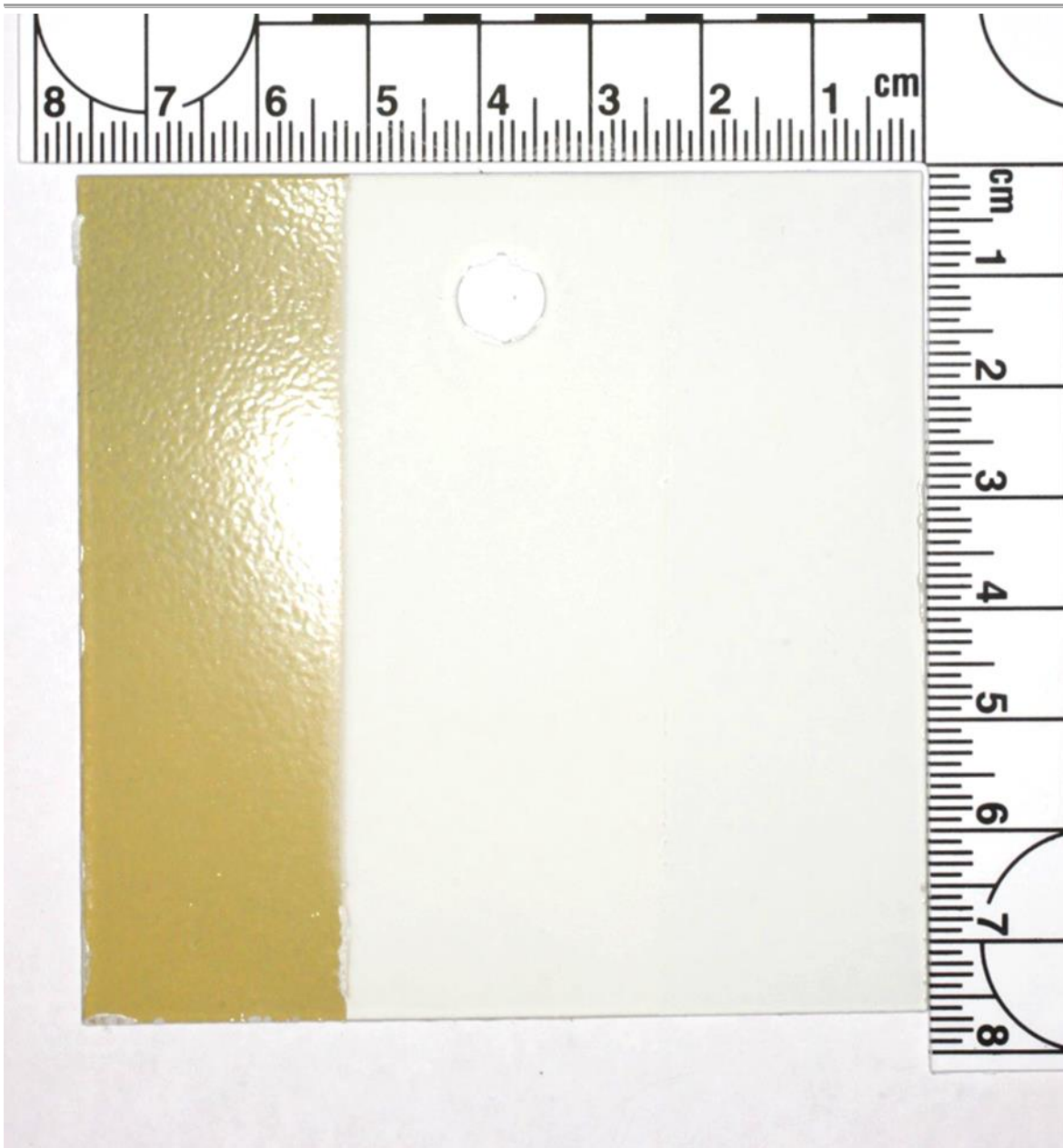


Figure 111: Example of an as-coated AkzoNobel coating system 3 – Coupon # 177(AA2024-T3 substrate).

11.2. Coating Systems supplied by PPG

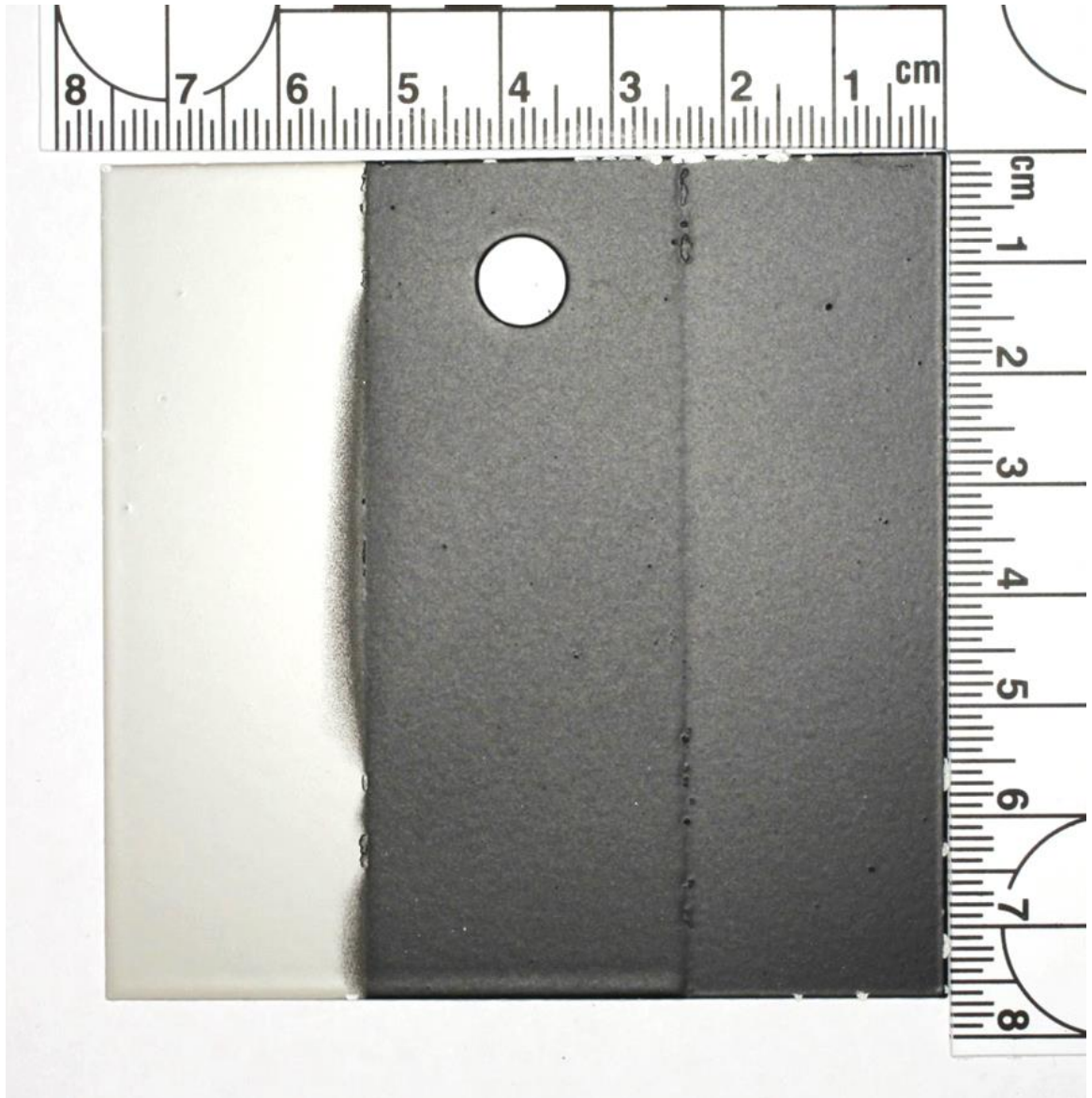


Figure 112: Example of an as-coated PPG coating system 4 – Coupon # 199 (AA7075-T6 substrate).

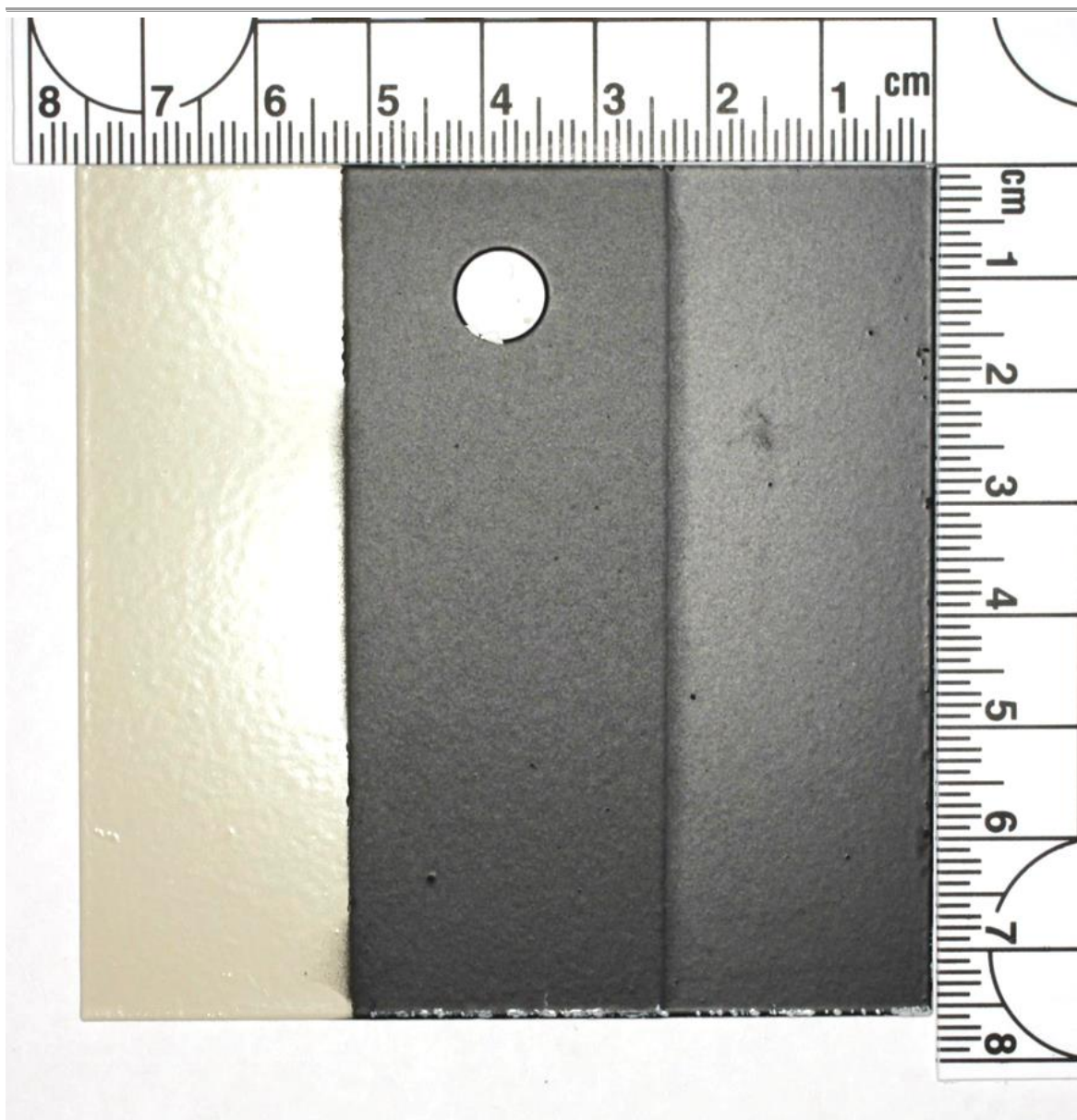


Figure 113: Example of an as-coated PPG coating system 5 – Coupon # 273 (AA2024-T3 substrate).

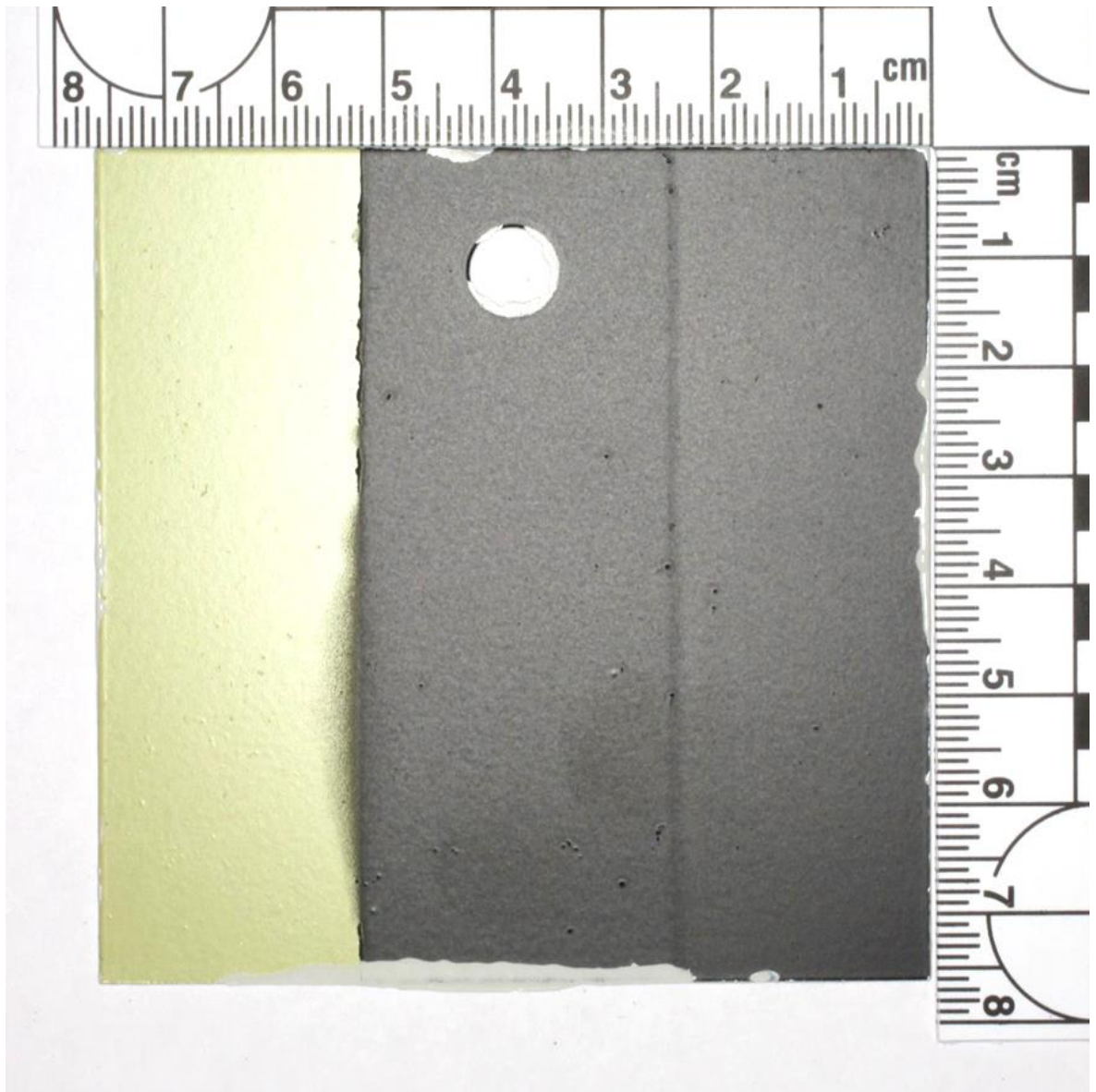


Figure 114: Example of an as-coated PPG coating system 6 – Coupon # 197 (AA2024-T3 substrate).

11.3. Natural exposure rack design

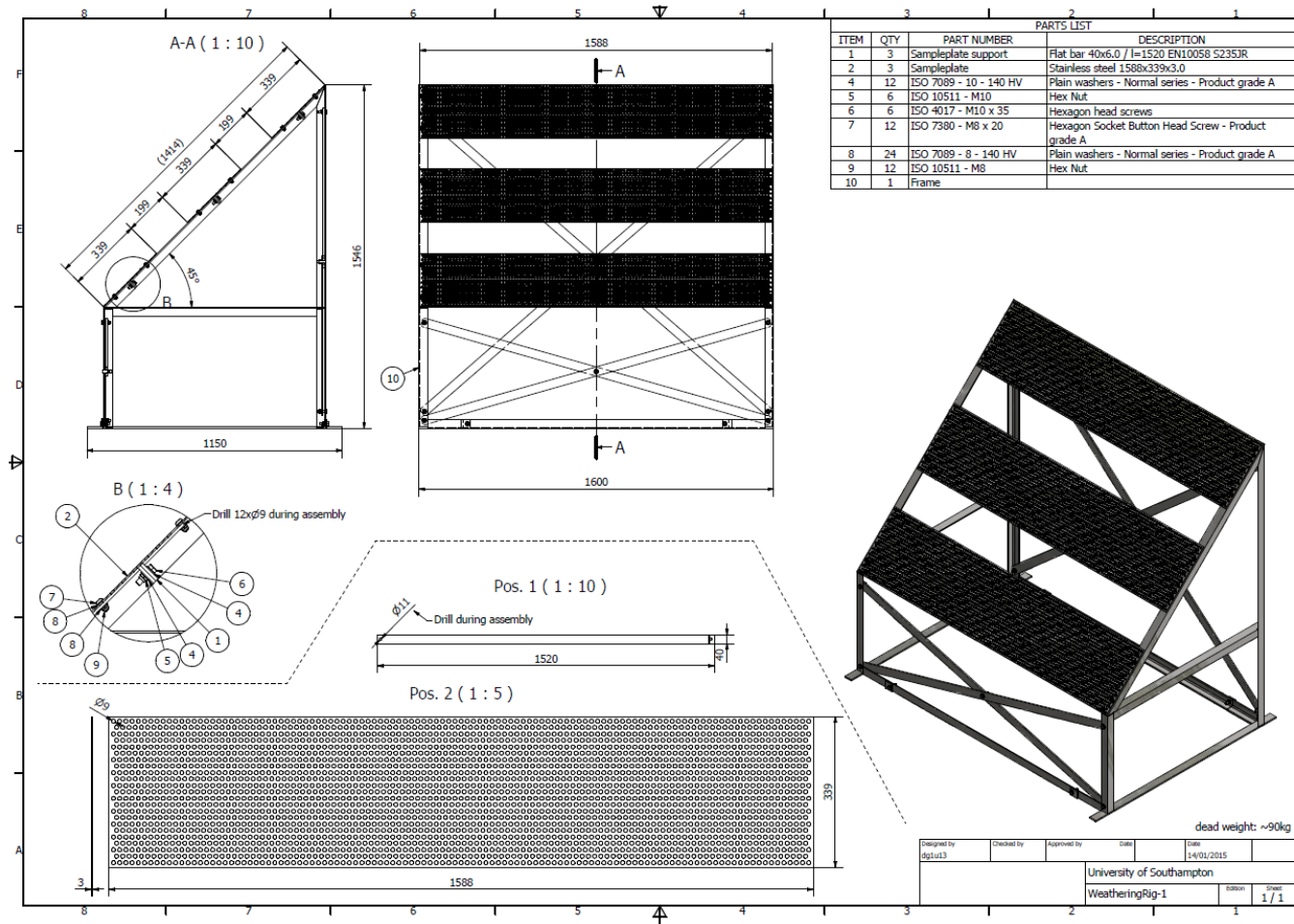


Figure 115: Exposure rig drawings page 1.

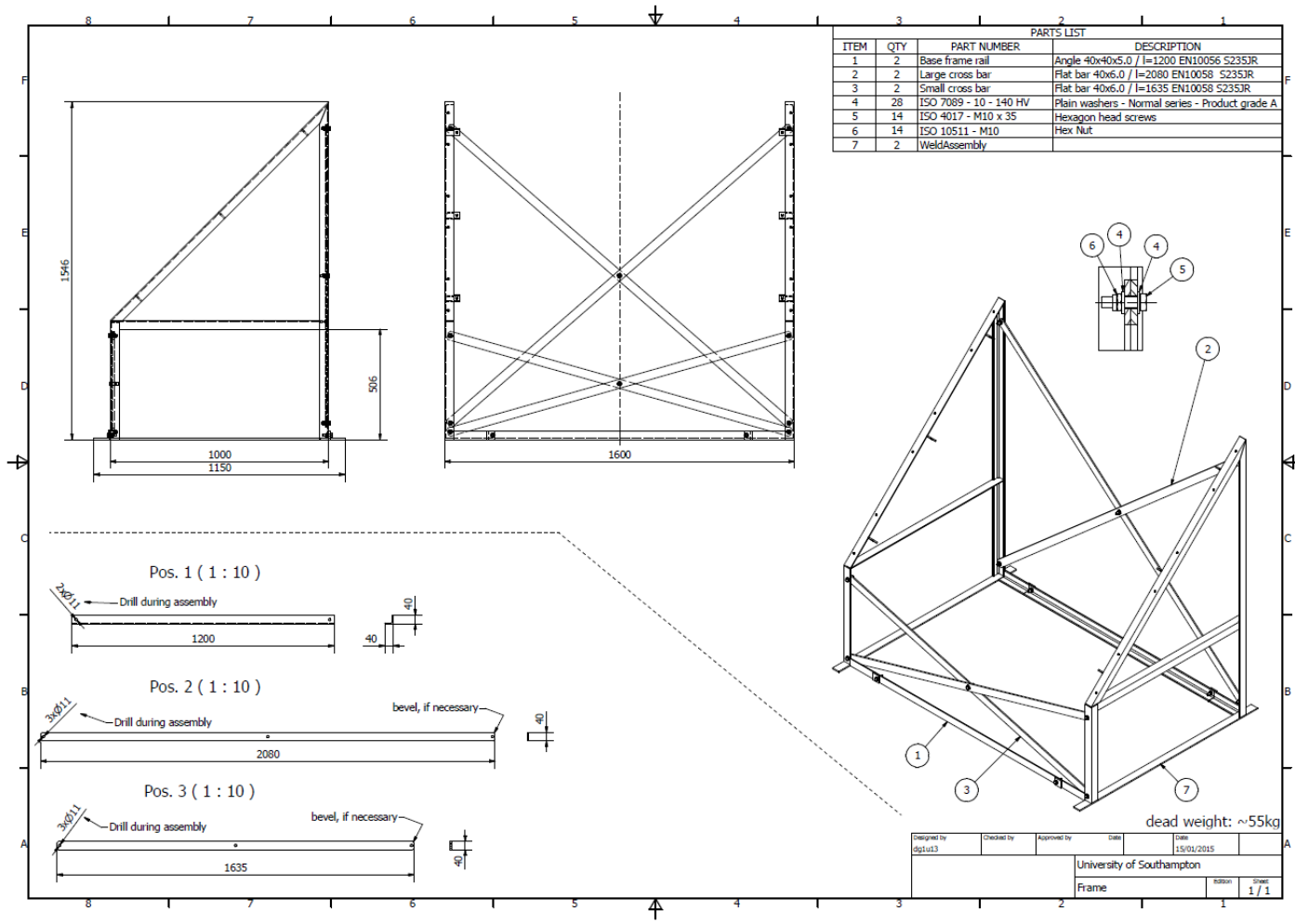


Figure 116: Exposure rig drawings page 2.

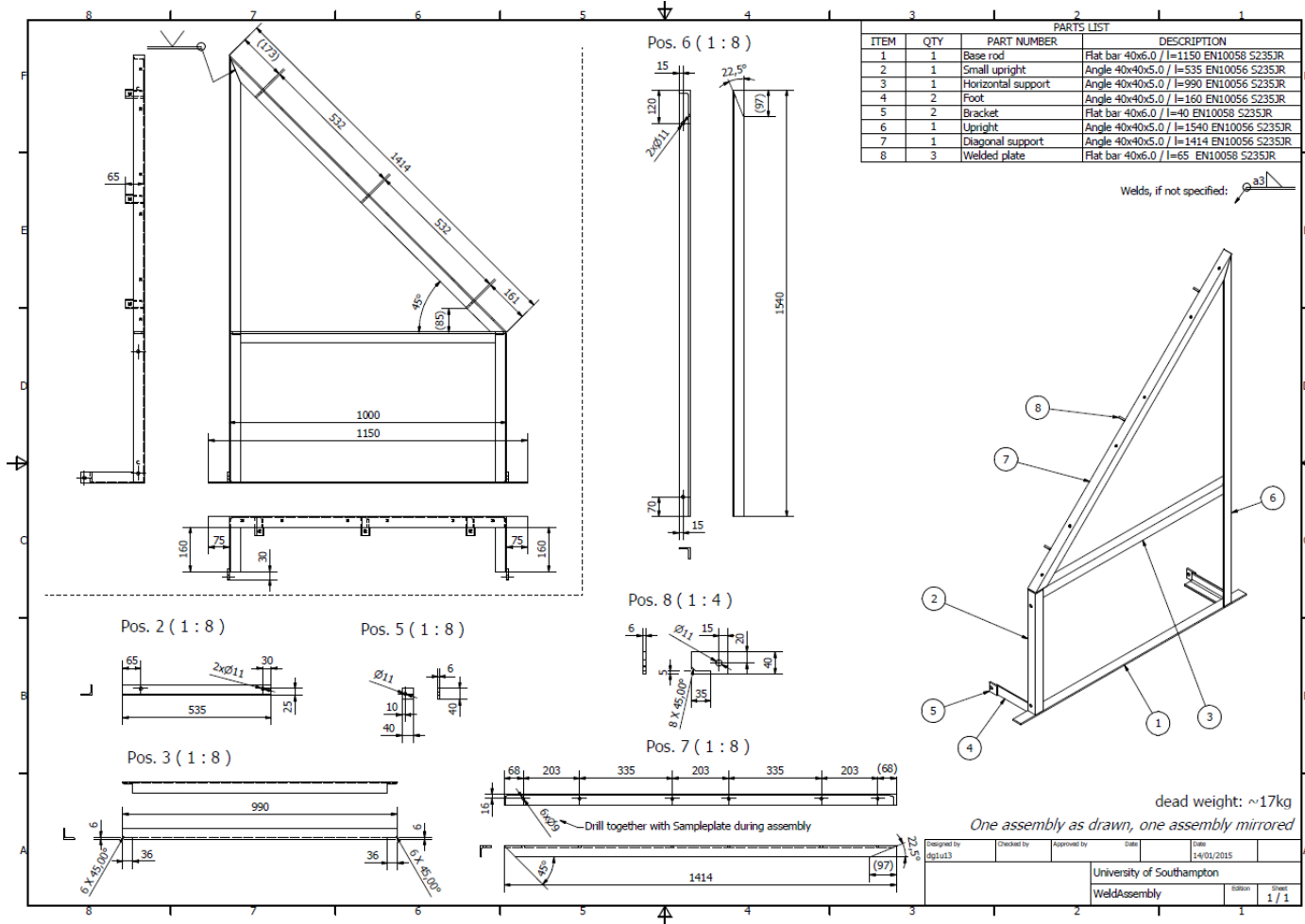


Figure 117: Exposure rig drawings page 3.

11.4. Additional data from testing of Ascott chamber

Thermocouple experiment 2

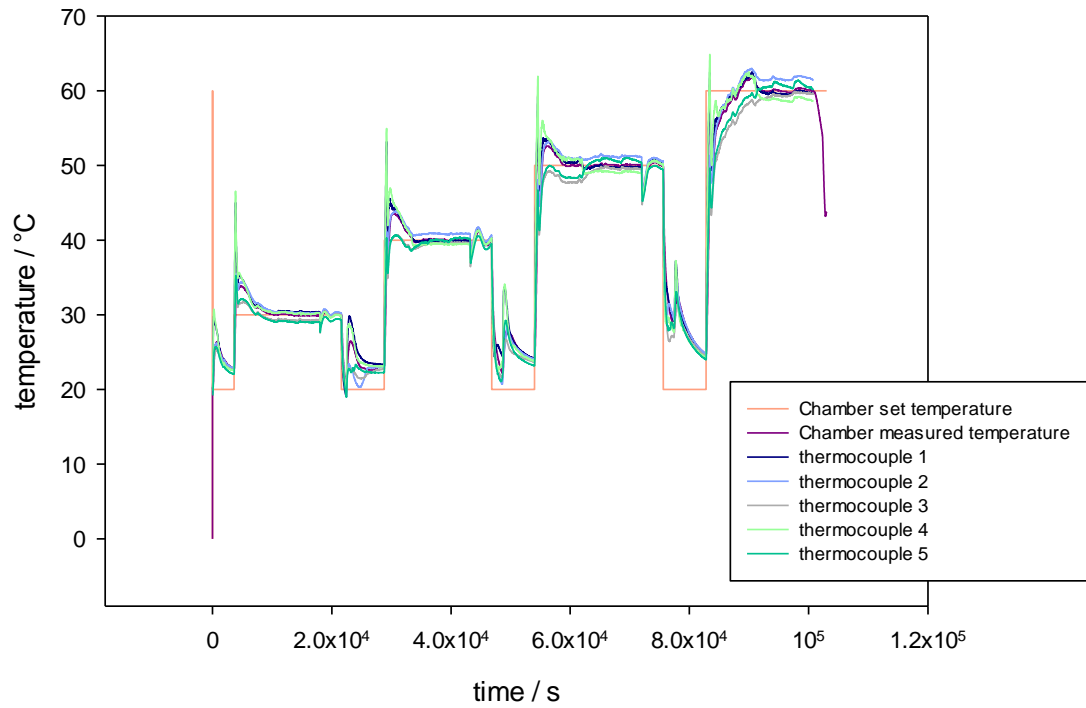


Figure 118: Understanding the accelerated environment thermocouple sample arrangement 2.

Thermocouple experiment 3

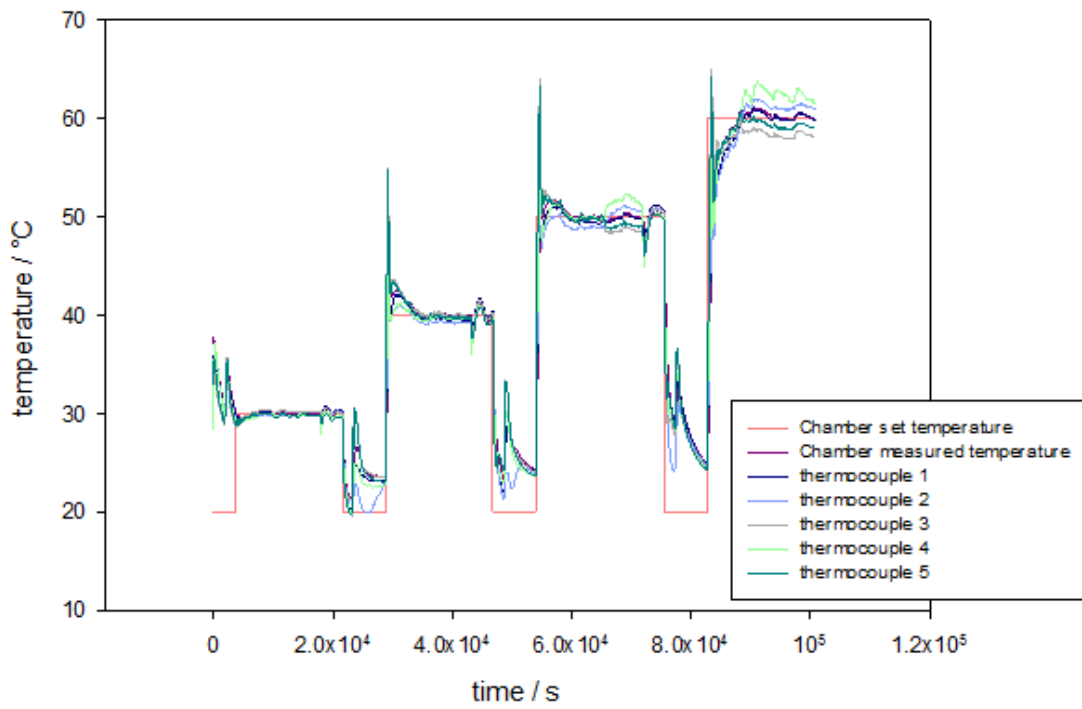


Figure 119: Understanding the accelerated environment thermocouple sample arrangement 3.

Thermocouple experiment 4

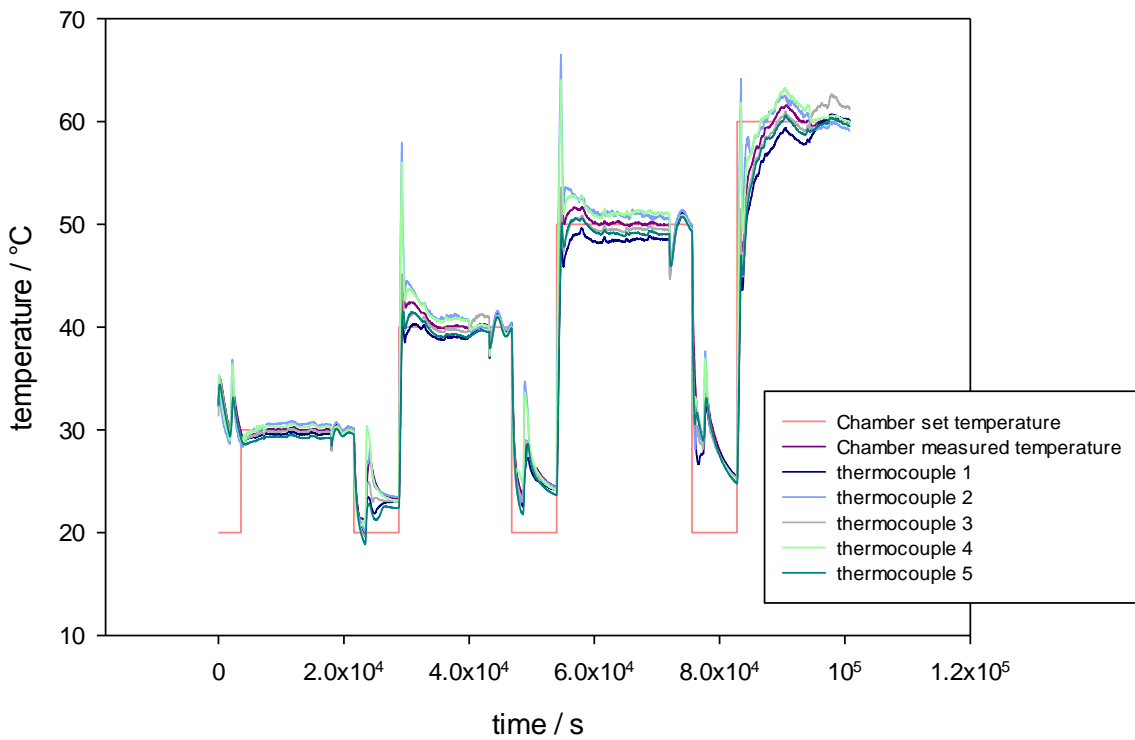


Figure 120: Understanding the accelerated environment thermocouple sample arrangement 4.

Thermocouple experiment 5

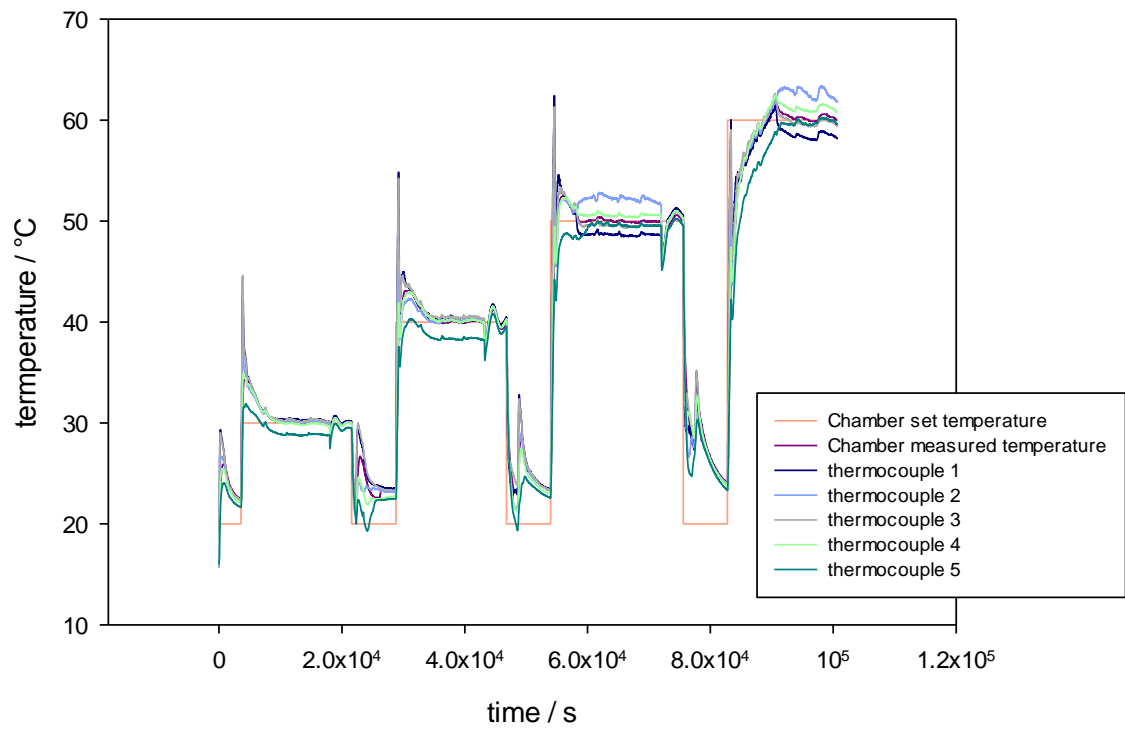


Figure 121: Understanding the accelerated environment thermocouple sample arrangement 5.

11.5. Full factorial design as analysed

Experimental Conditions					Analytical Inputs				
Coupon number	Substrate	Coating system	Experiment	Time point	% area thermography topcoat	85° gloss primer	ΔE 200 primer	Konig Hardness primer/topcoat	60° Gloss for primer/topcoat
1	AA2024 - T3	6	Temperate Inland	4	0.0	8.5	11.8	121	4.2
2	AA2024 - T3	5	Accelerated 3	2	0.0	80.7	0.7	156	3.9
3	AA2024 - T3	3	Temperate Inland	4	0.0	56.4	1.0	28	2.7
4	AA2024 - T3	3	BS EN ISO 9227	5	17.8	19.8	3.2	27	3.5
5	AA2024 - T3	3	Tropical Inland	6	19.3	58.5	0.6	29	3.5
6	AA2024 - T3	3	Accelerated 4	5	0.0	60.5	0.9	23	3.0
7	AA7075-T6	3	Temperate Coastal	2	0.0	62.2	0.9	24	3.0
8	AA2024 - T3	1	Accelerated 3	5	0.0	1.4	3.9	32	2.9
9	AA7075-T6	6	Accelerated 4	3	0.0	26.0	8.0	131	3.4
10	AA7075-T6	1	Accelerated 1	4	39.7	0.9	15.3	40	1.7
11	AA7075-T6	1	Accelerated 1	6	34.1	2.4	19.6	42	1.9
12	AA2024 - T3	3	Accelerated 2	5	1.8	62.9	0.9	27	3.0
13	AA2024 - T3	1	Accelerated 3	2	0.0	2.2	1.8	34	2.3

Experimental Conditions					Analytical Inputs				
Coupon number	Substrate	Coating system	Experiment	Time point	% area thermography topcoat	85° gloss primer	ΔE 200 primer	Konig Hardness primer/topcoat	60° Gloss for primer/topcoat
14	AA2024 - T3	4	Accelerated 4	1	0.0	66.8	0.3	127	6.3
15	AA7075-T6	4	BS EN ISO 9227	2	0.0	33.2	1.9	127	5.1
16	AA7075-T6	5	Temperate Inland	3	1.6	36.3	1.8	138	4.5
17	AA2024 - T3	3	BS EN ISO 9227	4	33.0	19.5	0.2	28	3.6
18	AA7075-T6	3	Accelerated 2	2	0.0	87.5	3.2	26	2.9
19	AA7075-T6	1	Accelerated 2	6	5.9	1.8	1.5	41	2.1
20	AA7075-T6	1	Accelerated 2	7	23.3	1.5	4.0	37	2.0
21	AA7075-T6	6	Accelerated 2	2	0.0	44.6	4.9	126	4.8
22	AA2024 - T3	1	Accelerated 2	2	0.0	1.1	12.1	36	2.2
23	AA2024 - T3	1	Accelerated 2	1	0.0	1.7	1.9	34	2.4
24	AA7075-T6	1	Accelerated 2	4	4.7	1.7	0.3	39	2.1
25	AA7075-T6	1	Accelerated 1	5	53.4	0.8	5.1	110	1.8
26	AA2024 - T3	4	Accelerated 2	6	0.0	64.6	16.8	36	7.3
27	AA2024 - T3	1	Accelerated 1	7	40.8	2.6	0.2	29	2.1

Experimental Conditions					Analytical Inputs				
Coupon number	Substrate	Coating system	Experiment	Time point	% area thermography topcoat	85° gloss primer	ΔE 200 primer	Konig Hardness primer/topcoat	60° Gloss for primer/topcoat
28	AA2024 - T3	1	Accelerated 1	6	42.5	1.0	15.1	43	2.0
29	AA2024 - T3	1	Accelerated 1	2	3.8	1.7	16.8	98	2.0
30	AA2024 - T3	1	Accelerated 1	3	8.8	3.5	13.6	28	2.1
31	AA2024 - T3	1	Temperate Inland	3	0.0	1.3	17.9	127	2.4
32	AA7075-T6	6	Tropical Coastal	5	81.5	7.7	2.7	34	2.2
33	AA2024 - T3	1	Accelerated 3	6	0.0	1.2	10.9	140	2.3
34	AA7075-T6	6	Accelerated 3	4	0.3	24.0	2.8	35	4.5
35	AA7075-T6	1	Accelerated 3	1	0.0	1.3	10.1	28	2.1
36	AA7075-T6	3	Temperate Inland	7	3.9	59.2	0.1	38	2.5
37	AA7075-T6	1	Accelerated 3	3	0.0	2.0	0.9	38	2.0
38	AA7075-T6	1	Accelerated 3	4	0.0	1.2	5.6	94	1.8
39	AA2024 - T3	1	Accelerated 4	5	0.2	0.9	4.0	38	2.3
40	AA7075-T6	1	Accelerated 4	6	0.0	1.3	3.4	37	2.1
41	AA2024 - T3	1	Accelerated 4	7	0.0	0.9	4.5	38	2.2

Experimental Conditions					Analytical Inputs				
Coupon number	Substrate	Coating system	Experiment	Time point	% area thermography topcoat	85° gloss primer	ΔE 200 primer	Konig Hardness primer/topcoat	60° Gloss for primer/topcoat
42	AA7075-T6	1	Accelerated 4	1	0.0	1.6	2.8	34	2.2
43	AA7075-T6	1	Accelerated 4	2	0.0	2.6	0.4	36	2.2
44	AA2024 - T3	1	Accelerated 4	3	0.0	1.7	1.3	36	2.1
45	AA2024 - T3	1	Accelerated 4	4	0.0	1.3	1.9	38	2.2
46	AA2024 - T3	1	Tropical Coastal	5	95.0	0.5	3.3	38	1.8
47	AA7075-T6	1	Tropical Coastal	6	64.5	2.3	15.4	42	1.7
48	AA7075-T6	5	Tropical Coastal	7	86.4	6.3	19.1	74	2.0
49	AA2024 - T3	1	Tropical Coastal	1	0.0	2.1	3.5	29	2.4
50	AA7075-T6	1	Tropical Coastal	2	29.3	0.9	0.2	35	2.0
51	AA7075-T6	1	Tropical Coastal	3	44.4	2.0	7.7	37	1.9
52	AA2024 - T3	1	Tropical Coastal	4	100.0	1.0	7.5	31	1.9
53	AA7075-T6	1	Tropical Inland	5	21.8	1.3	11.7	41	2.3
54	AA2024 - T3	1	Tropical Inland	6	13.8	1.7	16.3	40	2.5
55	AA7075-T6	1	Tropical Inland	7	33.5	1.0	18.0	37	2.2

Experimental Conditions					Analytical Inputs				
Coupon number	Substrate	Coating system	Experiment	Time point	% area thermography topcoat	85° gloss primer	ΔE 200 primer	Konig Hardness primer/topcoat	60° Gloss for primer/topcoat
56	AA2024 - T3	3	Tropical Inland	1	0.0	93.5	16.6	25	2.9
57	AA2024 - T3	1	Tropical Inland	2	4.8	1.8	0.9	32	2.3
58	AA2024 - T3	1	Tropical Coastal	7	95.3	0.8	9.5	45	2.0
59	AA2024 - T3	1	Tropical Inland	4	2.5	1.7	na	35	2.4
60	AA7075-T6	1	Temperate Inland	5	4.1	1.6	11.8	35	2.3
61	AA2024 - T3	1	Temperate Inland	6	1.5	1.2	15.0	33	2.4
62	AA7075-T6	1	Temperate Inland	7	13.6	1.9	17.2	36	2.2
63	AA2024 - T3	1	Temperate Inland	1	0.0	1.1	16.0	35	2.2
64	AA2024 - T3	2	Temperate Inland	7	0.0	3.0	0.9	31	2.4
65	AA2024 - T3	2	Temperate Inland	3	0.0	1.1	2.6	23	2.7
66	AA7075-T6	2	Temperate Inland	4	0.0	11.8	1.6	36	2.5
67	AA2024 - T3	4	Temperate Coastal	5	0.0	8.4	0.9	146	5.3
68	AA2024 - T3	2	Temperate Coastal	6	0.8	10.4	6.5	28	2.6
69	AA2024 - T3	2	Temperate Coastal	7	0.0	2.2	3.7	35	2.4

Experimental Conditions					Analytical Inputs				
Coupon number	Substrate	Coating system	Experiment	Time point	% area thermography topcoat	85° gloss primer	ΔE 200 primer	Konig Hardness primer/topcoat	60° Gloss for primer/topcoat
70	AA7075-T6	2	Temperate Coastal	1	0.0	10.2	2.9	27	2.7
71	AA2024 - T3	2	Temperate Coastal	2	0.0	3.3	0.8	32	2.7
72	AA7075-T6	2	Temperate Coastal	3	0.0	6.6	1.2	34	2.3
73	AA2024 - T3	2	Tropical Coastal	4	77.9	0.5	1.5	28	2.3
74	AA7075-T6	2	BS EN ISO 9227	5	14.1	43.8	1.4	29	3.5
75	AA2024 - T3	2	BS EN ISO 9227	6	25.1	16.8	1.7	30	3.1
76	AA7075-T6	2	BS EN ISO 9227	7	24.6	43.8	0.4	29	3.2
77	AA2024 - T3	2	BS EN ISO 9227	1	0.0	59.5	1.6	29	2.7
78	AA2024 - T3	2	BS EN ISO 9227	2	0.4	11.8	0.5	26	3.2
79	AA2024 - T3	2	BS EN ISO 9227	3	59.4	2.6	0.8	28	3.3
80	AA7075-T6	6	BS EN ISO 9227	6	14.3	33.6	1.8	118	4.3
81	AA7075-T6	2	Accelerated 2	5	0.0	11.5	6.7	32	2.6
82	AA7075-T6	2	Temperate Inland	2	0.0	8.1	0.5	32	2.6
83	AA2024 - T3	2	Accelerated 2	7	1.7	2.1	1.7	29	2.8

Experimental Conditions					Analytical Inputs				
Coupon number	Substrate	Coating system	Experiment	Time point	% area thermography topcoat	85° gloss primer	ΔE 200 primer	Konig Hardness primer/topcoat	60° Gloss for primer/topcoat
84	AA7075-T6	2	Accelerated 2	6	6.1	62.4	2.1	131	2.7
85	AA7075-T6	2	Accelerated 2	1	0.0	49.9	1.3	31	2.8
86	AA7075-T6	2	Accelerated 1	3	37.2	61.9	0.9	28	2.6
87	AA7075-T6	2	Accelerated 2	4	3.0	41.2	0.9	29	2.6
88	AA7075-T6	2	Accelerated 1	5	87.3	30.0	0.7	127	2.5
89	AA2024 - T3	4	Accelerated 1	1	0.0	65.3	1.2	114	6.8
90	AA7075-T6	2	Temperate Coastal	4	0.4	1.8	0.3	33	2.6
91	AA2024 - T3	2	Accelerated 1	1	0.0	18.1	2.5	29	2.8
92	AA2024 - T3	4	Accelerated 2	2	0.0	63.6	0.8	117	5.7
93	AA7075-T6	2	Accelerated 1	2	4.5	4.2	0.3	27	2.9
94	AA2024 - T3	2	Accelerated 1	4	62.2	12.0	0.8	62	2.5
95	AA2024 - T3	2	Accelerated 3	5	0.0	16.8	1.1	32	2.5
96	AA7075-T6	2	Accelerated 3	6	0.0	21.0	1.4	32	2.7
97	AA7075-T6	2	Accelerated 3	7	0.9	2.8	1.8	32	2.6

Experimental Conditions					Analytical Inputs				
Coupon number	Substrate	Coating system	Experiment	Time point	% area thermography topcoat	85° gloss primer	ΔE 200 primer	Konig Hardness primer/topcoat	60° Gloss for primer/topcoat
98	AA2024 - T3	2	Accelerated 3	1	0.0	11.4	1.2	31	2.8
99	AA7075- T6	2	Accelerated 3	2	0.0	48.0	0.8	30	2.7
100	AA2024 - T3	2	Accelerated 3	3	0.0	3.8	2.0	32	2.6
101	AA7075- T6	2	Accelerated 3	4	0.0	33.5	0.9	32	2.7
102	AA7075- T6	2	Accelerated 4	5	0.0	11.9	2.8	37	2.6
103	AA2024 - T3	3	Accelerated 4	6	0.0	69.7	1.4	28	3.0
104	AA7075- T6	2	Accelerated 4	7	2.6	16.1	0.7	34	2.6
105	AA7075- T6	2	BS EN ISO 9227	4	25.5	51.1	0.8	28	3.2
106	AA7075- T6	5	Accelerated 4	1	0.0	82.4	1.7	143	3.4
107	AA7075- T6	2	Accelerated 4	3	0.0	56.9	0.0	29	2.8
108	AA2024 - T3	2	Accelerated 4	4	0.0	11.3	2.1	34	2.8
109	AA2024 - T3	2	Tropical Coastal	5	85.0	1.6	1.0	78	2.2
110	AA2024 - T3	2	Tropical Coastal	6	100.0	0.4	2.0	27	2.0
111	AA7075- T6	2	Tropical Coastal	7	100.0	0.6	2.1	36	1.9

Experimental Conditions					Analytical Inputs				
Coupon number	Substrate	Coating system	Experiment	Time point	% area thermography topcoat	85° gloss primer	ΔE 200 primer	Konig Hardness primer/topcoat	60° Gloss for primer/topcoat
112	AA7075-T6	2	Tropical Coastal	1	0.0	6.0	3.2	29	2.7
113	AA2024 - T3	2	Accelerated 3	7	0.0	11.5	1.3	31	2.7
114	AA7075-T6	2	Tropical Coastal	3	100.0	2.8	1.0	36	2.2
115	AA7075-T6	3	Tropical Coastal	6	58.9	11.5	0.7	32	2.0
116	AA7075-T6	5	Temperate Inland	5	0.3	44.7	2.1	127	4.4
117	AA7075-T6	2	Tropical Inland	6	93.8	2.6	1.2	47	2.9
118	AA7075-T6	5	Tropical Inland	7	11.2	4.0	1.3	134	3.1
119	AA7075-T6	2	Tropical Inland	1	0.0	26.1	0.2	20	3.2
120	AA7075-T6	2	Tropical Inland	2	0.0	13.7	2.7	29	2.8
121	AA2024 - T3	1	Tropical Inland	3	2.7	34.8	3.9	34	2.8
122	AA2024 - T3	2	Tropical Inland	4	21.0	1.8	1.2	27	1.9
123	AA2024 - T3	2	Temperate Inland	5	1.4	4.5	2.1	27	3.0
124	AA2024 - T3	2	Accelerated 1	6	34.7	4.7	0.5	25	2.8
125	AA2024 - T3	2	Tropical Inland	7	36.4	8.7	2.1	28	2.3

Experimental Conditions					Analytical Inputs				
Coupon number	Substrate	Coating system	Experiment	Time point	% area thermography topcoat	85° gloss primer	ΔE 200 primer	Konig Hardness primer/topcoat	60° Gloss for primer/topcoat
126	AA2024 - T3	2	Accelerated 4	1	0.0	1.1	1.4	30	3.0
127	AA2024 - T3	3	Temperate Inland	2	0.0	69.6	0.5	25	2.7
128	AA7075- T6	1	Temperate Coastal	4	0.0	65.1	11.0	34	2.8
129	AA7075- T6	2	Temperate Inland	1	0.0	1.3	0.9	37	2.4
130	AA7075- T6	3	Temperate Coastal	5	3.7	136.6	0.8	26	2.7
131	AA7075- T6	3	Temperate Coastal	6	0.8	78.6	0.8	30	2.7
132	AA7075- T6	6	Temperate Coastal	7	0.4	71.4	12.1	140	2.7
133	AA2024 - T3	3	Temperate Coastal	1	0.0	8.3	0.2	27	3.7
134	AA2024 - T3	3	Temperate Coastal	2	0.0	92.4	0.6	26	3.0
135	AA7075- T6	3	Temperate Coastal	3	0.0	87.2	0.7	22	3.0
136	AA2024 - T3	3	Temperate Coastal	4	0.0	76.6	0.6	30	2.8
137	AA7075- T6	6	BS EN ISO 9227	1	0.0	79.3	13.8	131	2.8
138	AA7075- T6	3	BS EN ISO 9227	6	46.2	36.0	3.8	26	4.9
139	AA7075- T6	2	Tropical Inland	3	0.0	9.8	1.1	27	3.4

Experimental Conditions					Analytical Inputs				
Coupon number	Substrate	Coating system	Experiment	Time point	% area thermography topcoat	85° gloss primer	ΔE 200 primer	Konig Hardness primer/topcoat	60° Gloss for primer/topcoat
140	AA2024 - T3	6	BS EN ISO 9227	1	0.0	33.7	0.2	131	3.0
141	AA2024 - T3	3	BS EN ISO 9227	3	49.7	44.0	2.4	24	5.7
142	AA7075-T6	1	BS EN ISO 9227	3	6.1	31.8	8.1	36	3.6
143	AA7075-T6	6	Accelerated 3	5	0.0	1.1	8.6	142	2.4
144	AA7075-T6	3	Tropical Inland	5	21.1	18.5	1.2	30	4.0
145	AA2024 - T3	3	Accelerated 2	6	0.0	62.5	0.7	26	3.3
146	AA2024 - T3	3	Accelerated 2	7	0.0	72.6	1.2	25	3.0
147	AA7075-T6	3	Accelerated 2	1	0.0	61.5	0.6	30	9.2
148	AA2024 - T3	4	Tropical Coastal	4	0.0	95.9	8.5	132	2.9
149	AA2024 - T3	2	Accelerated 2	3	0.0	4.6	0.4	33	3.3
150	AA7075-T6	3	Accelerated 2	4	1.0	80.1	1.6	30	2.8
151	AA2024 - T3	3	Accelerated 1	5	13.4	79.7	1.2	119	2.9
152	AA2024 - T3	3	Accelerated 1	6	14.5	28.2	2.0	134	2.6
153	AA7075-T6	3	Accelerated 1	7	49.1	25.7	1.7	25	2.6

Experimental Conditions					Analytical Inputs				
Coupon number	Substrate	Coating system	Experiment	Time point	% area thermography topcoat	85° gloss primer	ΔE 200 primer	Konig Hardness primer/topcoat	60° Gloss for primer/topcoat
154	AA2024 - T3	3	Accelerated 1	2	0.0	23.0	1.0	27	2.5
155	AA7075-T6	6	Accelerated 1	2	1.7	58.1	10.2	145	2.8
156	AA2024 - T3	2	Tropical Coastal	3	53.6	25.8	0.7	25	4.2
157	AA7075-T6	3	Accelerated 1	3	7.4	10.0	0.9	26	3.0
158	AA7075-T6	3	Accelerated 3	5	0.0	53.5	0.6	28	2.6
159	AA2024 - T3	3	Accelerated 3	6	0.0	84.0	1.0	27	3.4
160	AA2024 - T3	1	Accelerated 3	7	0.0	76.2	3.3	38	3.1
161	AA2024 - T3	3	Tropical Coastal	2	19.2	1.1	1.0	29	2.1
162	AA2024 - T3	3	Accelerated 3	2	0.0	49.9	0.5	26	2.5
163	AA2024 - T3	3	Accelerated 2	3	0.0	89.2	0.8	31	3.0
164	AA2024 - T3	3	Accelerated 3	4	0.0	74.9	0.9	28	3.0
165	AA7075-T6	6	Temperate Coastal	6	0.0	72.3	5.2	142	3.0
166	AA2024 - T3	4	Tropical Coastal	7	0.0	8.7	9.9	153	3.4
167	AA7075-T6	3	Accelerated 4	7	2.4	19.5	2.3	29	2.6

Experimental Conditions					Analytical Inputs				
Coupon number	Substrate	Coating system	Experiment	Time point	% area thermography topcoat	85° gloss primer	ΔE 200 primer	Konig Hardness primer/topcoat	60° Gloss for primer/topcoat
168	AA2024 - T3	3	Accelerated 4	1	0.0	90.6	0.8	26	3.1
169	AA7075-T6	3	Accelerated 4	2	0.0	80.6	0.3	27	2.9
170	AA2024 - T3	3	Accelerated 4	3	0.0	71.3	0.3	25	3.0
171	AA7075-T6	3	Accelerated 4	4	0.0	66.5	2.0	164	2.7
172	AA7075-T6	3	Tropical Coastal	5	51.6	10.2	2.6	98	2.2
173	AA2024 - T3	4	Temperate Inland	6	0.0	6.7	7.9	121	5.1
174	AA2024 - T3	3	Tropical Coastal	7	100.0	18.5	2.3	38	1.9
175	AA7075-T6	3	Accelerated 1	1	0.0	93.4	0.1	29	4.2
176	AA7075-T6	3	BS EN ISO 9227	1	0.0	83.6	0.3	27	2.9
177	AA2024 - T3	3	Tropical Coastal	3	42.5	42.3	1.1	27	2.3
178	AA7075-T6	6	Accelerated 1	4	4.6	26.5	8.7	125	3.2
179	AA2024 - T3	6	Tropical Inland	5	8.3	18.1	9.0	126	4.4
180	AA7075-T6	3	Tropical Coastal	4	68.4	30.2	0.9	24	2.4
181	AA7075-T6	3	Accelerated 3	7	0.2	78.4	0.6	28	2.8

Experimental Conditions					Analytical Inputs				
Coupon number	Substrate	Coating system	Experiment	Time point	% area thermography topcoat	85° gloss primer	ΔE 200 primer	Konig Hardness primer/topcoat	60° Gloss for primer/topcoat
182	AA2024 - T3	3	BS EN ISO 9227	7	13.2	16.3	3.8	25	3.6
183	AA7075-T6	1	Accelerated 1	1	0.0	1.7	0.5	37	2.0
184	AA7075-T6	3	Tropical Inland	3	7.3	64.8	0.8	28	3.2
185	AA7075-T6	3	Tropical Inland	4	14.1	63.2	1.1	27	3.1
186	AA7075-T6	3	Temperate Inland	1	0.0	53.4	0.9	29	2.9
187	AA7075-T6	3	Temperate Inland	6	0.0	26.0	1.8	25	2.8
188	AA2024 - T3	3	Tropical Inland	7	28.9	42.9	0.7	12	3.4
189	AA2024 - T3	3	Tropical Coastal	1	0.0	87.7	1.0	27	2.8
190	AA2024 - T3	4	Temperate Inland	2	0.0	41.7	3.1	88	4.7
191	AA7075-T6	4	Temperate Inland	3	0.0	6.6	6.4	104	5.4
192	AA7075-T6	4	Temperate Inland	4	0.0	4.4	7.9	118	4.9
193	AA7075-T6	6	Tropical Inland	5	2.1	17.7	10.5	114	4.2
194	AA2024 - T3	4	Temperate Coastal	6	0.0	11.2	8.8	141	4.8
195	AA7075-T6	4	Temperate Coastal	7	0.0	1.4	10.8	123	3.4

Experimental Conditions					Analytical Inputs				
Coupon number	Substrate	Coating system	Experiment	Time point	% area thermography topcoat	85° gloss primer	ΔE 200 primer	Konig Hardness primer/topcoat	60° Gloss for primer/topcoat
196	AA2024 - T3	4	Temperate Coastal	1	0.0	64.3	0.2	117	6.4
197	AA2024 - T3	6	Temperate Coastal	2	0.0	16.4	8.8	146	5.3
198	AA2024 - T3	4	Temperate Coastal	3	0.0	14.0	5.2	133	5.5
199	AA7075-T6	4	Temperate Coastal	4	0.0	14.8	6.4	128	4.4
200	AA2024 - T3	4	BS EN ISO 9227	5	0.0	57.9	2.2	61	5.7
201	AA2024 - T3	4	Tropical Inland	6	0.0	17.4	6.8	130	5.2
202	AA2024 - T3	4	BS EN ISO 9227	7	1.1	50.8	2.4	109	5.7
203	AA2024 - T3	4	Accelerated 3	1	0.0	59.7	0.2	112	5.0
204	AA2024 - T3	6	Tropical Coastal	2	20.0	17.2	9.3	136	3.5
205	AA7075-T6	4	BS EN ISO 9227	3	0.0	51.3	2.0	115	4.7
206	AA7075-T6	3	BS EN ISO 9227	5	44.2	11.7	3.5	32	3.4
207	AA7075-T6	4	Accelerated 2	5	0.0	58.4	0.3	116	4.5
208	AA7075-T6	5	Accelerated 4	6	0.0	70.5	1.2	107	4.9
209	AA7075-T6	4	Tropical Coastal	4	0.0	3.2	9.1	138	3.1

Experimental Conditions					Analytical Inputs				
Coupon number	Substrate	Coating system	Experiment	Time point	% area thermography topcoat	85° gloss primer	ΔE 200 primer	Konig Hardness primer/topcoat	60° Gloss for primer/topcoat
210	AA7075-T6	6	Accelerated 3	1	0.0	37.8	13.8	144	4.4
211	AA7075-T6	4	Accelerated 2	2	0.0	59.6	0.7	118	4.5
212	AA7075-T6	1	Accelerated 2	3	1.9	1.3	3.9	38	2.0
213	AA2024 - T3	4	Accelerated 2	4	0.0	66.0	0.3	112	6.8
214	AA7075-T6	4	Accelerated 1	5	0.0	54.6	0.9	124	4.1
215	AA7075-T6	4	Accelerated 1	6	0.0	56.6	0.5	149	4.1
216	AA7075-T6	5	Accelerated 1	7	14.2	39.1	0.6	155	1.9
217	AA7075-T6	4	Temperate Coastal	1	0.0	53.2	0.2	98	4.4
218	AA2024 - T3	4	Accelerated 1	2	0.0	53.2	0.5	137	5.6
219	AA7075-T6	2	Accelerated 1	7	86.9	22.4	1.0	101	2.4
220	AA2024 - T3	4	Accelerated 1	3	0.0	51.9	0.9	117	6.4
221	AA2024 - T3	4	Accelerated 3	5	0.0	43.2	1.8	126	5.2
222	AA7075-T6	4	Accelerated 3	6	0.0	39.4	4.0	119	4.7
223	AA7075-T6	4	Accelerated 3	7	0.0	39.1	3.7	121	4.1

Experimental Conditions					Analytical Inputs				
Coupon number	Substrate	Coating system	Experiment	Time point	% area thermography topcoat	85° gloss primer	ΔE 200 primer	Konig Hardness primer/topcoat	60° Gloss for primer/topcoat
224	AA7075-T6	4	BS EN ISO 9227	6	0.0	50.1	2.7	107	4.8
225	AA7075-T6	4	Accelerated 3	2	0.0	63.6	0.6	163	4.5
226	AA7075-T6	3	Accelerated 3	3	0.0	83.3	0.3	24	3.3
227	AA2024 - T3	3	Accelerated 1	4	19.3	42.4	0.7	22	2.7
228	AA7075-T6	4	Accelerated 4	5	0.0	26.4	2.1	126	3.9
229	AA2024 - T3	4	Accelerated 4	6	0.0	37.0	2.3	115	6.9
230	AA7075-T6	1	Accelerated 4	7	0.1	1.0	2.8	113	2.1
231	AA7075-T6	4	BS EN ISO 9227	1	0.0	59.1	0.2	105	5.1
232	AA7075-T6	4	Accelerated 4	2	0.0	61.1	0.3	113	4.2
233	AA7075-T6	4	Accelerated 4	3	0.0	54.6	0.5	56	4.0
234	AA7075-T6	4	Accelerated 2	1	0.0	66.9	0.5	81	5.1
235	AA7075-T6	4	Tropical Coastal	5	1.4	2.1	8.3	111	1.9
236	AA7075-T6	4	Tropical Coastal	6	0.0	2.6	9.9	148	3.2
237	AA7075-T6	4	Tropical Coastal	1	0.0	66.5	0.3	100	6.9

Experimental Conditions					Analytical Inputs				
Coupon number	Substrate	Coating system	Experiment	Time point	% area thermography topcoat	85° gloss primer	ΔE 200 primer	Konig Hardness primer/topcoat	60° Gloss for primer/topcoat
238	AA7075-T6	4	Temperate Coastal	2	0.0	40.3	2.4	110	4.6
239	AA2024 - T3	4	Tropical Coastal	2	0.3	11.5	5.6	121	3.6
240	AA2024 - T3	4	Tropical Coastal	3	0.0	6.5	8.9	132	3.6
241	AA7075-T6	6	Accelerated 1	3	2.9	25.9	9.5	110	3.6
242	AA2024 - T3	4	Tropical Inland	5	0.0	16.0	7.2	126	5.0
243	AA7075-T6	1	Tropical Inland	2	10.1	2.0	10.4	37	2.1
244	AA2024 - T3	4	Tropical Inland	7	0.0	13.6	6.8	111	5.0
245	AA7075-T6	4	Tropical Inland	1	0.0	54.9	0.1	94	5.9
246	AA7075-T6	3	Tropical Inland	2	4.8	54.7	1.4	26	2.9
247	AA2024 - T3	4	Tropical Inland	2	0.0	30.9	3.4	126	4.8
248	AA7075-T6	4	Tropical Inland	4	0.0	21.7	6.4	126	4.4
249	AA2024 - T3	4	Temperate Inland	5	0.0	4.9	8.5	123	4.7
250	AA2024 - T3	4	Accelerated 3	4	0.0	48.8	0.7	165	6.5
251	AA2024 - T3	4	Accelerated 4	7	0.0	28.4	2.6	41	6.1

Experimental Conditions					Analytical Inputs				
Coupon number	Substrate	Coating system	Experiment	Time point	% area thermography topcoat	85° gloss primer	ΔE 200 primer	Konig Hardness primer/topcoat	60° Gloss for primer/topcoat
252	AA2024 - T3	4	Temperate Inland	1	0.0	37.5	0.6	88	6.9
253	AA2024 - T3	5	Temperate Inland	2	0.5	63.4	1.5	99	4.3
254	AA2024 - T3	3	Temperate Inland	3	0.2	62.6	1.0	27	2.7
255	AA2024 - T3	5	Temperate Inland	4	0.0	38.0	1.8	129	3.9
256	AA2024 - T3	5	Temperate Coastal	5	0.0	58.5	2.1	15	3.8
257	AA2024 - T3	5	Temperate Coastal	6	0.0	37.6	9.0	149	3.8
258	AA7075-T6	5	Temperate Coastal	7	0.0	32.3	2.9	146	2.4
259	AA2024 - T3	5	Accelerated 1	4	0.6	52.4	0.3	146	3.5
260	AA7075-T6	5	Temperate Coastal	2	0.0	72.7	1.7	139	6.0
261	AA7075-T6	2	Temperate Inland	6	0.0	1.8	2.0	32	2.6
262	AA7075-T6	5	Temperate Coastal	4	0.0	45.8	1.5	155	4.1
263	AA7075-T6	5	BS EN ISO 9227	5	2.4	75.7	20.4	141	4.2
264	AA2024 - T3	5	BS EN ISO 9227	6	36.7	82.8	0.3	148	4.7
265	AA2024 - T3	5	BS EN ISO 9227	7	7.6	80.4	0.3	158	5.0

Experimental Conditions					Analytical Inputs				
Coupon number	Substrate	Coating system	Experiment	Time point	% area thermography topcoat	85° gloss primer	ΔE 200 primer	Konig Hardness primer/topcoat	60° Gloss for primer/topcoat
266	AA2024 - T3	5	BS EN ISO 9227	1	0.0	69.8	0.1	132	4.7
267	AA7075-T6	5	BS EN ISO 9227	2	12.1	77.2	0.2	134	3.4
268	AA7075-T6	5	BS EN ISO 9227	3	22.2	72.7	0.2	142	4.1
269	AA2024 - T3	1	BS EN ISO 9227	4	30.8	1.9	4.1	31	2.8
270	AA2024 - T3	5	Accelerated 2	5	0.0	83.9	0.3	126	3.7
271	AA7075-T6	5	Accelerated 2	6	4.2	79.9	0.4	130	4.2
272	AA7075-T6	5	Accelerated 2	7	0.6	73.7	0.4	135	4.2
273	AA2024 - T3	5	Accelerated 2	1	0.0	89.1	0.1	131	5.4
274	AA2024 - T3	2	Accelerated 4	2	0.0	2.1	0.9	27	2.8
275	AA7075-T6	5	Accelerated 2	3	1.5	72.1	0.3	137	4.0
276	AA2024 - T3	5	Accelerated 2	4	0.2	91.9	0.3	123	5.0
277	AA2024 - T3	5	Accelerated 1	5	0.0	54.4	0.4	157	4.5
278	AA2024 - T3	5	Accelerated 1	6	0.2	62.5	0.4	154	3.2
279	AA2024 - T3	3	Temperate Coastal	7	3.8	58.3	0.7	30	2.6

Experimental Conditions					Analytical Inputs				
Coupon number	Substrate	Coating system	Experiment	Time point	% area thermography topcoat	85° gloss primer	ΔE 200 primer	Konig Hardness primer/topcoat	60° Gloss for primer/topcoat
280	AA7075-T6	5	Accelerated 1	1	0.0	81.2	0.1	118	3.5
281	AA7075-T6	5	Accelerated 1	2	1.1	45.2	0.6	97	3.5
282	AA2024 - T3	5	Accelerated 1	3	0.0	52.4	0.6	157	3.1
283	AA7075-T6	4	Accelerated 1	4	0.0	47.2	0.6	107	4.4
284	AA7075-T6	5	Accelerated 3	5	0.0	74.4	1.2	150	4.9
285	AA7075-T6	5	Accelerated 3	6	0.0	68.7	1.5	138	6.3
286	AA2024 - T3	5	Accelerated 3	7	1.2	65.5	1.7	138	3.9
287	AA7075-T6	5	Accelerated 3	1	0.0	74.7	0.2	152	4.6
288	AA7075-T6	3	BS EN ISO 9227	2	23.7	38.8	2.4	28	3.4
289	AA7075-T6	5	Accelerated 3	3	0.0	77.5	1.0	136	5.1
290	AA7075-T6	5	BS EN ISO 9227	4	3.8	71.1	0.3	156	4.2
291	AA7075-T6	5	Accelerated 4	5	0.0	70.9	1.0	145	4.1
292	AA7075-T6	2	Accelerated 4	6	0.0	23.5	2.0	35	2.6
293	AA2024 - T3	5	Accelerated 4	7	0.1	70.5	1.3	138	3.6

Experimental Conditions					Analytical Inputs				
Coupon number	Substrate	Coating system	Experiment	Time point	% area thermography topcoat	85° gloss primer	ΔE 200 primer	Konig Hardness primer/topcoat	60° Gloss for primer/topcoat
294	AA2024 - T3	5	Accelerated 4	6	0.0	74.1	1.2	137	3.5
295	AA2024 - T3	2	Accelerated 2	2	0.0	14.3	1.3	33	2.6
296	AA2024 - T3	5	Accelerated 4	2	0.0	89.5	0.6	149	4.0
297	AA7075-T6	5	Accelerated 4	4	0.0	79.1	0.9	124	3.3
298	AA2024 - T3	5	Tropical Coastal	5	21.7	13.7	2.4	136	2.3
299	AA2024 - T3	5	Tropical Coastal	6	29.4	22.9	2.3	144	3.3
300	AA2024 - T3	5	Tropical Coastal	7	38.7	14.2	2.9	3	3.0
301	AA2024 - T3	5	Tropical Coastal	1	0.0	72.8	0.3	124	4.4
302	AA7075-T6	5	Tropical Coastal	2	21.3	43.8	0.7	147	2.9
303	AA2024 - T3	5	Accelerated 4	3	0.0	77.4	0.9	187	4.8
304	AA7075-T6	5	Tropical Coastal	3	43.5	45.6	1.6	150	2.9
305	AA7075-T6	5	Tropical Inland	5	3.7	59.3	0.9	140	4.4
306	AA7075-T6	5	Tropical Inland	6	9.1	67.0	1.0	137	3.4
307	AA2024 - T3	5	Tropical Inland	3	0.0	53.5	1.5	142	4.9

Experimental Conditions					Analytical Inputs				
Coupon number	Substrate	Coating system	Experiment	Time point	% area thermography topcoat	85° gloss primer	ΔE 200 primer	Konig Hardness primer/topcoat	60° Gloss for primer/topcoat
308	AA2024 - T3	5	Tropical Inland	1	0.0	89.1	0.1	118	4.6
309	AA2024 - T3	5	Tropical Inland	2	0.0	72.4	0.9	129	4.1
310	AA2024 - T3	4	Accelerated 2	3	0.0	57.3	0.6	106	10.5
311	AA7075-T6	5	Tropical Coastal	4	65.5	40.9	1.0	37	2.8
312	AA2024 - T3	3	Temperate Inland	5	0.2	45.9	1.0	28	2.7
313	AA7075-T6	5	Temperate Inland	6	0.0	46.2	3.0	137	3.4
314	AA2024 - T3	5	Temperate Inland	7	0.0	38.6	2.9	133	3.6
315	AA7075-T6	5	Temperate Inland	1	0.0	77.3	0.2	117	3.7
316	AA7075-T6	6	Temperate Inland	2	0.0	14.8	6.9	114	4.6
317	AA7075-T6	6	Temperate Inland	3	0.2	9.2	3.5	116	5.3
318	AA7075-T6	6	Temperate Coastal	3	0.0	7.1	4.2	158	4.0
319	AA2024 - T3	6	Temperate Coastal	5	0.0	16.9	11.4	132	5.1
320	AA2024 - T3	1	Temperate Coastal	1	0.0	1.1	1.1	29	2.2
321	AA2024 - T3	6	Accelerated 2	7	2.8	40.2	3.7	116	5.8

Experimental Conditions					Analytical Inputs				
Coupon number	Substrate	Coating system	Experiment	Time point	% area thermography topcoat	85° gloss primer	ΔE 200 primer	Konig Hardness primer/topcoat	60° Gloss for primer/topcoat
322	AA7075-T6	6	Temperate Coastal	1	0.0	48.9	13.8	98	4.3
323	AA7075-T6	2	Temperate Coastal	5	1.1	17.4	2.2	31	2.7
324	AA2024 - T3	5	Temperate Coastal	3	0.0	51.3	0.8	124	4.2
325	AA2024 - T3	6	Temperate Coastal	4	0.2	12.2	12.0	154	5.2
326	AA2024 - T3	6	BS EN ISO 9227	5	20.7	35.5	7.1	109	4.7
327	AA2024 - T3	6	Accelerated 2	4	21.1	37.0	3.3	124	5.4
328	AA7075-T6	6	BS EN ISO 9227	7	7.9	35.4	6.4	98	4.8
329	AA2024 - T3	6	Temperate Inland	1	0.0	30.2	0.6	115	7.0
330	AA2024 - T3	6	BS EN ISO 9227	2	17.3	30.6	5.8	139	5.2
331	AA2024 - T3	6	BS EN ISO 9227	3	17.9	41.4	6.3	134	5.7
332	AA7075-T6	6	BS EN ISO 9227	4	5.4	31.7	6.9	120	4.4
333	AA7075-T6	6	Accelerated 2	5	1.3	32.4	9.9	103	4.7
334	AA2024 - T3	6	Accelerated 2	6	7.6	39.7	3.5	116	6.1
335	AA7075-T6	4	Accelerated 2	7	0.0	54.9	0.5	123	4.5

Experimental Conditions					Analytical Inputs				
Coupon number	Substrate	Coating system	Experiment	Time point	% area thermography topcoat	85° gloss primer	ΔE 200 primer	Konig Hardness primer/topcoat	60° Gloss for primer/topcoat
336	AA2024 - T3	6	Accelerated 2	1	0.0	32.5	0.3	118	3.7
337	AA7075-T6	5	Accelerated 2	2	0.0	87.1	0.2	131	4.7
338	AA7075-T6	6	Accelerated 2	3	0.0	36.9	11.5	113	4.8
339	AA7075-T6	6	Accelerated 4	4	0.0	19.0	8.0	128	3.2
340	AA2024 - T3	6	Accelerated 1	5	15.1	30.0	5.3	124	3.8
341	AA7075-T6	6	Accelerated 1	6	3.3	24.7	8.2	35	3.0
342	AA2024 - T3	6	Accelerated 1	7	37.3	45.1	5.6	184	4.2
343	AA2024 - T3	6	Accelerated 1	1	0.0	43.3	0.2	112	5.7
344	AA2024 - T3	6	Accelerated 1	3	25.3	36.0	4.8	146	4.7
345	AA7075-T6	5	Tropical Inland	4	2.6	59.0	0.7	162	3.5
346	AA2024 - T3	4	Accelerated 4	4	0.0	45.4	0.8	176	6.5
347	AA2024 - T3	2	Tropical Inland	5	26.1	17.7	25.2	30	4.1
348	AA2024 - T3	6	Accelerated 3	6	0.3	1.5	15.5	127	3.0
349	AA2024 - T3	4	Accelerated 3	3	0.0	19.3	7.3	104	5.0

Experimental Conditions					Analytical Inputs				
Coupon number	Substrate	Coating system	Experiment	Time point	% area thermography topcoat	85° gloss primer	ΔE 200 primer	Konig Hardness primer/topcoat	60° Gloss for primer/topcoat
350	AA2024 - T3	3	Accelerated 3	1	0.0	59.9	0.4	128	6.6
351	AA7075-T6	6	Accelerated 3	2	0.0	67.9	0.4	148	3.0
352	AA2024 - T3	6	Accelerated 3	3	0.0	35.3	12.5	142	4.3
353	AA2024 - T3	4	BS EN ISO 9227	4	0.0	44.9	2.6	122	5.7
354	AA2024 - T3	6	Accelerated 4	5	0.2	53.6	1.9	155	5.3
355	AA2024 - T3	6	Accelerated 4	6	0.0	19.3	10.6	133	5.1
356	AA2024 - T3	6	Accelerated 4	7	0.1	14.0	7.9	107	5.3
357	AA7075-T6	6	Accelerated 4	1	0.0	11.4	9.0	127	4.9
358	AA2024 - T3	6	Accelerated 4	2	0.0	33.5	13.8	132	3.5
359	AA2024 - T3	4	Accelerated 1	7	0.0	53.2	2.4	41	5.4
360	AA2024 - T3	5	Accelerated 3	4	0.0	54.0	0.9	143	4.6
361	AA2024 - T3	6	Accelerated 3	7	0.2	64.9	1.4	133	3.8
362	AA2024 - T3	6	Tropical Coastal	6	60.2	16.1	8.5	116	4.9
363	AA7075-T6	6	Tropical Coastal	7	100.0	9.0	11.1	126	3.5

Experimental Conditions					Analytical Inputs				
Coupon number	Substrate	Coating system	Experiment	Time point	% area thermography topcoat	85° gloss primer	ΔE 200 primer	Konig Hardness primer/topcoat	60° Gloss for primer/topcoat
364	AA7075-T6	6	Tropical Coastal	1	0.0	6.0	20.0	121	2.7
365	AA7075-T6	2	Tropical Coastal	2	85.3	42.0	13.8	32	5.2
366	AA2024 - T3	6	Tropical Coastal	3	19.7	26.9	1.4	123	2.3
367	AA2024 - T3	6	Tropical Coastal	4	43.3	14.1	9.9	123	3.8
368	AA7075-T6	6	Accelerated 2	4	0.0	11.3	11.4	129	3.3
369	AA7075-T6	6	Tropical Inland	6	7.5	38.6	11.0	129	4.4
370	AA7075-T6	6	Tropical Inland	7	12.5	18.3	11.1	109	4.2
371	AA2024 - T3	6	Tropical Inland	1	0.0	12.7	11.5	118	3.6
372	AA7075-T6	6	Tropical Inland	2	0.6	45.8	0.2	119	6.0
373	AA2024 - T3	6	Tropical Inland	3	4.6	26.6	10.6	130	3.8
374	AA2024 - T3	6	Tropical Inland	4	2.9	20.5	7.4	94	4.4
375	AA7075-T6	6	Temperate Inland	5	0.5	10.4	8.8	129	4.3
376	AA2024 - T3	6	Temperate Inland	6	0.4	5.3	4.7	128	4.9
377	AA2024 - T3	6	Temperate Inland	7	0.2	10.2	12.2	135	4.6

Experimental Conditions					Analytical Inputs				
Coupon number	Substrate	Coating system	Experiment	Time point	% area thermography topcoat	85° gloss primer	ΔE 200 primer	Konig Hardness primer/topcoat	60° Gloss for primer/topcoat
378	AA7075-T6	4	Temperate Inland	7	0.0	8.7	12.3	122	3.7
379	AA7075-T6	1	Temperate Inland	2	0.0	0.8	10.2	37	2.1
380	AA7075-T6	4	Tropical Inland	3	0.0	21.3	3.1	128	4.3
381	AA7075-T6	1	Temperate Inland	4	0.5	0.8	5.5	42	2.1
382	AA7075-T6	1	Temperate Coastal	5	8.2	0.9	13.8	40	2.0
383	AA7075-T6	1	Temperate Coastal	6	3.8	0.6	10.3	48	2.0
384	AA2024 - T3	1	Temperate Coastal	7	0.0	0.7	12.5	32	2.3
385	AA7075-T6	1	Tropical Inland	1	0.0	1.5	0.2	39	2.3
386	AA7075-T6	1	Temperate Coastal	2	0.0	1.4	2.9	29	2.1
387	AA2024 - T3	1	Temperate Coastal	3	0.0	0.7	4.2	38	2.1
388	AA2024 - T3	1	Temperate Coastal	4	0.0	0.7	9.1	36	2.1
389	AA7075-T6	1	BS EN ISO 9227	5	25.8	1.5	11.0	41	2.5
390	AA2024 - T3	1	BS EN ISO 9227	6	19.3	2.9	6.3	31	2.6
391	AA7075-T6	1	BS EN ISO 9227	7	15.1	1.6	11.1	41	2.5

Experimental Conditions					Analytical Inputs				
Coupon number	Substrate	Coating system	Experiment	Time point	% area thermography topcoat	85° gloss primer	ΔE 200 primer	Konig Hardness primer/topcoat	60° Gloss for primer/topcoat
392	AA7075-T6	5	Temperate Coastal	1	0.0	70.8	0.1	134	4.0
393	AA2024 - T3	1	BS EN ISO 9227	2	4.8	1.3	5.5	32	2.7
394	AA2024 - T3	2	Temperate Inland	6	0.0	15.6	2.3	30	2.6
395	AA7075-T6	1	BS EN ISO 9227	1	0.0	1.2	0.2	33	1.6
396	AA2024 - T3	1	Accelerated 2	5	1.7	1.2	3.3	38	2.2